

GEOLOGICA ULTRAIECTINA

**Mededelingen van de
Faculteit Aardwetenschappen
Universiteit Utrecht**

No. 156

**THE SMALL MAMMALS FROM THE UPPER MIOCENE
OF THE TERUEL-ALFAMBRA REGION (SPAIN):
PALEOBIOLOGY AND PALEOCLIMATIC RECONSTRUCTIONS**



JAN A. VAN DAM

GEOLOGICA ULTRAIECTINA

**Mededelingen van de
Faculteit Aardwetenschappen
Universiteit Utrecht**

No. 156

**THE SMALL MAMMALS FROM THE UPPER MIOCENE
OF THE TERUEL-ALFAMBRA REGION (SPAIN):
PALEOBIOLOGY AND PALEOCLIMATIC RECONSTRUCTIONS**

Cover illustration by Jaap Luteijn

ISBN 90-5744-014-8

**The small mammals from the upper Miocene
of the Teruel-Alfambra region (Spain):
paleobiology and paleoclimatic reconstructions**

**De kleine zoogdieren van het boven Mioceen van het
Teruel-Alfambra gebied (Spanje):
paleobiologie en paleoklimaatsreconstructies**

(met een samenvatting in het Nederlands)

PROEFSCHRIFT

ter verkrijging van de graad van doctor aan de Universiteit Utrecht op gezag van de rector magnificus Prof. dr H. O. Voorma ingevolge het besluit van het college van dekanen in het openbaar te verdedigen op maandag 15 december 1997 des namiddags te 16.15 uur.

door

Jan Arie van Dam

geboren op 20 maart 1959,

te Krimpen a/d IJssel

PROMOTOR: PROF. DR J.E. MEULENKAMP

CO-PROMOTOR: DR A.J. VAN DER MEULEN

Research was carried out at the Research Institute for Paleoenvironments and Paleoclimate Utrecht (IPPU) of the Netherlands Research School of Sedimentary Geology (NSG). This is NSG publication number 970165.

Field campaigns were partly carried out within the framework of the projects "Paleoecología y paleoclimatología del Neógeno continental de la fosa Calatayud-Teruel" (PB92-0013) and "Evolución paleoambiental de sucesiones con alta resolución bioestratigráfica en el Neógeno continental: area de Daroca-Teruel (Aragón-España)" (PB95-0114), financed by the Dirección General de Investigación y Técnica, Spain.

Address of the author:
Faculty of Earth Sciences
Utrecht University
Budapestlaan 4
3584 CD Utrecht
The Netherlands
tel.: 31-302535178/302535122
fax: 31-302535030
E-mail: jdam@earth.ruu.nl

Voor mijn ouders

Voor Agnes

CONTENTS

Publications	8
Samenvatting (Summary in Dutch)	9
Chapter 1: Introduction and synopsis	13
Chapter 2: Mammal successions of the Teruel-Alfambra region: biostratigraphy and biochronology	17
Chapter 3: The Murinae from the upper Vallesian and lower Turolian of the Teruel - Alfambra region (NE Spain)	37
Chapter 4: Stephanodonty in fossil murids: a landmark-based morphometric approach	73
Chapter 5: Paleoclimatic reconstruction on the basis of micromammal faunal compositions, with special reference to life-history aspects	87
Chapter 6: Reconstruction of the late Miocene climate of Spain using rodent paleocommunity successions: an application of end-member modelling	111
Chapter 7: The small mammals from the upper Miocene of the Teruel-Alfambra region: faunal dynamics and events	153
Appendix A: Taxonomic remarks	171
Appendix B: Age estimates for mammal localities	175
Appendix C: A biometric analysis on fossil and extant murine molars	183
References	187
Acknowledgements	201
Curriculum vitae	204

Publications

Chapter 2: will be published in an extended form as: van Dam, J. A., L. Alcalá, A. Alonso Zarza, J. P. Calvo, M. Garcés, and W. Krijgsman. High-resolution late Miocene mammal biochronology and paleoecology of the Teruel-Alfambra region (NE Spain). (to be submitted to the *Journal of Vertebrate Paleontology*)

Chapter 3: to be submitted to *Palaeontographica*.

Chapter 4: has been published as: van Dam, J.A. 1996. Stephanodonty in fossil murids: a landmark-based morphometric approach. Pp. 449-461 in Marcus, L. F., M. Corti, A. Loy, G. J. P. Naylor and D. E. Slice, eds. *Advances in Morphometrics*. NATO volume 284. Plenum, New York.

Chapter 5: submitted to *Paleobiology*.

Chapter 6: will be published as: van Dam, J. A. and G. J. Weltje. Reconstruction of the late Miocene climate of Spain using rodent paleocommunity successions: an application of end-member modelling. (submitted to *Palaeogeography, Palaeoclimatology, Palaeoecology*)

Samenvatting (Summary in Dutch)

Het onderzoek aan fossiele kleine zoogdieren is in de jaren 60 in een stroomversnelling geraakt, toen ontdekt werd dat grote hoeveelheden gebitselementen konden worden verkregen door grondmonsters te onderwerpen aan de techniek van het "nat zeven". Met het uitwerken van de taxonomie werd al snel duidelijk dat met name knaagdieren zeer geschikt zijn voor het bedrijven van continentale biostratigrafie, hetgeen te danken is aan de hoge diagnostische waarde van hun gebitselementen en aan hun snelle evolutie. Daarnaast worden vanaf het einde van de jaren 70 associaties van kleine zoogdieren steeds vaker gebruikt voor de reconstructies van paleomilieu en klimaat. Het onderzoek in Spaanse Neogene bekkens heeft hierbij een belangrijke rol gespeeld. De uitzonderlijke rijkdom aan zoogdierresten in de fossiele meerafzettingen van deze bekkens maken het opstellen van hoge resolutie stratigrafische opeenvolgingen mogelijk, hetgeen een absolute randvoorwaarde is om gedetailleerde fauna- en omgevingsveranderingen naar behoren te kunnen registreren.

Het belangrijkste doel van dit proefschrift is de gedetailleerde reconstructie van trends en gebeurtenissen ("events") in fauna, omgeving en klimaat gedurende het laat Mioceen (Vallesien en Turolien) van Spanje. Als onderzoeksgebied is gekozen het gebied tussen Teruel en Alfambra in het bekken van Teruel, noordoost Spanje. De keuze voor dit gebied is mede bepaald door het feit dat eerder onderzoek een solide taxonomisch en biostratigrafisch raamwerk had opgeleverd.

Gedurende een reeks van veldwerkcampagnes in de jaren 90, in samenwerking met collega's van de Complutense Universiteit en het Nationaal Museum voor Natuurwetenschappen in Madrid, is het aantal vindplaatsen van fossiele kleine zoogdieren in het boven Mioceen praktisch verdubbeld. Dit heeft geresulteerd in een sequentie van 89 lokaliteiten, waarvan in totaal zo'n 20.000 gebitselementen zijn bestudeerd. De meeste van deze vindplaatsen bevinden zich in secties met meerdere fossielhoudende niveaus boven elkaar. Gedurende het onderzoek zijn vijf van deze profielen bemonsterd voor magnetostratigrafische analyse. De combinatie van de gevonden magnetische polariteitspatronen en de dateringen van zonegrenzen in andere Spaanse bekkens maakt een correlatie van de zoogdiersuccessie naar de geomagnetische polariteits tijdschaal (GPTS) mogelijk.

De eerste stap na het verzamelen is de determinatie van de fossielen. Na een korte bespreking van de geologische setting van het onderzoeksgebied en de voornaamste lithologische aspecten van de fossielhoudende secties, worden in **hoofdstuk 2** nieuwe range charts van de verschillende groepen kleine zoogdieren gepresenteerd. De gevonden knaagdieren, die het zwaartepunt van het onderzoek vormen, zijn zonder veel problemen in reeds gedefiniëerde soorten ingepast. De insekteneters en lagomorfen zijn tot op genusniveau gedetermineerd en de zeldzame vleermuizen tot op familieniveau. Het overzicht wordt gecomplementeerd met een range chart van de grote zoogdieren uit het onderzoeksgebied. Drie nieuwe lokale biostratigrafische subzones voor het boven Vallesien worden gedefiniëerd op basis van muriden. Een groot deel van de lokaliteiten,

alsmede verschillende zone/etage grenzen worden gecorreleerd naar de numerieke tijdschaal. De resultaten voor de Masía de la Roma sectie zijn consistent met de ouderdom van 9.7 miljoen jaar geleden voor de Onder-Boven Vallesien (MN9-10) grens, zoals die bepaald is in het Vallès-Penedès bekken. De ouderdom van de Vallesien-Turolien (MN10-11) grens is bepaald op 8.7 miljoen jaar geleden in de La Gloria sectie. Ouderdommen van twee andere subzone grenzen in het boven Vallesien zijn geschat op respectievelijk 9.3 en 9.0 miljoen jaar geleden. De magnetostratigrafische controle voor het midden en boven Turolien van het Teruel bekken is minder goed. Ouderdommen voor de vindplaatsen in dit traject zijn geschat door middel van biostratigrafische correlaties met secties in het Cabriel bekken.

Hoofdstuk 3 beschrijft de stand van zaken voor wat betreft de taxonomie van de muriden (Muridae, muisachtigen), voor zover deze groep voorkomt in het boven Vallesien en onder Turolien van het Teruel-Alfambra gebied. De familie van de muriden de meest voorkomende groep kleine zoogdieren in het Mediterrane gebied gedurende het laat Mioceen en vroeg Pliocceen. Het eerste regelmatige voorkomen van muriden in het Teruel bekken is gedateerd op ongeveer 9.6 miljoen jaar geleden. Verscheidene karakteristieken van de eerste bovenkaaksmolaar van deze vroegste muriden (*Progonomys hispanicus*) wijzen op een nauwe verwantschap met *Progonomys cathalai*, een iets grotere vorm die rond 9.3 miljoen jaar geleden in het gebied verschenen is. Met het identificeren van *Parapodemus gaudryi* in verschillende onder Turolien vindplaatsen is aangetoond dat de verspreiding van deze soort niet beperkt was tot zuidoost Europa. De oorsprong van de soort is niet helemaal duidelijk, maar het is aannemelijk dat *Progonomys cathalai* de directe voorouder was. Dit zou inhouden dat het genus *Parapodemus* polyphyletisch is (meerdere keren is ontstaan).

In **hoofdstuk 4** wordt een nieuwe manier besproken om vormvariatie in muridenkieszen te beschrijven. De methode gaat uit van van te voren gedefiniëerde homologe punten ("landmarks") op het horizontaal geprojecteerde kauwvlak, waarvan de x en y coördinaten worden gemeten. De toepassing van verschillende op deze landmarks gebaseerde morphometrische technieken op een set van 250 eerste bovenkaaksmolaren van acht verschillende laat Miocene en Pliocene Spaanse associaties laat zien dat een clustering van populaties op grond van morphometrische parameters de taxonomische indeling redelijk goed, maar niet precies weerspiegelt. De analyses laten ook zien, dat de evolutionaire ontwikkeling naar een apart soort richelpatroon op de bovenkaakskieszen van muriden (stephanodontie) correleert met specifieke veranderingen in de omtrek van de kies en de positie van knobbels. Eén van de opvallendste trends is het "oplijnen" van landmarks langs twee parallelle banen. Een mogelijke functionele verklaring hiervoor is het ondersteunen van een lange en krachtige kauwbeweging, die nodig is om meer vezelrijk voedsel (gras) te kunnen verwerken.

Klimaatreconstructies zijn het onderwerp van de hoofdstukken 5 en 6. **Hoofdstuk 5** bespreekt de aanpassingen aan en voorkeuren van kleine zoogdieren voor verschillende klimaataspecten, en het gebruik van veranderingen in de relatieve aantallen van kleine

Samenvatting (Summary in Dutch)

zoogdieren in stratigrafische opeenvolgingen voor het reconstrueren van klimaatsveranderingen. Trends in twee verschillende ariditeit-gerelateerde maten, het % individuen dat aangepast is aan het consumeren van grassen en het % individuen dat een terrestrische levenswijze heeft, wijzen op een droog interval tussen 9 en 8 miljoen jaar geleden. Gedurende dit interval blijkt ook de soortendiversiteit lager te zijn geweest dan normaal. In dit hoofdstuk wordt er voor gepleit om kennis over recente "life history" strategieën, zoals die tot uiting komen in demografische parameters (zoals levensverwachting) en energiehuishouding (reproductie vs. overleving), toe te passen in paleoklimaatsreconstructies. In de eerste plaats zouden verschillen in gemiddelde levensverwachting bij de geboorte gebruikt kunnen worden om relatieve aantallen van groepen in geleidelijk geaccumuleerde fossiele associaties te corrigeren. In de tweede plaats kunnen fluctuaties in het voorkomen van bepaalde life history strategieën gebruikt worden om veranderingen in seizoenaliteitstype (aan humiditeit dan wel aan temperatuur gerelateerde seizoenaliteit) en veranderingen in klimaatsvoorspelbaarheid (het niveau van interjaarlijkse variatie) van het klimaat te modelleren. Als hypothese wordt voorgesteld dat de vervanging van hamsterachtigen (Cricetidae) door uit Zuid Azië afkomstige muisachtigen (Muridae) in de subtropische gordel van de Oude Wereld gedurende het vroege laat Mioceen het gevolg is geweest van een omslag naar een meer onvoorspelbaar, nat-droog seizoenaal klimaat in dit deel van de wereld. De oorzaak van deze klimaatsomslag zou gelegen kunnen zijn in een veranderde atmosferische circulatie op het Noordelijk Halfrond, als die op haar beurt weer veroorzaakt zou zijn door de opheffing van een deel van Zuid Azië (Tibetaans Plateau / Himalaya).

Een meer verfijnde klimaatsreconstructie wordt uitgevoerd in **hoofdstuk 6** op basis van de methode van eindleden modellering ("end-member modelling"). Deze methode wordt toegepast op een matrix van relatieve aantallen van 67 laat Miocene knaagdierassociaties uit Spanje, Frankrijk, Oostenrijk en Griekenland. Het model heeft in de eerste plaats als invoer de relatieve aantallen van negen ecologisch en demografisch gedefiniëerde groepen knaagdieren, en in de tweede plaats scores (positief, negatief of intermediair) voor de preferenties en aanpassingen van deze groepen voor en aan verschillende klimaatsparameters. De preferenties en aanpassingen zijn gebaseerd op functioneel morfologische en actualistische principes, (paleo)biogeografische verspreidingspatronen, en demografische karakteristieken. Op basis van de klimaatskarakteristieken van de gemodelleerde eindleden kunnen uit de bijdragen van deze eindleden aan de 67 composities klimaatscurves en gradiënten worden afgeleid. De tijdelijk verhoogde bijdrage van twee meer "noordelijke" eindleden in de Spaanse successie tussen 11.5 en 8.5, rond 7 en rond 6 miljoen jaar geleden wordt geïnterpreteerd als het optreden van meer gematigde (koelere en nattere) klimaatsomstandigheden. Het toenemen van de relatieve bijdrage van deze eindleden reflecteert mogelijk een zuidwaartse migratie van de gematigde klimaatszone. Verder suggereren de modelresultaten een belangrijke verandering van koud-warm naar nat-droog seizoenaliteit tussen 9.4 en 8.2 miljoen jaar geleden. Afkoelingsmaxima rond 9.4 en 7 miljoen jaar geleden correleren met clusters van mariene gebeurtenissen die samenhangen met maxima van globaal ijsvolume.

De hypothese van "coordinated stasis" veronderstelt dat lange periodes van stabiliteit in levensgemeenschappen worden afgewisseld worden met relatief korte perioden van faunaverandering. In **hoofdstuk 7** wordt deze hypothese getest voor de opeenvolging van kleine zoogdieren in het Teruel-Alfambra gebied. De resultaten steunen de "coordinated stasis" hypothese maar ten dele. In tegenstelling tot wat deze hypothese voorspelt, treden verschillende typen gebeurtenissen zoals extinctions, immigraties, veranderingen in relatieve aantallen, en veranderingen in de verdeling van lichaamsgroottes in kleine zoogdieren in het algemeen niet tegelijk op. Ook gaan belangrijke veranderingen in een bepaalde orde (knaagdieren of insekteneters) vaak voorbij aan de andere orde. Wel kunnen desondanks een aantal belangrijke gebeurtenissen worden onderscheiden, die onder de aanduiding "Small Mammal events" (SM events) zijn opgenomen in een chronologisch overzicht. Het zijn: 1) de vervanging van cricetiden door muriden in termen van aantallen individuen rond 9.6 miljoen jaar geleden; 2) een extinctie gebeurtenis rond 9.1 miljoen jaar geleden; 3) een immigratie event van knaagdieren rond 8.7 miljoen jaar geleden; 4) een immigratie event van met name insekteneters rond 8.1 miljoen jaar geleden, en 5) een gecombineerde immigratie en extinctie event in knaagdieren 7.0-6.6 miljoen jaar geleden. De resultaten van de fauna analyse bevestigen het beeld van corresponderende marien-continentale, klimaats-geïnduceerde veranderingen zoals behandeld in hoofdstuk 6. Snelle en/of sterke mondiale opwarming zou het min of meer gelijktijdig plaatsvinden van de SM events van 8.7 en 7.0-6.6 miljoen jaar geleden in Spanje en stabiele isotopen events in de noord-oostelijke Atlantische Oceaan die globale afname van poolijs aanduiden, kunnen verklaren.

Study the past if you would divine the future.

Confucius
(The Analects)

Chapter 1

Introduction and synopsis

Small mammal paleontology reached maturity during the 1960s. From then onward the introduction of efficient screen-sieving techniques allowed to collect large amounts of skeletal and dental remains. Initially, the use of small mammals was mainly confined to biostratigraphy, which was based on the highly diagnostic value of the teeth, and the rapid evolution of many groups. From the late 1970s onwards, however, fossil small mammal associations have also increasingly been used for the reconstruction of paleoenvironments and climatic fluctuations. In this context much work has been done in the Neogene basins of Spain. The exceptional richness of mammal remains in the fossil lacustrine deposits of these basins has allowed the construction of a high-resolution stratigraphic framework, which is a prerequisite for the detailed reconstruction of causes and effects of faunal and environmental changes.

The main aim of this thesis is to unravel in greatest possible detail trends and events in fauna, environment and climate in NE Spain during the late Miocene (Vallesian and Turolian). The Teruel-Alfambra region in the Teruel basin has been chosen as the study area, because earlier studies in the 1960s and 1970s had already provided a firm taxonomic and biostratigraphic framework. In order to further increase the small mammal faunal resolution in the area, several field campaigns have been organized during the 1990s in close collaboration with colleagues from Complutense University and the National Museum of Natural Sciences, Madrid. This has finally resulted in a total number of 89 upper Miocene fossil localities, i.e. almost twice as much as were known before. The majority of the localities have been found in stratigraphic superposition in the field. In the course of the study, various key sections have been sampled for magnetostratigraphic analysis. The combination of the polarity patterns in the Teruel and in other Spanish basins allows the correlation of the studied small mammal succession to the Geomagnetic Polarity Time Scale (GPTS).

After a short introduction on the geological setting of the study area and the main lithological aspects of the small mammal containing sections, updated small mammal distribution charts are presented in **chapter 2**. Rodents, which constitute the main group of study, have been identified at the species level. Insectivores and lagomorphs have been

identified at the genus level and the rare bats at the family level. An up to date large mammal distribution chart is also included in this chapter. Three new local biostratigraphic subzones for the upper Vallesian have been defined on the basis of murids. Various zone/stage boundaries have been dated using combined magneto- and biostratigraphy. Data from the lower part of the Masía de la Roma section are consistent with the age of 9.7 Ma for the lower-upper Vallesian (MN9-10) boundary, as determined in the Vallès-Penedès basin (NE Spain). The age of the Vallesian-Turolian boundary is estimated at 8.7 Ma in the La Gloria section. The ages of two other upper Vallesian subzones are estimated at 9.3 and 9.0 Ma, respectively. Time control for the middle and upper Turolian sections is still relatively poor. Ages for the localities in this interval are estimated by biostratigraphic correlation to the Cabriel basin (eastern Spain), where a magnetic polarity pattern has been correlated to the GPTS.

In **chapter 3** the upper Vallesian and lower Turolian murine succession of the Teruel - Alfambra region is reviewed in the light of the new material. Murinae (true mice) are the dominant small mammal group in the Mediterranean area during the late Miocene. The first regular occurrence of murines in the Teruel basin is dated at 9.6 Ma. Various features of the first upper molar of the earliest murines (*Progonomys hispanicus*) indicate a close relationship with the slightly larger *Progonomys cathalai*, which appears in the area at about 9.3 Ma. *Parapodemus gaudryi* has been recognized in various lower Turolian localities of the Teruel-Alfambra region; hitherto it was known only from the eastern Mediterranean. The origin of this species is not entirely clear, but its most probable ancestor is *Progonomys cathalai*, which would imply that *Parapodemus* is a polyphyletic genus. *P. gaudryi* is thought to be the direct ancestor of *Apodemus gudrunae*, and *Parapodemus lugdunensis* is thought to be the ancestor of *P. barbarae*.

Chapter 4 describes the application of landmark-based morphometrics to the study of size and shape variation in murid teeth. Nineteen homologous points (the landmarks) are defined on the horizontally projected occlusal surface of the first upper molar, and measured by their *x* and *y* coordinates. Statistical analysis of the landmark patterns of eight upper Miocene and Pliocene Spanish associations shows that a clustering of the populations on the basis of morphometric parameters reflects the taxonomy reasonably well, except perhaps for the studied population of *Stephanomys ramblensis*, of which the shape is very close to that of *Occitanomys*. The analyses also show that the evolution towards a specialized crown structure (stephanodonty) correlates well to specific changes in the outline of the tooth and the position of some cusps. One of the most interesting findings is the alignment of landmarks in the longitudinal direction during the evolution towards the stephanodont pattern. Presumably, such a configuration allows a longer and more efficient power stroke, which is necessary for the bulk consumption of fibrous foods such as grass.

Paleoclimatic reconstructions are the subject of chapters 5 and 6. **Chapter 5** deals with the adaptations and preferences of small mammals for various climatic parameters, and with the use of changes in relative abundances in stratigraphic successions in the

reconstruction of climatic fluctuations. Trends in two aridity-related measures, the % individuals which (partially) graze and the % individuals with a terrestrial way of life, indicate the presence of an arid interval between 9 and 8 Ma ago. This dry interval is characterized by low species diversity. It is proposed to use the knowledge on extant life history strategies, as expressed for example by demographic parameters (life expectancy) and by patterns of energy expenditure (reproduction versus survival) for paleoclimatic reconstructions. Firstly, differences in mean life expectancies at birth can be used to correct relative abundances in gradually accumulating assemblages. Such a correction may have a clear effect on the distribution of groups, as is shown by an example from Spain. Secondly, fluctuations in the relative abundances of three basic demographic groups can be used for the reconstruction of type of seasonality (humidity- or temperature-related) and degree of interannual climatic variation (predictability). It is proposed that the competitive replacement of cricetids by murids (which are supposed to have originated in South Asia) in the subtropics of the Old World during the early late Miocene is the result of a shift to a more unpredictable, wet-dry seasonal climate in this part of the world. This climatic transition may have resulted from a changing atmospheric circulation, which in its turn may have been induced by increased rates of uplift of the Himalaya/Tibetan plateau.

Chapter 6 presents a climatic reconstruction by using end-member modelling. This method is applied to a data set of relative abundances of 67 late Miocene rodent associations (11-6 Ma) from Spain, France, Austria and Greece. The input of the model is formed by 1) relative abundances of nine ecologically defined rodent groups, and 2) the preference and adaptation scores (either positive, negative or intermediate) of these groups to the climatic parameters humidity, temperature, seasonality type and predictability. Humidity preferences and adaptations are based on actualistic and functional morphological interpretations of the dentition and locomotion, and temperature preferences are based on paleobiogeographic distribution patterns. Levels of adaptation to seasonality type (wet-dry or cool-warm seasonality) are assigned on the basis of diversities in present-day climate/vegetation zones, and the ability of extant relatives to hibernate. Demographic data are used to formulate adaptations to climatic (un)predictability. After a climatic characterization of the end-members, their contributions to the 67 compositions is used to construct climatic curves and gradients. The temporary high contribution of more "northern" end members in the Spanish succession between ~10.5 and ~8.5 Ma, around 7, and around 6 Ma is interpreted in terms of more temperate (cooler and wetter) climatic conditions. The presence of such conditions in Spain might be explained by southward migrations of the transitional zone between temperate and subtropical-dry climatic belts and their associated vegetation types. Two cooling maxima at 9.4 and 7 Ma are approximately time-equivalent with clusters of marine events which mirror maxima of global ice volume. Superimposed on this humidity/temperature pattern is a shift from a more predictable, cool-warm seasonal climate towards a more unpredictable, wet-dry seasonal climate between 9.4 and 8.2 Ma.

The "coordinated stasis" hypothesis suggests that there is a common pattern in the fossil record, which is characterized by long intervals of community stability, which alternate with short episodes of abrupt faunal change. In **chapter 7**, the small mammal succession of the Teruel-Alfambra region is analyzed to test this hypothesis. The coordinated stasis hypothesis is only partly corroborated by the results. Changes in different faunal aspects (relative abundance, immigration, extinction, size) are not coeval, which is in conflict with the hypothesis. Furthermore, important changes in particular faunal aspects of rodent associations are not accompanied by corresponding changes in insectivores, or vice-versa. A number of important small mammal events (SM events) are defined. These include the expansion of murids at ~9.6 Ma, the extinction amongst rodents and insectivores at ~ 9.1 Ma leading to a rodent diversity drop at ~ 8.9 Ma, the rodent immigration at ~8.7 Ma, the immigration of various taxa (mainly insectivores) at ~ 8.1 Ma, and the rodent extinction and migration between 7.0 and 6.6 Ma. The faunal analyses confirm the existence of coeval climate-induced changes in the marine and continental records. Two "glacial"- "interglacial" reversals at 8.6 and 6.7 Ma, inferred from the stable oxygen isotope record from the NE Atlantic, more or less coincide with SM events. These correlations can best be explained in terms of major climatic warmings.

*Go, my sons, buy stout shoes, climb the mountains,
search....the deep recesses of the earth....
In this way and in no other you will arrive
at a knowledge of the nature and properties of things.*

Severinus

Chapter 2

Mammal successions of the Teruel-Alfambra region: biostratigraphy and biochronology

Abstract

An extended and revised mammal succession of 90 fossil localities from the upper Miocene sediments of the Teruel basin (NE Spain) is presented. A detailed biozonation for the upper Vallesian based on Muridae is proposed. Magnetostratigraphic correlation of various key sections to the Geomagnetic Polarity Time Scale (GPTS) allows a fairly accurate dating of most mammal localities and zonal boundaries. Time control of the middle and upper Turolian sections is still relatively poor.

2.1. Introduction

The Teruel-Alfambra region in NE Spain (figs. 2.1 and 2.2) is a classical area for mammal paleontology. Documentation of fossil bones dates back to the first part of the eighteenth century, when Feijoo (1736) mentioned the occurrence of "varios huesos de el cuerpo humano, y otras, que representan huesos de bestias" near the village of Concué (see Alcalá, 1994 for a historical review). During the nineteenth and first part of the twentieth century an increasing amount of (obviously non-human) bones from Concué were taxonomically described. From the nineteenforties onwards, the Spanish paleontologists Crusafont, Truyols and Villalta started to explore the region more systematically, and discovered various other important macromammal sites. One of the results of these field campaigns was the introduction of the term "Turolian" to indicate "les niveaux de Teruel" (Crusafont, 1965). A formal definition of the Turolian as a continental stage was given somewhat later (Marks, 1971; Aguirre et al., 1975).

Many new, particularly micromammal localities became known from the sixties onwards, when Adrover started his extensive prospections of the area around Teruel. His

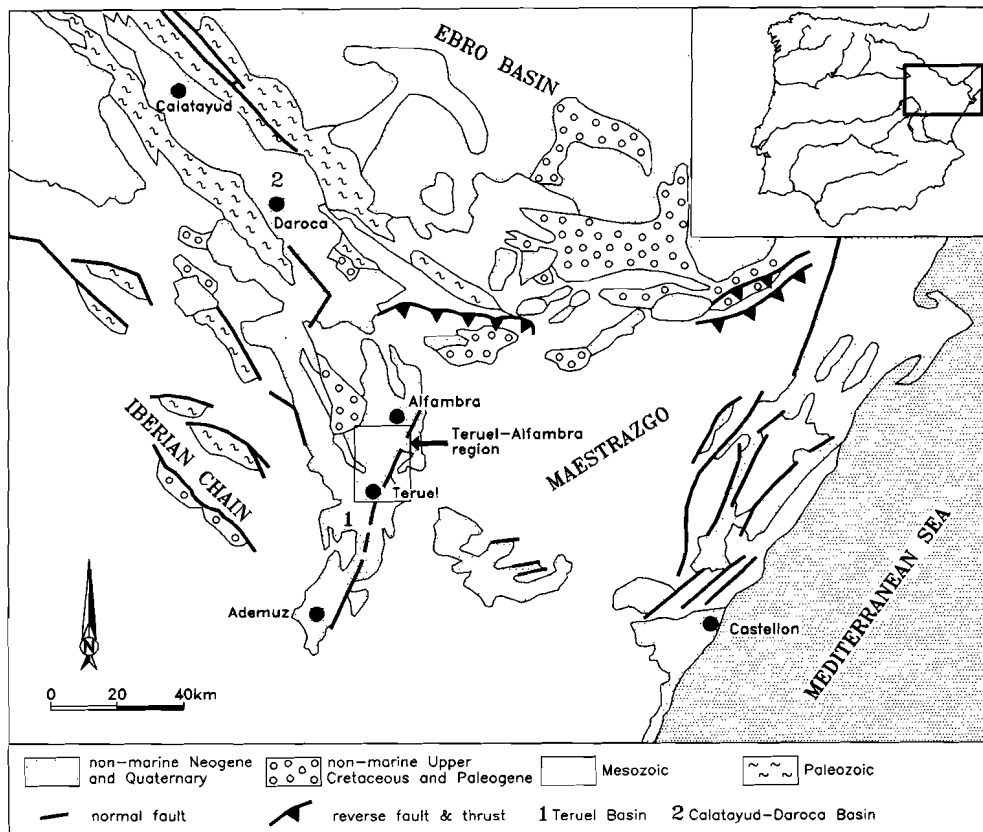


Figure 2.1. Schematic map of the Teruel basin and surrounding areas (NE Spain).

contribution to the mammal paleontology of the area is enormous and is contained in many publications (see bibliography in Adrover, 1986). Some other important studies resulted from Dutch-Spanish cooperation starting slightly later. Among these are the monography on *Hipparion* by Sondaar (1971) and the work of van de Weerd (1976) on rodents. The latter study was the first paleontological study of the area based on modern bio- and chronostratigraphic concepts, coupled with sampling of sections with series of superposed micromammal localities. Van de Weerd's study resulted in a firmly-established biozonation based on Muridae. Recently, latest Miocene to Pliocene gaps in the zonation were bridged by the Spanish-French team of Adrover, Mein and Moissenet (Mein et al., 1990).

During the nineties paleontological research took various new directions. The number of micromammal localities was considerably increased by renewed intensive sampling, and the degree of stratigraphic resolution was further increased by the correlation of key sections to the Geomagnetic Polarity Time Scale (GPTS) (Krijgsman et al., 1996; Garcés et al., submitted). The "high-resolution" magnetobiostratigraphic approach (*sensu*

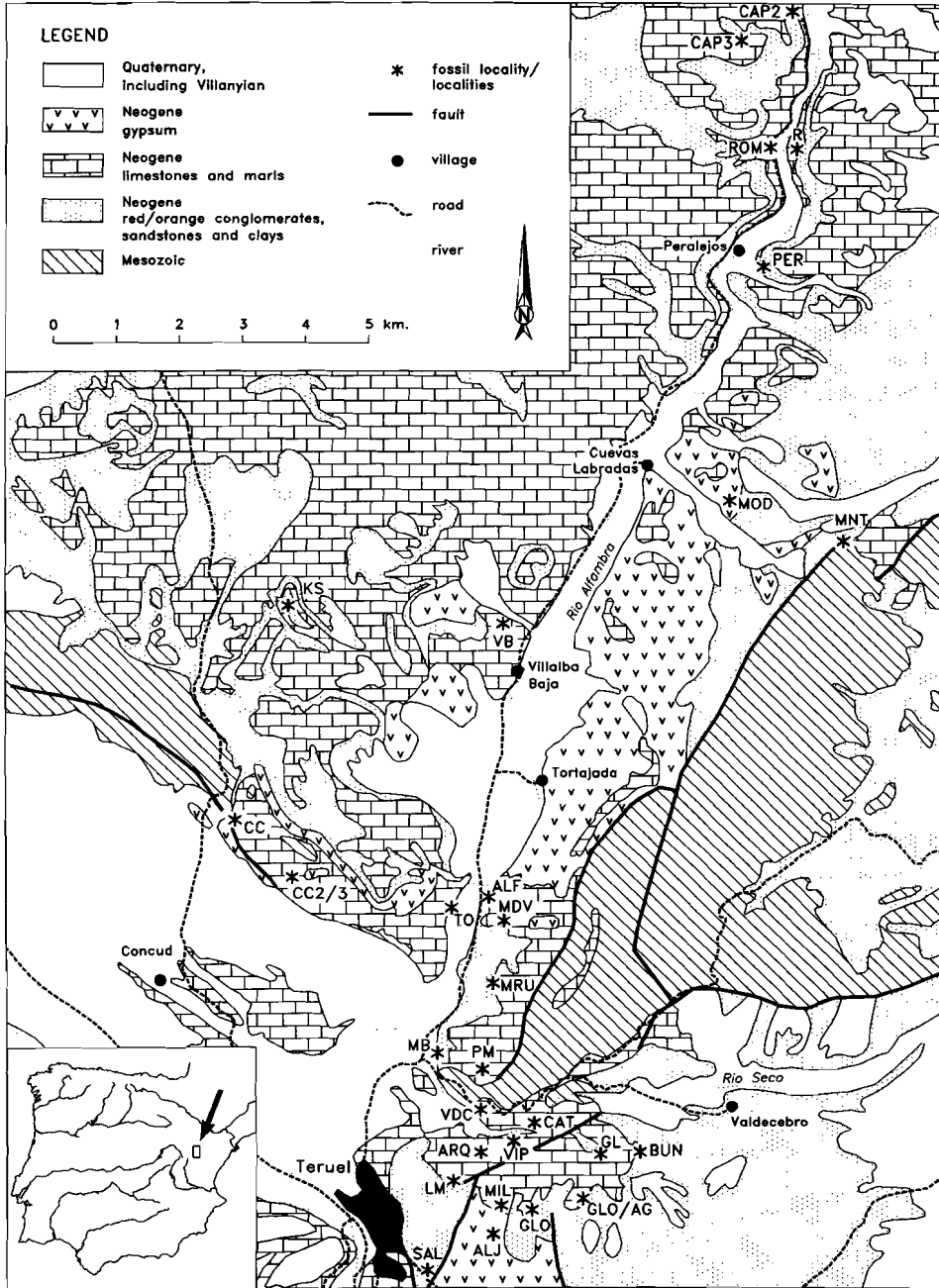


Figure 2.2. Schematic geological map of the northern part of the Teruel basin (Teruel-Alfambra region) with positions of sections and mammal localities. See tables 2.1 and 2.2 for locality names. Note that GLO= La Gloria 6, 14A and B, GL= La Gloria 4 and 5, and GLO/AG= other La Gloria and Los Aguanaces localities.

Lindsay, see Woodburne, 1996) not only improved the chronology of mammal localities and zones (this chapter), but also yielded the temporal framework for paleoecological and paleoclimatological studies based on relative abundances in rodents (chapters 5 and 6) and the analysis of small mammal events (chapter 7). A shift towards paleoenvironmental reconstructions has also characterized the work on the macromammals. For instance Alcalá (1994) combines detailed taphonomic analyses with paleoecological studies of body-size distribution and ecological diversity spectra.

2.2. Geological setting and lithology

The backbone of the biostratigraphic framework consists of a series of sections with fossil localities in the central part of the Teruel-Alfambra region, which is situated between the town of Teruel in the South and the village of Alfambra in the North. The majority of the sections are situated in or close to the valley of the Rio Alfambra (fig. 2.2). The Teruel-Alfambra region comprises half of the northern part of the Teruel Basin, a NNE-SSW oriented basin in the northeastern part of the Iberian Peninsula (fig. 2.1). The basin covers an area of approximately 100 km in length, and 15 km in width. It is filled with a fairly complete middle to late Neogene succession exceeding 500 m in thickness (Moissenet, 1983, 1989). According to Anadón and Moissenet (1996) the basin should be regarded as a half-graben, with the NNE-SSW oriented master fault running along the eastern border of the basin (fig. 2.1).

In the Teruel-Alfambra region (fig. 2.2), the Neogene succession is predominantly bounded by Triassic clastic and evaporite formations and Jurassic carbonates. Along the eastern margin of the basin (fig. 2.2), the oldest Neogene deposits (early Aragonian after unpublished data of the Montalbos fauna in the Teruel-Alfambra region, locality MNT in fig. 2.2) unconformably overlie carbonate formations of late Jurassic age. However, most of the basin fill sequence that can be observed in the central part (the river Alfambra valley) is composed of sediments of early late Miocene (early Vallesian) to early Pliocene (Ruscinian) age. Overall, these sediments were deposited in distal alluvial fan and shallow lake environments.

The main mammal-containing sections are schematically represented in figures 2.3 and 2.4. Figure 2.3 shows eleven sections in the southern part of the Teruel-Alfambra region, close to Teruel. Figure 2.4 shows three sections in the northern part, which will be referred to as the Peralejos area (after the village of Peralejos, see fig. 2.2). Both areas are separated from each other by about 15 km. Correlations between sections are either based on the position of individual marker beds, or on the position of (boundaries between) lithostratigraphic units described in the literature (van de Weerd, 1976; Hernandez et al., 1983). The mammal locality codes in the figures correspond with the codes on the map of figure 2.2.

Most fossil mammal remains are found in organic-rich marlstones and claystones, or lignites associated with a carbonate lithofacies, although some localities are associated with distal alluvial facies (e.g. MBA) or gypsum facies (e.g. LM and LM2). The relation between lithofacies and the accumulation of mammal remains has been tentatively studied

by Albesa et al. (1997) but a comprehensive approach to the factors controlling the formation of the mammal sites is still in progress.

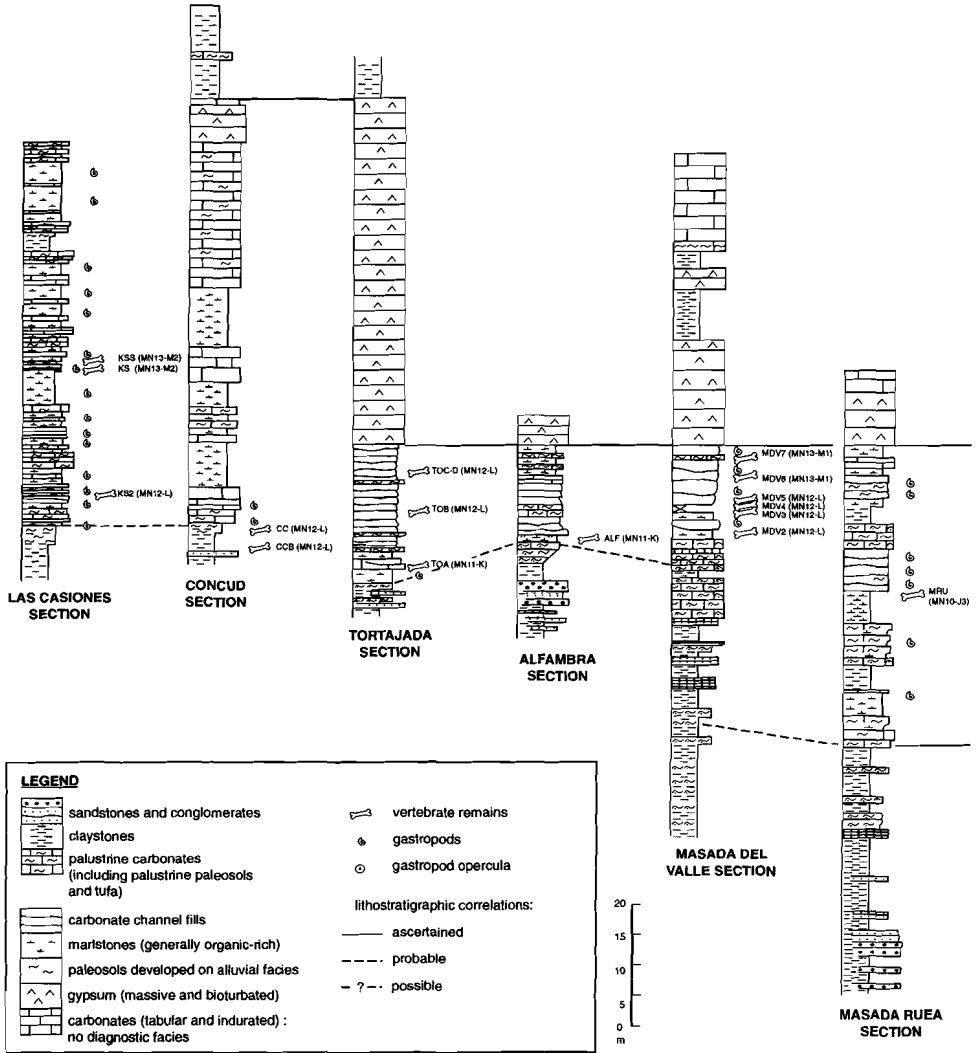
The studied fossiliferous organic-rich marls belong to the carbonate facies units M_3 and M_{4m} as described by Hernandez et al. (1983), and to the Alfambra formation of van de Weerd (1976). The carbonates associated with these facies units display features typical of sedimentation in shallow lake environments and include: 1) carbonate paleosols showing distinct maturation stages (Machette, 1985); 2) carbonate pond sequences (Sanz et al., 1995); 3) palustrine carbonates, i.e. rooted micrites and biomicrites (Platt, 1989; Alonso-Zarza et al., 1992), mottled carbonates and marls, and nodular carbonates; 4) tufa deposits (Pedley, 1990); 5) carbonate channel fills, locally rich in gastropod opercula; and 6) tabular, gastropod-rich carbonate beds. Superposition of carbonates displaying extensive rooting and other palustrine features on primary carbonate lithofacies, especially tufas and carbonate channel fills, are common features. This suggests that the shallow lakes underwent episodic lake level oscillations.

Facies M_3 is exposed in the Peralejos area, where it forms the lowest part of the hills bordering the river Alfambra. Its top can easily be recognized in the field (half-way the hill slope in fig. 2.5) and is used for correlation between the sections of La Roma, Masía de la Roma and Peralejos (fig. 2.4). Carbonate channel fills are predominant in the lower part and palustrine carbonates and paleosols in the upper part. The carbonate beds alternate with organic-rich marls which contain mammal remains and abundant gastropod remains. A maximum thickness of almost 50 m is observed in the Masía de la Roma section.

Facies unit M_{4m} is well exposed in the area close to Teruel, where it typically forms the top of escarpments (e.g. fig. 2.6) and *cuestas*. The characteristic thick tabular and indurated capping limestone beds (type 6) have been used for correlation purposes, as for instance shown in figure 2.3 between the middle part of the Masía del Barbo section and the upper part of the Puente Minero section, and between the La Gloria and El Bunker sections. (Note that the uppermost carbonate unit in the latter two sections is included in M_{4m} .) The carbonates may alternate with greyish marls and clays or black lignites, all of which may contain mammal remains. The unit reaches maximum thickness of more than 60 m.

The (reddish) claystone-dominated intervals in the studied sections belong to facies unit M_2-Pl_2 of Hernandez et al. (1983). This unit contains the major part of the Miocene and Pliocene clastic sediments (claystones, sandstones, conglomerates) of the basin and is mainly developed along the basin margin. It is more or less equivalent to the Peral Formation of van de Weerd (1976) and may locally reach thicknesses of 200 m.

Both the carbonate and claystone facies may laterally grade into evaporites, e.g. in Los Mansuetos (LM) (figure 2.3) and at Los Aljezares (ALJ, see figure 2.2). More to the north-west, this evaporitic facies reaches thicknesses of 60 m (Tortajada and Concu sections, TO and CC, figure 2.4). A maximum thickness of about 150 m is estimated close to the village of Tortajada (Hernandez et al., 1983). These latter, more northern gypsum exposures constitute van de Weerd's (1976) Tortajada Formation. This formation comprises massive, meter-thick gypsum beds with a fabric consisting of strongly



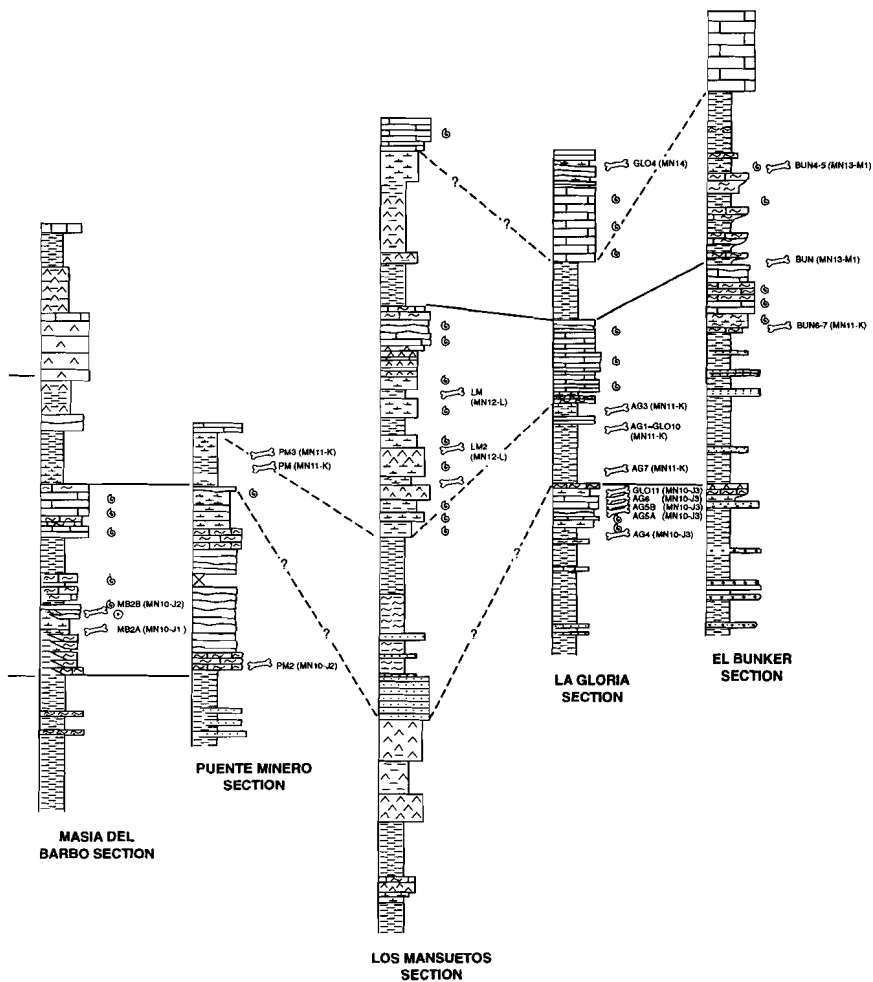


Figure 2.3. Stratigraphic columns for the southern part of the Teruel-Alfambra region. MN 10-14 and J1-M1 refer to biostratigraphic assignments of mammal localities (section 2.4).

bioturbated (chironomids) lenticular gypsum, which accumulated extensively in moderately saline lake waters (Rodríguez-Aranda and Calvo, 1997).

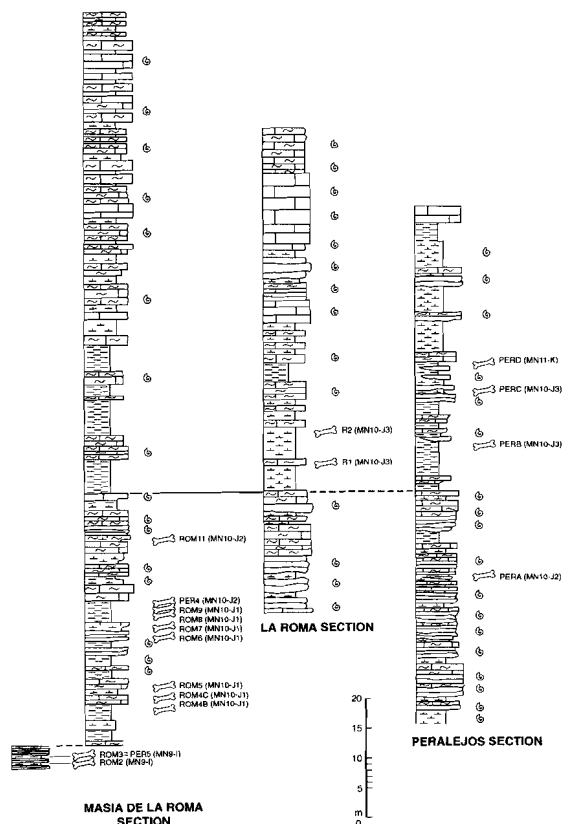


Figure 2.4. Stratigraphic columns for the northern part of the Teruel-Alfambra region (the Peralejos area). MN 9-I 1 and I-K refer to biostratigraphic assignments of mammal localities (section 2.4).

2.3. The sequence of mammal localities

The composite Vallesian-Turolian mammal succession of the area (tables 2.1-2.2) consists of 90 assemblages. All except one contain micromammals and 27 contain both micro- and macromammals. The stratigraphic order of the localities is based on the interpretation of litho-, bio- and magnetostratigraphic data. The position of isolated, poorly documented assemblages in the sequence of localities is only approximate, which

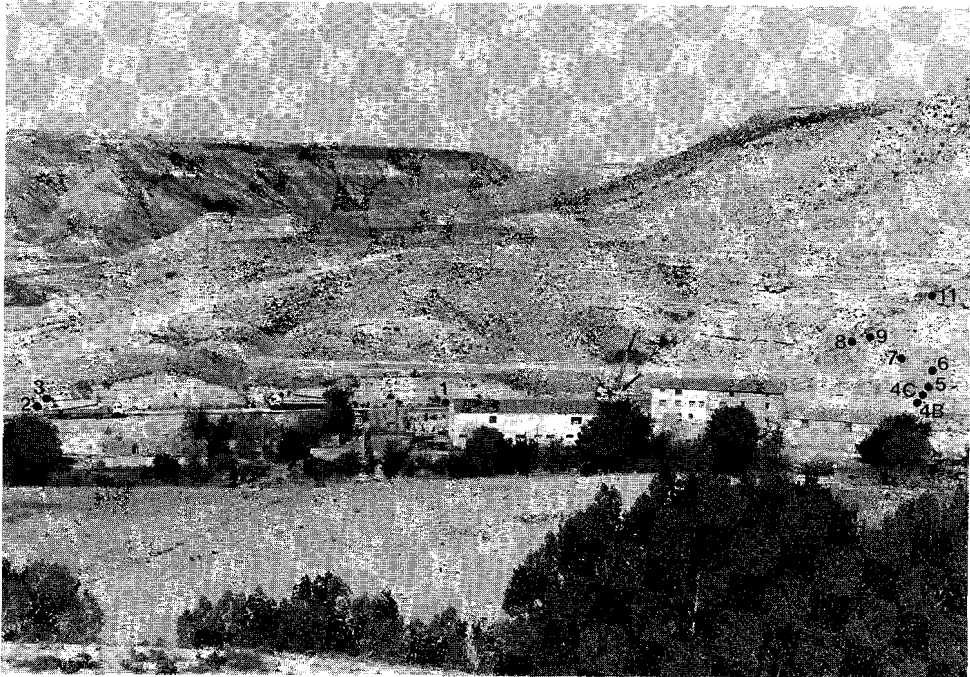


Figure 2.5. The Masía de la Roma (ROM) area. All mammal localities (indicated by numbers) belong to carbonate facies unit M₃ of Hernandez et al. (1983). The local top of this unit can be easily recognized by the extensive white limestone bed, which is situated about 8 m above locality ROM11. The limestones are followed by some 25 m of predominantly reddish mudstones, which, in turn, are succeeded by limestones constituting the top of the cuesta.

implies that the degree of resolution for those assemblages is not better than that of the biozone. Rodent data for MBA-B, PER4, PERA-D, ALF (partly), TOA-C, VIP (a small fraction), MDV2-7, TO, VB, VB2 (a small fraction), CC, CCB, CCL, CC2-3, TO, LM, and VDC3 are from van de Weerd (1976). Species identifications of Desmaninae (Talpidae) are from Rümke (1985). *Desmanella* (Talpidae) from CC3 and LM was described by Rümke (1974). Lagomorphs from MBB, VIP, CC3 and MDV2, 4 and 6 were described by López Martínez (1989). The remaining micromammal data from ALJB and a part of the data from VIP and R2, as well as the micromammal data from SAL, REG2-5, AG, BUN, VDC6, GLO5-6, and AQ1 and 4 are from Adrover (1986), Adrover and Mein (1996), Adrover et al. (1982a, 1982b, 1984, 1993) and Mein et al. (1990). The data for PM are from Alcalá et al. (1991). All other micromammal data are new. (New localities: PER5; ROM1, 3, 4B, 4C, 5, 6, 7, 8, 9, 11; PM2, 3, 5A, 5B; GLO10, 11, 14A, 14B; CAT2; R1; MRU; AG1, 3, 4, 5A, 5B, 6,7; BUN4, 5, 6, 7; KS, KS2, KSS; CAP2, 3; MOD. Extended samples: R2, ALF, VIP, VB2/2C). For a review of the upper Vallesian-lower Turolian Muridae is referred to chapter 3. Additional relevant taxonomic remarks are included in appendix A. The insectivores and lagomorphs from the new localities were identified at the genus level. New bats were identified at the family level.

Macromammals were identified for 19 localities. Identifications for CAT are from Alcalá et al. (1986), for PM from Alcalá et al. (1991), for VDC5 from Adrover et al. (1986), for BUN and VDC3 from Alberdi et Alcalá (1990). The data for AF are compiled by Alcalá and Montoya (1990), and those from ALJB by Alcalá (1987). The rest of the macromammal associations (ROM1, MBB, R2, VIP, MDV2, LP, CCL, LM, CC, KS, ML and AQ1) are described by Alcalá (1994). Besides new data, this work includes the updating and completion of faunal lists from Alcalá et al. (1994), Alcalá and Morales (1997), Azanza et al. (1997), Fraille et al. (1997) and van der Made et al. (1997).



Figure 2.6. The La Gloria-Los Aguanaces area. Numbers refer to mammal localities. Mammal localities are indicated by dots. AG1 and 3, of which the stratigraphic positions are indicated by arrows, are situated 400 m south-west of the other AG localities. Three main carbonate units can be seen: the lower one contains AG4-7, the middle one AG1 and 3 and the upper one the Ruscinian locality GLO4 (not included in this study). The carbonate units alternate with detrital sediments units which mainly consist of reddish mudstones.

2.4. Biozones

The biozonation used here is a modification of the Vallesian-Turolian part of the zonation of van de Weerd (1976), who defined range zones for the area on the basis of Muridae (Rodentia). A first refinement of van de Weerd's scheme was published by Mein et al. (1990) who proposed a tripartition of the upper Turolian *Stephanomys ramblensis* Zone.

Table 2.1. The sequence of Vallesian and Turolian localities of the Teruel-Alfambra region: micromammals. See appendix B for locality age estimates.

LOCAL ZONE	CODE	RODENTIA																
		CRICETIDAE				GLIRIDAE				SCIURIDAE			EO-MY- ID.	ZA- POL- DID	CAS- TOM- DAE	HYS- TRIX- CHD.		
		<i>Dipreictodon sulcatus</i> / <i>Hispanomys aff. peralensis</i> <i>Hispanomys peralensis</i> <i>H. proteusaff. peral.</i> / <i>H. proteus</i> <i>Megascricetodon dobrajini</i> <i>Cricetodon karrenber- geri</i> <i>Eumyarion</i> sp. <i>Hispanomys</i> sp. A <i>Hispanomys freudenthali</i> <i>Hispanomys</i> sp. B <i>Kovalevia occidentalis</i> <i>Ruscinomys schencki</i> / <i>Cricodonomys</i> indet. <i>Cricetinae</i> indet. <i>Ruscinomys branovi</i> <i>Cricetus kormosi</i> <i>Blancomys sanzii</i> <i>Myomimus delahmi</i>	<i>Tempestia karrenbergeri</i> <i>Muscardinus hispanicus</i> <i>Eliomys tracti</i> <i>Myomimus</i> sp. A <i>Eliomys</i> sp. A <i>Muscardinus aff. hispanicus</i> <i>Muscardinus pilocentus</i> <i>Heteroxerus grivensis</i> <i>Atlantoxerus adoveri</i> <i>Spermophilus breda- turollensis</i> <i>Spermophilus turollensis</i> <i>Heteroxerus</i> sp. <i>Atlantoxerus</i> sp. <i>Heteroxerus maria-</i> <i>herensis</i> <i>Myomimus canabonatus</i> <i>Eoziphus intermixtus</i> <i>Crataomys saegeri</i> <i>Dipodops problematicus</i> <i>Hystrix primgenia</i>															
M3	AQ4	■ identified species	■	■	■	■	■	■	■	■	■	■	■	■	■	■	■	
M2	AQ1	□ sp. A	□	□	□	□	□	□	□	□	□	□	□	□	□	□	□	
	GLO5	○ cf. species	○	○	○	○	○	○	○	○	○	○	○	○	○	○	○	
M1/2/3	ML	● identified genus (sp.)	●	●	●	●	●	●	●	●	●	●	●	●	●	●	●	
	KSS	○ cf. genus (sp.)	○	○	○	○	○	○	○	○	○	○	○	○	○	○	○	
M1	KS	◇ cf. genus-species	◇	◇	◇	◇	◇	◇	◇	◇	◇	◇	◇	◇	◇	◇	◇	
	VB1	◇ genus et sp. indet.	◇	◇	◇	◇	◇	◇	◇	◇	◇	◇	◇	◇	◇	◇	◇	
L	MOD																	
	CAP3																	
	CAP2																	
	REG5																	
	BUN4/5																	
	VDC6																	
	VDC3																	
	MDV7																	
	BUN																	
	GLO6																	
	GLO1																	
	MDV6																	
	VDC5																	
	K	CC																
		CC3																
LM																		
ALJB																		
CCL																		
CC2																		
TO																		
VB2/2C																		
REG4																		
REG3																		
MDV5																		
MDV4																		
TOD																		
TOC																		
KS2																		
MDV3																		
J3	CB																	
	MDV2																	
	LM2																	
	TOB																	
	BUN6/7																	
	VIP																	
	TOA																	
J2	AG3																	
	AG																	
	REG2																	
	ALF																	
	PM3																	
	GLO10																	
	AG1																	
J1	PMSA/B																	
	PM																	
	AG7																	
	PERD																	
	GLO11																	
	CAT																	
	AG6																	
I	MRU																	
	AG5A																	
	PERC																	
	AG4																	
	R2																	
	PERB																	
	R1																	
I	CAT2																	
	GL14A/B																	
	PM2																	
	ROM11																	
	MBB																	
	PERA																	
	SAL																	
I	ROM1																	
	PER4																	
	ROM9																	
	ROM8																	
	MBA																	
	ROM7																	
	ROM6																	
I	ROM5																	
	ROM4C																	
	ROM4B																	
	ROM3																	
I	PER5																	

Table 2.2. The sequence of Vallesian and Turolian localities of the Teruel-Alfambra region: macromammals.

STAGE	VALLESIAN			TUROLIAN																	
	L	UPPER	J3	LOW.	MIDDLE	UPPER															
LOCAL ZONE	I	J2	J3	K	L		M1	M2													
LOCALITY	Masa de la Roma 2 (RON2)	Masa del Barco B (MBB)	La Roma 2 (R2)	La Cañera (CAT)	Puente Milnero (PM)	Los Agnaces (AG)	Vivero de Pinos (VIP)	Masa del Valle 2 (MDV2)	Concud 2 (CC2)	Concud barranco (CCL)	Aljazar B (ALJB)	Los Mansuecos (LM)	Concud (CC)	Valdecebro 5 (VDC5)	Bunker de Valdecebro (BUN)	Valdecebro 3 (VDC3)	Las Casinas (KS)	Milagros (ML)	El Aquillo 1 (AQ1)		
CARNIVORA	CANIDAE	<i>Canis cipio</i>																			
	URSIDAE	<i>Indarctos atticus</i> <i>Agriotherium robesli</i>																			
	MUSTELIDAE	<ul style="list-style-type: none"> ■ identified species □ cf. species ● identified genus ○ cf. genus ◆ suprageneric taxa 																			
		<i>Simocyon primigenius</i>																			
		<i>Plesiogulo</i> sp.																			
		<i>Plesiogulo monspessulanus</i>																			
		<i>Mustela</i> sp.																			
		<i>Sabadellictus</i> sp.																			
	HYAENIDAE	<i>Baranogale adroveri</i>																			
		<i>Martes</i> cf. <i>paleosinensis</i>																			
		<i>Martes basilii</i>																			
		<i>Sivaonyx lluecai</i>																			
		Mustelidae indet.																			
		Hyaenidae indet.																			
	FELIDAE	<i>Plioiviverrops guerini</i>																			
Ictitheriinae indet.																					
<i>Ictitherium</i> aff. <i>pannonicum</i>																					
<i>Thalassictis hipparionum</i>																					
<i>Thalassictis</i> sp.																					
<i>Lycyaena chaeretic</i>																					
ARTIO-DACTYLA	SUIDAE	<i>Felis attica</i> /Felis sp.																			
		<i>Metailurus major</i>																			
		<i>Metailurus parvulus</i>																			
	HIPPOPOTAMIDAE	<i>Paramachairodus orientalis</i>																			
		<i>Machairodus</i> sp.																			
		<i>Amphimachairodus giganteus</i>																			
	TRAGULIDAE	Felidae indet.																			
		<i>Microstonyx erymanthius</i>																			
		<i>Microstonyx major</i>																			
	GIRAFFIDAE	<i>Propotamochoerus provincialis</i>																			
		<i>Suidae</i> indet.																			
		<i>Hexaprotodon crusafonji</i>																			
	BOVIDAE	<i>Dorcatherium nani</i>																			
		<i>Decennatherium pacheoi</i>																			
		<i>Birgerbohlinia schaubi</i>																			
<i>Tragoportyx gaudryi</i>																					
<i>Tragoportyx</i> sp.																					
<i>Boselaphini</i> indet. 1																					
<i>Boselaphini</i> indet. 2																					
<i>Palaoryx pallasi</i>																					
<i>Protoryx carolinae</i>																					
<i>Gazella deperdita</i>																					
CERVIDAE	<i>Hispanodorcas torrubiæ/H.</i> sp.																				
	<i>Aragoral mudejar</i>																				
	Bovidae indet.																				
EQUIDAE	<i>Micromeryx flourensianus/M.</i> sp.																				
	<i>Lucentia</i> aff. <i>piensis</i>																				
	<i>Turiacemus concudensis</i>																				
RHINOCEROTIDAE	<i>Pliocervus</i> aff. <i>matheroni</i>																				
	<i>Pliocervus turolensis</i>																				
	Cervidae indet.																				
PERISSO-DACTYLA	<i>Hipparion primigenium</i>																				
	<i>Hipparion concudense</i>																				
	<i>Hipparion gromovae</i>																				
HYRACOIDEA	<i>Hipparion periafricanum</i>																				
	<i>Alicornops alfumbrense</i>																				
	<i>Aceratherium incisivum</i>																				
PRO-BOSCIDEA	<i>Lartetotherium</i>																				
	<i>Pliohyrax</i> cf. <i>gracius</i>																				
	<i>Deinotherium giganteum</i>																				
MASTODONTIDAE	<i>Tetralophodon longirostris</i>																				
	cf. <i>Anancus avernensis</i>																				
PROBOSCIDEA	<i>Zugolophodon turicensis</i>																				
	Proboscidea indet.																				

Here we propose also a tripartition for the upper Vallesian *Progonomys hispanicus* Zone. For the sake of convenience, we adopt and extend the letter system (A, B up to I) introduced by Daams and Freudenthal (1981) for the Aragonian and Vallesian sediments of the neighbouring Calatayud-Daroca Basin. We use this system next to the zone names of van de Weerd, which are retained. We introduce zones J to M, with J (*Progonomys hispanicus* Zone) and M (*Stephanomys ramblensis* Zone) subdivided into subzones J1-3 and M1-3, respectively. The zones are described below.

Zone I (upper part of lower Vallesian, corresponding to a late MN9 age); Daams and Freudenthal (1981).

Diagnosis: The lower boundary is defined by the entry of the cricetid *Cricetulodon* and the glirid *Ramys multicrestatus*. The base of the next-higher zone is not defined by the authors, but is taken here at the first regular occurrence of *Progonomys hispanicus*.

Additional micromammal data: *Cricetulodon* and *Hispanomys* are important. *Megacricetodon debruijni* is present, *M. ibericus* is absent. Among the Gliridae *Myomimus dehmi*, *Tempestia hartenbergeri*, *Muscardinus hispanicus* and *Ramys multicrestatus* are common. Some rare eomyids (*Leptodontomys catalaunicus*) and murids (*Progonomys* cf. *hispanicus*) occur in this zone. *Miosorex* is a common soricid, together with an as yet unnamed genus (gen. et sp. 1).

Characteristic macromammals have not been found in the Teruel-Alfambra region.

Zone J (upper Vallesian, corresponding to an MN10 age); *Progonomys hispanicus* Zone of van de Weerd (1976).

Diagnosis: *Progonomys hispanicus*-*Parapodemus lugdunensis* interval zone, from the first regular occurrence of *P. hispanicus* to the entry of *Parapodemus lugdunensis*.

Additional micromammal data: The murid *Progonomys hispanicus* is the dominant rodent; the range of this species, however, is not confined exactly to the nominate zone. The cricetid *Hispanomys peralensis* is mainly restricted to this zone. Sciurids (*Heteroxerus*) are rare. Many species have their last occurrences: the cricetids *Cricetulodon* and *Democricetodon*, the glirids *Tempestia*, *Muscardinus hartenbergeri*, and *Myomimus dehmi*, and the soricids *Miosorex*, *Crusafontina* and genus and species 1. *Crusafontina* shows an acme. Another soricid, *Paenelimnoecus* has its first occurrence.

Additional macromammal data: Macromammals are scarce and poorly studied. The presence of the robust equid *Hipparion primigenium* and rhinocerotids is characteristic. The latter family is represented by three genera, of which *Alicornops alfambrense* is restricted to this zone until now. The girafid *Decennatherium pachecoi* and the suid *Microstonyx* are common. Bovids are represented by *Tragoportax gaudryi* (Boselaphini), a species which is also present in the Turolian, and by *Aragoral mudejar*, a form considered to be ancestral to the caprines. No cervids are documented although *Micromeryx* (Moschidae) is common. The carnivore record is poor.

Subzone J1 (lower part of the upper Vallesian, corresponding to an early MN10 age).

Diagnosis: *P. hispanicus*-*P. cathalai* interval zone, from the entry of *P. hispanicus* to the entry of *P. cathalai*. Additional micromammal data: *Progonomys hispanicus* is the

dominant rodent and the only murid present. The cricetid *Megacricetodon* is absent and *Cricetulodon* is rare. Among the glirids, *Muscardinus*, *Tempestia*, and particularly *Myomimus dehmi* are common. The soricid *Miosorex* is a common insectivore. The talpid *Desmanella* is absent.

Subzone J2 (middle part of the upper Vallesian, corresponding to a middle MN10 age):

Diagnosis: *Progonomys cathalai* range zone, characterized by the total range zone of *Progonomys cathalai*.

Additional micromammal data: *Progonomys cathalai* and *P. hispanicus* are the only murids. *Cricetulodon* and glirids are rare. *Crusafontina* is a common insectivore. *Desmanella* is rare.

Subzone J3 (upper part of the upper Vallesian, corresponding to a late MN10 age):

Diagnosis: *Huerzelerimys minor-Parapodemus lugdunensis* interval zone, from the entry of *Huerzelerimys minor* to the entry of *Parapodemus lugdunensis*.

Additional micromammal data: *Huerzelerimys minor* and *Progonomys hispanicus* are the only murids present. *Myomimus* sp. is restricted to this subzone. *Myomimus dehmi*, *Tempestia* and *Muscardinus* are absent. Among the insectivores, *Desmanella* is common.

Zone K (lower Turolian, corresponding to MN11); *Parapodemus lugdunensis* Zone of van de Weerd (1976).

Diagnosis: Range zone, characterized by the total range of *Parapodemus lugdunensis*.

Additional micromammal data: The complete range of *Parapodemus lugdunensis* is included in this zone. This range corresponds also more or less to the ranges of the murids *Occitanomys sondaari* and *Huerzelerimys vireti*. *Parapodemus gaudryi* and the cricetids *Hispanomys freudenthali* and *Kowalskia occidentalis* start their range at about the base of the zone. The range of the zapodid *Eozapus intermedius* is restricted to this zone. Sciurids (*Heteroxerus*) are very rare. Although still very rare, the castorid *Dipoides*, the soricid *Blarinella* and the talpids *Archaeodesmana* and *Talpa* start their ranges within this zone. Generally, the diversity of insectivores is low, and only three species belonging to *Galerix*, *Desmanella* and *Paenelimnoecus* are common. The only Rhinolophidae (Chiroptera) known from the studied interval occur in this zone.

Additional macromammal data: *Plioviverrops guerini* occurs for the first time, and it coexists with *Indarctos atticus*, *Adcrocuta exima* and *Paramachairodus orientalis*. The giraffid *Decennatherium* is replaced by *Birgerbohlinia schaubi*. *Dorcatherium* and *Micromeryx* have their last occurrence. Typical for the zone is the cervid *Lucentia*. Among the rest of the artiodactyls, *Microstonyx* and *Tragoportax* continue their presence. In PM, *Hipparion primigenia* is associated with *H. gromovae*, a small species otherwise known from the upper Turolian. This diversification of *Hipparion* contrasts with a decline in rhinocerotid diversity.

Zone L (middle Turolian, corresponding to MN12); *Parapodemus barbarae* Zone of van de Weerd (1976).

Diagnosis: *Parapodemus barbarae*-*Stephanomys ramblensis* interval zone, from the entry of *Parapodemus barbarae* to the entry of *Stephanomys ramblensis*.

Additional micromammal data: The range of *Parapodemus barbarae* is not confined exactly to the nominate zone. The zone comprises the total ranges of *Occitanomys adroveri* and *Huerzelerimys turoliensis*. It includes the last occurrence of *P. gaudryi*. *Ruscinomys* starts its range in this zone. *Eliomys truci* and the sciurids *Spermophilinus turoliensis* and *Atlantoxerus adroveri* are common. The latter is entirely restricted to this zone. Insectivore diversity is much higher than in zone K. *Archaeodesmana turolese* is common.

Additional macromammal data: very characteristic for this zone is the first known occurrence of canines (*Canis cipio*). Carnivora are very diverse, especially hyaenids and felids. Zone L is the last zone with *Microstonyx*. The girafid *Birgerbohlinia* continues to be present. This zone is characterized by a marked proliferation of bovids, who are, apart from Boselaphini, represented by hippotragines (*Palaeoryx pallasii* and *Protoryx carolinae*) and antilopines (*Gazella deperdita* and *Hispanodorcas torrubiae*). Cervids start their range with two species, including *Turiacemas concudensis*. *Hipparion concudense* is the common equid in this zone. Zone L is the only zone with more than one proboscidean genus.

Zone M (upper Turolian, corresponding to MN13); *Stephanomys ramblensis* Zone of van de Weerd (1976).

Diagnosis (based on Mein et al. 1990): *Stephanomys ramblensis*-*Celadensia* interval zone, from the entry of *Stephanomys ramblensis* to the entry of the cricetid *Celadensia*.

Additional micromammal data: The zone roughly corresponds to the range zone of *Apodemus gudrunae* and the cricetids *Blancomys sanzi* and *Cricetus* cf. *kormosi*. *Occitanomys alcalai* and *Castromys inflatus* enter the area at the base of this zone. *Castromys inflatus* is present only in the lower part of the zone and *Paraethomys miocaenicus* in the uppermost part. Sciurids are very rare. The insectivore association resembles that of zone L, except that *Crusafontina* is replaced by *Amblycoptus*, and *Archaeodesmana turolese* and *A. adroveri* by *A. luteyni* and *A. major*. Among the lagomorphs, *Prolagus crusafonti* is replaced by *P. michauxi*.

Additional macromammal data: The medium-sized hyaenid *Thalassictis hipparionum* and large-sized sabertooth tigre *Amphimachairodus giganteus* are abundant. Among the mustelids a large-sized form (*Plesiogulo monspessulanus*) is present. Within the group of ursids, *Indarctos* is replaced by *Agriotherium*. The most characteristic artiodactyls are *Hexaprotodon crusafonti* (the oldest hippopotamid known from Eurasia) and two species of the cervid *Pliocervus*, known from this zone only. *Tragoptax* and antilopines continue to be present, and the medium-sized suid *Propotamochoerus* appears for the first time. Various species of *Hipparion* co-occur, among which is *Hipparion periafricanum*, the smallest *Hipparion* known. Rhinocerotids are reduced to one species, the large-sized *Lartetotherium schleiermacheri*.

Zone M1 (lower part of the upper Turolian):

Diagnosis: Range zone, characterized by the total range of of *Castromys inflatus*.

Zone M2 (middle part of the upper Turolian):

Diagnosis: *Castromys inflatus-Paraethomys miocaenicus* interval zone, from the exit of *Castromys inflatus* to the entry of *Paraethomys miocaenicus*.

Additional micromammal data: this zone includes the first occurrence of *Hystrix*.

Zone M3 (upper part of the upper Turolian):

Diagnosis: *Paraethomys miocaenicus-Celadensia* interval zone, from the entry of *Paraethomys miocaenicus* to the entry of *Celadensia*.

2.5. Numerical ages

The most suitable sections have been subjected to magnetostratigraphic studies in order to provide numerical age constraints for the biorecord. Especially the reddish coloured sediments in the area usually provide reliable paleomagnetic results. The whitish limestones appear to have much lower magnetic intensities, and their demagnetisation diagrams are generally more difficult to interpret. Our preferred correlations of the polarity sequences of the La Gloria, El Bunker de Valdecebro, Masada Rueva, Masada del Valle, and La Roma sections are shown in figure 2.7. They underlie the chronology for the continental record in Spain from the Vallesian to lower Turolian. Ages for most of the localities (table 2.1) were estimated by linear interpolation of sediment thicknesses within polarity zones and sections, lithostratigraphic correlations between sections, and linear interpolation of quantified evolutionary stages of *Progonomys* and *Occitanomys* (Muridae, Rodentia). For paleomagnetic details is referred to Krijgsman (1996), Krijgsman et al. (1996), and Garcés et al. (submitted). For detailed information on the estimation of the ages of individual localities and zone boundaries is referred to appendix B.

The magnetobiostratigraphic data of the lower part of the Masía de la Roma section are consistent with the age of 9.7 Ma for the lower-upper Vallesian (MN9-10) boundary in the Vallès-Penedès basin as determined by Garcés et al. (1996). The J1-J2 local biozone boundary is positioned between ROM9 and PER4 in the Masía de la Roma section, and between MBA and MBB in the Masía del Barbo-Masada Rueva sections, and can be estimated at 9.3 Ma. The J2-J3 boundary can be estimated at 9.0 Ma on the base of estimated ages for ROM11, R2 and PM2. The magnetic polarity patterns of the La Gloria section and the lower part of the overlapping El Bunker section have been correlated to interval C5n.2n-C4n.2n (figure 2.7). This correlation allows the estimation of the Vallesian-Turolian (MN10-11) boundary at 8.7 Ma between the localities AG5B and AG7 (Krijgsman et al., 1996). Biostratigraphic details are given in appendix B.

Magnetostratigraphic control for the middle and upper Turolian (MN12 and 13) in the Teruel-Alfambra region is poor. For the age of the MN11-12 boundary we use 7.5 Ma on the basis of a reinterpretation by Krijgsman et al. (1996) of Opdyke et al. 's (1990) results for the Cabriel Basin (eastern Spain). This implies that a gap corresponding to the upper

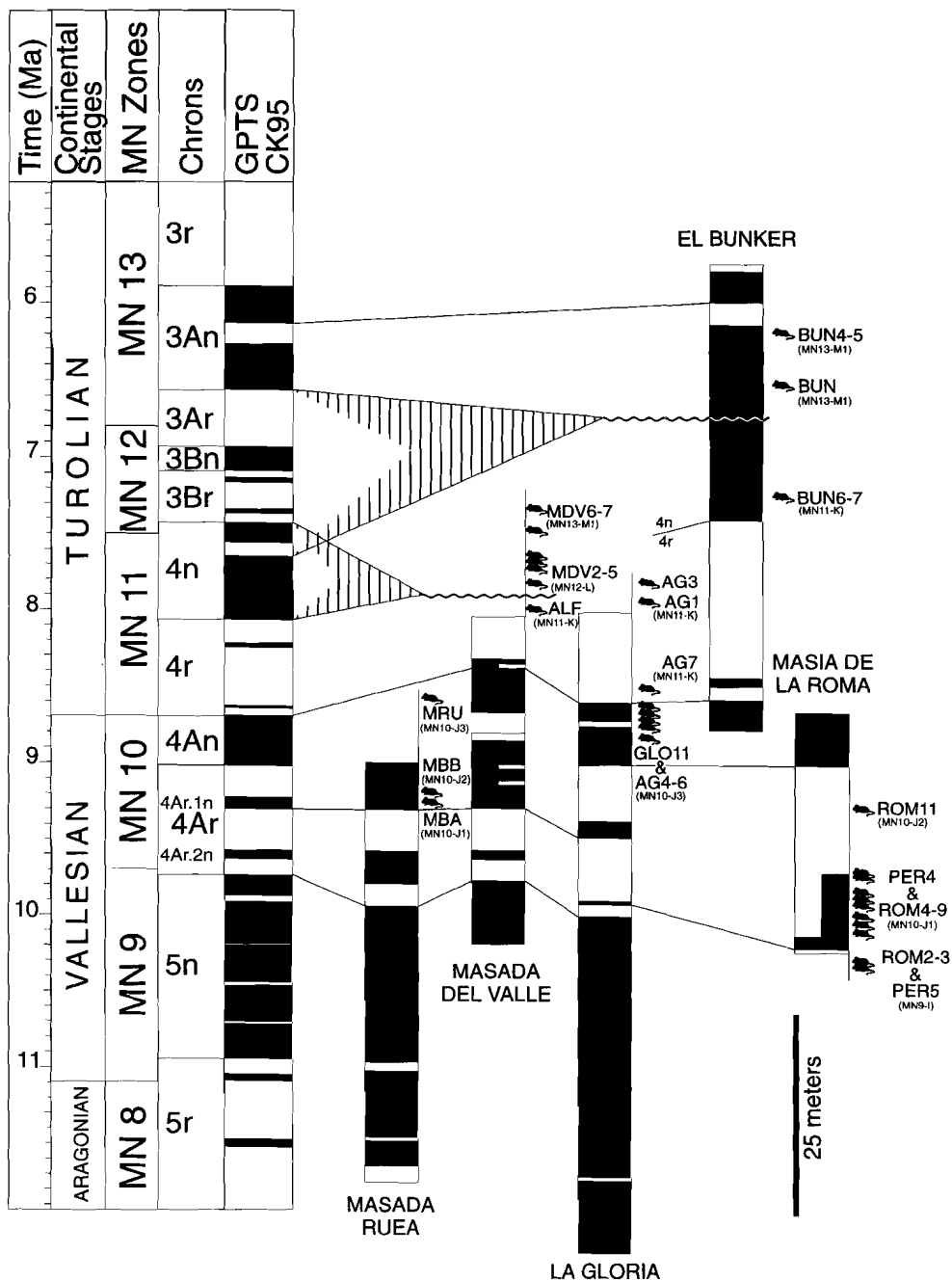


Figure 2.7. Correlation of key sections to the Geomagnetic Polarity Time Scale of Cande and Kent (1995). Fossil localities are indicated, along with their zonal assignments. Modified after Krijgsman (1996), Krijgsman et al. (1996) and Garcés et al. (in press).

part of the lower Turolian and chron C4n is present in the Masada del Valle and Alfambra parallel sections (figure 2.7). An another major gap, which probably includes the entire middle Turolian, is present in the El Bunker section (fig. 2.7). A tentative age of 6.8 Ma is assigned to the MN12-13 boundary on the basis of a) the polarity pattern and the presence of lower upper Turolian (zone M1) micromammals in the upper part of the El Bunker section (table 2.1), and b) a constraint for a minimum age of about 6 Ma (5.9 or 6.3 Ma according to two different recalibrated interpretations of Opdyke et al., 1990) for the locality Venta del Moro in the Cabriel basin, which can be correlated to our zone M3. For further details is referred to appendix B. An age of 6.8 Ma for the MN12/13 boundary is consistent with the post-Tortonian age (i.e. younger than 7.12 Ma according to Krijgsman et al. 1994a) for the mammal locality Casa del Acero in the Fortuna basin (Murcia, Spain) (Agustí et al., 1985).

Aristotle maintained that women have fewer teeth than men; although he was twice married, it never occurred to him to verify this statement by examining his wives' mouths.

[Lord] Bertrand Russell
(The impact of Science on Society, 1952)

Chapter 3

The Murinae from the upper Vallesian and lower Turolian of the Teruel-Alfambra region (NE Spain)

Abstract

The murine succession of 42 localities from the upper Vallesian and lower Turolian sediments of the Teruel-Alfambra region (NE Spain) is reviewed in the light of new material. The stratigraphic range of *Progonomys hispanicus* described by van de Weerd (1976) is extended further downward, and the morphological change through time within this species is discussed. Evolutionary trends in the *P. hispanicus*-*Occitanomys sondaari* and *P. cathalai*-*Huerzelerimys vireti* lineages are analyzed. The current status and diagnoses of the genera *Progonomys*, *Occitanomys* and *Huerzelerimys* are discussed.

Parapodemus gaudryi, formerly only known from the eastern Mediterranean area, is described from lower Turolian localities of the Teruel-Alfambra region, where it occurs together with *Parapodemus lugdunensis*. *Progonomys cathalai* is the most probable ancestor of *P. gaudryi*, which implies that *Parapodemus* would be polyphyletic. *P. gaudryi* is seen as the direct ancestor of *Apodemus gudrunae*, and *P. lugdunensis* of *P. barbarae*. The phylogenetic relationships between all studied murines are discussed.

3.1. Introduction

The late Miocene sediments from the Teruel-Alfambra region (Calatayud-Daroca and Teruel basins, NE Spain) are well-known for their rich succession of fossil Murinae (van de Weerd, 1976; Adrover, 1986; Mein et al., 1990). Murines probably originated in South Asia (Jacobs, 1978; de Bruijn and Hussain, 1984; de Bruijn et al., 1996) where the first true murine (*Progonomys*) developed out of *Antemus* at about 12 Ma ago (Jacobs and Downs, 1994). Murinae started to migrate to Europe about 1-2 m.y. later, but they remained rare during the early Vallesian. They became much more numerous at the beginning of the late Vallesian, when *Progonomys* replaced low-crowned cricetids. By

Table 3.1. Localities and numbers of cheek teeth studied. For local zones see chapter 2. Numerical ages are calibrated to the time scale of Cande and Kent (1995) and are after after Krijgsman et al. (1996), Garcés et al. (in press), chapter 2 and appendix B. cf. designations are indicated next to the number of teeth and they all relate to complete species names (e.g. cf. *Progonomys hispanicus*).

locality	code	local zone	MN zone	age (Ma)	<i>Progonomys hispanicus</i>	<i>Occitanomys sondaari</i>	<i>Progonomys cathalati</i>	<i>Huerzelerimys minor</i>	<i>Huerzelerimys vireti</i>	<i>Parapodemus gaudryi</i>	<i>Parapodemus lugdunensis</i>	<i>O. sond./P. lugd. M3+m3</i>	total
Bunker de Valdecebro 7	BUN7	K	11	7.9	0	cf 1	0	0	0	0	1	0	2
Bunker de Valdecebro 6	BUN6	K	11	7.9	0	cf 1	0	0	0	0	0	0	1
Vivero de Pinos	VIP	K	11	8.1	0	337	0	0	46	8	1	61	453
Tortajada A	TOA	K	11	8.1	0	201	0	0	29	15	6	28	279
Los Aguanaces 3	AG3	K	11	8.1	0	126	0	0	28	54	26	151	385
Alfambra	ALF	K	11	8.2	0	39	0	0	12	2	2	16	71
Puente Minero 3	PM3	K	11	8.2	0	40	0	0	8	1	0	19	68
La Gloria 10	GLO10	K	11	8.2	0	106	0	0	24	1	1	14	146
Los Aguanaces 1	AG1	K	11	8.3	0	110	0	0	8	0	0	40	158
Puente Minero 5B	PM5B	K	11	8.3	0	4	0	0	0	1	0	1	6
Puente Minero 5A	PM5A	K	11	8.3	0	3	0	0	0	0	0	0	3
Puente Minero	PM	K	11	8.3	0	794	0	0	110	4	0	35	943
Los Aguanaces 7	AG7	K	11	8.6	0	cf 1	0	0	cf 1	0	0	1	3
Peralejos D	PERD	K	11	8.7	116	0	0	3	0	0	1	0	120
La Gloria 11	GLO11	J3	10	8.7	cf 4	0	0	3	0	0	0	0	5
Masada Ruea	MRU	J3	10	8.7	2	0	0	cf 13	0	0	0	0	4
Los Aguanaces 5B	AG5B	J3	10	8.6	9	0	0	0	0	0	0	0	9
Los Aguanaces 5A	AG5A	J3	10	8.6	5	0	0	0	0	0	0	0	5
Peralejos C	PERC	J3	10	8.8	255	0	0	55	0	0	0	0	310
Los Aguanaces 4	AG4	J3	10	8.9	2	0	0	0	0	0	0	0	2
La Roma 2	R2	J3	10	8.9	33	0	0	17	0	0	0	0	50
Peralejos B	PERB	J3	10	9.0	2	0	0	3	0	0	0	0	5
La Roma 1	R1	J3	10	9.0	26	0	0	0	0	0	0	0	26
La Cantera 2	CAT2	J2	10	?	cf 1	0	2	0	0	0	0	0	3
La Gloria 14B	GLO14B	J2	10	?	2	0	5	0	0	0	0	0	7
La Gloria 14A	GLO14A	J2	10	?	3	0	cf 1	0	0	0	0	0	4
Puente Minero 2	PM2	J2	10	9.1	28	0	1	0	0	0	0	0	29
Masía de la Roma 11	ROM11	J2	10	9.2	100	0	54	0	0	0	0	0	154
Masía del Barbo 2B	MBB	J2	10	9.2	241	0	123	0	0	0	0	0	364
Peralejos A	PERA	J2	10	9.3	7	0	14	0	0	0	0	0	21
La Salle	SAL	J2	10	?	6	0	2	0	0	0	0	0	8
Masía de la Roma 1	ROM1	J2	10	9.3	1	0	1	0	0	0	0	0	2
Peralejos 4	PER4	J2	10	9.3	37	0	8	0	0	0	0	0	45
Masía de la Roma 9	ROM9	J1	10	9.4	54	0	0	0	0	0	0	0	54
Masía de la Roma 8	ROM8	J1	10	9.4	19	0	0	0	0	0	0	0	19
Masía del Barbo 2A	MBA	J1	10	9.4	103	0	0	0	0	0	0	0	103
Masía de la Roma 7	ROM7	J1	10	9.4	56	0	0	0	0	0	0	0	56
Masía de la Roma 6	ROM6	J1	10	9.4	4	0	0	0	0	0	0	0	4
Masía de la Roma 5	ROM5	J1	10	9.5	5	0	0	0	0	0	0	0	5
Masía de la Roma 4C	ROM4C	J1	10	9.5	56	0	0	0	0	0	0	0	56
Masía de la Roma 4B	ROM4B	J1	10	9.6	20	0	0	0	0	0	0	0	20
Pedregueras 2C	PED2C	1	9	9.9?	cf 1	0	0	0	0	0	0	0	1

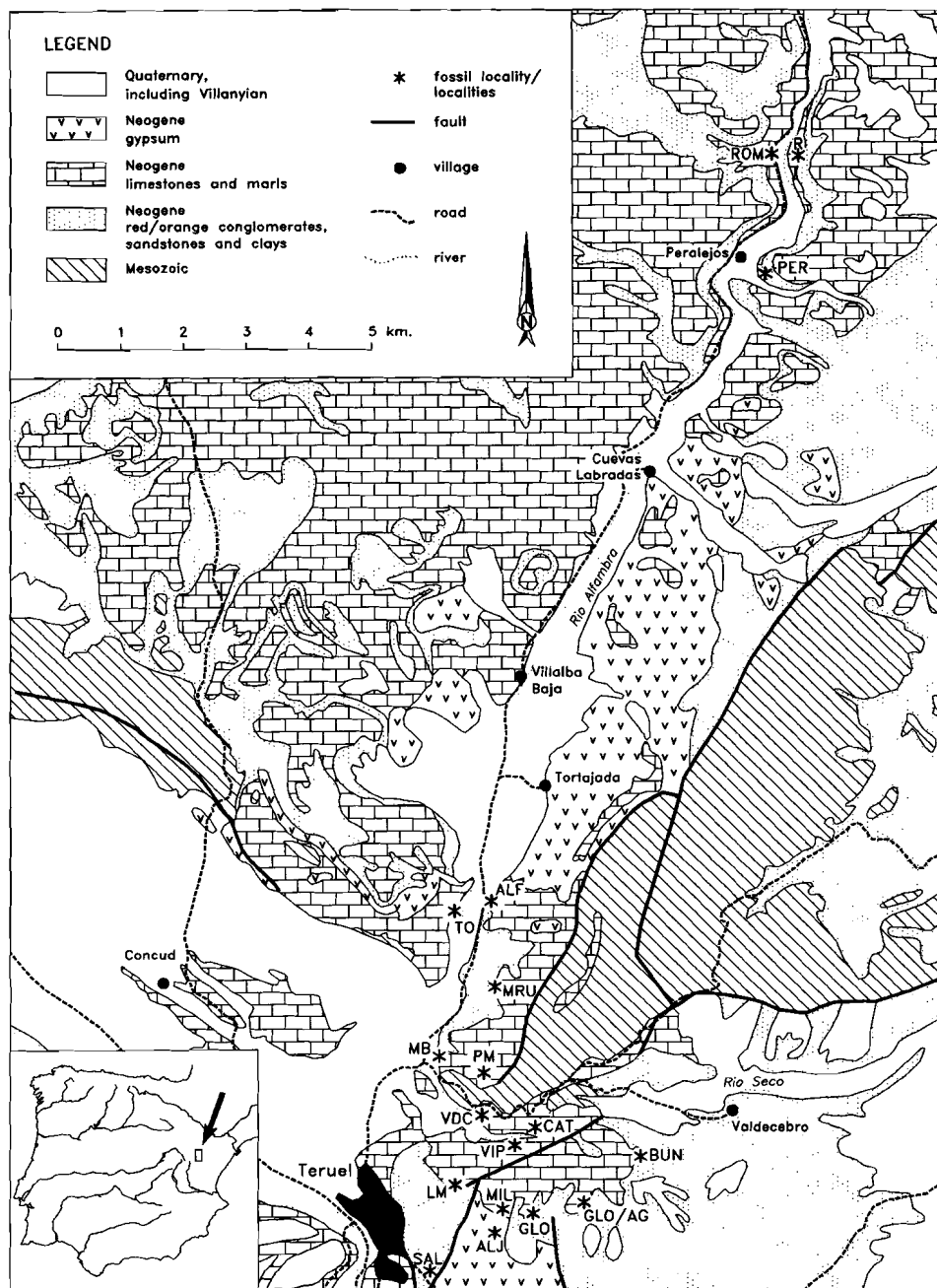


Figure 3.1. Schematic geological map of the Teruel-Alfambra region with positions of fossil localities. Locality codes: see table 3.1. Note that GLO=La Gloria 14A and B, and GLO/AG= other La Gloria and Los Aguanaces localities. ALJ=Aljezar B, LM=Los Mansuetos, VDC=Valdecebro.

the beginning of the Turolian (8.7 Ma), the new genera *Occitanomys*, *Huerzelerimys* and *Parapodemus* were well-established.

Renewed collecting in the Teruel-Alfambra region has allowed further extension and refining of the murine record. This has resulted in new insights into the evolution of Vallesian and early Turolian Murinae, to be presented and discussed below.

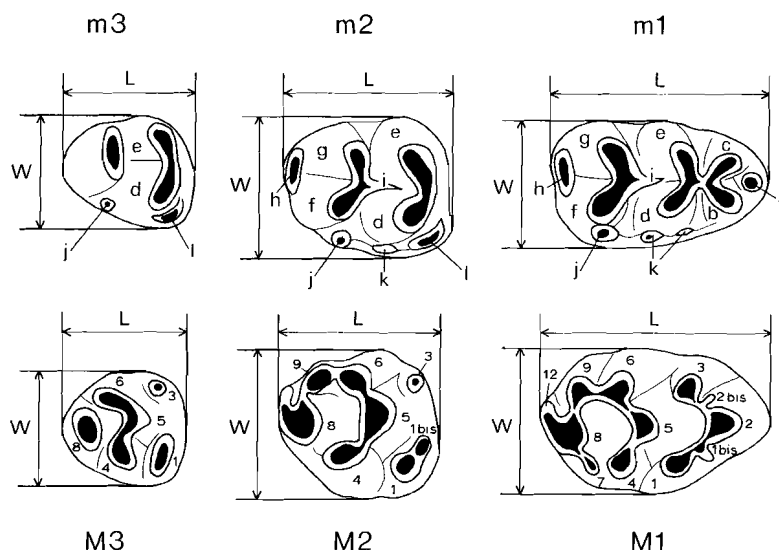


Figure 3.2. Terminology of the dental elements of the Murinae, demonstrated in drawings of the right upper and lower molars: a) antero-central cusp (=tma), b) antero-buccal cusp, c) antero-lingual cusp (in m1), d) protoconid, e) metaconid, f) hypoconid, g) entoconid, h) terminal heel, i) longitudinal spur, j) posterior accessory cusp (=c1), k) accessory cusps on the buccal cingulum, l) antero-labial cusp (in m2 and m3). Length and width are measured as indicated. After van de Weerd (1976).

3.2. Material and methods

Forty-two Vallesian and early Turolian murine associations are studied (table 3.1). The geographical position of the localities in the Teruel-Alfambra region is shown in figure 3.1. 29 localities are new: Peralejos 5, Masía de la Roma 1, 3, 4B, 4C, 5, 6, 7, 8, 9 and 11, Puente Minero 2, 3, 5A and 5B, La Gloria 10, 11, 14A and 14B, La Cantera 2, Los Aguanaces 1, 3, 4, 5A, 5B, 6, and 7, Masada Rueva, and Bunker de Valdecebro 6 and 7. Van de Weerd (1976) described the Murinae from Masía del Barbo 2A and 2B, Peralejos 4, A, B, C and D, 12, Tortajada, Alfambra and Vivero de Pinos (=Rambla de Valdecebro 4). Part of the material from Peralejos C and D was not described by van de Weerd (1976) and is included in this study. Van de Weerd's samples from Alfambra and Vivero de Pinos were small, and additionally sampled material from these localities is also included. The material from La Salle was described by Adrover et al. (1982a). Additional

sampling was done in La Roma 2, from which small mammals were earlier described by Adrover et al. (1982b). The major part of the material from Puente Minero was described by Alcalá et al. (1991). Los Aguanaces 3 was sampled in 1993 and 1995. From the second sample only *Parapodemus* is included in this study. Pedregueras 2C is the only locality which is not situated in the Teruel-Alfambra region. It is located about 100 km north, near the town of Daroca. It is the oldest locality containing Murinae in the basins of Teruel and Calatayud-Daroca.

The relative stratigraphic positions of the localities and their ages (table 3.1) are based on magneto-, litho- and biostratigraphic correlations which are discussed in chapter 2. The terminology of parts of the dentition and the measuring method are after van de Weerd (1976) (see figure 3.2).

3.3. The *Progonomys hispanicus*-*Occitanomys sondaari* lineage (pl. 1)

3.3.1. Introduction

On the basis of his study of the Murinae from the Teruel-Alfambra region, van de Weerd (1976) could demonstrate that early Turolian *Occitanomys sondaari* descended from late Vallesian *Progonomys hispanicus* by anagenetic evolution. The new material confirms this reconstruction. Furthermore, the Masía de la Roma section near Peralejos (ROM in fig. 3.1) allows the downward extension of the record of *Progonomys hispanicus* almost to the boundary with the lower Vallesian (appendix B), which is marked by the major late Miocene expansion of Murinae into the western Mediterranean (van de Weerd and Daams, 1978; Agustí and Moyà-Solà, 1990; de Bruijn et al., 1996).

New material will be described and discussed and evolutionary trends in the *P. hispanicus*-*O. sondaari* lineage will be analyzed. The status of the genera *Progonomys* and *Occitanomys* will be elaborated.

3.3.2. Comparison of *P. hispanicus* from Masía de la Roma 4 with *P. hispanicus* from its type locality (pl. 1: figs. 1-7, 10, 12, 13)

The oldest *P. hispanicus* assemblages in the Teruel-Alfambra region are from Masía de la Roma 4B and 4C (ROM4B and ROM4C) (fig. 3.1). These two levels, which are separated by ~1 meter of sediment from each other, will sometimes be collectively referred to as ROM4 for the sake of convenience. *P. hispanicus* from ROM4 differs from the type material from Masía del Barbo B (MBB) (fig. 3.1) in several aspects (see below and tables 3.2, 3.3, figs. 3.3-3.6).

M1. The M1 from ROM4 show a lower average width-length ratio than the M1 from MBB (figs. 3.5, and 3.6a-b). This lower ratio is mainly due to a reduction of length (figs. 3.3-3.5). *t*-tests show significant differences at the .05 confidence level between the mean for width/length in MBB and both ROM4B and ROM4C ($p=.002$ and $.022$, respectively) and length ($p=.017$; $p=.003$). Differences in mean widths are not significant ($p=.092$; $p=.516$).

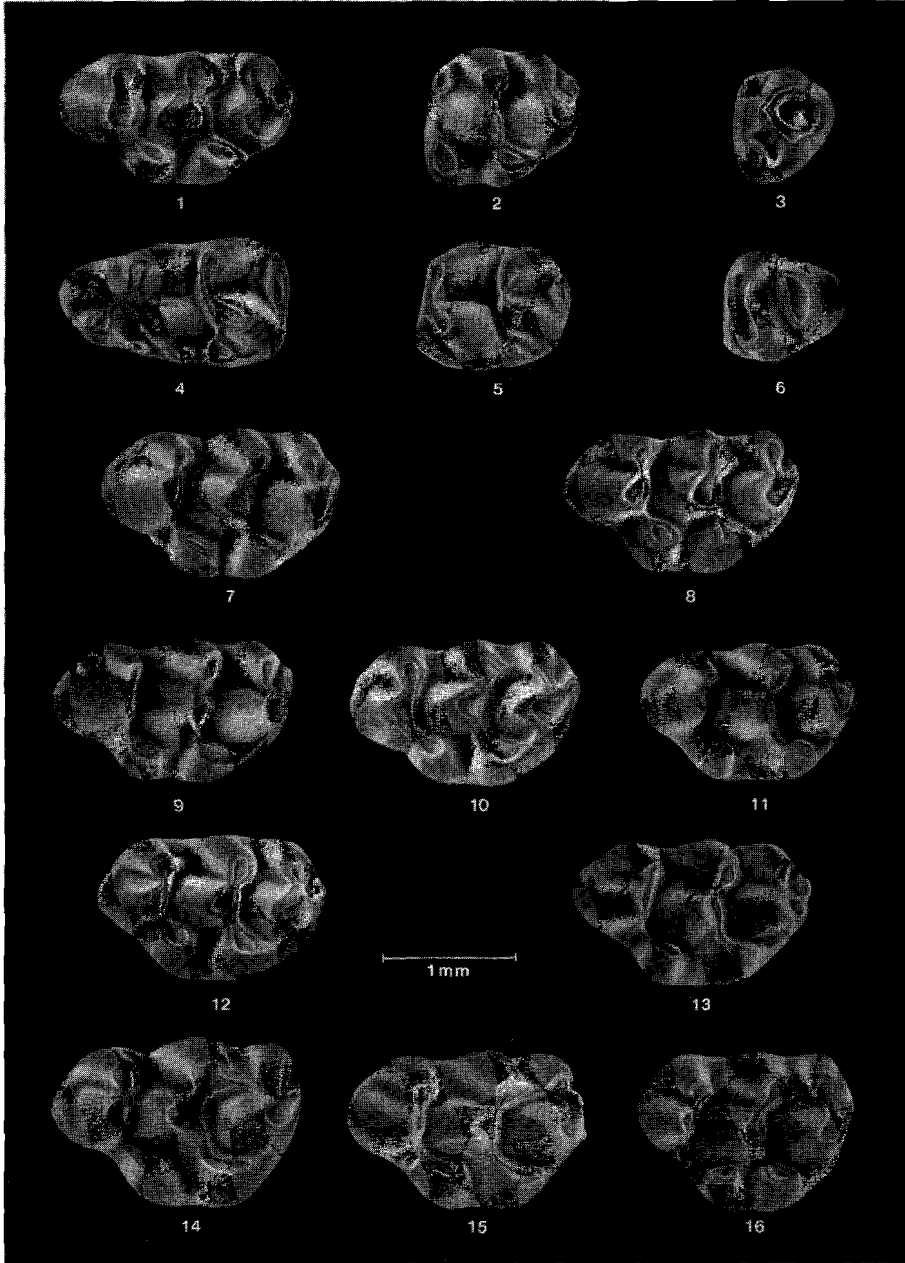


Plate 1. *Progonomys hispanicus*: 1) ROM4B-2: M1 sin. (rev.); 2) ROM4B-14: M2 sin.; 3) ROM4B-20: M3 sin.; 4) ROM4B-21: m1 sin.; 5) ROM4C-65: m2 sin.; 6) ROM4C-86: m3 sin.; 7) ROM4C-12: M1 dex. (rev.); 8) ROM9-9: M1 sin.; 9) BDB-102 from Biodrak: M1 sin.; 10) MBB-1145: M1 dex. (rev.); 11) AG5B-7: M1 dex. (rev.); 12) MBB-696: M1 dex. (rev.); 13) MBB-1161: dex. (rev.); 14) PERD-72: M1 dex. (rev.), *Occitanomys sondaari*: 15) AG3-411: M1 sin.; 16) AG3-412: M1 sin.

Murinae

Table 3.2. Length and width measurements of representatives of the *Progonomys hispanicus*-*Occitanomys sondaari* lineage. The M3 and m3 of *Occitanomys sondaari* and *Parapodemus lugdunensis* are unseparable. The populations of PED2C, GLO11, AG7 and BUN6 have cf. designations.

locality	length (in mm)					width (in mm)				
	n	min	mean	max	sd	n	min	mean	max	sd
<i>M1 Occitanomys sondaari</i>										
VIP	42	1.61	1.81	2.03	0.09	50	1.11	1.23	1.38	0.05
TOA	51	1.59	1.79	2.01	0.10	56	1.15	1.26	1.37	0.06
AG3	15	1.67	1.83	2.05	0.09	22	1.14	1.25	1.35	0.05
ALF	4	1.73	1.77	1.83	0.05	4	1.20	1.23	1.25	0.02
PM3	4	1.74	1.82	1.89	0.07	7	1.22	1.25	1.28	0.02
GLO10	13	1.67	1.81	1.88	0.06	16	1.14	1.26	1.33	0.05
AG1	10	1.70	1.80	1.93	0.07	11	1.20	1.26	1.32	0.04
PM	144	1.58	1.80	2.06	0.10	165	1.11	1.24	1.41	0.06
<i>M1 Progonomys hispanicus</i>										
GLO11	0	-	-	-	-	1	1.15	1.15	1.15	-
PERD	25	1.66	1.80	1.94	0.08	25	1.16	1.22	1.29	0.04
AG5B	3	1.64	1.70	1.80	0.08	3	1.06	1.13	1.17	0.06
AG5A	0	-	-	-	-	1	1.16	1.16	1.16	-
PERC	45	1.53	1.72	1.90	0.08	63	1.01	1.16	1.27	0.05
R2	3	1.69	1.77	1.85	0.08	5	1.05	1.18	1.23	0.07
PERB	1	1.66	1.66	1.66	-	1	1.11	1.11	1.11	-
R1	4	1.62	1.66	1.69	0.03	4	1.09	1.14	1.18	0.04
PM2	1	1.77	1.77	1.77	-	1	1.09	1.09	1.09	-
ROM11	8	1.58	1.71	1.79	0.07	9	1.07	1.11	1.19	0.04
MBB	43	1.64	1.77	1.91	0.06	45	1.00	1.13	1.26	0.05
PERA	1	1.78	1.78	1.78	-	2	1.15	1.15	1.15	0.00
SAL	1	1.65	1.65	1.65	-	1	1.12	1.12	1.12	-
PER4	5	1.70	1.72	1.75	0.02	6	1.01	1.08	1.14	0.05
ROM9	8	1.75	1.80	1.89	0.05	12	1.05	1.14	1.25	0.07
ROM8	2	1.86	1.89	1.91	0.03	4	1.10	1.15	1.17	0.04
MBA	19	1.65	1.78	1.92	0.07	20	1.03	1.12	1.20	0.04
ROM7	8	1.66	1.82	1.92	0.08	13	1.03	1.11	1.21	0.05
ROM5	0	-	-	-	-	1	1.03	1.03	1.03	-
ROM4C	8	1.71	1.85	1.97	0.07	11	1.00	1.12	1.17	0.05
ROM4B	4	1.81	1.87	1.91	0.04	5	1.08	1.09	1.11	0.01
<i>M2 Occitanomys sondaari</i>										
BUN6	1	1.34	1.34	1.34	-	1	1.25	1.25	1.25	-
VIP	41	1.21	1.32	1.44	0.06	41	1.06	1.21	1.33	0.07
TOA	49	1.11	1.26	1.36	0.06	49	1.05	1.23	1.45	0.08
AG3	17	1.22	1.33	1.44	0.06	17	1.11	1.24	1.32	0.05
ALF	7	1.22	1.35	1.52	0.10	9	1.13	1.27	1.38	0.07
PM3	3	1.31	1.37	1.41	0.05	4	1.22	1.24	1.25	0.01
GLO10	10	1.13	1.28	1.36	0.07	10	1.05	1.19	1.28	0.07
AG1	17	1.21	1.34	1.45	0.07	15	1.06	1.22	1.39	0.07
PM5B	1	1.28	1.28	1.28	-	1	1.30	1.30	1.30	-
PM	79	0.95	1.27	1.41	0.07	78	1.01	1.23	1.36	0.06

Table 3.2. (continued)

locality	length (in mm)					width (in mm)				
	n	min	mean	max	sd	n	min	mean	max	sd
<i>M2 Progonomys hispanicus</i>										
PERD	19	1.18	1.27	1.36	0.06	18	1.08	1.20	1.30	0.05
AG5A	1	1.15	1.15	1.15	-	1	0.98	0.98	0.98	-
PERC	40	1.13	1.24	1.36	0.06	38	1.01	1.15	1.26	0.05
R2	2	1.23	1.23	1.24	0.01	3	1.03	1.09	1.14	0.06
R1	4	1.07	1.17	1.30	0.10	4	1.02	1.12	1.17	0.07
PM2	1	1.12	1.12	1.12	-	2	1.01	1.08	1.16	0.11
ROM11	22	1.12	1.22	1.34	0.06	23	1.02	1.10	1.16	0.04
MBB	46	1.04	1.19	1.32	0.07	46	1.00	1.13	1.28	0.06
PERA	1	1.17	1.17	1.17	-	1	1.12	1.12	1.12	-
SAL	1	1.18	1.18	1.18	-	0	-	-	-	-
PER4	6	1.13	1.23	1.33	0.08	7	1.00	1.09	1.18	0.06
ROM9	6	1.16	1.24	1.32	0.06	7	1.03	1.14	1.22	0.06
ROM8	5	1.20	1.23	1.27	0.03	5	1.07	1.12	1.17	0.04
MBA	19	1.08	1.22	1.31	0.06	19	0.96	1.12	1.23	0.05
ROM7	11	1.12	1.24	1.35	0.06	11	1.03	1.11	1.26	0.07
ROM6	1	1.23	1.23	1.23	-	2	1.08	1.11	1.14	0.04
ROM5	2	1.12	1.13	1.14	0.02	2	1.05	1.06	1.07	0.01
ROM4C	11	1.17	1.25	1.33	0.05	10	1.00	1.11	1.19	0.06
ROM4B	6	1.17	1.22	1.30	0.05	7	1.06	1.09	1.12	0.03
<i>M3 Occitanomys sondaari + Parapodemus lugdunensis</i>										
VIP	16	0.79	0.86	0.98	0.05	18	0.81	0.90	1.01	0.04
TOA	10	0.82	0.90	1.00	0.06	10	0.87	0.94	1.05	0.06
AG3	51	0.71	0.86	0.96	0.05	49	0.81	0.91	1.08	0.06
ALF	8	0.77	0.83	0.94	0.05	9	0.76	0.91	1.00	0.07
PM3	9	0.82	0.89	0.94	0.05	9	0.83	0.94	1.01	0.05
GLO10	9	0.75	0.84	0.93	0.06	9	0.85	0.92	0.99	0.05
AG1	12	0.81	0.87	1.00	0.06	14	0.89	0.96	1.06	0.06
PM5A	1	0.93	0.93	0.93	-	1	0.87	0.87	0.87	-
PM	12	0.61	0.84	0.91	0.09	12	0.81	0.90	0.95	0.04
PERD	2	0.72	0.75	0.77	0.04	2	0.87	0.92	0.96	0.06
<i>M3 Progonomys hispanicus</i>										
PERC	2	0.71	0.74	0.77	0.04	2	0.79	0.81	0.84	0.04
R2	5	0.70	0.77	0.89	0.07	5	0.75	0.81	0.90	0.06
R1	2	0.82	0.85	0.88	0.05	2	0.85	0.87	0.89	0.03
PM2	1	0.74	0.74	0.74	-	1	0.75	0.75	0.75	-
ROM11	4	0.77	0.82	0.87	0.04	4	0.80	0.85	0.94	0.06
MBB	12	0.71	0.80	0.91	0.07	13	0.71	0.84	0.99	0.08
SAL	2	0.83	0.84	0.86	0.02	2	0.70	0.75	0.80	0.07
PER4	4	0.80	0.91	0.94	0.07	4	0.87	0.90	0.92	0.02
ROM9	2	0.74	0.78	0.81	0.05	2	0.80	0.83	0.86	0.04
MBA	5	0.75	0.80	0.83	0.03	5	0.75	0.81	0.89	0.06
ROM7	2	0.79	0.82	0.85	0.04	2	0.80	0.83	0.87	0.05
ROM6	1	0.87	0.87	0.87	-	1	0.88	0.88	0.88	-
ROM4C	1	0.80	0.80	0.80	-	1	0.85	0.85	0.85	-
ROM4B	1	0.71	0.71	0.71	-	1	0.79	0.79	0.79	-

Murinae

locality	length (in mm)					width (in mm)				
	n	min	mean	max	sd	n	min	mean	max	sd
<i>m1 Occitanomys sondaari</i>										
AG3	17	1.57	1.71	1.87	0.08	19	0.90	1.05	1.17	0.07
ALF	9	1.55	1.67	1.83	0.09	9	1.00	1.08	1.17	0.05
PM3	5	1.63	1.66	1.71	0.03	8	0.99	1.03	1.09	0.04
GLO10	10	1.57	1.67	1.78	0.06	14	0.95	1.04	1.14	0.05
AG1	10	1.68	1.71	1.74	0.02	11	0.96	1.03	1.09	0.04
PM	171	1.42	1.66	1.91	0.08	172	0.94	1.06	1.21	0.05
<i>m1 Progonomys hispanicus</i>										
GLO11	1	1.76	1.76	1.76	-	1	1.05	1.05	1.05	-
PERD	17	1.50	1.63	1.73	0.05	18	0.93	1.02	1.10	0.04
PERC	42	1.48	1.60	1.78	0.06	49	0.85	0.98	1.07	0.05
R2	4	1.46	1.55	1.64	0.09	2	0.88	0.88	0.88	0.00
R1	1	1.69	1.69	1.69	-	1	1.05	1.05	1.05	-
GL14A	1	1.53	1.53	1.53	-	1	0.94	0.94	0.94	-
PM2	5	1.56	1.61	1.68	0.05	5	0.92	0.99	1.06	0.05
ROM11	4	1.53	1.59	1.67	0.06	6	0.87	0.92	1.00	0.05
MBB	42	1.50	1.61	1.70	0.05	45	0.88	0.97	1.06	0.04
SAL	1	1.66	1.66	1.66	-	1	0.99	0.99	0.99	-
ROM1	0	-	-	-	-	1	0.99	0.99	0.99	-
PER4	6	1.56	1.60	1.62	0.02	6	0.93	0.96	1.00	0.03
ROM9	5	1.56	1.60	1.66	0.04	8	0.91	0.99	1.05	0.06
ROM8	3	1.50	1.56	1.61	0.05	3	0.94	0.97	0.99	0.03
MBA	22	1.49	1.59	1.70	0.05	24	0.88	0.96	1.07	0.04
ROM7	8	1.50	1.60	1.71	0.07	8	0.91	1.00	1.07	0.06
ROM6	0	-	-	-	-	1	0.91	0.91	0.91	-
ROM5	2	1.56	1.58	1.59	0.02	2	0.92	0.93	0.94	0.01
ROM4C	9	1.55	1.61	1.68	0.05	11	0.89	0.96	1.06	0.05
ROM4B	2	1.67	1.68	1.70	0.02	2	0.95	0.97	0.99	0.03
<i>m2 Occitanomys sondaari</i>										
VIP	71	1.11	1.25	1.38	0.05	72	0.93	1.12	1.31	0.07
TOA	47	1.09	1.23	1.39	0.06	47	1.03	1.13	1.35	0.06
AG3	16	1.08	1.24	1.33	0.06	14	1.05	1.15	1.22	0.05
ALF	8	1.15	1.24	1.33	0.07	9	1.08	1.15	1.23	0.05
PM3	6	1.12	1.24	1.32	0.07	7	1.02	1.10	1.15	0.05
GLO10	11	1.16	1.23	1.34	0.05	16	1.02	1.11	1.18	0.04
AG1	13	1.14	1.24	1.39	0.06	13	1.02	1.13	1.23	0.05
PM5A	1	1.29	1.29	1.29	-	1	1.15	1.15	1.15	-
PM	148	1.05	1.24	1.40	0.06	142	0.98	1.13	1.29	0.06
AG7	1	1.25	1.25	1.25	-	1	1.21	1.21	1.21	-
<i>m2 Progonomys hispanicus</i>										
PERD	16	1.17	1.22	1.28	0.03	16	1.03	1.08	1.13	0.03
MRU	1	1.20	1.20	1.20	-	0	-	-	-	-
AG5A	2	1.13	1.16	1.18	0.04	2	0.96	1.02	1.08	0.08
PERC	47	1.05	1.17	1.38	0.06	43	0.97	1.05	1.15	0.05
AG4	0	-	-	-	-	1	1.03	1.03	1.03	-
R2	3	1.16	1.17	1.19	0.02	3	1.02	1.06	1.13	0.06

locality	length (in mm)					width (in mm)				
	n	min	mean	max	sd	n	min	mean	max	sd
<i>m2 Progonomys hispanicus</i> (continued)										
MBB	51	1.05	1.17	1.30	0.06	49	0.95	1.05	1.19	0.05
PERA	1	1.15	1.15	1.15	-	1	0.97	0.97	0.97	-
SAL	1	1.11	1.11	1.11	-	1	0.99	0.99	0.99	-
PER4	4	1.12	1.16	1.19	0.04	5	0.95	1.01	1.05	0.04
ROM9	12	1.11	1.17	1.27	0.05	14	0.95	1.03	1.11	0.04
ROM8	3	1.16	1.21	1.25	0.05	3	1.00	1.08	1.14	0.07
MBA	25	1.09	1.18	1.25	0.04	26	0.94	1.07	1.19	0.05
ROM7	10	1.09	1.18	1.24	0.05	11	0.97	1.06	1.14	0.05
ROM4C	12	1.13	1.20	1.26	0.04	12	0.99	1.04	1.10	0.04
ROM4B	1	1.15	1.15	1.15	-	1	0.98	0.98	0.98	-
<i>m3 Occitanomys sondaari + Parapodemus lugdunensis</i>										
VIP	33	0.85	0.95	1.06	0.05	33	0.77	0.86	0.97	0.05
TOA	18	0.81	0.96	1.10	0.06	18	0.82	0.88	0.96	0.04
AG3	64	0.84	0.97	1.06	0.04	64	0.79	0.88	0.98	0.04
ALF	7	0.95	0.99	1.04	0.03	7	0.83	0.87	0.92	0.04
PM3	7	1.00	1.04	1.06	0.02	7	0.84	0.89	0.92	0.03
GLO10	4	0.88	0.96	1.02	0.06	4	0.82	0.85	0.89	0.03
AG1	11	0.85	0.93	1.06	0.07	11	0.70	0.86	0.96	0.07
PM	20	0.77	0.93	1.04	0.07	18	0.78	0.87	0.99	0.05
AG7	1	1.00	1.00	1.00	-	1	0.89	0.89	0.89	-
<i>m3 Progonomys hispanicus</i>										
PERD	9	0.88	0.97	1.02	0.05	9	0.73	0.85	0.90	0.06
R2	2	0.86	0.87	0.88	0.01	2	0.79	0.79	0.79	0.00
R1	4	0.79	0.83	0.89	0.05	4	0.80	0.82	0.89	0.04
GL14B	1	0.83	0.83	0.83	-	1	0.79	0.79	0.79	-
GL14A	1	0.90	0.90	0.90	-	1	0.75	0.75	0.75	-
PM2	3	0.80	0.93	1.00	0.11	3	0.67	0.78	0.83	0.09
ROM11	4	0.92	0.94	0.98	0.03	3	0.77	0.80	0.82	0.02
MBB	33	0.82	0.92	1.00	0.04	33	0.70	0.82	0.90	0.04
PER4	4	0.92	0.96	0.99	0.03	4	0.78	0.84	0.88	0.05
ROM9	3	0.90	0.92	0.95	0.03	3	0.82	0.85	0.87	0.03
ROM8	2	0.98	0.98	0.98	0.00	2	0.85	0.85	0.85	0.00
MBA	4	0.83	0.96	1.06	0.10	4	0.80	0.86	0.93	0.05
ROM7	4	0.91	0.96	1.01	0.05	4	0.84	0.87	0.89	0.02
ROM4C	6	0.88	0.92	0.96	0.04	6	0.78	0.84	0.89	0.04
ROM4B	3	0.88	0.91	0.95	0.03	2	0.78	0.81	0.85	0.05
PED2C	1	0.84	0.84	0.84	-	1	0.77	0.77	0.77	0.04

Table 3.2. (continued)

The M1 from ROM4 show neither a t6-t9 connection (n=15) nor a t1bis (n=18) (table 3.3). Both features are present in 9% of the M1 from MBB, but sample sizes of the latter locality are larger (n=43 and 46, respectively). t1 is placed slightly more anteriorly in ROM4 than in MBB (compare fig. 3.6a and 3.6b). t12 is larger in the specimens from

ROM4.

The M1 from ROM4 are more homogeneous than those from the type locality. In MBB, the variability of the M1 in general shape, position of the t1, development of the t6-t9 connection, and other features is large (pl. 1: figs. 10, 12, 13). ROM7 is the oldest locality showing heterogeneity (fig. 3.7).

M2. *t*-tests show that the width-length ratio in MBB is significantly higher than in ROM4B and ROM4C ($p=.025$ and $p<.001$) (see also fig. 3.5). Mean length difference between MBB and ROM4 is significant at the .05 level only for ROM4C (MBB-ROM4B: $p=.260$; MBB-ROM4C: $p=.015$). Mean widths cannot be separated statistically at the $p=.05$ level ($p=.086$; $p=.307$). In ROM4, t6 and t9 are connected in one out of 18 M2 (=6%). In MBB the t6-t9 connection occurs more frequently (22%, $n=46$).

M3. The one specimen from ROM4B (pl.3: fig. 3) is very small. Its length is equal to the minimum length recorded for the M3 from MBB ($n=32$) (table 3.3).

m1. The dimensions of the m1 from ROM4 and MBB are about equal. The relative frequencies of the longitudinal spur do not differ significantly. The presence of the antero-central cusp increases from 0% in ROM4 ($n=12$) to 21 % in MBB ($n=42$).

m2. Only one m2 is present in ROM4B. The mean width/length ratios from ROM4C and MBB differ significantly ($n=12$, $p=.016$), although mean length and width do not ($p=.088$ and $.457$ respectively). One specimen from ROM4C shows a longitudinal spur (8%, $n=13$). This percentage is comparable to that for MBB (12%, $n=43$).

m3. The m3 from ROM4 and MBB have similar dimensions and do not differ morphologically.





In summary, *Progonomys hispanicus* from ROM4 is more primitive than that from MBB. The molars from ROM4, notably the M1, M2 and m2, are more slender. The antero-central cusp in the m1 from ROM4 is absent. The M1 from this locality have a slightly more anteriorly positioned t1, and a larger t12. *Occitanomys* morphotypes in the M1 are absent in ROM4, whereas some of these morphotypes occur in MBB. The complete *Progonomys hispanicus*-*Occitanomys sondaari* sequence will be studied in the next section.

3.3.3. Evolutionary trends

Length, width, and relative width (table 3.2, figs. 3.3, 3.4, and 3.5)

Size increase in the M1-2 and m1-2 is concentrated in the middle part of the sequence (zone J3). It starts at the levels of PM2 and R1 and continues until the levels of PERD and PM. Lower in the sequence length and width remain more or less constant, except for the length of M1, which shows a decrease. Higher in the sequence size remains more or less constant. The decrease of length in M1 explains the consistent rise of the width/length ratio of M1 throughout zone J (late Vallesian) (fig. 3.5). The relative width in the M2 and m2 increases less, whereas in m1 it remains more or less constant.

Table 3.3. Relative frequencies of selected molar structures in the *Progonomys hispanicus*-*Occitanomys sondaari* lineage. Percentages based on n<10 are not shown and indicated by *.

locality	t6-t9 connection M1		t1 bis M1		longitudinal spur m1		antero-central cusp m1	
	n	%	n	%	n	%	n	%
								
<i>Occitanomys sondaari</i>								
VIP	55	75	55	67	87	62	41	37
TOA	50	79	53	64	44	59	41	39
AG3	20	75	20	65	36	58	16	37
ALF	*		*		13	46	16	56
PM3	*		*		10	75	*	
GLO10	19	53	14	57	25	60	17	41
AG1	19	58	18	50	24	54	12	25
PM	138	48	142	50	208	56	172	31
<i>Progonomys hispanicus</i>								
PERD	31	32	29	24	20	30	18	23
PERC	68	40	54	24	56	45	43	28
ROM11	11	9	*		11	27	*	
MBB	43	9	46	9	42	21	42	21
ROM9	12	0	12	8	10	0	*	
MBA	19	5	20	0	26	15	23	22
ROM7	10	0	13	0	12	8	10	20
ROM4C	10	0	13	0	12	17	10	0

Other morphological features (tables 3.3 and 3.4, fig. 3.6)

Table 3.3 shows the trends in the relative frequencies of four features: the t6-t9 connection in M1, the t1bis in M1, the longitudinal spur in m1, and the antero-central cusp in m1. The presence of each of these features is generally agreed upon to be apomorph. Just as in the case of size, the J2-J3 boundary (i.e. between ROM11 and PERC in table 3.3) marks an important change: the M1 show an increase of the t6-t9 connection and the presence of the t1bis from about 10% to 25% or more. The J-K (Vallesian-Turolian) transition marks another rise of these percentages and also of that of the longitudinal spur in m1. At this point, all three features occur in about 50% of the specimens. Higher in the sequence (AG3, TOA and VIP) the relative frequency of the t6-

Murinae

t9 connection in M1 reaches values of 70-80%, and the relative frequency of t1bis rises to 60-70%. The relative frequency of m1 having an antero-central cusp gradually increases throughout the sequence, up to the point where it exceeds 50% in ALF. The higher localities VIP and TOA show again somewhat lower percentages. There is no consistent trend in the presence of t4-t8 connection in the M1 in *P. hispanicus* (table 3.4).

Table 3.4. Relative frequency of t4-t8 connection in M1 of *Progonomys hispanicus* (n≥10).

locality	n	%
PERD	29	72
PERC	62	58
ROM11	12	25
MBB	45	36
MBA	19	63
ROM4C	11	45

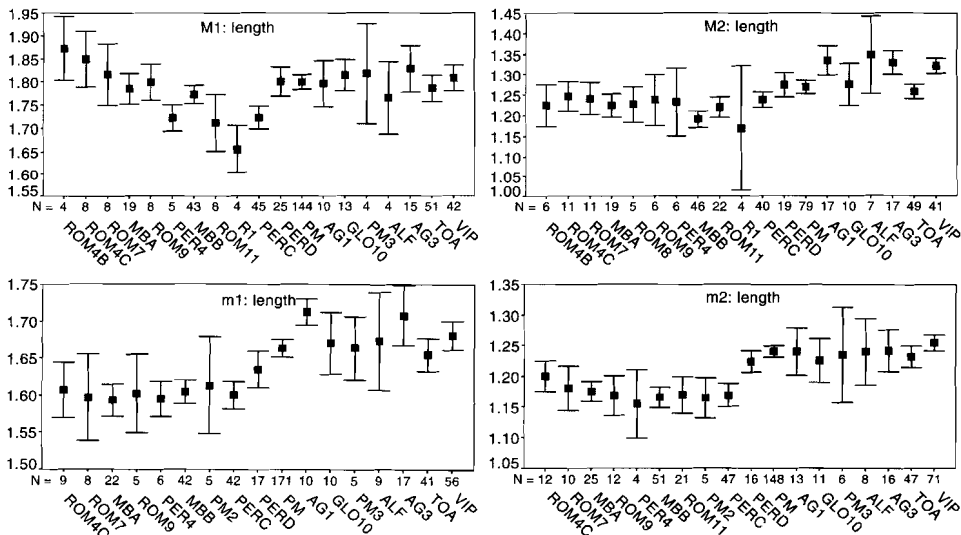


Figure 3.3. 95% confidence intervals for mean length in assemblages of the *Progonomys hispanicus-Occitanomys sondaari* lineage. Only those localities are included for which n>3.

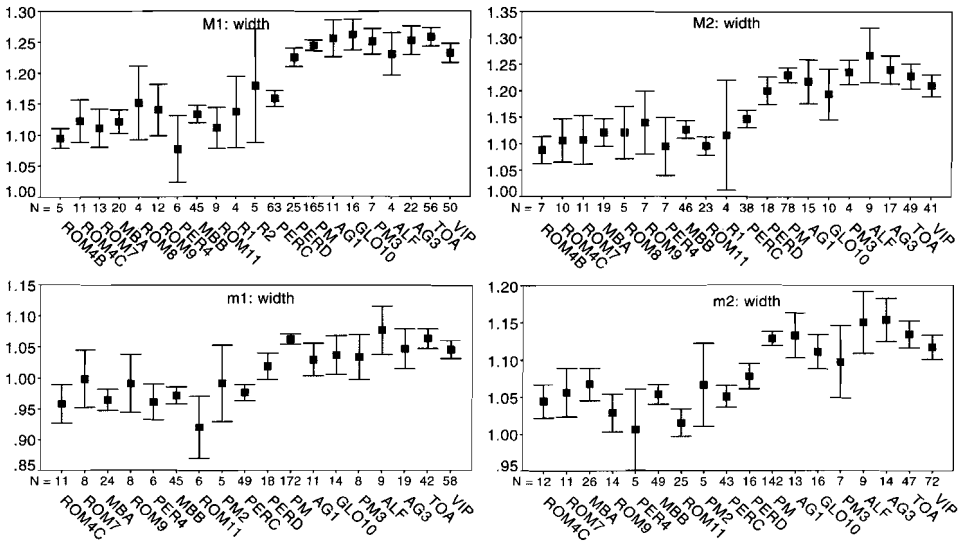


Figure 3.4. 95% confidence intervals for mean width in assemblages of the *Progonomys hispanicus-Occitanomys sondaari* lineage. Only those localities are included for which $n > 3$.

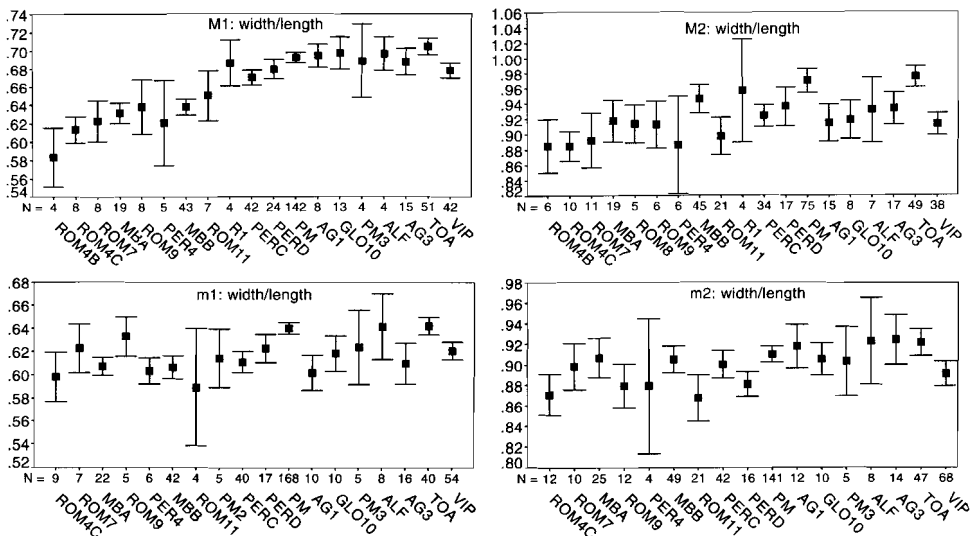


Figure 3.5. 95% confidence intervals for mean width-length ratio in assemblages of the *Progonomys hispanicus-Occitanomys sondaari* lineage. Only those localities are included for which $n > 3$.

Murinae

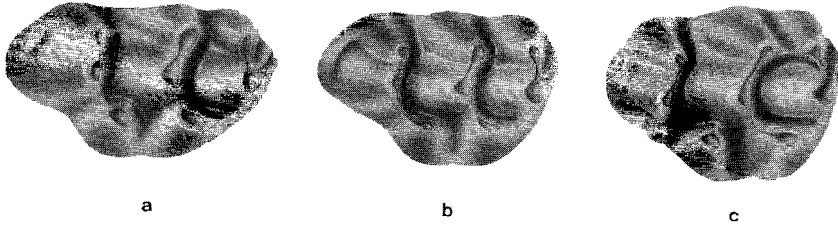


Figure 3.6. Morphological trend in the M1 of the *Progonomys hispanicus*-*Occitanomys sondaari* lineage. a) *P. hispanicus* specimen ROM4B-1 (zone J1); b) *P. hispanicus* specimen MBB-885 (holotype, zone J2); c) *O. sondaari* specimen TOA-785 (zone K). Enlargement $\pm 19 \times$.

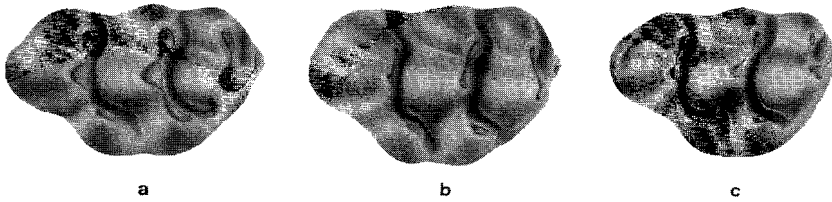


Figure 3.7. Morphological variation in the M1 of *Progonomys hispanicus* from ROM7. a) ROM7-1; b) ROM7-5; c) ROM7-6. Enlargement $\pm 19 \times$.

The morphological change in the M1 is illustrated in the three stages of figure 3.6, which shows examples from ROM4B, MBB and TOA. The morphological difference between *P. hispanicus* from MBB and *O. sondaari* from TOA is also discussed in the morphometric study of chapter 4 (van Dam, 1996), where trends in the outline and the positions of cusps in the M1 are quantified. Apart from the increase in relative width, that study shows trends such as the straightening of the posterior border and the relative anterior displacement of the central cusps in M1. These two features (and most other *Occitanomys* features discussed above) are even more pronounced in the advanced murine *Stephanomys*.

3.3.4. Discussion: *Progonomys hispanicus* or *Occitanomys hispanicus*?

Mein et al. (1993) proposed to transform *Progonomys* Schaub, 1938 from a paraphyletic into a monophyletic genus, and to redefine the genus. They restricted *Progonomys* to the Anatolian/European lineage *Progonomys* sp. (only locality thus far: Sinap Tepe, Anatolia)-*P. cathalai*-*P. woelferi*. They excluded various other Asiatic, African and European populations and species from *Progonomys*. Among the excluded species is *P. hispanicus*, which was placed into *Occitanomys*.

The diagnosis of *Progonomys* of Mein et al. (1993, p. 44) is as follows: "Muridae with lengthened and slender molars, without longitudinal connections between the tubercles, and slightly larger than those of the extant *Mus musculus*. M1 with an almost elliptical outline, with the t1 in an anterior position (not placed backwards) and without t1bis. t4

united to t5 by a high connection, and with a tendency to fuse with t8 by a low crest, that never forms a t7. Upper molars with t6 and t9 generally separated. m1 with a reduced or absent tma; the anteroconid-metaconid connection is generally absent, except in very much worn specimens. Upper molars with one single lingual root. m1 with two main roots and a small central one."

The following remarks can be made:

1) The general absence of the anteroconid-metaconid connection in m1 should not be used as a character, because the connection is generally present in the type species *P. cathalai* (see section 3.4).

2) *Progonomys* sensu Mein et al. (1993) still is paraphyletic, because the phylogenetic tree proposed by the authors includes *Huerzelerimys* and *Anthracomys* among the descendants of the ancestor species *Progonomys* sp.

3) Evolutionary taxonomy is generally preferred above cladistic taxonomy by the author of this thesis, and hence the suggestion to include *P. hispanicus* into *Occitanomys* is not supported. Cladistic taxonomy ignores the amount of morphological divergence between groups, and considers only the order of branching in the phylogenetic tree. Evolutionary taxonomy is based on both morphological difference and phylogeny, and because *P. hispanicus* is morphologically much closer to the type species of *Progonomys* (*P. cathalai*) than to the type species of *Occitanomys* (*O. brailloni*), inclusion into *Progonomys* is preferred.

The morphological differences between *P. hispanicus* and *P. cathalai* are small, and when the two species co-occur there is overlap in both size and in morphology (Michaux, 1971; van de Weerd, 1976). The difference between *P. hispanicus* and *O. brailloni* is much larger. The latter species is characterized by many apomorph features such as a trapezoidal outline, a reduced t12, and a t1bis in M1, and a longitudinal spur in m1. The *P. hispanicus* assemblage from the type locality MBB shows *Occitanomys* features in a very incipient form only: e.g. only 9% shows a t6-t9 connection, and 9% shows the presence of a t1bis. As outlined above, the main part of the evolution towards *Occitanomys sondaari* occurs in the interval J3 which is stratigraphically higher than the type locality of *Progonomys hispanicus*.

It is suggested here to draw the line between *Progonomys* and *Occitanomys* between PERD and PM, a position corresponding to one of the two morphological breaks in the lineage (see above). It is preferred over the break between PM2 and R1, because at the former boundary various relative frequencies of morphotypes almost reach, or cross the 50% level (table 3.3). The most important size break occurs between PERC and PERD (see above), but a morphological break is preferred to draw the line between the two genera.

The earliest *Progonomys hispanicus* assemblages (e.g. ROM4) are morphologically more distinct from *Occitanomys* than the assemblages known thus far. The former start to resemble *P. cathalai* in various aspects: the shape of the M1 is elongate and, on the average, the position of the t1 is close to t2 (e.g. fig. 3.6a). A useful character to discriminate between the earliest *P. hispanicus* on the one hand and *P. cathalai* on the other hand is the position of t8 relative to t9 in M1 (fig. 3.8). t9 is lateral of t8 in *P. hispanicus* and the orientation of the t8-9 pair is more or less at right angles to the

Murinae

longitudinal axis of the molar (fig. 3.8a). This is a plesiomorph feature already present in *Antemus*. It also characterizes the lineage *Progonomys debruijni-Mus* in South Asia (Jacobs, 1978). A more anterior position of the t9 (fig. 3.8b) occurs in *P. cathaloi*, and is also characteristic for the *Parapodemus-Apodemus* group.

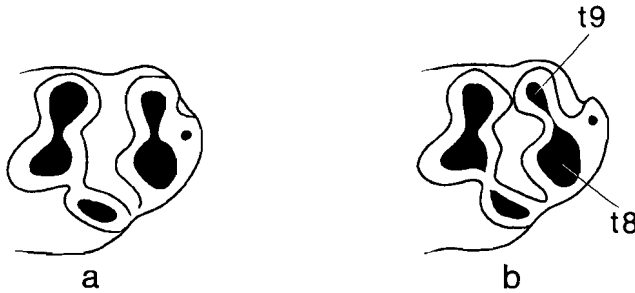


Figure 3.8. Position of the t9 relative to the t8 in a) *Progonomys hispanicus* and b) *Progonomys cathaloi*.

3.3.5. Populations included into *Progonomys hispanicus*

"*P. cathaloi*" from Biodrak (pl.1: fig.9)

Because the morphological variation within *P. hispanicus* is much better known now, some former species identifications need to be revised. The "*P. cathaloi*" specimens from Biodrak (de Bruijn, 1976) are transferred to *P. hispanicus*. Their size is small for *P. cathaloi* and corresponds to the average size of *P. hispanicus*. Morphologically these specimens resemble *P. hispanicus* very well, because of the elongated t1 and t4 and the posterior position of t9 in M1.

"*P. cathaloi*" specimen KA2-45 from Kastellios Hill 2A (fig. 3.9)

De Bruijn et al. (1971) and de Bruijn and Zachariasse (1979) described *P. cathaloi* and *P. woelferi* from Kastellios Hill (Crete, Greece). A small M1 no. KA2A-45 (fig. 3.9) is included in *P. hispanicus*. This specimen was also figured in de Bruijn and Zachariasse (1979: fig. 3) and Mein et al. (1993: fig. 2d). (Note that the latter authors mention KA3 as the locality, which is not correct). The length (1.77 mm.) and width (1.17 mm.) of the specimen are at the lower limit of the variation of *P. cathaloi* in its type locality (Aguilar, 1982). It has almost the mean size of *Progonomys hispanicus* in MBB (table 3.2). Its morphology is characterized by a strongly reduced t12, an elongate t1, and a posteriorly placed t9, features which are characteristic for *P. hispanicus*.

3.3.6. Problematic populations

cf. *Progonomys hispanicus* from Pedregueras 2C (fig. 3.10)

A murine m3 has been reported from the lower Vallesian (MN9) locality Pedregueras 2C (Calatayud-Daroca basin) (Freudenthal, 1968), but it was never described. Its length and width are .84 and .77 mm respectively (see table 3.2), which is smaller than the

smallest m3 of *P. cathalai* from Montredon. The anterior-buccal cusp is medium-sized. A tiny c1 is present. Size and morphology fall within the range of *P. hispanicus*, a small *Occitanomys* or a small *Parapodemus*. Here it is designated as cf. *Progonomys hispanicus*. From a chronological viewpoint it is improbable that the molar belongs to *Occitanomys*. Although *Occitanomys* is present in Anatolia during late MN10 (de Bruijn et al. 1996), in Europe it typically occurs from MN11 onwards. Similarly, *Parapodemus* is not known in SW Europe until late MN10-early MN11.

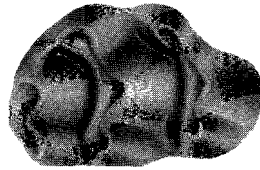


Figure 3.9. M1 of *Progonomys hispanicus* from Kastellios Hill (KA2A-45). Enlargement ± 19 x.

***Progonomys* sp. from Can Llobateres**

Two M1 from the early Vallesian locality Can Llobateres 1 (Vallès-Penedès basin, Spain) were identified as *P. aff. cathalai* by Thaler (1966) and later as *P. cathalai* by Michaux (1971). The mean length and width of the two specimens are 1.93 and 1.15 (Michaux, 1971), which is about the average of *P. cathalai* from Montredon, and large for *P. hispanicus*. The relatively posterior positions of both t1 and t9 (e.g. Pl. I: figs. 9-10 in the work of Michaux) are similar as in *P. hispanicus*. Mein et al. (1993) refer to this lower Vallesian material and to unpublished upper Vallesian material from Can Llobateres 2 (upper Vallesian). These authors suggest that both localities contain one and the same murid species *Progonomys* sp. "of larger size than *P. cathalai* from its type-locality". The specimens from Can Llobateres 1, however, do not have a size which is significantly different from *P. cathalai*.



Figure 3.10. m3 of cf. *Progonomys hispanicus* from Pedregueras 2C. Enlargement ± 41 x.

***Progonomys* cf. *cathalai* from Priay, level δ**

Welcomme et al. (1991) described an anterior part of an m1 and an M3 of *Progonomys* cf. *cathalai* from the early Vallesian faunule of Priay, level δ (Ain, France). Judging by the measurements, description and figures, the specimens could either belong to *P. cathalai* or to *P. hispanicus*. The size of the M3 (length= .89 mm, width= .94 mm) is about average for *P. cathalai* from Montredon, and equivalent to the larger specimens in the *P. hispanicus* assemblage from Masía del Barbo B (tables 3.2 and 3.5). However, the extrapolated length of the fragmented m1 is ~1.5 mm, which is very small for *P. cathalai*: the association of Montredon contains one outlier of length 1.45 mm, all other m1 have lengths ranging from 1.53-1.90 (Aguilar, 1982). 1.5 mm is also small for *P. hispanicus*; the m1 from the type locality have a length range of 1.50-1.70 mm.

3.4. The *Progonomys cathalai*-*Huerzelerimys minor*-*Huerzelerimys vireti* lineage (pl. 2)

3.4.1. Introduction

Van de Weerd (1976) described specimens from Peralejos B, C and D (PERB-D) which strongly resemble *Progonomys cathalai* from MBB, but have a slightly larger size and a higher relative frequency of the t6-t9 connection in M1 and M2. Van de Weerd included these specimens into *Parapodemus* (sp. A). According to the emended diagnosis for *Parapodemus* given by the Bruijn (1976) a strong t4-t8 connection in the M1-2 is the critical diagnostic feature for *Parapodemus*. However, this connection is weak in five out of seven M1 from PERC (the largest assemblage), and in the other two specimens it is absent (table 3.6). 11 out of 13 M2 from PERC show a weak to moderately strong t4-t8 connection. Recently, Mein et al. (1993) included these specimens into the genus *Huerzelerimys* (*H. minor*, type locality Ambérieu 2C, southern France). A relative frequency larger than 50% of the t6-t9 connection (75% in PERC, see table 3.6), and a weakly developed t4-t8 connection in these specimens fit the diagnosis for *H. minor* given by the authors. (In 4.6 this diagnosis is further discussed.)

3.4.2. Comparison of *P. cathalai* from Masía del Barbo B with the type material

Michaux (1971) and van de Weerd (1976) both compared *P. cathalai* from MBB with the type material from Montredon (Hérault, southern France). Michaux noted that both assemblages are very similar, but that the assemblage from Montredon is more primitive because of smaller size, less robust cusps, the absence of a well-developed anterior-central cusp in m1, and a lower frequency of the t6-t9 connection in M1. 23% of the M1 from Montredon show a t6-t9 connection (Aguilar, 1982), which is about twice as low as in MBB (table 3.6). Another characteristic morphological difference between the two assemblages relates to the shape of the t1 in M1. Whereas this cusp is rounded in the Spanish material, four out of six M1 from Montredon in the Utrecht collection show a semi-circular shaped t1: the buccal side of the t1 is straight, and posteriorly connected to the base of t5 (for example pl. 2: fig. 3).

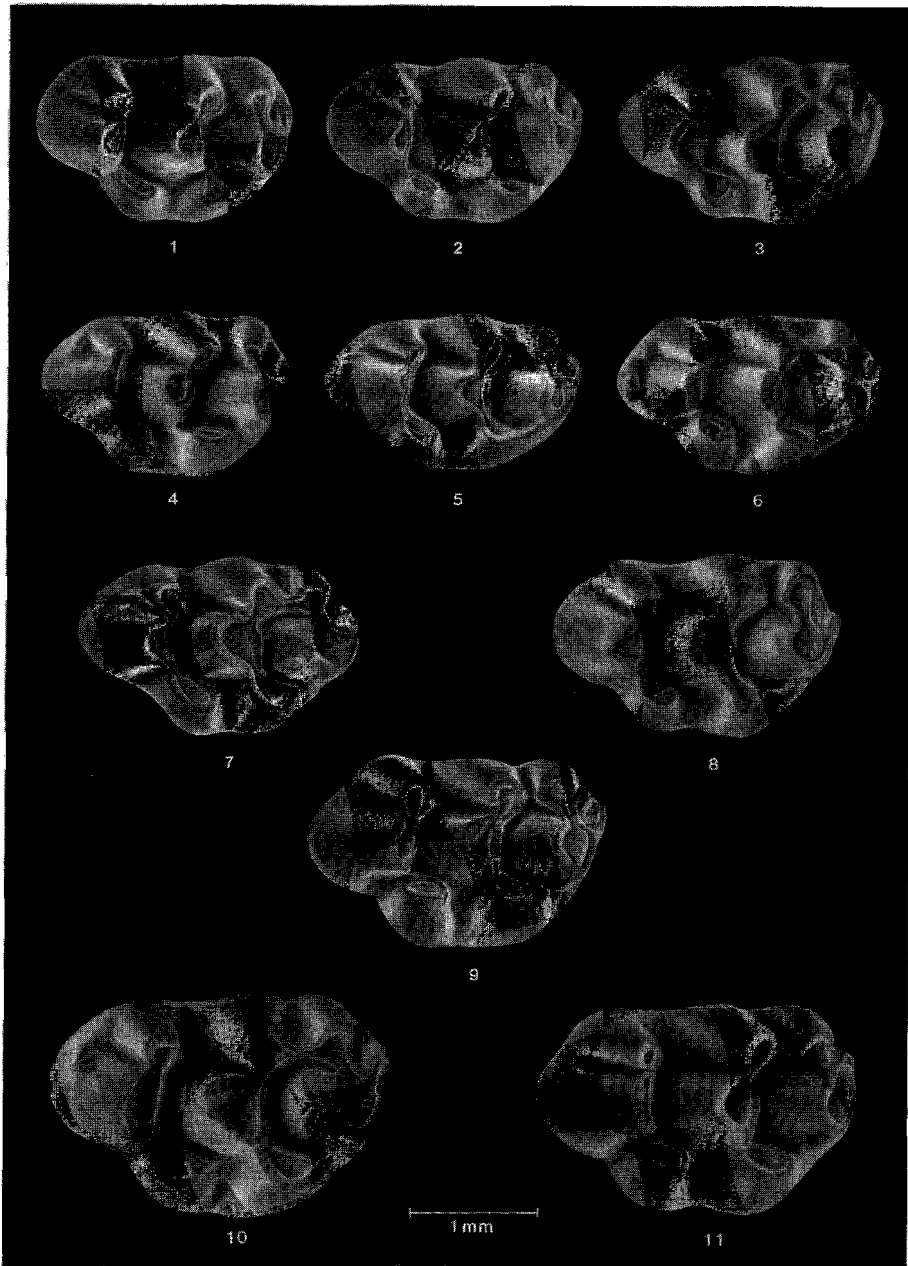


Plate 2. *Progonomys cathalai*: 1) ROM11-9: M1 sin.; 2) PER4-64: M1 sin.; 3) MR-232 from Montredon: M1 dex. (rev.); 4) MBB-1182 dex. (rev.); 5) MBB-1189: dex. (rev.); 6) MBB-1181: dex. (rev.). *Huerzelerimys minor*: 7) M1 from Ambérieu 2C; 8) PERC-582: M1 dex. (rev.); 9) R2-1: M1 sin. *Huerzelerimys vireti*: 10) AG3-6: M1 dex. (rev.); 11) AG3-3: M1 sin.

Murinae

Table 3.5. Length and width measurements of representatives of the *Progonomys cathalae*-*Huerzelerimys minor*-*Huerzelerimys vireti* lineage. The populations of GLO14A, MRU and AG7 have cf. designations.

locality	length (in mm)					width (in mm)				
	n	min	mean	max	sd	n	min	mean	max	sd
<i>M1 Huerzelerimys vireti</i>										
VIP	6	2.29	2.48	2.67	0.15	6	1.60	1.63	1.66	0.02
TOA	1	2.72	2.72	2.72	-	1	1.66	1.66	1.66	-
AG3	5	2.36	2.47	2.72	0.15	6	1.60	1.68	1.80	0.07
ALF	5	2.39	2.58	2.80	0.17	6	1.53	1.64	1.74	0.07
PM3	0	-	-	-	-	1	1.58	1.58	1.58	-
GLO10	1	2.37	2.37	2.37	-	1	1.60	1.60	1.60	-
AG1	3	2.29	2.37	2.42	0.07	2	1.50	1.58	1.65	0.11
PM	15	2.26	2.46	2.86	0.14	17	1.47	1.59	1.79	0.07
<i>M1 Huerzelerimys minor</i>										
PERD	2	2.11	2.18	2.24	0.09	2	1.31	1.38	1.46	0.11
PERC	5	2.02	2.14	2.31	0.13	7	1.32	1.39	1.48	0.06
R2	1	2.20	2.20	2.20	-	1	1.47	1.47	1.47	-
PERB	2	2.06	2.08	2.09	0.02	2	1.30	1.31	1.31	0.01
<i>M1 Progonomys cathalae</i>										
GL14B	1	1.85	1.85	1.85	-	1	1.25	1.25	1.25	-
PM2	1	1.98	1.98	1.98	-	1	1.22	1.22	1.22	-
ROM11	2	1.88	1.90	1.92	0.03	5	1.20	1.24	1.28	0.03
MBB	15	1.91	1.99	2.09	0.06	20	1.18	1.27	1.35	0.05
PERA	3	1.92	1.94	1.95	0.02	3	1.24	1.27	1.31	0.04
SAL	0	-	-	-	-	1	1.19	1.19	1.19	-
ROM1	1	1.86	1.86	1.86	-	1	1.20	1.20	1.20	-
PER4	1	1.92	1.92	1.92	-	1	1.23	1.23	1.23	-
<i>M2 Huerzelerimys vireti</i>										
VIP	2	1.76	1.78	1.80	0.03	2	1.63	1.63	1.64	0.01
TOA	3	1.78	1.79	1.80	0.01	5	1.59	1.67	1.76	0.07
AG3	7	1.61	1.80	1.96	0.11	6	1.62	1.67	1.72	0.04
PM3	1	1.75	1.75	1.75	-	1	1.57	1.57	1.57	-
GLO10	2	1.63	1.65	1.67	0.03	2	1.58	1.58	1.58	0.00
AG1	2	1.62	1.73	1.85	0.16	2	1.56	1.57	1.59	0.02
PM	13	1.48	1.68	1.81	0.08	14	1.44	1.58	1.72	0.07
<i>M2 Huerzelerimys minor</i>										
MRU	1	1.43	1.43	1.43	-	1	1.27	1.27	1.27	-
PERC	9	1.33	1.45	1.59	0.08	11	1.28	1.34	1.41	0.05
R2	3	1.49	1.51	1.53	0.02	3	1.34	1.41	1.48	0.07
<i>M2 Progonomys cathalae</i>										
ROM11	7	1.29	1.38	1.48	0.07	8	1.16	1.25	1.33	0.06
MBB	22	1.28	1.37	1.47	0.05	22	1.10	1.24	1.39	0.08
PERA	3	1.32	1.38	1.43	0.06	3	1.18	1.23	1.29	0.06
SAL	1	1.40	1.40	1.40	-	1	1.29	1.29	1.29	-

locality	length (in mm)					width (in mm)				
	n	min	mean	max	sd	n	min	mean	max	sd
<i>M2 Progonomys cathalai</i> (continued)										
PER4	3	1.32	1.37	1.45	0.07	3	1.12	1.22	1.34	0.11
<i>M3 Huerzelerimys vireti</i>										
VIP	5	1.17	1.24	1.28	0.05	4	1.18	1.25	1.32	0.06
TOA	1	1.28	1.28	1.28	-	1	1.30	1.30	1.30	-
AG3	5	1.23	1.32	1.42	0.07	5	1.25	1.29	1.31	0.02
ALF	1	1.30	1.30	1.30	-	1	1.26	1.26	1.26	-
GLO10	3	1.15	1.19	1.26	0.06	3	1.21	1.26	1.33	0.07
PM	3	1.14	1.21	1.26	0.07	4	1.23	1.27	1.31	0.03
<i>M3 Huerzelerimys minor</i>										
PERC	7	0.93	1.00	1.08	0.06	7	0.93	1.02	1.09	0.07
R2	4	0.97	1.00	1.03	0.03	4	0.98	1.06	1.09	0.05
PERB	1	0.97	0.97	0.97	-	1	1.04	1.04	1.04	-
<i>M3 Progonomys cathalai</i>										
ROM11	5	0.92	0.96	1.02	0.04	5	0.90	0.97	1.03	0.05
MBB	15	0.84	0.94	1.05	0.06	16	0.82	0.96	1.06	0.05
PERA	2	0.89	0.90	0.90	0.01	2	0.90	0.96	1.01	0.08
<i>m1 Huerzelerimys vireti</i>										
VIP	6	2.04	2.14	2.26	0.09	7	1.30	1.36	1.47	0.07
TOA	6	2.04	2.11	2.22	0.06	6	1.35	1.40	1.45	0.03
AG3	3	2.13	2.23	2.38	0.13	4	1.43	1.44	1.46	0.01
ALF	1	2.11	2.11	2.11	-	1	1.31	1.31	1.31	-
PM3	2	2.20	2.22	2.23	0.03	3	1.30	1.33	1.39	0.05
GLO10	2	2.14	2.14	2.15	0.01	1	1.38	1.38	1.38	-
AG1	1	2.20	2.20	2.20	-	1	1.37	1.37	1.37	-
PM	21	1.96	2.18	2.37	0.11	24	1.27	1.40	1.57	0.08
<i>m1 Huerzelerimys minor</i>										
GLO11	2	1.82	1.87	1.93	0.08	1	1.08	1.08	1.08	-
PERD	1	2.19	2.19	2.19	-	0	-	-	-	-
PERC	9	1.76	1.88	1.96	0.07	11	1.12	1.18	1.27	0.05
R2	2	1.86	1.94	2.02	0.11	2	1.10	1.17	1.24	0.10
<i>m1 Progonomys cathalai</i>										
GL14B	1	1.82	1.82	1.82	-	1	1.14	1.14	1.14	-
ROM11	6	1.67	1.78	1.85	0.07	9	1.02	1.08	1.16	0.04
MBB	19	1.69	1.77	1.88	0.06	19	0.99	1.08	1.18	0.05
PERA	3	1.63	1.69	1.72	0.05	4	1.00	1.03	1.06	0.03
<i>m2 Huerzelerimys vireti</i>										
VIP	9	1.49	1.70	1.79	0.09	9	1.34	1.49	1.58	0.09
TOA	11	1.63	1.71	1.89	0.08	11	1.46	1.53	1.64	0.06
AG3	3	1.67	1.74	1.81	0.07	3	1.45	1.51	1.57	0.06
ALF	2	1.59	1.70	1.82	0.17	2	1.49	1.54	1.58	0.06
GLO10	5	1.62	1.70	1.79	0.07	5	1.44	1.49	1.53	0.04
PM	27	1.44	1.66	1.87	0.09	27	1.34	1.48	1.64	0.08

locality	length (in mm)					width (in mm)				
	n	min	mean	max	sd	n	min	mean	max	sd
<i>m2 Huerzelerimys minor</i>										
GLO11	1	1.52	1.52	1.52	-	1	1.31	1.31	1.31	-
PERC	5	1.43	1.46	1.50	0.03	8	1.19	1.27	1.32	0.04
R2	2	1.35	1.41	1.47	0.09	2	1.14	1.19	1.24	0.07
CAT2	1	1.33	1.33	1.33	-	1	1.17	1.17	1.17	-
<i>m2 Progonomys cathalai</i>										
GL14B	1	1.36	1.36	1.36	-	1	1.26	1.26	1.26	-
ROM11	7	1.29	1.33	1.37	0.03	9	1.05	1.15	1.22	0.05
MBB	25	1.20	1.31	1.42	0.05	25	1.08	1.16	1.27	0.05
PERA	1	1.28	1.28	1.28	-	1	1.14	1.14	1.14	-
PER4	1	1.28	1.28	1.28	-	1	1.17	1.17	1.17	-
<i>m3 Huerzelerimys vireti</i>										
VIP	7	1.23	1.33	1.43	0.08	10	1.05	1.22	1.35	0.09
TOA	2	1.40	1.42	1.43	0.02	2	1.28	1.34	1.39	0.08
AG3	1	1.35	1.35	1.35	-	1	1.24	1.24	1.24	-
PM3	2	1.41	1.41	1.41	-	2	1.32	1.32	1.32	0.00
GLO10	2	1.44	1.45	1.45	0.00	3	1.27	1.29	1.33	0.03
AG1	1	1.35	1.35	1.35	-	1	1.28	1.28	1.28	-
PM	5	1.34	1.42	1.54	0.10	4	1.19	1.27	1.38	0.09
<i>m3 Huerzelerimys minor</i>										
AG7	1	1.36	1.36	1.36	-	1	1.24	1.24	1.24	-
PERC	1	1.13	1.13	1.13	-	1	1.05	1.05	1.05	-
R2	1	1.10	1.10	1.10	-	1	1.04	1.04	1.04	-
<i>m3 Progonomys cathalai</i>										
ROM11	7	1.03	1.08	1.17	0.06	6	0.92	0.97	1.02	0.04
MBB	13	0.95	1.06	1.13	0.06	13	0.88	0.96	1.01	0.04
PER4	2	1.20	1.21	1.22	0.01	2	0.99	1.02	1.04	0.04

Table 3.5. (continued)

3.4.3. Comparison of *H. minor* from the Teruel-Alfambra region with *H. minor* from its type locality (pl. 2: figs. 7-9)

With 55 specimens the assemblage from PERC is the richest of the *H. minor* assemblages from the Teruel-Alfambra region. The teeth from PERC are slightly smaller than those from the type locality Ambérieu 2C (Ain, France) described by Mein et al. (1993). The mean length-width ratio of M1 of .65 given by these authors is very close to that of the PERC material (fig. 3.13). The material from PERC fits the morphological descriptions of the type material in all relevant aspects. The relative frequencies of all selected characters in PERC in table 3.6 have values >50%. Percentages higher than 50% were also observed in the type material (Mein et al., 1993).

3.4.4. Comparison of *H. vireti* from the Teruel-Alfambra region with *H. vireti* from its type locality (pl. 2: figs. 10-11)

The measurements of *H. vireti* from Mollon (Ain, France) (collections of Basel and Lyon) presented by van de Weerd (1976) show that the assemblage from the type locality and the Spanish assemblages have similar sizes. The relative frequencies of the t6-t9 connection in the M1 are comparable: 70-100% in the Spanish assemblages (table 3.6) and four out of five M1 in Mollon (the holotype in Schaub, 1938 from the Basel collection and the paratypes in Michaux, 1971 from the Lyon collection). The t4-t8 connection in the M1 from Mollon is weak or absent. The Spanish assemblages show a t4-t8 connection in the majority of specimens (table 3.6), but the limited number of teeth from Mollon do not permit a statistically reliable comparison. The same is true for the relative frequency of connection between the anterior pair of cusps in m1. It is 80-100% in the Spanish assemblages (table 3.6), and present in three out of four specimens from

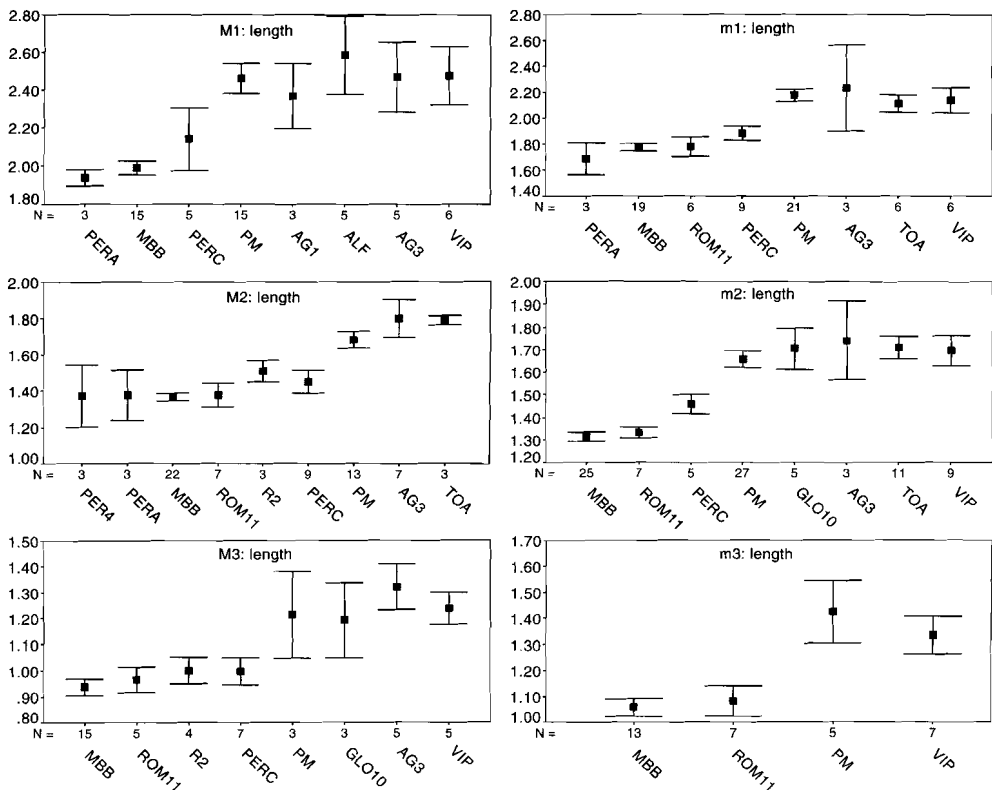


Figure 3.11. 95% confidence intervals for length in assemblages of the *Progonomys catalai*-*Huerzelerimys minor*-*Huerzelerimys vireti* lineage. Only those localities are included for which $n > 2$.

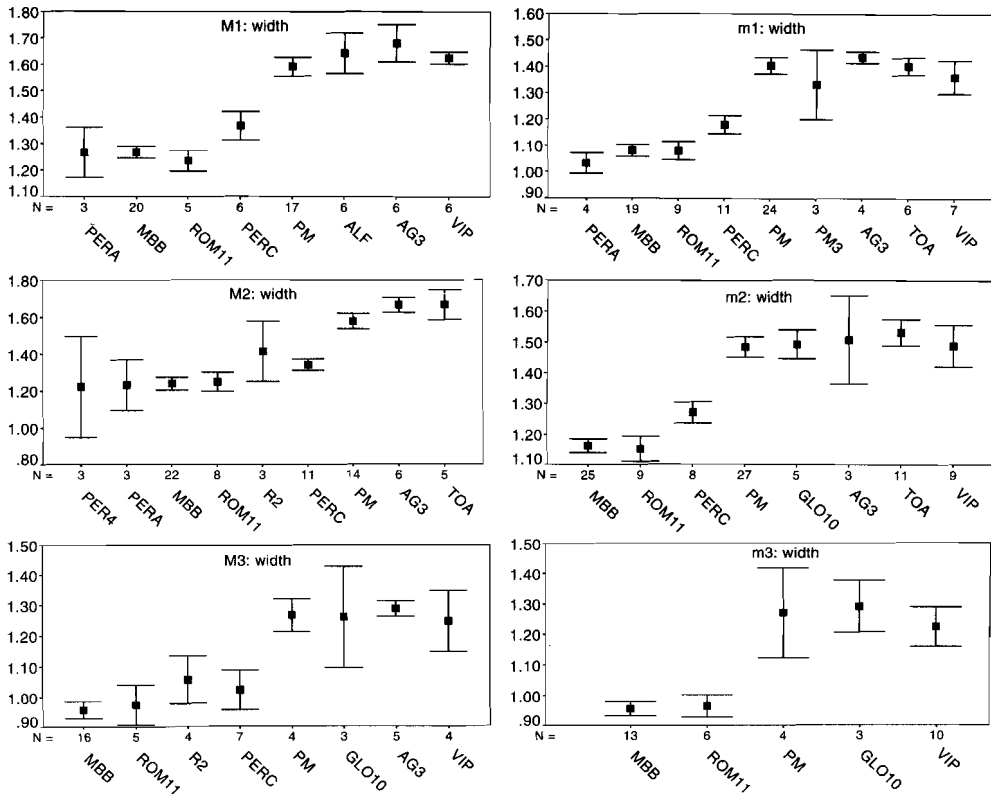


Figure 3.12. 95% confidence intervals for width in assemblages of the *Progonomys cathalai*-*Huerzelerimys minor*-*Huerzelerimys vireti* lineage. Only those localities are included for which $n > 2$.

Mollon (Schaub, 1938; Michaux, 1971). According to Michaux (1971), a minuscule antero-central cusp in the m1 can be present. In Spain the relative frequency of this cusp in *H. vireti* is variable (table 3.6).

3.4.5. Evolutionary trends

Length, width and relative width (table 3.5, figs. 3.11-3.13)

The size of *H. minor* is intermediate between that of *P. cathalai* and *H. vireti* except for the M3 and possibly the m3. Unlike the *P. hispanicus*-*O. sondaari* lineage, the *P. cathalai*-*H. minor*-*H. vireti* lineage shows only isometric size increase: the width-length ratio remains more or less constant.

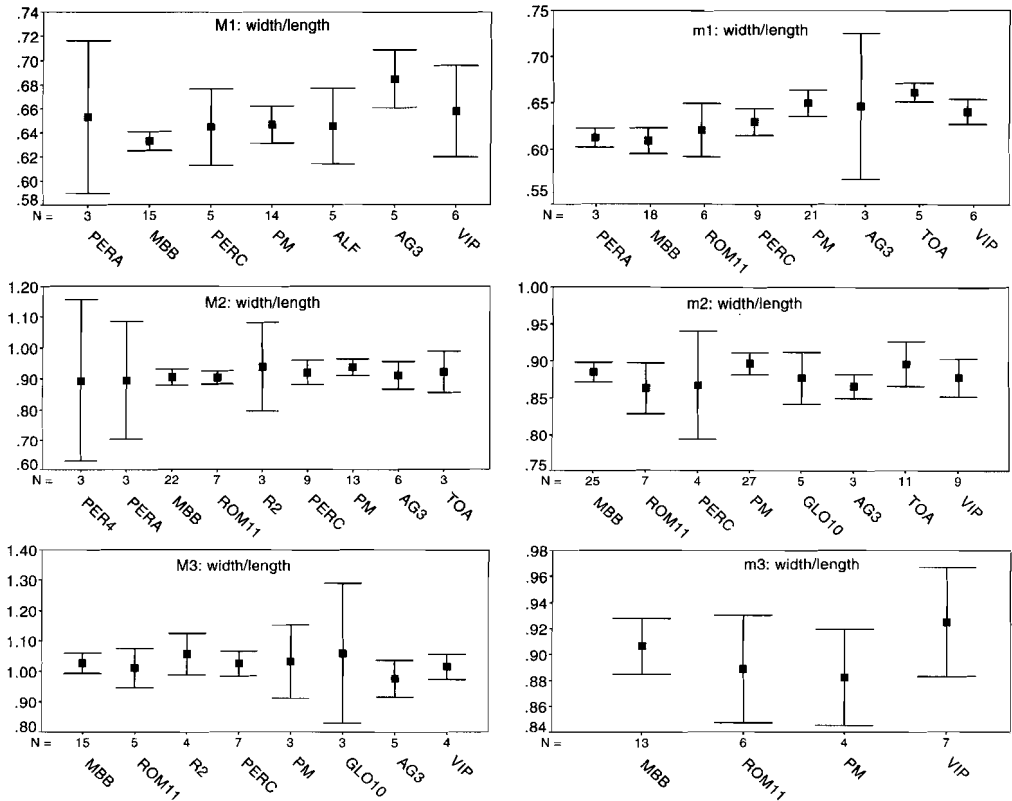


Figure 3.13. 95% confidence intervals for width-length ratio in assemblages of the *Progonomys catalai*-*Huerzelerimys minor*-*Huerzelerimys vireti* lineage. Only those localities are included for which $n > 2$.

Morphological trends (table 3.6)

The lineage shows an increase in the relative frequency of the t6-t9 connection in M1 throughout the studied interval. From PERC onwards this frequency is higher than 50%. Due to the limited number of teeth, it is difficult to observe a trend in the percentage of the t4-t8 connection in M1. It is observed, however, that the height of the t4-t8 connection in the studied *Huerzelerimys* assemblages from Spain is lower than that of its ancestor *P. catalai*. Other trends are the reduction of the t12 and the elongation and longitudinal imbrication of the central cusps in M1-2. This feature is most pronounced in the youngest and most advanced *Huerzelerimys* species, *H. turoliensis* which is not further discussed here.

The relative frequency of the antero-central cusp and the connection between the two anterior pairs of cusps in m1 do not show any clear trend.

Murinae

Table 3.6. Relative frequencies of selected molar structures in the *Progonomys cathalal-Huerzelerimys minor-Huerzelerimys vireti* lineage. Percentages based on n<5 are not shown and indicated by *.

locality	t6-t9 connection M1		t4-t8 connection M1		antero-central cusp m1		anterior connection m1	
	n	%	n	%	n	%	n	%
<i>Huerzelerimys vireti</i>								
VIP	7	100	6	67	11	89	8	88
TOA	*		*		6	33	7	100
AG3	5	80	6	83	6	50	8	88
ALF	7	71	6	67	*		*	
PM	21	81	18	72	19	42	25	84
<i>Huerzelerimys minor</i>								
PERC	8	75	7	71	14	71	13	100
<i>Progonomys cathalal</i>								
ROM11	*		5	60	6	67	7	86
MBB	16	44	9	89	19	53	20	80

3.4.6. The genera *Progonomys* and *Huerzelerimys*

The genus *Huerzelerimys* has been defined by Mein et al. (1993, p. 49) as follows: "Molars smaller than or similar in size to those of extant *Rattus rattus*, and with a poor development of the longitudinal connections between tubercles. Upper molars without t7, but with t4 and t8 connected by a weak crest. M1 and M2 with a well-developed t9, and with t6 and t9 united in more than 50% of the specimens. M3 without t9. m1 with a reduced tma, and with a connection between the anterior pairs of tubercles; three roots; cingular margin moderately developed. Tendency towards a strong size increase in the course of time." The differential diagnosis of *Huerzelerimys* with regard to *Progonomys* is as follows: "Differs from *Progonomys* by having a connection between the two anterior pairs of tubercles in the m1; t6 and t9 are connected.". The diagnosis of *Progonomys* (section 3.4) includes the general absence of the anterior connection in m1. However, this connection is present in 90% (n=39) of the m1 from the type locality Montredon of the type species of *Progonomys* (Aguilar and Michaux, 1996). In *P. cathalal* from Masía del Barbo B this percentage is 75% (n=16). Table 3.6 shows that there is no trend in the percentage of the anterior connection in the lineage segment *P. cathalal-H. minor-H. vireti* in Spain. This observation implies that there is no justification to use this character in the diagnoses of *Huerzelerimys* and *Progonomys*.

Huerzelerimys and *Progonomys* molars are rather similar in their general habitus. Among the most important differences are the high percentage of the t6-t9 connection, the reduced t12, and the imbricated pattern of cusps in the M1-2 in *Huerzelerimys* (see above). There is a marked trend towards larger size in the lineage *P. cathalai*-*H. minor*-*H. vireti*-*H. turoliensis*. However, morphologically *Huerzelerimys* is still relatively close to its ancestor *Progonomys*.

3.4.7. Populations attributed to *H. minor*

"*Parapodemus pasquierae*" from Lo Fournas 6

Aguilar and Michaux (1996) describe a new species, *Parapodemus pasquierae* from Lo Fournas 6 (Rousillion, France). This population is assigned to *Huerzelerimys minor* because the description and measurements of *P. pasquierae* fit very well.

3.5. *Parapodemus*

3.5.1. Introduction

Parapodemus lugdunensis is the only early Turolian *Parapodemus* species described from the Teruel-Alfambra region until now (van de Weerd, 1976; Adrover 1986; Alcalá et al., 1991). The relatively rich *Parapodemus* sample from Los Aguanaces 3 (AG3) shows that *P. gaudryi* was also present in the region at that time. The morphological distinction between *P. gaudryi* and *P. lugdunensis* which is clear in this locality, also allows their separation in localities which contain only a few specimens. Both *P. gaudryi* and *P. lugdunensis* will be described and compared on the basis of the material from AG3. The material from the other assemblages (PERD, PM5B, ALF, TOA, VIP) will not be described separately because it falls within the variation of the species. The measurements are shown in tables 3.7-3.8 and figure 3.14.

3.5.2. *Parapodemus gaudryi* from Los Aguanaces 3 (pl. 3: figs. 1-7, 9)

Description:

Slightly hypsodont molars with steep, rounded cusps. Transverse valleys are narrow and deep. Wear surfaces are relatively horizontal on the lower molars, on the M3 and on the central cusps of the M1 and M2.

M1. The M1 have an elliptical outline. t1 is round and there is no ridge between this cusp and t2. t1 is positioned anteriorly (only slightly posteriorly with regard to t3). t3 is large and shows a posterior spur in seven out of eight specimens. A posterior spur on the t4 and a lingual spur on the t8 form a crest, on which an incipient t7 is present in two out of eight specimens. The connection between the t6 and the t9 is variable in height and may be absent (pl. 3: fig. 1). In most cases it is low compared to the height of the t6 and the t9 in unworn state. t12 is well developed. A small fourth, central root is present in one of the two specimens in which the roots are preserved.

Table 3.7. Length and width measurements of *Parapodemus gaudryi*.

element	locality	length (in mm)					width (in mm)				
		n	min	mean	max	sd	n	min	mean	max	sd
M1	VIP	3	1.97	2.04	2.09	0.06	3	1.17	1.23	1.28	0.06
	TOA	1	1.98	1.98	1.98	-	1	1.25	1.25	1.25	-
	AG3	5	1.90	2.06	2.14	0.09	6	1.26	1.29	1.31	0.02
	PM5B	1	1.93	1.93	1.93	-	1	1.25	1.25	1.25	-
	PM	2	1.99	2.04	2.10	0.08	2	1.21	1.21	1.22	0.01
M2	VIP	1	1.38	1.38	1.38	-	1	1.26	1.26	1.26	-
	TOA	5	1.37	1.44	1.55	0.08	4	1.23	1.28	1.34	0.05
	AG3	13	1.32	1.42	1.49	0.05	9	1.19	1.29	1.37	0.06
M3	TOA	1	0.95	0.95	0.95	-	1	0.93	0.93	0.93	-
	AG3	7	0.91	0.98	1.07	0.06	6	0.95	0.98	1.01	0.02
	PM3	1	1.06	1.06	1.06	-	1	1.04	1.04	1.04	-
	GLO10	1	0.98	0.98	0.98	-	1	0.94	0.94	0.94	-
m1	TOA	4	1.80	1.83	1.89	0.04	4	1.08	1.12	1.16	0.03
	AG3	2	1.80	1.80	1.80	0.00	3	1.12	1.14	1.16	0.02
	PM	1	1.79	1.79	1.79	-	1	1.16	1.16	1.16	-
m2	VIP	0	-	-	-	-	1	1.18	1.18	1.18	-
	TOA	2	1.44	1.49	1.54	0.07	2	1.17	1.24	1.30	0.09
	AG3	5	1.34	1.43	1.53	0.08	6	1.18	1.21	1.25	0.03
	PM	1	1.32	1.32	1.32	-	1	1.17	1.17	1.17	-
m3	VIP	1	1.08	1.08	1.08	-	2	0.96	0.98	1.01	0.04
	TOA	1	1.17	1.17	1.17	-	1	0.91	0.91	0.91	-
	AG3	7	1.09	1.14	1.20	0.04	7	0.98	1.05	1.12	0.05
	ALF	2	1.11	1.11	1.12	0.01	2	1.05	1.15	1.24	0.14

Table 3.8. Length and width measurements of *Parapodemus lugdunensis*.

element	locality	length (in mm)					width (in mm)				
		n	min	mean	max	sd	n	min	mean	max	sd
M1	TOA	3	1.79	1.83	1.90	0.06	4	1.12	1.17	1.20	0.03
	AG3	8	1.72	1.80	1.94	0.07	9	1.07	1.13	1.17	0.03
	ALF	1	1.81	1.81	1.81	-	1	1.09	1.09	1.09	-
	PERD	1	1.87	1.87	1.87	-	0	-	-	-	-
M2	AG3	5	1.20	1.25	1.32	0.06	7	1.04	1.12	1.17	0.06
m1	BUN7	1	1.57	1.57	1.57	-	1	0.90	0.90	0.90	-
	VIP	1	1.59	1.59	1.59	-	1	0.93	0.93	0.93	-
	TOA	2	1.62	1.62	1.62	0.00	2	0.98	0.99	0.99	0.01
	AG3	2	1.62	1.65	1.69	0.05	2	0.96	0.97	0.97	0.01
	ALF	1	1.61	1.61	1.61	-	1	0.98	0.98	0.98	-
m2	TOA	1	1.24	1.24	1.24	-	1	1.04	1.04	1.04	-
	AG3	4	1.19	1.23	1.29	0.04	4	0.99	1.02	1.06	0.03

M2. t1 is rounded, and the outline of the molar shows a marked re-entrant between t1 and t4 in about half of the specimens. There is no posterior spur on t3. Seven out of 13 specimens show an incipient t7. t6-t9 connection as in M1.

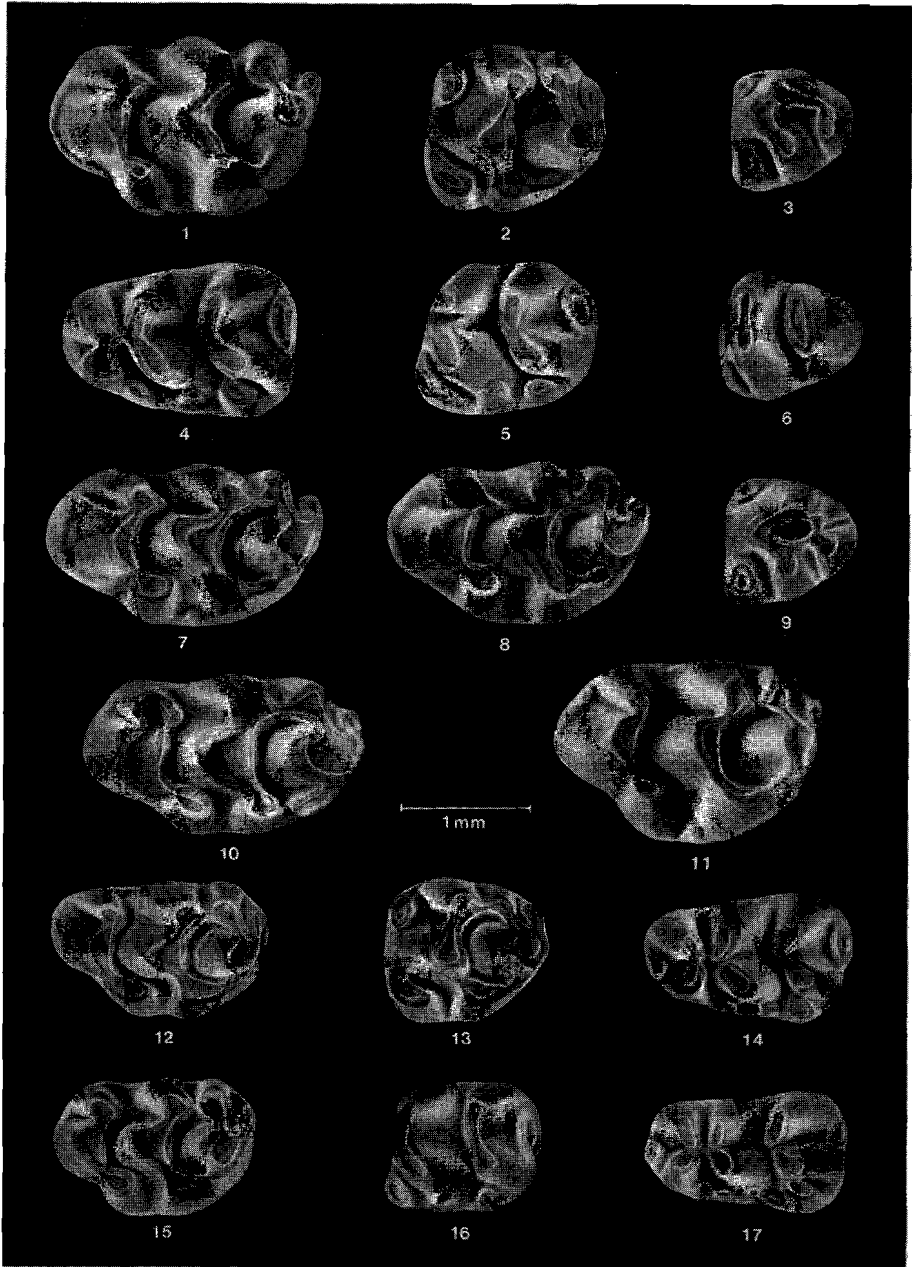


Plate 3. *Parapodemus gaudryi*: 1) AG3-827: M1 dex. (rev.); 2) AG3-154: M1 dex. (rev.); 3) AG3-847: M3 dex. (rev.); 4) AG3-851: m1 sin.; 5) AG3-861: m2 sin.; 6) AG3-882: m3 sin.; 7) VIP-22: M1 sin.; 8) PK4-174 from Pikermi (neotype): M1 sin.; 9) AG3-846: M3 dex. (rev.). *Apodemus gudrunae*: 10) VDC3-352 from Valdecebro 3 (holotype): M1 dex. (rev.). *Parapodemus barbarae*: 11) LM-416 from Los Mansuetos (holotype): M1 dex. (rev.). *Parapodemus lugdunensis*: 12) AG3-147: M1 dex. (rev.); 13) AG3-151: M1 sin.; 14) AG3-816: m1 dex. (rev.); 15) AG3-142: M1 sin.; 16) AG3-819: m2 dex. (rev.); 17) VIP-351: m1 sin.

M3. Most specimens show a broad t6-t8 connection. t4 and t8 are generally separated. One specimen (pl. 3: fig. 9) is different from the rest in having a distinct t9, and a buccally-positioned t4-t8 connection.

m1. The anteroconid complex is symmetrical. An antero-central cusp is present in three out of five specimens. The connection between the two anterior pairs of cusps is present in all specimens. The c1 is large. The buccal ridge is distinct with two or three conules in front of the c1. The terminal heel has an elliptical outline. A small third root is present in one specimen out of three in which the root pattern is preserved.

m2. The anterior and posterior width of the m2 are about equal. The development of the buccal ridge varies from specimen to specimen, but an accessory cusp (k, see fig. 3.2) is always present lingually of the protoconid. In most specimens, the anterior-buccal cusp is elongate, and posteriorly connected to the accessory cusp k by a cingulum ridge.

m3. The m3 have an antero-labial cusp. They show a c1 in six out of nine specimens.

3.5.3. Comparison of *P. gaudryi* from Los Aguanaces 3 with *P. gaudryi* from its type locality

The size of *P. gaudryi* from AG3 is very close to that of *P. gaudryi* from the Greek type locality Pikermi (PK4) (de Bruijn, 1976). The dental patterns are very similar, although the Spanish assemblage is slightly more primitive. Firstly, the t6-t9 connection in M1-2 of AG3 is lower on the average, and may be absent. Secondly, the posterior spur on t3 in M1 is less well developed; in PK4 it even occasionally reaches t6. Thirdly, the antero-central cusp in the m1 from AG3 is less distinct. Fourthly, the anterior-buccal cusp in the m2 from AG3 is more elongated and generally connected to accessory cusp k (fig. 3.2), whereas in PK4 it is rounded and tends to be isolated. Finally, six out of nine m3 from AG3 show a c1, some of which are very distinct, whereas only two out of six specimens from PK4 show a weak c1.

Although the M1 of AG3 show a t7 less frequently (AG3: 25%, n=8; PK4: 42%, n=12, see table 3.7), this is not the case for the M2 (AG3: 54%, n=13; PK4: 40%, n=5). However, the differences between AG3 and PK4 in these relative frequencies are probably not significant, because numbers are relatively small.

3.5.4. *Parapodemus lugdunensis* from Los Aguanaces 3 (pl. 3: figs. 12-16)

Description:

M1. The t1 is slightly elongate in a posterior-lingual direction. A spur on t3 is present in three out of eight specimens. t4 and t8 are connected, but there is no t7. All M1 show a firm t6-t9 connection. t12 is well developed. An incipient, very small fourth, central root is present in three of the four specimens in which the roots are preserved.

M2. There is no posterior spur on t3. t7 is absent. A t6-t9 connection is present, except in one specimen. t12 is small and ridge-shaped.

M3. Not described because it cannot be distinguished from the M3 of *O. sondaari*.

m1. The anteroconid complex is symmetrical. All four specimens show an antero-central cusp. The connection between the two anterior pairs of cusps is present in three

specimens, and virtually absent in one specimen (pl. 3: fig. 14). The low buccal ridge contains one, two or three accessory cusps anteriorly of c1. One specimen has its two roots preserved.

m2. The anterior and posterior width of the m2 are about equal. The buccal ridge is less developed than in m1. An accessory cusp buccally of the protoconid is present in three out of four specimens.

m3. Not described because it cannot be distinguished from the m3 of *O. sondaari*.

3.5.5. Comparison of *Parapodemus lugdunensis* from Los Aguanaces 3 with *Parapodemus lugdunensis* from its type locality

P. lugdunensis from AG3 and the type locality Mollon (Ain, France) are of similar size (van de Weerd, 1976: his fig. 14). The holotype (M1) in Schaub, 1938 shows an elongate and slightly posteriorly situated t1. This feature also characterizes the M1 from AG3. (It is not characteristic for *P. gaudryi*.)

3.5.6. Comparison of *P. gaudryi* and *P. lugdunensis* from Los Aguanaces 3

The main differences between *P. gaudryi* and *P. lugdunensis* from AG3 are summarized in table 3.9. Figure 3.14 shows length-width scatter diagrams for both species. There is no size overlap except in the length and width of the M1. The m1 show a size gap, but this can be due to the low numbers of specimens. The M3 of *P. gaudryi* show a small overlap with the combined M3 of *P. lugdunensis* and *O. sondaari* (compare tables 3.2 and 3.8). The m3 show no overlap.

Table 3.9. Main differences between *Parapodemus gaudryi* and *Parapodemus lugdunensis* populations from Los Aguanaces (AG3).

feature	<i>Parapodemus gaudryi</i>	<i>Parapodemus lugdunensis</i>
size	larger	smaller
hypsoodonty	stronger	weaker
shape M1	more elliptical	less elliptical
position t1 in M1	more anteriorly	more posteriorly
shape t1 in M1	round	more elongated
size t3 in M1	relatively large	relatively small
posterior spur on t3 in M1	present in most specimens	absent in most specimens
t6-t9 connection in M1 and M2	variable height and sometimes absent	always present
t7 in M1 and M2	incipient t7 may be present	absent
antero-central cusp m1	may be absent	present
buccal ridge in m1 and m2	well-developed	less well-developed
antero-labial cusp m2	more elongated	more round
orientation wear surfaces	more horizontal	more inclined

3.5.7. Populations attributed to *P. gaudryi*

The rich sample of "*Parapodemus lugdunensis*" from VIP studied by Adrover (1986, his figure 46) shows a size gap in the M1. It is almost certain that the larger specimens belong to *P. gaudryi*.

The middle Turolian assemblage of *Parapodemus* "sp." from Aljezar B (Adrover, 1986) in the same region fits the description of *P. gaudryi* very well and is attributed to this species. This extends the record of *P. gaudryi* in Spain from the lower to the middle Turolian.

3.6. Discussion

The proposed phylogenetic relationships between the Murinae present in the Teruel-Alfambra region between about 10 and 6 Ma is shown in figure 3.15. *Progonomys hispanicus* is the first murine recorded in the Teruel-Alfambra region. It appears in the basal part of the lower Vallesian around 9.6 Ma, where it becomes the dominant small mammal. The find of a tooth of cf. *Progonomys hispanicus* in the lower Vallesian locality Pedregueras 2C (~10.0 Ma) in the Daroca area (see section 3.3.6) proves, however, that murines were already present in NE Spain during the early Vallesian (MN9). The

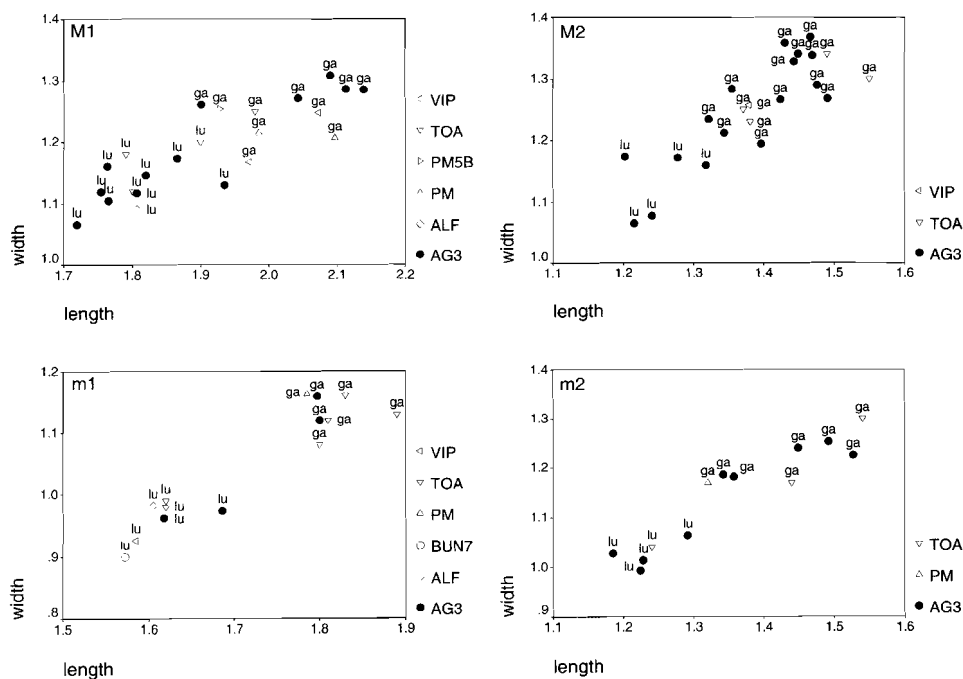


Figure 3.14. Scatter diagrams for the M1-2 and m1-2 of *Parapodemus* from the lower Turolian of the Teruel-Alfambra region.

expansion of the geographical range of the Murinae into NE Spain around the lower-upper Vallesian transition (9.7 Ma) appears to have been an abrupt event, since the lower Vallesian assemblages from ROM3 and PER5 (~ 9.7 Ma) do not contain a single murine tooth.

Supposedly, *Progonomys hispanicus* arrived in SW Europe during the late early Vallesian (late MN9) as evidenced by its presence in Pedregueras 2C and Ampudia 9 in the Duero Basin (López Martínez et al., 1986). Aguilar et al. (1991) claim a much earlier find of late Aragonian-early Vallesian (MN7/8-9) *P. cf. hispanicus* in the karst locality Castelnou 1B (eastern Pyrenees, France). However, this assignment is uncertain because of the possibility of faunal mixing in fissure deposits.

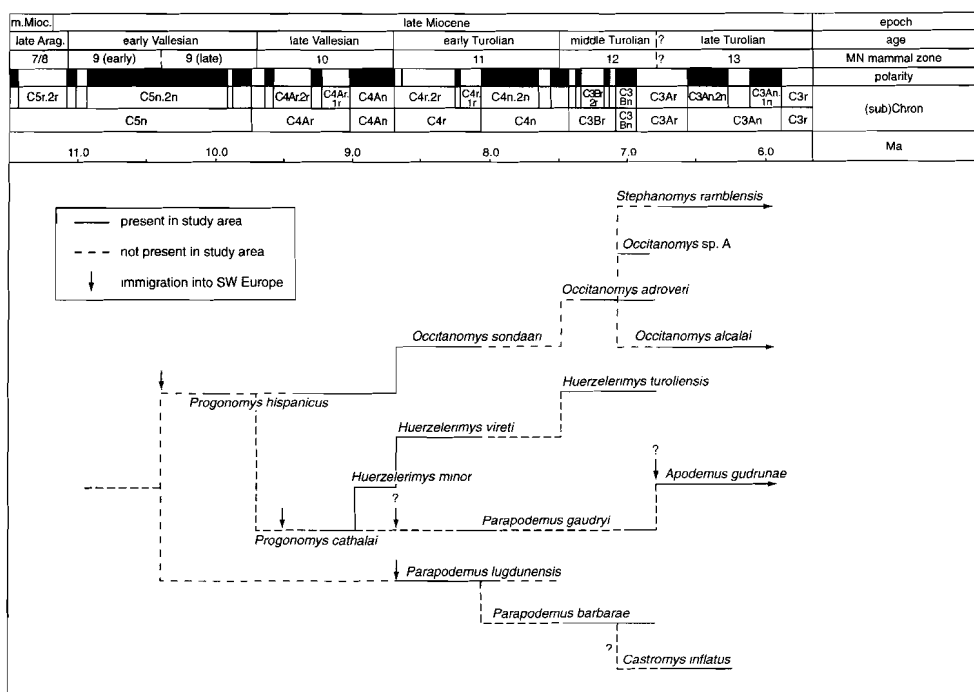


Figure 3.15. Proposed phylogenetic relationships between the Murinae present in the Teruel-Alfambra region between about 10 and 6 Ma. Solid lines indicate presence in the Teruel-Alfambra region (gaps shorter than 0.5 m.y. are ignored). Numerical ages of ranges and MN zonal boundaries according to Krijgsman et al. (1996), Garcés et al. (in press), and chapter 2. Time scale according to Cande and Kent (1995); dating of marine stages according to Berggren et al. (1996).

The origin of *Progonomys hispanicus* is not clear. The material from Sinap Tepe, Anatolia (Sen, 1997) is of interest in this context. It includes murines from two lower Vallesian (MN9) localities: locality 108, dated at 10.4-10.3 Ma, and locality 8A, which is slightly younger. The small assemblage from 8A shows *Progonomys* and *Parapodemus* morphotypes, but seems to represent one species. Specimens from Mahmutköy, European Turkey, mentioned by Ünay and de Bruijn (1984), also shows mixed *Progonomys*-

Parapodemus features. There are, however, uncertainties concerning the age of this locality. It could be either MN9 (*Myocricetodon* is still present) or MN10. In Pakistan, *Progonomys* is known from ~12 Ma onwards (Jacobs and Downs, 1994; Flynn et al., 1995). Because the oldest species (cf. *Progonomys* sp.) is neither described nor pictured, statements on the relationship of this species and the Vallesian murines from Europe cannot be made. *Progonomys debruijni* is probably not the ancestor of *P. hispanicus*, because its first appearance is relatively late (9.8-9.7 Ma, recalibration based on Barry et al., 1982; Flynn and Jacobs, 1982; Jacobs et al., 1989), and its morphology too derived. (The t1 and t4 are more elongate and the t12 more reduced than in the M1 of the earliest *P. hispanicus*.)

The immigration of *Progonomys cathalai* in the Teruel-Alfambra region occurs at 9.3 Ma. Its arrival seems to be a diachronous event, because in Kastellios Hill (Crete), it occurs between the localities KA1 and KA2A (de Bruijn and Zachariasse, 1979) which corresponds to an age of ~9.6 Ma (Woodburne et al., 1996). In section 3.3.4 it was shown that the earliest assemblages of *P. hispanicus* in the upper Vallesian (MN10) of Spain resemble *P. cathalai* in various features. Because, as it seems, there is no clear evidence for a lower Vallesian record of *P. cathalai*, it is hypothesized that *P. hispanicus* gave rise to *P. cathalai* in the late early or early late Vallesian.

P. hispanicus develops into *Occitanomys sondaari* in SW Europe during the latest Vallesian and earliest Turolian (van de Weerd, 1976, and above). By the middle Turolian (MN12) the small-sized *O. sondaari* is replaced by its medium-sized descendant *O. adroveri* (van de Weerd, 1976). The latter can be considered as the ancestor of the large middle Turolian *Occitanomys* sp.A (see appendix A), the small middle Turolian to Ruscinian *O. alcalai*, and the genus *Stephanomys*. *Stephanomys* (*S. stadii*) appears first in southern France and southern Spain in the middle Turolian (Mein and Michaux, 1979; Martín Suárez and Freudenthal, 1994). The first *Stephanomys* species entering the Teruel-Alfambra region is the slightly more advanced *S. ramblensis*. The entry of this species is used to define the base of the upper Turolian boundary (van de Weerd, 1976, and chapter 2).

Huerzelerimys is considered to be a descendant of *P. cathalai* (Mein et al., 1993). The size increase marking the transition from *H. minor* to *H. vireti* was discussed in section 3.4.5. It is followed by another size increase characterizing the transition from *H. vireti* to the middle Turolian (MN12) species *H. turoliensis* (van de Weerd, 1976).

The ancestry of the Turolian *Parapodemus* species is rather complex. In my opinion, there are two possibilities for the direct ancestor of *Parapodemus gaudryi*:

1) *Progonomys cathalai*. This species has a similar size as *Parapodemus gaudryi*. The elliptical shape of the outline of the M1 of *Parapodemus gaudryi* is present in *Progonomys cathalai* morphotypes (e.g. pl.2: figs. 5 and 6), and both species have the relatively anterior position of t1, t4 and t9 in M1 in common. The evolutionary trend from *P. cathalai* to *P. gaudryi* would involve an increase in hypsodonty, and in the relative frequencies of the t4-t8 connection (including the development of an incipient t7) in M1-2, the t6-t9 connection in M1-2, the antero-central cusp in m1, and the c1 in m3.

2) *Parapodemus lugdunensis*. Evolution towards *P. gaudryi* would involve size increase, transformation of the t1 in M1 towards a more rounded shape and a shift of the

t1 towards a more anterior position, and various other features (see table 3.9). An argument against this possibility is that a well-delimited antero-central cusp in the m1 is not always present in early assemblages of *P. gaudryi* (e.g. four out of six m1 have this cusp in AG3), whereas this cusp is always well developed in *P. lugdunensis*. For this reason the first hypothesis is preferred over the second one.

If hypothesis 1 is correct, then *Parapodemus* is almost certainly polyphyletic. Given this hypothesis, the only possibility for a single-rooted origin of the genus would be the case where *P. gaudryi* gave rise to the other *Parapodemus* species as well. Because *Parapodemus* species (not *P. gaudryi*) of MN10 age (de Bruijn et al., 1996) and even MN9 age (reinterpretation by Mein et al., 1993 of data of Lungu, 1981) are reported, the speciation from *Progonomys cathalai* to *Parapodemus gaudryi* and the subsequent evolution towards the earliest *Parapodemus* species should both have occurred very early, probably during the early Vallesian. Since there is no clear evidence for the presence of *Progonomys cathalai* in lower Vallesian deposits, and for *Parapodemus gaudryi* in lower and upper Vallesian deposits, a single-rooted origin of *Parapodemus* is improbable in view of hypothesis 1.

The ancestor of *Parapodemus lugdunensis* is expected to show a morphology resembling *Progonomys hispanicus* (see above). Evolutionary changes towards *P. lugdunensis* would include a further development of the t4-t8 and t6-t9 connections in M1-2 and of the anterior central cusp in m1.

P. lugdunensis could very well be the ancestor of *P. barbarae* as advocated by van de Weerd (1976). Both species have relatively low and flat cusps, the t1 in a relative posterior position and the t7 very poorly developed. The main difference is the large size of *P. barbarae* implying a size increase in this lineage. Both species occur together in the lower Turolian (MN11) locality Lobrieu, southern France (Demarcq et al., 1989) whereas in Spain *P. barbarae* characterizes the middle Turolian (MN12).

Except for a smaller percentage of the t7 in M1-2, and a less well-developed spur on t3 in M1, *P. gaudryi* from the early Turolian (MN11) of Spain and from the middle Turolian (MN12) of Greece are almost indistinguishable from the late Turolian *Apodemus gudrunae* (MN13) (e.g. pl. 3: figs. 1, 7, 8, and 10). I therefore place these two species in one lineage. The reasons not to follow van de Weerd's (1976) reconstruction of a lineage *P. barbarae*-*A. gudrunae*, and that the molars of *P. barbarae* are less hypsodont than those of *P. gaudryi* and *A. gudrunae* that the M1 of *P. barbarae* do not show the elliptical shape which is characteristic for the other two species (compare pl. 3: figs. 1, 7, 8 and 10 with pl. 3: fig. 11), and that the t7 in the M1-2 of *P. barbarae* is (almost) absent.

Whereas *P. lugdunensis* and *P. gaudryi* occur with about equal percentages in the lower Turolian (MN11) of the Teruel-Alfambra region, almost all middle Turolian (MN12) assemblages from this area contain only *P. barbarae*. Middle Turolian *P. gaudryi* is only known from the extremely rich assemblage of Aljezar B (see 3.5.7). In other middle Turolian localities, e.g. Masada del Valle 2 (van de Weerd, 1976) occasionally "*P. gaudryi* morphotypes" occur, but their low number and the morphological variability within the dominant species *P. barbarae* does not permit their recognition as a separate species.

Ubi materia, ibi geometria.
[Where there is matter, there is geometry.]

Johannes Kepler

Chapter 4

Stephanodonty in fossil murid: a landmark-based morphometric approach¹

Abstract

Landmark-based morphometric methods were used to study shape variation in fossil murid teeth. Nineteen landmarks were defined and recorded on the occlusal surfaces of first upper molars belonging to eight populations from upper Miocene and Pliocene localities in Spain. The study focused on an evolutionary sequence characterized by development towards a specialized crown structure known as stephanodonty. Population differences were investigated using Bookstein shape coordinates and analyzed using analysis of variance and Mahalanobis distances. Relative warp analysis was used to study the nature of the shape variation among the landmarks. The results are consistent with the accepted taxonomic classification, although the taxonomic position of one of the populations is problematic. The analyses show that the development towards stephanodonty (a feature defined by the presence of ridges) is correlated with changes in shape, which are themselves correlated with size in the evolutionary sequence studied. It is apparent that landmark-based approaches show promise for functional morphological and paleoenvironmental interpretations of fossil murid teeth.

4.1. Introduction

The number of applications of landmark-based morphometrics is growing, and more biological shapes are being described and analyzed with these new geometric methods (Bookstein, 1991). This study explores the potential of these methods for interpreting shape differences among lineages of fossil teeth from murid rodents during their Old

¹ Published as: Dam, J.A. van. 1996. Stephanodonty in fossil murid: a landmark-based morphometric approach. Pp. 449-461 in Marcus, L. F., M. Corti, A. Loy, G. J. P. Naylor and D. E. Slice, eds. *Advances in Morphometrics*. NATO volume 284. Plenum, New York.

World radiation evidenced in late Miocene and Pliocene sediments of Spain (Misonne, 1969; Michaux, 1971; van de Weerd, 1976). The study focuses on an extinct group of south-western European murids that show an evolutionary development towards stephanodonty (Schaub, 1938; Cordy, 1976). In complete stephanodonty (*sensu* Cordy, 1976) all cusps of the upper molars are connected by ridges, resulting in a garland - type dental pattern. Figure 4.1 shows this evolutionary trend in the first right upper molars of the sequence *Progonomys hispanicus*-*Occitanomys sondaari*-*Occitanomys adroveri*-*Stephanomys ramblensis*-*Stephanomys medius*-*Stephanomys donnezani*. This evolutionary trend is accompanied by a size increase and the development of a special type of hypsodonty (elongation of the cusps in an oblique, posterior direction).

The *P. hispanicus*-*O. sondaari*-*O. adroveri* lineage, described by van de Weerd (1976) and in the previous chapter, is an excellent example of anagenetic evolution (Chaline and Mein, 1979). The sequence *S. ramblensis*-*S. medius*-*S. donnezani* was interpreted as an evolutionary lineage by Cordy (1976 and 1978) and Adrover (1986). The suggested relationship of these two lineages is shown in figure 4.1, with *S. ramblensis* descending from *Occitanomys* (van de Weerd, 1976; Cordy, 1976).

A *Castillomys* species (*C. gracilis*) is included in this study because the genus shows stephanodonty, but the molars are small and brachiodont (van de Weerd, 1976; Martín Suárez and Mein, 1991). An *Apodemus* species is included as an outgroup. *Castillomys gracilis* and *Apodemus* aff. *jeanteti* are shown in their respective phylogenetic positions in figure 4.1.

4.2. Material and methods

In total, 250 first upper molars from eight populations were studied. Each population consisted of a different species. These eight species belong to five genera (table 4.1; figure 4.1). The first upper molar was chosen because it represents the most diagnostic element of the murid dentition.

The oldest four populations come from the basin of Teruel in northeastern Spain (van de Weerd, 1976). The most recent population comes from the Layna locality in central Spain (Cordy, 1976). The Caravaca locality of southwestern Spain is represented with three species: *Stephanomys medius* (Adrover, 1976), *Castillomys gracilis* (van de Weerd, 1976) and *Apodemus* aff. *jeanteti* (de Bruijn et al., 1975). One locality from each MN biochronologic zone (Mein, 1990, de Bruijn et al., 1992) from MN 10 to MN 15 was included. Absolute ages range from circa 9.5 up to circa 3 Ma. All material examined is stored in the collection of the Institute of Earth Sciences, Utrecht University. Nineteen landmarks were defined on the occlusal surface of the first upper molar (fig. 4.2), 13 along the outline and 6 on top, all in occlusal view. The 6 landmarks on top of the occlusal surface were defined in valleys between the cusps, rendering their location virtually independent of wear.

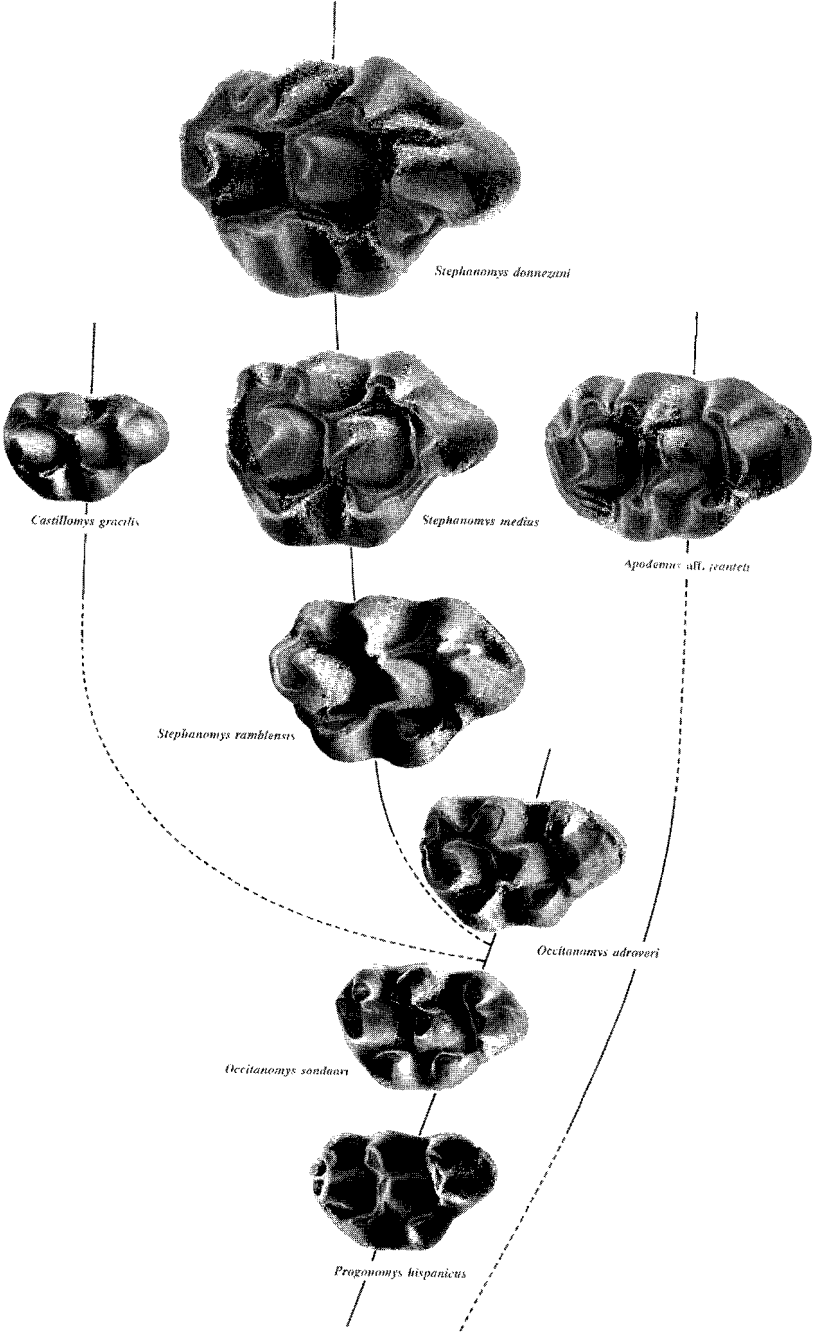


Figure 4.1. Evolutionary relationships among murid species used in this chapter, represented by their right upper molars. Dashed lines represent likely lineages. Enlargement: ca. 15x.

Table 4.1. Species used in this study and their collection data.

species	locality	MN biozone	Ma ¹	sample size
<i>Apodemus</i> aff. <i>jeanteti</i>	Caravaca	14	5	57
<i>Castillomys gracilis</i>	Caravaca	14	5	9
<i>Stephanomys donnezani</i>	Layna	15	3	12
<i>Stephanomys medius</i>	Caravaca	14	5	32
<i>Stephanomys ramblensis</i>	Villalba Baja 1	13	5.5	3
<i>Occitanomys adroveri</i>	Masada del Valle 2	12	7.5	66
<i>Occitanomys sondaari</i>	Tortajada A	11	8.5	37
<i>Progonomys hispanicus</i>	Masía del Barbo 2B	10	9.5	34
Total				250

¹ During preparation of the publication (van Dam, 1996) the detailed numerical time frame of chapter 2 had not been yet developed. Estimated ages in this column are based on van de Weerd (1976), Pevzner and Vangenheim (1993) and Steininger et al. (1990).

Landmarks 3, 5, 8, 10 and 12 are type 2 landmarks in the classification of Bookstein (1991): they are points of maximum curvature of the outline and are associated with cusps. Similarly, 4, 6, 7, 9, 11 and 13 are type 2 landmarks: they are points of maximum curvature associated with valleys. (Note that these last 6 landmarks could also be defined as intersections, namely of a valley with the outline. Interpreted in this way they become type 1 landmarks. However, the bottoms of these valleys usually do not form distinct lines but rather represent lines of maximum curvature between adjacent cusps.) Landmarks 14, 15, 17, 18 and 19 come close to type 1 landmarks: they are defined as the "intersections" of the central valleys (which do approach distinct lines) with lines perpendicular to these valleys running through the lowest part of the connections between the two adjacent cusps. In a number of specimens one or two additional small cusps have developed next to the central anterior cusp (i.e. *S. ramblensis* in fig. 4.1): a cuspule called t1-bis at the position of landmark 2, and a cuspule called t3-bis between the landmarks 13 and 15. In this cases, landmark 14 and 15 are defined by the intersections of the central valleys with lines perpendicular to these valleys running through the points of maximum curvature of the cuspules. Fig. 4.2b shows the construction in the case of t1-bis. Landmark 16 is best classified as type 2. It is defined as the meeting point of three valleys in the *Progonomys*, *Occitanomys* and *Apodemus* species. For the *Stephanomys* and *Castillomys* specimens a construction had to be made for this landmark (fig. 4.2b). Landmark 2 is a true type 2 landmark, being a point of maximum curvature of the outline. However, in some specimens the t1-bis was so large that it filled up the inner curve of the outline where landmark 2 was defined. When this was the case the position of this landmark was estimated as indicated in figure 4.2b. Landmark 1 is the anterior extreme of the molar in the orientation of figure 4.2. It is a type 3 landmark.

The *S. medius* and *S. donnezani* samples consist of specimens characterized by a moderate to high state of wear, because the landmarks 14, 15, 17 and 18 would not have been visible in specimens with little wear.

The specimens were placed horizontally, and x and y coordinates of the landmarks were recorded using a Reflex three dimensional measuring microscope. Coordinates of left-side specimens were re-calculated as though they came from the right side.

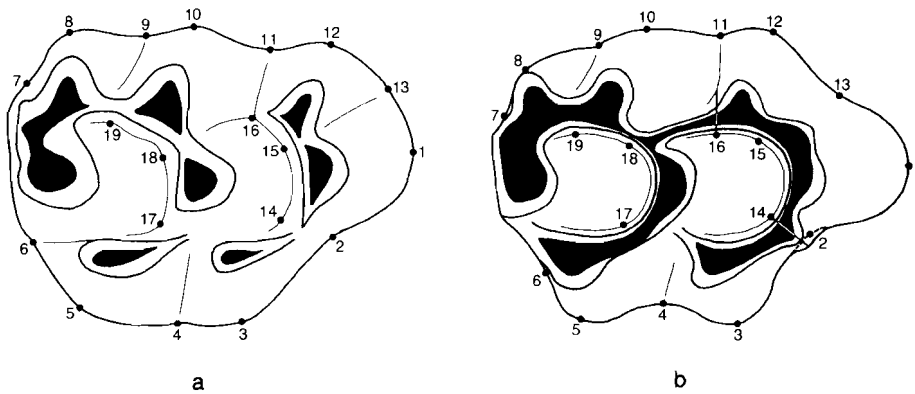


Figure 4.2. Location of landmarks on the occlusal surface of the right upper molar of a) an *Occitanomys*-type molar and b) an advanced *Stephanomys*-type molar. Orientation: right is anterior and bottom is lingual.

Landmarks 4 and 11 were chosen as endpoints for the baseline (Bookstein, 1991). This baseline was chosen instead of one in the direction of the long axis of the tooth, because landmarks such as 1, 13, 6 or 7 could be measured with relatively less precision.

Coordinates were rotated and scaled to the baseline with endpoints (0,0) and (1,0) to produce "size-free" Bookstein shape coordinates. The calculations were done by the program XY written by Baylac (1993), which was also used to calculate centroid sizes.

Uni- and multivariate analysis of variance were used to test for population differences. This was done with the SAS procedure CANDISC, which also produced Mahalanobis distances, D , between the populations. These distances were transformed into F values and were adjusted to compensate for bias according to Marcus (1993). An UPGMA clusteranalysis was performed on the adjusted squared D .

Generalized Least Square (GLS) fitting was performed to find consensus specimens for each of the eight populations. Consensus specimens were fitted by least square fitting to the consensus specimen of the most primitive species, *Progonomys hispanicus*. The fits were calculated using the program GRF-ND written by Slice (1993).

The fitted consensus configurations were compared using relative warps (Bookstein, 1991; Rohlf, 1993) with the TPSRW program of Rohlf (1993b).

Different options within the program were explored, such as the use of the parameter α , whose values influences the scale of the non-linear deformations, and the option to include the uniform component (the linear part of shape change) as estimated by the method of Bookstein (1996). When the latter option is used the relative warps summarize non-linear as well as linear shape variation between the consensus specimens. The program TPSPLINE was used to visualize deformations of grids between a number of consensus specimens.

Partial warp scores (Bookstein, 1991; Rohlf, 1993a) and uniform components of the consensus specimen shapes were regressed on centroid size and geological time for the

P. hispanicus-*S. donnezani* evolutionary sequence by means of TPSREGR (Rohlf, 1993c). The consensus configuration of *P. hispanicus* was used as the reference. Deformation grids were produced for values of the independent variable. In each case, the initial condition was the average landmark pattern.

4.3. Results

4.3.1. Statistical differences between the populations

Table 4.2 shows the univariate F ratios and probability values for the separate x and y Bookstein shape coordinates (except those of the baseline, which have fixed values of (0,0) and (1,0)) that resulted from a one-way analysis of variance (ANOVA). Population differences were clearly significant for all the coordinates, except for x_{15} , and significant for all coordinates together (table 4.3). Table 4.4 shows the pairwise Mahalanobis D between the populations. The D are all significant with probability values less than 0.0001. Figure 4.3 shows the phenogram resulting from an UPGMA cluster analysis based on the adjusted Mahalanobis distances. It is interesting that *S. ramblensis* does not

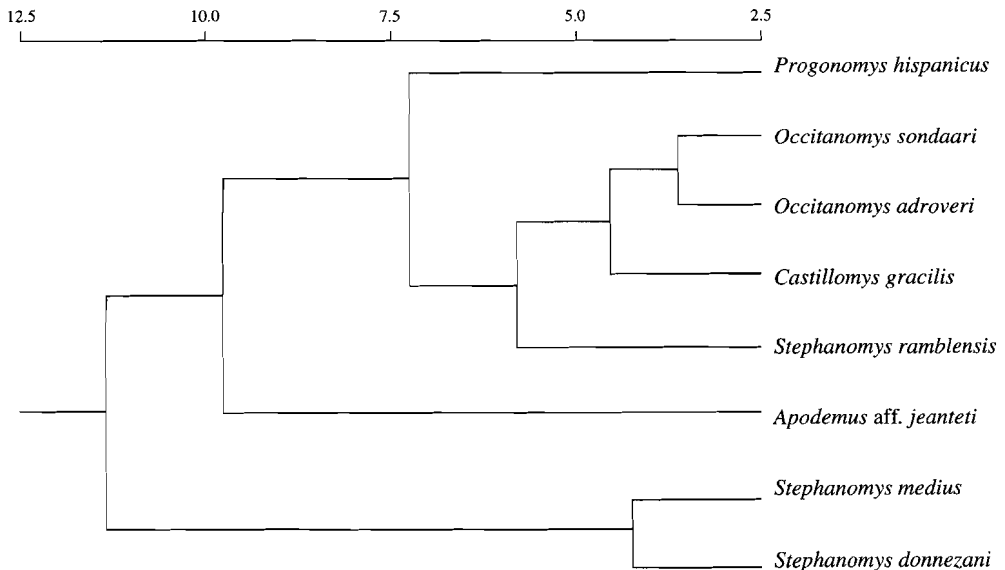


Figure 4.3. The UPGMA phenogram of populations based on adjusted Mahalanobis distances (see text) computed on 34 Bookstein shape coordinates.

Landmark-based morphometrics

cluster with the other *Stephanomys* populations, but with *Occitanomys* and *Castillomys*. That the *Apodemus* species does not form a tight cluster with the other species is consistent with its relative more distant taxonomic position.

Table 4.2. The *F* Statistics and probability values (df 7, 242) from one-way ANOVA (SAS procedure CANDISC) testing population variation for the Bookstein shape coordinates.

variable	<i>F</i>	<i>p</i> > <i>F</i>	variable	<i>F</i>	<i>p</i> > <i>F</i>
X1	36.37	0.0001	Y1	19.01	0.0001
X2	16.84	0.0001	Y2	7.63	0.0001
X3	23.10	0.0001	Y3	9.32	0.0001
X5	5.84	0.0001	Y5	22.07	0.0001
X6	112.34	0.0001	Y6	39.98	0.0001
X7	20.60	0.0001	Y7	121.47	0.0001
X8	4.07	0.0003	Y8	60.63	0.0001
X9	3.45	0.0015	Y9	64.05	0.0001
X10	4.17	0.0002	Y10	54.82	0.0001
X12	6.52	0.0001	Y12	32.27	0.0001
X13	30.56	0.0001	Y13	13.31	0.0001
X14	7.68	0.0001	Y14	34.52	0.0001
X15	1.24	0.2802	Y15	32.31	0.0001
X16	15.38	0.0001	Y16	9.75	0.0001
X17	4.52	0.0001	Y17	120.17	0.0001
X18	25.87	0.0001	Y18	103.19	0.0001
X19	14.58	0.0001	Y19	48.79	0.0001

Table 4.3. Multivariate statistics, *F* approximations and probability values (df 7, 242) from multivariate analysis of variance (SAS procedure CANDISC), testing population variation for the Bookstein shape coordinates.

statistic	value	<i>F</i>	numerator df	denomin. df	<i>p</i>
Wilks' Lambda	0.00	15.00	238	1448.11	0.0001
Pillai's Trace	3.92	8.04	238	1505.00	0.0001
Hotelling-Lawley Trace	35.96	31.32	238	1451.00	0.0001
Roy's Greatest Root	19.84	125.46	34	215.00	0.0001

Table 4.4. Mahalanobis distances between populations computed using Bookstein shape coordinates. Values below the diagonal are adjusted to remove bias.

	<i>A.aff.j.</i>	<i>C.g.</i>	<i>S.d.</i>	<i>S.m.</i>	<i>S.r.</i>	<i>O.a.</i>	<i>O.s.</i>	<i>P.h.</i>
<i>Apodemus aff. jeanteti</i>	0.0	10.0	14.2	13.0	12.5	9.6	9.5	7.5
<i>Castillomys gracilis</i>	9.8	0.0	10.8	8.8	6.2	4.3	4.7	7.0
<i>Stephanomys donnezani</i>	13.9	10.5	0.0	4.3	10.9	11.1	11.6	14.0
<i>Stephanomys medius</i>	12.8	8.6	4.1	0.0	9.5	9.5	10.0	12.3
<i>Stephanomys ramblensis</i>	12.2	5.9	10.6	9.2	0.0	5.0	6.9	10.3
<i>Occitanomys adroveri</i>	9.5	4.2	10.9	9.3	4.6	0.0	3.6	6.9
<i>Occitanomys sondaari</i>	9.4	4.5	11.4	9.8	6.6	3.5	0.0	5.8
<i>Progonomys hispanicus</i>	7.4	6.8	13.7	12.1	10.0	6.8	5.6	0.0

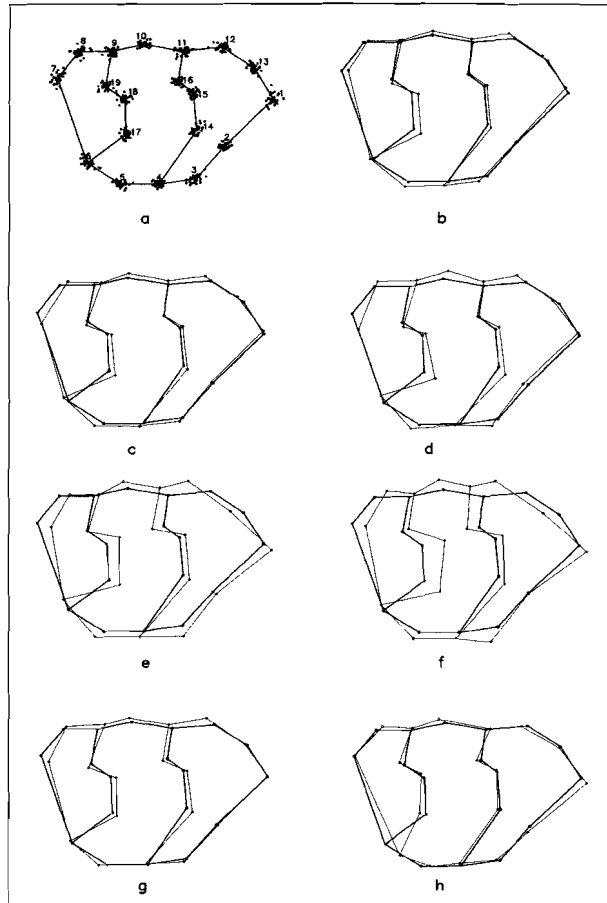


Figure 4.4. a) Generalized Least Square (GLS) fitted consensus specimen for the *Progonomys hispanicus* population together with the landmark points of all the fitted specimens. The landmark shape differences relative to the *P. hispanicus* consensus specimen (thin lines) of the consensus specimens (thick lines) of the populations of b) *Occitanomys sondaari*, b) *O. adroveri*, d) *Stephanomys ramblensis*, e) *S. medius*, f) *S. donnezani*, g) *Castillomys gracilis*, and h) *Apodemus* aff. *jeanteti*.

4.3.2. Landmark shape differences between the populations

Figure 4.4a shows the GLS fitted consensus specimen for the *Progonomys hispanicus* population along with all the fitted specimens of this population. Figure 4.4b-h show the landmark shape differences of the consensus specimens of the other species relative to the *Progonomys hispanicus* consensus specimen. The trends shown by the figures 4.4a-f are the general broadening of the molars, the straightening of the posterior border, the relative broadening and the anterior shift of the central region, and the sharpening of the anterior part in *Stephanomys medius* and *Stephanomys donnezani* by means of posterior-buccal movement of landmarks 10, 11 and in particular 12. The shape of *Castillomys gracilis* (fig. 4.4g) is very similar to that of the *Occitanomys* species. The largest

difference between *A. aff. jeanteti* and the reference specimen is the position of landmark 6, which has moved in the antero-lingual direction. This shift is associated with the formation of a new cusp, the so-called t7 (see fig. 4.1).

Table 4.5. Results of relative warp analysis on consensus specimens, based on the consensus specimen of the *Progonomys hispanicus* population as the reference. Reported for the first three relative warps are singular values, proportion of explained variance and probability values for equality of the remaining singular values. Results are given for three different combinations of program options. The $\alpha=0$ and $\alpha=1$ options give more weight to small-scale and large-scale variations, respectively. In case of $\alpha=1$ singular values are adjusted (see TPSRW documentation; Rohlf, 1993b).

relative warp analysis									
relative warp	$\alpha=0$, uniform component not included			$\alpha=0$, uniform component included			$\alpha=1$, uniform component not included		
	singular value	proportion variance	<i>p</i>	singular value	proportion variance	<i>p</i>	singular value	proportion variance	<i>p</i>
1	0.158	0.808	0.000	0.078	0.776	0.000	0.269	0.789	0.000
2	0.066	0.141	0.001	0.029	0.104	0.384	0.101	0.110	0.164
3	0.030	0.030	0.234	0.023	0.067	0.528	0.067	0.049	0.411

The results of relative warp analysis are presented in table 4.5 and figure 4.5. Table 4.5 shows that in all three cases a large part of the variation is explained by the first relative warp (80.8, 77.6 and 78.9 %, respectively). Inspection of the relative warp loadings (not shown) indicate that the value of α had little effect on the first relative warp. However, inclusion of the of the uniform component estimate resulted in significant differences between relative warp 2 and those higher, and yielded a meaningful second relative warp that did not reflect statistical error. The largest differences between the loadings of the first relative warp from analyses with and without the uniform component were localized in the posterior-lingual area of the teeth. Figure 4.5a shows the loadings as vectors for the first relative warp with estimation of the uniform component included. In the analysis excluding this uniform component, the vectors of landmarks 4, 5, 6 point more to the posterior side of the teeth (not shown here). Figures 4.5a and 4.5b show that transversal deformation is mainly represented by relative warp 1 whereas longitudinal deformation is represented in relative warp 2. The unique morphology of *Apodemus* is reflected in relative warp 2 by the anteriorly directed vectors from landmarks 5 and especially 6 (compare with fig. 4.4h). Figure 4.5c shows the first relative warp as a deformed grid (all eight populations included, $\alpha=1$). The inflation and relative anterior movement of the central region, and the generally symmetric shape (caused by the posterior movement of landmark 12 and the straightening of the posterior border) compared with the reference specimen were already observed in figure 4.4e and f. Figure 4.5d and e show a similar clustering of populations, indicating that the *x* and the *y* part of the uniform component contribute strongly to relative warp 2 and 1, respectively. Both

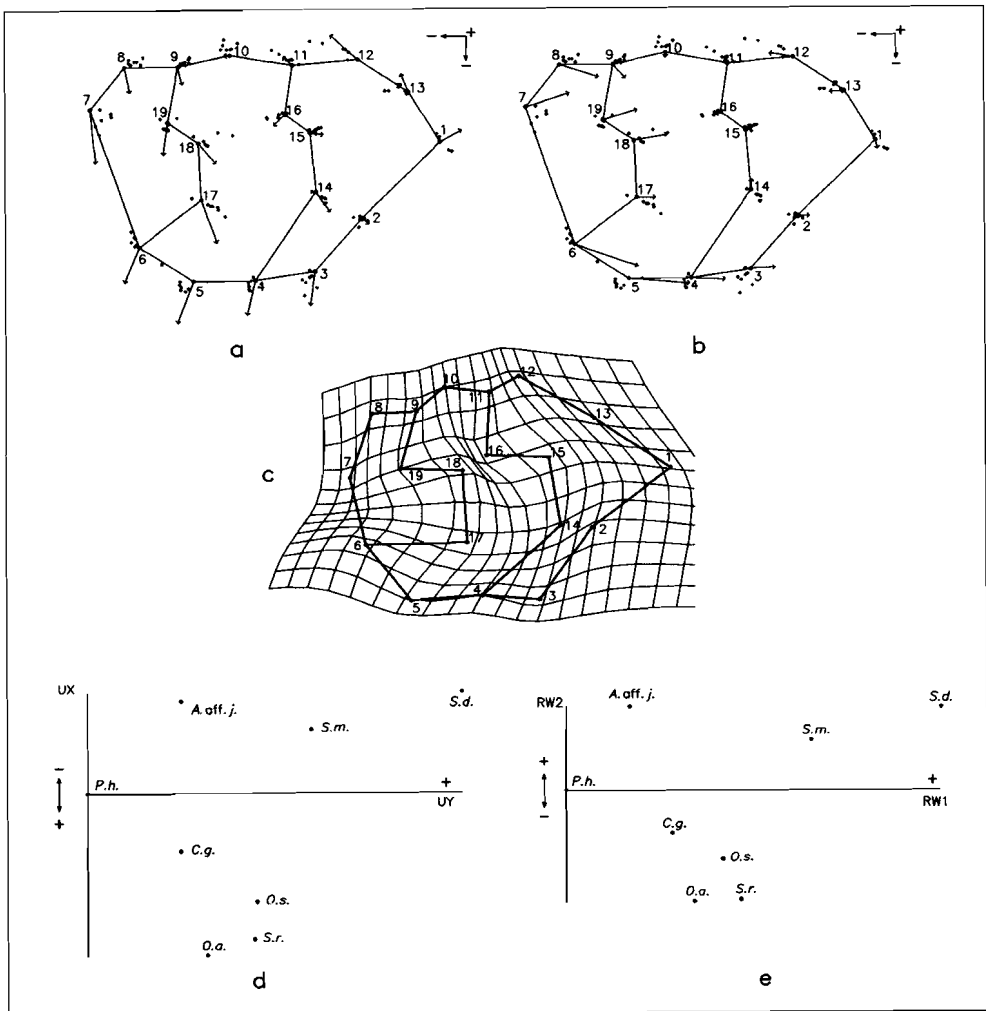


Figure 4.5. a) Vectors of landmark changes for the first relative warp. Estimation of uniform component included, $\alpha=0$, and all populations used. b) Vectors of landmark changes for the second relative warp. Options as in a). c) Deformation grid for the first relative warp. Estimation of uniform component not included, $\alpha=1$, and all populations used. d) Plot of uniform x (Ux) and uniform y (Uy). Options as in a). e) Plot of the first two relative warps. Options as in a).

plots are concordant with the phenogram of figure 4.3. It can be seen from the positions of the points in figure 4.5d that the order of the evolutionary sequence *P. hispanicus*-*S. donnezari* correlates well with the scores on relative warp 1, except for the relative "advanced" position of *O. sondaari*. Relative warp 2 separates the oldest four populations of the sequence (*Progonomys hispanicus*, the two *Occitanomys* species and *Stephanomys*

ramblensis) from the two most recent populations (*S. medius* and *S. donnezani*), which like *Apodemus* aff. *jeanteti* are characterized by stronger longitudinal shifts of landmarks. Both *A.* aff. *jeanteti* and *C. gracilis* remain relatively close to the primitive form, *P. hispanicus*.

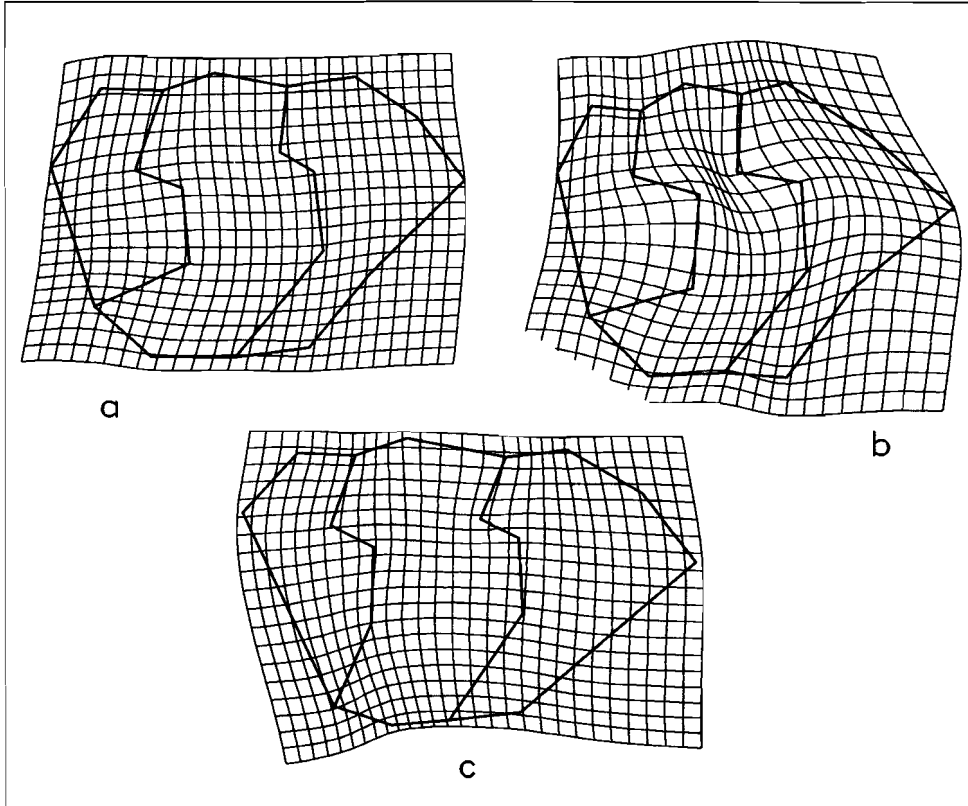


Figure 4.6. Thin-plate spline grid deformations from the *Progonomys hispanicus* consensus specimen into consensus specimens for a) *Occitanomys adroveri*, b) *Stephanomys donnezani*, c) *Apodemus* aff. *jeanteti*.

The figures 4.6 a, b and c show grid deformations from the primitive form to *O. adroveri*, *S. donnezani* and *A.* aff. *jeanteti*, respectively. The grids in figures 4.6a and b reflect the first relative warp (compare figure 4.5c). The deformation seen in figure 4.6b appears essentially to be a magnification seen in figure 4.6a, and corresponds to a more advanced evolutionary state. The deformation in figure 4.6c is of a different type, reflecting relative warp 2.

4.3.3. Regressions of landmark shape on size and geological age

Least-square regressions of the partial warp scores and uniform components of the consensus specimens for the populations of the *P. hispanicus*-*S. donnezani* sequence were performed on centroid size and on geological age by means of the TPSREGR program (Rohlf, 1993c). (See table 4.1 for ages. Average centroid sizes are 2.62 (*P. hispanicus*), 2.75 (*O. sondaari*), 2.99 (*O. adroveri*), 3.59 (*S. ramblensis*), 3.79 (*S. medius*) and 4.75 (*S. donnezani*)). The initial average conditions of the deformations in both figures 4.7a and b correspond to stages between *O. adroveri* and *S. ramblensis*, whereas in both cases the resulting conditions were chosen so that they were close to those of *S. donnezani*. Both grids can not be distinguished from each other by eye. This is not at all surprising because these two variables are highly correlated for this sequence ($r=0.98$).

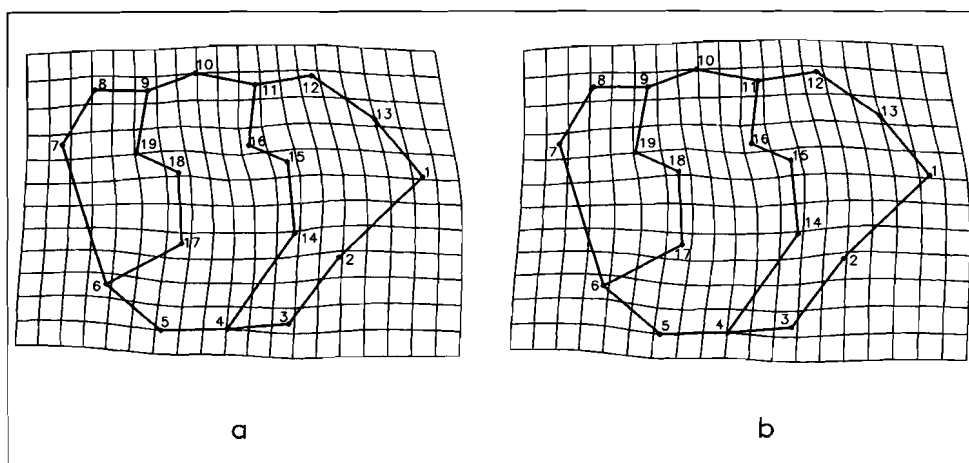


Figure 4.7. Deformation grid resulting from a least-square regression of the partial warp scores and uniform component for consensus specimens of the *P. hispanicus*-*S. donnezani* sequence on centroid size (centroid size= 4.483). The *P. hispanicus* consensus configuration was used as the reference. b) deformation grid resulting from a regression as in a) but with absolute ages as independent variable (absolute age= 3.25 Ma).

Figures 4.7a and b resemble strongly figure 4.6a, which represents the older part of the studied sequence. It is evident that the results of this regression analysis express, in another way, the effects of the first relative warp described above. However, as the shape changes are now explicitly related to size and time, we are justified in saying that allometry has played a major role in this evolutionary sequence.

4.4. Discussion

4.4.1. Taxonomy

The taxonomy of the murid species studied is largely confirmed, except for *Stephanomys ramblensis* van de Weerd, 1976, which clusters not so much with the other *Stephanomys* species as with the *Occitanomys* species. In this respect it is interesting that this author considers this species to be intermediate between *Occitanomys* and *Stephanomys* on the basis of size and stage of stephanodonty. He classifies it as *Stephanomys* because it fits in with the supposed evolutionary lineage toward the type species of this genus, *Stephanomys donnezani*. The sample size of the *S. ramblensis* population examined was very small ($n=3$), but this does not account for the observed clustering. New material of this species will be available soon for further work. The results presented here suggest a shape of *S. ramblensis* which is much closer to *Occitanomys* than it is to *Stephanomys*.

The shape of *Castillomys gracilis* as defined by the landmarks is also similar to that of *Occitanomys*. This is in agreement with the van de Weerd's (1976) observation that the molars of the two genera closely resemble one another in shape but not in size.

4.4.2. Evolutionary trends

The data presented above show that the degree of stephanodonty is correlated with changes in the pattern of landmarks as defined along the outline and on the surface of the molars. For instance, the anterior shift of the central landmarks allow an increase of oblique hypsodonty. Similarly, the lingual-buccal symmetry of the garland-like dental pattern in the true stephanodont forms corresponds to lingual-buccal symmetry in the landmark patterns. Trends towards broadening of the molars and the straightening of the posterior border, associated with increasing stephanodonty, have been mentioned in the literature. Results presented here show that the evolution towards a stephanodont pattern is adequately described by the first relative warp.

4.4.3. Functional morphology

Increase in stephanodonty and has been interpreted as adaptation to grass-eating (Michaux, 1982; appendix B). This interpretation is based on comparison of the dental morphology and diet of certain living African murids showing similar specializations (Misonne, 1969), and on the observation that the *Occitanomys-Stephanomys* cladogenesis occurs approximately simultaneously with the expansion of the steppe dwellers among the large mammals. In addition to an increase in stephanodonty, the molars of the *Progonomys hispanicus-Stephanomys donnezani* sequence also show a general increase in hypsodonty. The association of hypsodonty in herbivores with the bulk consumption of calory-poor and relatively abrasive food (such as grasses) is well established in rodents (Rensberger, 1975) and mammals in general (Janis and Fortelius, 1988).

An interesting finding revealed from this study is the trend towards alignment of the "valley" landmarks 7, 19, 18, 16 and 15 on the one hand, and 6, 17, and 14 on the other (fig. 4.5c). Presumably, such a configuration allows a longer and more efficient power stroke, with increased guidance of movement by longitudinal ridges (see also Weijs and Dantuma, 1975 on mastication in *Rattus norvegicus*). During the power stroke the cusp rows of the lower molars move anteriorly and longitudinally across the upper molars. The two anterior cuspules, the t1-bis and the t3-bis of stephanodont forms allow an even longer power stroke. In order to test such correlations and to make inferences about diet and paleoenvironment, more information concerning the function of the masticatory apparatus and wear patterns in recent murids is needed.

4.5. General conclusions

This study shows that complex three-dimensional shapes like those of teeth can be described by landmark patterns. The example of stephanodonty makes it clear that landmark-based morphometrics are a very useful tool to analyze shape in fossil murid molars. Population differences, evolutionary trends and allometry can be adequately described. The results are promising for taxonomic, evolutionary and functional morphological studies.

*The mammal is a highly-tuned physiological machine
carrying out with superlative efficiency
what the lower animals are content to muddle through with.*

James Arthur Ramsey

Chapter 5

Paleoclimatic reconstruction on the basis of micromammal faunal compositions, with special reference to life-history aspects

Abstract

The use of stratigraphic successions of relative abundances of micromammal species is discussed from the paleoclimatic point of view. Humidity trends can be inferred from relative abundance data, when combined with functional morphological interpretations of the dentition and locomotion, and with habitat preferences of extant relatives. The estimation of temperature trends is problematic without additional data on (paleo)biogeographic distributions. It is further suggested that small mammals can be used as proxies for seasonal aspects of climate, because their life-history strategies are strongly linked to the annual cycle. The subdivision into three demographic groups is a useful starting point for the reconstruction of seasonality type (humidity- or temperature-related) and the degree of interannual climatic variation (predictability).

Three applications are presented. All three use data from the late Miocene micromammal record of the Calatayud-Daroca and Teruel basins, NE Spain (age interval 11-6 Ma). The first application shows that the compositions of the gradually accumulated assemblages from these basins are biased by the differential life expectancies of the constituent groups. In the second application various measures of humidity are constructed and compared. They all point to an aridity maximum between 9 and 8 Ma. In the third application the early late Miocene competitive replacement of cricetids with low crowns by murines in Spain and southern Eurasia is examined. A link is hypothesized between this replacement and a postulated late middle to early late Miocene acme of Tibetan-Himalayan uplift. The regional, monsoonal effects of uplift would have favoured the evolution towards extremely reproduction-oriented murines in South Asia, while the supposed atmospheric effects

on Mediterranean wet-dry seasonality would have enabled the murine populations to expand and diversify in this area as well.

5.1. Introduction

Since Kretzoi (1957) published his micromammal-based Quaternary temperature estimates, successions of fossil small mammal assemblages have shown more and more their usefulness for quantitative paleoecological and paleoclimatic reconstructions. Especially teeth have proven to be valuable tools because generally they are well preserved, they can be extracted relatively easily from sediments by bulk sampling and screen-washing, and they are useful for taxonomic purposes. These advantages have stimulated the building of long, high-resolution sequences enabling long-term continental paleoenvironmental reconstructions (Daams et al., 1988; Barry et al., 1990; van der Meulen and Daams, 1992; Krijgsman et al., 1994b; Barry et al., 1995).

Andrewartha (1961) defined ecology as "the scientific study of the distribution and abundance of organisms". Although this is one of the more restrictive definitions of ecology, it stresses the importance of abundances for the understanding of ecosystems. In paleoecology, abundances are equally important, but it requires more steps before proper ecological conclusions can be drawn. According to van Couvering (1980), a sound paleoecological study should be based on the following types of information: (1) detailed species distributions; (2) type of sample bias; (3) correction for this bias; (4) body sizes of species; (5) guilds of species; (6) relative abundances of species. Besides the importance of high-quality data, this enumeration stresses two other important aspects.

The first aspect relates to sampling effects. For instance, differential preservation may seriously distort micromammal compositions (Andrews, 1990a, 1990b; Kowalski 1990). In the case of local successions of assemblages, paleoenvironmental interpretations may be less problematic, especially if the presence of "isotaphonomic" conditions (Behrensmeyer and Hook, 1992) may be assumed. The second aspect concerns the problem how ecological preferences of extinct taxa have to be inferred. To tackle this question, taxon-free methods have proven to be very useful in mammal paleoecology (Andrews et al., 1979; Van Couvering, 1980; Nesbit Evans et al., 1981; Artemiou, 1984; Damuth, 1992; Harris, 1993; Andrews, 1995). Typically, these methods are not based on taxonomic classifications, but on classifications of ecologically relevant features such as diet, locomotion, size, etc. The advantage of such methods is that they allow direct ecological comparisons with extant communities and environments.

In this paper it is attempted to sketch the potential of successions of micromammal assemblages for paleoclimatic reconstructions. In addition to the more conventional applications such as humidity and temperature reconstructions, special attention is paid to the potential use of life-history characteristics of small mammals for the reconstruction of seasonal aspects of climate. An important step in this direction was set by van der Meulen and Daams (1992) who explained part of the variation in their

Miocene rodent succession by r- and K- selectedness of groups. Their approach is elaborated here by investigating the possibility to use micromammals for the explicit estimation of seasonality type (temperature or humidity-related) and interannual variation or predictability. With regard to this kind of reconstructions, small mammals have a large potential because mean life expectancies at birth are in the order of seasons (typically a few months up to one year), making survival across seasons "a matter of life and death".

First, the general use of stratigraphic sequences of micromammal faunal compositions for the reconstruction of climate will be discussed. Next three applications will be presented. They all use data from the late Miocene micromammal succession of the Calatayud-Daroca and Teruel basins, NE Spain (11-6 Ma). In the first application the problem of compositional bias is discussed, and the effect of demographic bias on the composition of rodent families is tested. The second application deals with the reconstruction of humidity, and contains a comparison of four humidity-related measures and curves based on small mammals. The last application discusses the remarkable early late Miocene cricetid-murine replacement in the Old World. It is shown that the application of the actualistic principle towards life-history strategies leads to interesting hypotheses on the relations between tectonics, climate, competition and macroevolution in rodents.

5.2. Fossil micromammal abundances and climate

The relative importance of abiotic and biotic factors in the structuring of communities is subject of a long-lasting debate in ecology (Putman, 1994). Abiotic factors such as climate are known to affect animal communities in many ways, both directly and indirectly (by vegetation), but at the same time the reality of biotic processes such as interspecific competition is demonstrated in many extant groups, e.g. in rodents (Grant, 1972). Here the view is taken that abiotic factors such as climate define the "ecological space" for micromammals, but that the actual occupation of habitats is primarily mediated by the process of interspecific competition. This implies that it is assumed that relative abundances of species reflect relative abundances of certain adaptations to abiotic factors, which in turn reflect the levels of these abiotic factors (high temperature, high humidity etc.). Although extrapolation of classical competition theory from the ecological to the geological timescale is not without problems (Sepkoski, 1996), most paleobiological models that attempt to explain replacement of species (and the taxonomic levels directly above it) see a major role for competition. Only in particular cases such as mass extinctions or expansions into entirely new niches, the role of competition in replacement seems to be secondary to other factors (Benton, 1991, 1996).

In this section, the reconstruction of four climatic factors from fossil micromammal assemblages will be discussed. The discussion is slightly biased towards Neogene European groups. First, compositional bias is discussed.

5.2.1. Compositional bias

Paleoclimatic reconstructions based on relative abundances have to take into account the various types of bias that have affected the compositions. Taphonomical processes may cause serious biases in mammal assemblages (Behrensmeyer and Kidwell, 1985; Andrews, 1990a; Behrensmeyer and Hook, 1992), as may demographic characteristics (see below). However, bias in compositions does not automatically mean that paleoenvironmental reconstructions based on these compositions are wrong. The crucial point is whether the objective of study is the reconstruction of the life assemblage in an absolute sense (reconstruction of the relative abundances of the taxa as they were in the biocoenosis), or whether the objective is to infer only relative differences between assemblages. In the second case, it may not be necessary to estimate specific correction factors, because they may cancel in the calculation of differences between samples (isotaphonomy).

Relatively little attention has been paid to the demographic bias in fossil attritional (= gradually accumulating) assemblages. However, demographic bias in the relative abundances and calculations based on them (such as diversity) may be profound. Although discussed or touched upon by several authors (e.g. Johnson, 1964; Van Valen, 1964; Voorhies, 1969; Behrensmeyer et al., 1979; Western, 1980; Damuth, 1982), detailed studies on the consequences of differential turnover rates or generation times have remained relatively sparse.

In short, relative frequencies in attritional death assemblages are inherently wrong estimators of the relative frequencies in living populations, because the numbers of deaths (D_i) are based on counts within a time interval, whereas population numbers (P_i) have to be counted at a certain moment. In demography the two kinds of data are called "flow statistics" and "stock statistics" respectively. In ecology, "rate of turnover" and "standing crop" describe the same difference. In paleoecology the terms "normal population" and "census population" have been used to make this distinction (Hallam, 1972). Whereas normal populations are fossil assemblages accumulated after attritional mortality, census populations are brought about by catastrophic mortality (e.g. flooding or starvation).

Under the assumption of stationary populations a simple relation must hold between P_i and D_i :

$$P_i = D_i * e_{oi}$$

where P_i = population size of population i

D_i = number of deaths of taxon i in one year

e_{oi} = life expectancy at birth (e_0) of taxon i in years

Thus, numbers of deaths have to be multiplied by life expectancies (or equivalently, divided by their crude death or birth rate, which are equal in stationary populations) to have correct estimations for the contributions of the populations. For example, if fossils from species A and B are found in equal numbers, and it is known that on the

average members of species A live twice as long as members of species B, then the true population size of species A was twice that of B, all other things equal. Under the assumption that a fossil sample is a "residue" of an area of a certain size (e.g. an average hunting area in the case of predation of small mammals) also the density of A can be estimated to be twice that of B.

Both demographic and taphonomical bias will be further discussed within the context of the concrete example of section 3.1.

5.2.2. Paleohumidity

Changes in relative paleohumidity can be inferred from changes in frequency distributions of adaptations in the dentition and locomotion of micromammals. For example, open, relatively arid environments such as grasslands will be characterized by relatively many species and individuals adapted to ground-dwelling. The frequency of dentitions adapted to diets with a large proportion of fibrous components (such as in grasses) will be high. More humid environments such as forests contain more species and individuals that are adapted to an arboreal or scansorial type of locomotion and to diets containing a low proportion of fibrous components. Dietary and locomotory adaptations are inferred on the basis of functional morphology and by extrapolation from extant relatives (the principle of actualism).

Several classifications have been used for diets of fossil mammals (Andrews et al., 1979; Damuth, 1992; Collinson and Hooker, 1993; Harris, 1993; Gunnell et al., 1995). In studies where only micromammals are considered, the use of very detailed ecological classifications is deemed questionable. Firstly, the food spectra of many small mammals are broad. For instance, although often characterized as vegetarians, many rodent species are in fact omnivores (Landry, 1970). Secondly, exact dietary compositions are known for only a relative small number of extant species. For this reason it is not a simple task to classify even extant species, let alone their fossil relatives, into closely related diet categories such as granivory, frugivory, soft browsing etc.

Fortunately, reconstructions of humidity do not necessarily require a detailed classification of diets. For example, the identification of a grazing component is already very informative, because (by definition) grazing indicates the presence of grass, which replaces forest vegetation with decreasing humidity. Dental adaptations to grazing are well described in the literature and do not differ essentially in micro- and macromammals (Rensberger, 1973, 1975, 1982, 1986; Fortelius, 1985; Osborn and Lumsden, 1978; Weijs and Dantuma, 1981; Janis, 1988; Janis and Fortelius, 1988; Martin, 1993; Weijs, 1994). The basic adaptation is increase in tooth volume, realized by hypsodonty and/or the enlargement of the effective occlusal area. Volume increase is necessary because of the abrasive effect of fibrous food with low caloric value, necessitating bulk consumption, and of grit. Additional efficiency is provided by occlusal stress concentration on enamel edges with a preferred direction perpendicular to the power stroke.

Various classifications have been used for locomotion in fossil mammals and terrestrial animals in general (e.g. Andrews et al., 1979; Damuth, 1992). For humidity

reconstructions we consider a subdivision into the three categories ground-dwelling/fossorial, arboreal/scansorial, and semi-aquatic as sufficiently detailed.

5.2.3. Paleotemperature

Temperature adaptations in micromammals are not expressed very well in the skeleton, perhaps except for body size (e.g. Tchernov, 1979). More valuable are data on (paleo)biogeographic distributions (particularly North-South ranges). For example, an increase of northern groups at some point in a certain succession on the Northern Hemisphere may be interpreted as a cooling. Distributional data have the advantage that no knowledge is required of underlying physiological adaptations. Micromammal-based temperature reconstructions for the Quaternary have been produced this way already four decades ago (Kretzoi, 1957). Multivariate analyses are helpful in tracing a temperature component in a data set of compositions (Thackeray, 1987; van der Meulen and Daams, 1992).

5.2.4. Paleoseasonality

Almost all continental areas in the world (including the tropics) have seasonal climates. In such climates annual temperature and/or humidity fluctuations lead to fluctuations in plant production, and hence to fluctuations in resource availability for animals. Mammals have developed various types of life history and energy expenditure strategies to cope with seasonal variations in resource availability (Boyce, 1979, 1988; Bronson, 1989). Two extreme strategies are: (1) increase in reproductive effort, in order to exploit more efficiently the "good" season, and (2) increase in resource storage effort and fasting endurance (fat production, hibernation, etc.) in order to survive the "bad" season. Both strategies as well as intermediates, are found among small mammals, and will now be examined from the point of view of demography, thermoregulation, and food availability.

5.2.4.1. Demography

Continent-wide comparisons of the timing and length of reproductive seasons within species and genera of mammals demonstrate that variations in seasonality are partly buffered by shifts in the timing of reproduction (Bronson, 1989). Nevertheless, clear "ways of life" exist above the genus level. French et al. (1975) subdivide extant small mammals into three types according to demographic characteristics:

1) a group consisting of "murid" and "microtine" types with low survival rates and high reproduction rates, high mean densities and high interseasonal ranges of density. Mean life expectancies at birth commonly amount to 2-3 months in the wild. Maximum longevities in the wild typically are about 1.5 year (Niethammer and Krapp, 1978; Nowak, 1991; Lange et al., 1994). In energetic terms, the production/respiration ratios in this group are high.

2) a type consisting of 'cricetine' type of rodents and soricid insectivores, characterized by moderate survival rates, moderate reproduction rates and much lower

densities than the first group. Life expectancies and longevities are about twice those of the first group. New World cricetids such as Peromyscini are included as well as Gerbillinae. Old World Cricetinae are not included in the list of French et al. (1975), but they belong to this group according to their mortality, reproduction and density features (Nowak, 1991; Lange et al., 1994). Ochotonidae were tentatively put in the intermediate group, because the maximum longevity for some pika species is known to amount to about three years (Bernstein and Klevezal, 1965), which is a number similar to that of Old World Cricetinae.

3) a type with high survival rates, low reproduction rates and low densities. Life expectancies at birth are variable but the mean for the whole group is in the order of ten months, and the average maximum longevity is in the order of five years. Sciuridae, Petauristidae, Zapodidae, Heteromyidae and fossorial groups belong to this category. Gliridae, which are not included in the data set of French et al. may safely be placed in this group on the basis of their life history characteristics (Storch, 1978; Nowak, 1991; Lange et al., 1994). Extinct Eomyidae probably also belong to this group (van der Meulen and Daams, 1992). Erinaceidae were put into this group, because of the relative long lifespans of extant representatives (Nowak, 1991). No separate fourth category was created for the rare Castoridae and Hystricidae despite their high life expectancies. Since also their taphonomical bias is of a different type than of the other groups (much larger teeth, other predators) they were conservatively put into the third group.

In summary, values of demographic parameters in small mammals appear to be strongly determined by taxonomy (French et al., 1975; Stoddart, 1979; Bronson, 1989). This also implies that the theory of allometric scaling of life history characteristics on body size (e.g. Damuth, 1982; Reiss, 1989; Maiorana, 1990) does not work very well within micromammals alone. Although the larger species within (sub)families (e.g. *Rattus* species within Murinae) probably live somewhat longer than their smaller relatives, size appears to be secondary to taxonomy.

5.2.4.2. Thermoregulation

The demographic types appear to correlate rather well to certain strategies of thermoregulation. The prevailing thermoregulatory strategy against cold in Murinae and Arvicolidae is of the so-called metabolic type, and includes a large variety of biochemical and physiological changes which induce thermogenesis and increased basal metabolism (Banet, 1988; Gordon, 1993). The opposite strategy is adopted by many survival-oriented small mammals of group 3, the more northern representatives of which usually hibernate during the unfavourable season. Hibernation and related forms of heterothermy (such as daily torpor) in rodents are known in Dipodoidea (most of the genera), Heteromyidae (mainly species in the genus *Perognathus*), Gliridae (all genera, including the terrestrial representative *Myomimus*, see Peshev et al., 1960, and Kurtonur and Özkan, 1991), Cricetinae (two genera) and Sciuridae (tribes Marmotini and Tamiini) (Precht et al., 1973). Hibernation also occurs among Erinaceidae (Insectivora) and Chiroptera. For many of these groups it is assumed that

fossil representatives were similarly adapted (Cade, 1964). The group which is intermediate in terms of demographic characteristics (group 2) also shows intermediate types of seasonal heterothermy. New World cricetines such as *Peromyscus* and gerbils such as *Gerbillus* and *Meriones* never have developed hibernation although daily torpor occurs (Precht et al., 1973). The Old World hamsters *Cricetus cricetus* and *Mesocricetus auratus* show a weak form of hibernation under the proper circumstances with considerable individual variation (Pengelley, 1967; Robinson, 1968; Gordon, 1993). In evolutionary terms, the typical habit of food-hoarding in this group may represent only a first stage in the development towards pronounced seasonal preparations for hibernation, fattening being a more specialized stage (Cade, 1964).

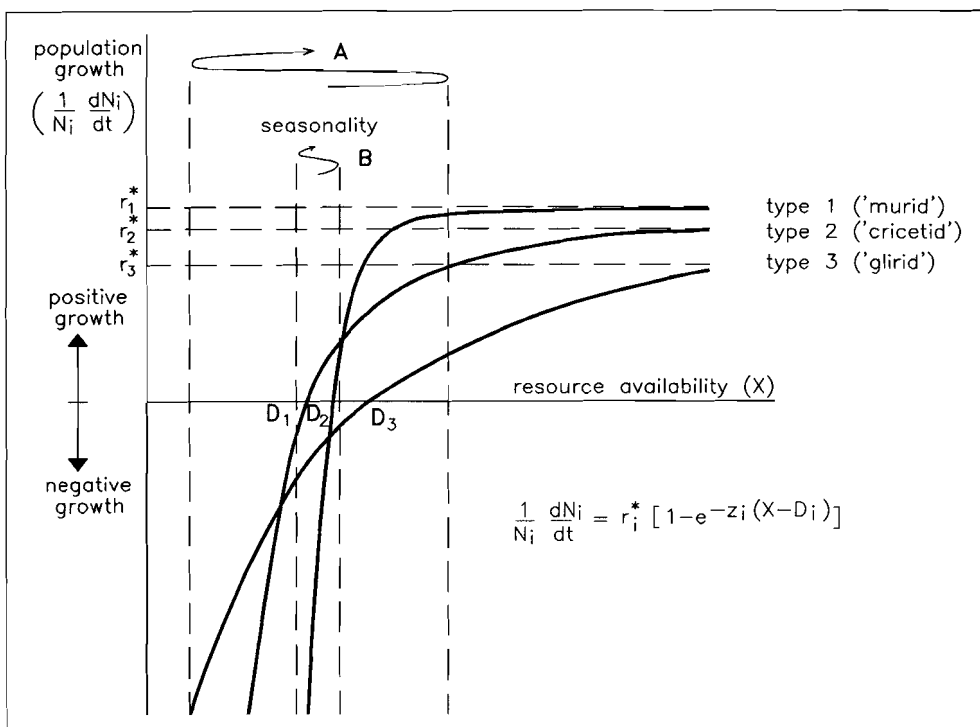


Figure 5.1. Theoretical model of seasonal population change for small mammal populations, which possess different types of life history strategies, and are in interspecific competition. The model is modified after Boyce (1979, 1988) who expresses fitness differences within populations as a function of the external factor of seasonality (in resource availability X) and the internal factors of reproductive potential (r'), resource demand (D), and fasting endurance (z). The resource availability X is dependent on both abiotic seasonal variation and consumer density. In the case of a strong seasonal amplitude (A) and a large food abundance, type 1 populations (see text) grow fastest. Type 3 populations decline least when food is scarce, and type 2 populations are superior in that part of the annual cycle which is not extreme in terms of resource availability. In the case of a less extreme seasonality amplitude (B), type 2 populations are superior during a large part of the year.

food-hoarding in this group may represent only a first stage in the development towards pronounced seasonal preparations for hibernation, fattening being a more specialized stage (Cade, 1964).

5.2.4.3. Food availability

The differences between the three demographic groups can also be described in terms of adaptations to seasonally fluctuating resources. Boyce (1979, 1988) proposed a model explaining fitness differences within populations during a certain period (typically an annual cycle) as a function of the external factor of resource availability X and the internal factors of reproductive potential (r^*), resource demand (D), and a factor which basically represents fasting endurance (z) (fig. 5.1). In this model the resource availability X is assumed to be dependent on abiotic seasonal variation and population density. This model is used as a conceptual framework to illustrate patterns of interspecific competition between rodents having different energy expenditure patterns. For example, let us examine the interspecific competition between representatives of the three demographic groups of figure 5.1. For the sake of

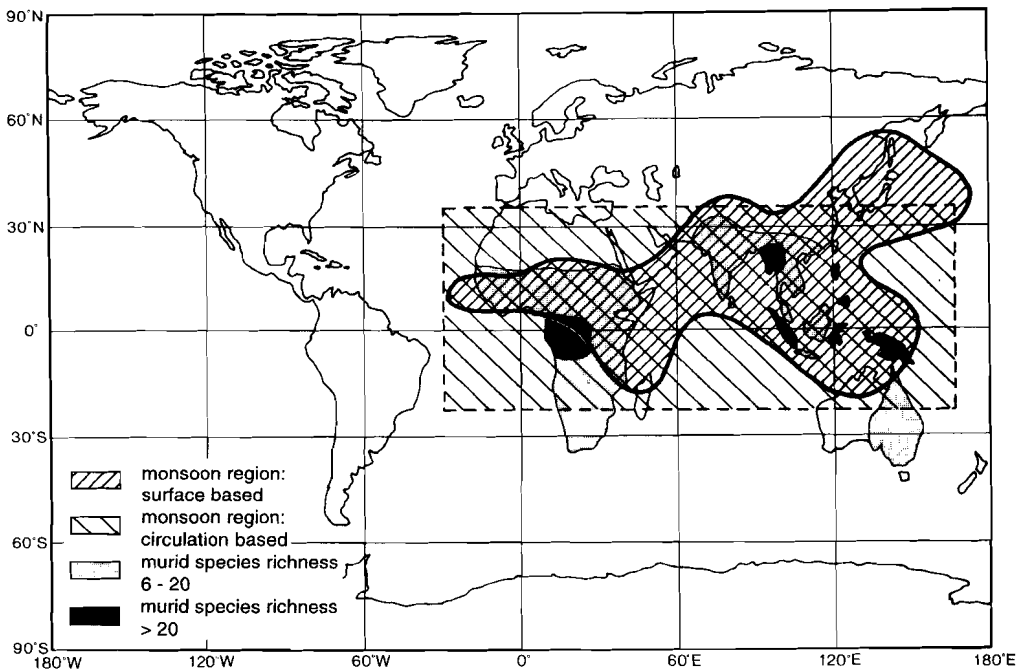


Figure 5.2. Monsoon region and murid species richness. The large overlap between the areas can be explained by the reproduction-oriented life history strategy of Muridae, enabling a rapid response to the between-year variability (unpredictability) in timing and amount of food availabilities. Monsoon region after Henderson-Sellers and Robinson (1994). Murid species richness after Misonne (1969).

simplicity, it is assumed that there are no differences in body size, diet and locomotion between these groups, and that reproduction is possible throughout the year. It follows from the model that one or the other group appears to be competitively superior over the others during certain parts of the annual cycle.

Let us first consider the case of a strong seasonal amplitude (A in fig. 5.1). When food is abundant, type 1 populations expand faster than type 2 and 3 populations because there is sufficient energy available for reproduction. The competitive advantage of type 1 is illustrated by the present-day success of murines in monsoon-dominated zones such as savannas, which are areas dominated by a wet-dry seasonality (fig. 5.2). When savanna grades into less productive biomes, murines give way to more survival-oriented groups, like gerbils (type 2) in the North African (semi) desert. When food is scarce, type 3 populations are superior because their populations decline less than those of the other two (fig. 5.1). Their superiority is related to a higher fasting endurance, made possible by large fat stores and hibernation, during which body temperature and activity are lowered. Glirids, which occur in all-year-wet temperate zones dominated by cool-warm seasonality (particularly cold winters) are a good example of a type 3 group.

Type 2 populations are superior in that part of the annual cycle which is not extreme in terms of resource availability. In the case of a less extreme seasonality amplitude (B in fig.1), these populations are competitively superior during a larger part of the year. Strategies like food hoarding and some weak hibernation in this group may be sufficient to cope with the slight seasonal decrease in resource availability. This decrease is too small to make deep hibernation efficient. The slight increase in resource availability during the favourable season is too small for type 1 species to take full advantage of their reproductive potential. Old World Cricetinae are an example of a type 2 group. The relative short period of favourable growth conditions for plants in extant steppe environments (Walter, 1994) would explain the success of Cricetinae relative to Muridae in these areas. Unfortunately, studies on interspecific competition between the two groups are very rare. (See Heisler, 1985 for an example of interspecific competition between more survival-oriented *Phodopus* and more reproduction-oriented *Mus*). It is not unreasonable to suppose that in times of enough food, murids have certain advantages over cricetids with similar diets because of a more efficient feeding apparatus. The possession of an additional lingual row of cusps in their upper dentition could be one of the adaptations allowing murids to process more food processed per unit time.

5.2.5. Paleopredictability

There is general agreement that (un)predictability is an important determinant of community structure (Pimm, 1978), and that predictable variations in resource availability can be accommodated by groups with appropriate life histories (Giller and Gee, 1986). Predictability is a climatic aspect which mainly relates to between-year variability, whereas seasonality relates to within-year variability.

An example of an adaptation to predictability are the "internal clocks" of deep hibernators of the efficiency-oriented group 3. These clocks regulate the tuning of

many physiological and behavioural changes to the annual cycle (e.g. Mrosovski, 1966, 1976; Precht et al., 1973; Ambid et al., 1990). Such tunings can only be efficient if the climate and food availability are fairly predictable.

By contrast, production-oriented species are better adapted to unpredictable environments. For example, various studies indicate that tropical savanna-dwelling murines (groups 1) tune their reproduction to the (unpredictable) rain period(s) and/or periods of abundant food supply (Delany, 1972; Taylor and Green, 1976; Cheeseman and Delany, 1979; Perrin, 1980; Delany and Monro, 1986; Leirs et al., 1993, 1994; Firquet et al., 1995). These animals show a tremendous adaptability of reproductive mechanisms, including post-partum oestrus, more rapid maturation in generations of females born early in the wet season, and anoestrus in the dry season.

Representatives of group 2 (the 'cricetine' type) are intermediately adapted with regard to predictability. The difference between this group and group 1 is reflected in the kind of reproductive triggers used. Whereas in Murinae the common reproductive trigger seems to be related to the presence of (certain) foods, a photoperiod trigger is common in Old World Cricetinae (Heideman and Bronson, 1993). Obviously, a reproductive cycle is more rigid (and predictable) when it is triggered by photoperiod than by food availability.

5.2.5.1. The concepts of r- and K selection

Adaptations to unpredictable and predictable climates have often been described as features of "r-selection" and "K-selection". The use of the concepts of r- and K-selection is avoided here on purpose, because these terms have led to considerable confusion in the ecological literature (Boyce, 1984, 1988). One of the major reasons of this confusion is that the original r-K model (MacArthur and Wilson, 1967; MacArthur, 1972) has been put in a loose, multi-interpretable form (Pianka, 1970, 1972). The original model is very simple, and basically deals with density-dependent, intrapopulation selection only. In the original formulation, the separation between r- ("production") and K- ("efficiency") selection is defined only for the special case where various genotypes have different fitness patterns (defined as per capita growth rates). If (and only if) the fitness profiles are such, that the order of fitnesses reverses at a certain population density, r-selection is defined as the selection at densities lower than this critical point, and K-selection is defined as the selection at densities higher than this point (MacArthur, 1972). The subsequent overextension of this simple intraspecific selection model to a continuum of species which are not assumed to interact in some way is bound to lead to confusion, because in absence of the reversal point, no definition of r- and K-selection can be given.

Another problem with the r-K model *sensu* Pianka, is the implicit assumption that per capita resources decrease in such a way that populations grow to some fixed carrying capacity K. However, in a seasonal or otherwise fluctuating regime, food availability is not only dependent on consumer density, but also on external abiotic variation in time. This external factor continuously modifies K, which may attain very low values during the unfavorable season. It is obvious that negative population growth has to be modeled explicitly along with positive growth (figure 5.1). However,

negative growth was not formulated in the original models, probably because these models were first formulated in the context of island colonization.

According to r-K theory, "K-selected species" should have higher average densities than "r-selected species", because they use resources more efficiently. However, in small mammals the opposite pattern is observed: so-called "r-selected", fast-reproducing murids and arvicolids have much higher average densities than other groups (French et al., 1975). This is because true saturation at a fixed K will almost never occur in seasonally fluctuating regimes. This will be particularly true for small mammals because their mean life expectancies are often lower than the length of the annual cycle. During the unfavorable season some kind of density-dependent "K-

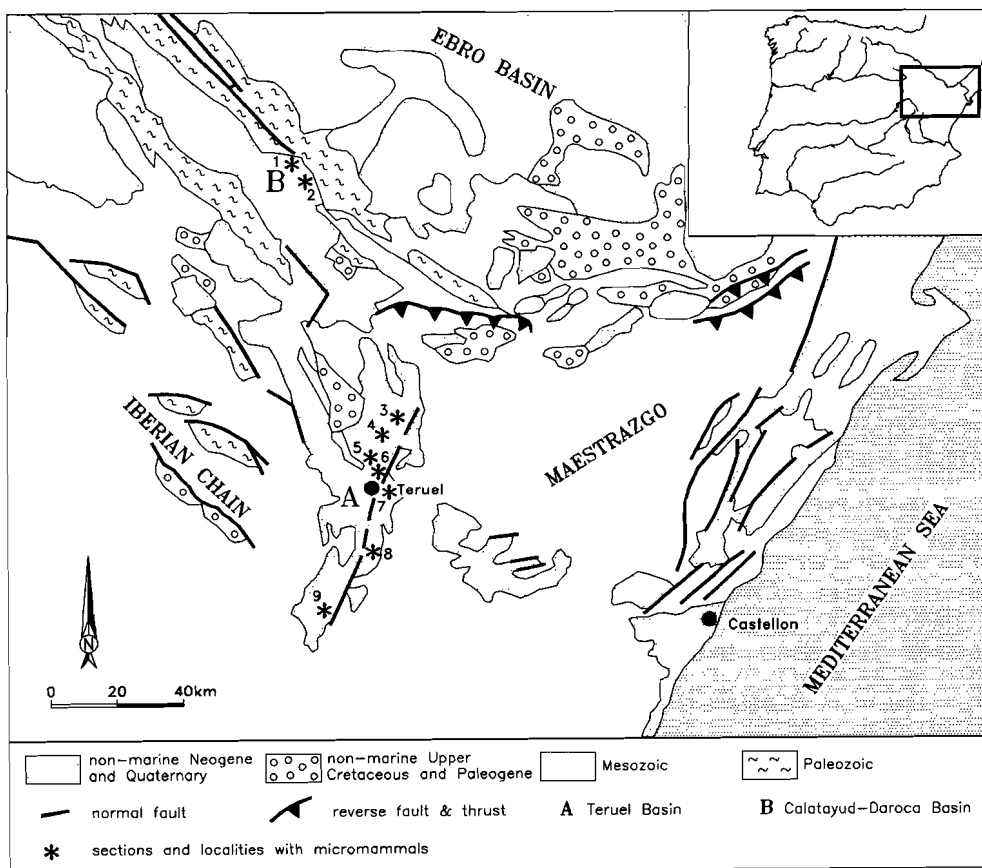


Figure 5.3. Locations of the sections and localities with micromammals in the Calatayud-Daroca and Teruel basins 1: Pedregueras (PED), Carrilanga (CAR); 2: Nombrevilla (NOM); 3: La Roma (R), Masía de la Roma (ROM), Peralejos (PER); 4: Las Casiones (KS); 5: Concul (CC); 6: Tortajada (TO), Masada del Valle (MDV), Masía del Barbo (MB), Puente Minero (PM); 7) Vivero de Pinos (VIP), Rambla de Valdecebro (VDC); Los Mansuetos (LM), La Gloria (GLO), Los Aguanaces (AG); 8) Cubla (CU); 9) Casas Altas (CASAL).

advantage" can be said to occur, although in the negative sense. In this case, the superiority of the so-called K-selected species (with high fasting endurance) is not associated with population increase, but with population decrease, which is less than the decrease in the so-called r-selected species (see also Fowler, 1981).

5.3. Three applications

Three applications are presented. They all use data from the 11-6 Ma old late Miocene micromammal succession from the Calatayud-Daroca and Teruel basins in NE Spain (van de Weerd, 1976; Daams et al., 1988; chapter 2, see fig. 5.3 for the position of the fossil localities). These are (mainly) extensional basins filled by alluvial-fan and shallow-lake sediments. Relative abundances of micromammals were calculated as the number of first and second molars, except for the Lagomorpha, of which the abundances were calculated as twice the number of third premolars. In case these elements were absent but other teeth or skeletal material was present, then frequencies were counted as one. Frequencies were also counted as one, in case

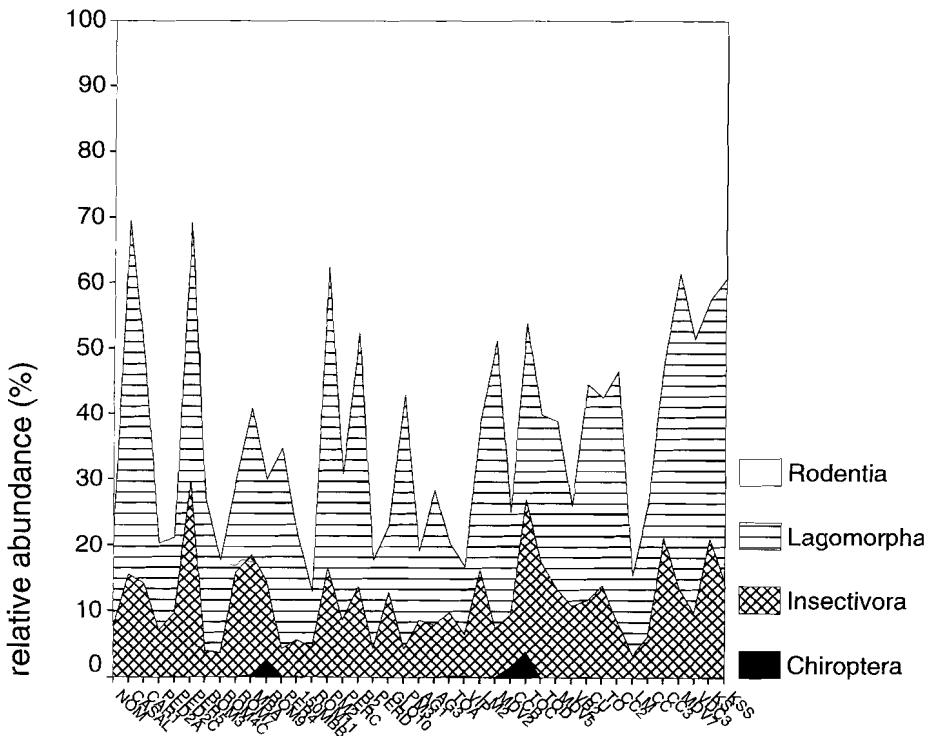


Figure 5.4. Relative abundances of orders in the upper Miocene micromammal assemblages of the Calatayud-Daroca and Teruel basins.

skeletal material (e.g. teeth of Castoridae) originated from a macromammal sample. Apparently, some material sampled in the seventies has been lost (Erinaceidae from Pedregueras 2C, Tortajada A and Valdecebro 3, Lagomorpha from Pedregueras 2C and Los Mansuetos 2, and *Paenelimnoecus* from Valdecebro 3). In these cases relative frequencies from time-equivalent samples were used to estimate missing values. Differences with counts of van de Weerd (1976) are mainly due to a different treatment of damaged specimens, and the addition of some unpublished material collected by van de Weerd. Abundance data can be obtained from the author on request.

Figure 5.4 shows the relative abundances of the four orders Rodentia, Insectivora, Lagomorpha and Chiroptera in the death assemblages. Figure 5.5 shows the frequency spectra for the rodent and insectivore genera. Lagomorphs are almost exclusively represented by representatives of the ochtonid *Prolagus*. The very rare bats belong to the Vespertilionidae and Rhinolophidae.

5.3.1. Compositional bias

5.3.1.1. Demographic bias

Rodent family compositions are used to illustrate the effect of demographic bias. Only localities with more than 300 first and second rodent molars are selected. Castoridae and Hystricidae are left out. The fine-grained clayey/marly lithologies of the sampled layers and the low average sedimentation rates suggest attritional (gradual) accumulation of many small mammal generations, rather than an instantaneous catastrophic accumulation. This implies that life-expectancy values should be used as weight factors to estimate the life-assemblage compositions.

The e_0 values used are based on averages for demographic types of French et al. (1975) mentioned above. We use 1.80 month for Muridae, 3.35 for Cricetidae, and 9.95 for Gliridae, Sciuridae and Zapodidae. Figure 5.6a shows the original death assemblages and figure 5.6b shows the distributions after correction with life expectancies. It appears that the adjusted compositions are much more homogeneous than the unadjusted ones, because the long-living families are not under-represented any more. The dominance of murids is less extreme than suggested by the number of their fossil remains, and sciurids and zapodids are less marginal than suggested by figure 5.6a. The average heterogeneity, as measured by Simpson's reciprocal index increases with 32% from 1.30 to 1.72.

This example shows that demographic bias seriously distorts fossil rodent compositions and diversity measures based on them. This implies that a diversity value for one areas and/or time slice cannot always be compared to that of an other area or time slice, unless some corrections are applied. A special case is represented by the comparison with extant assemblages. If the compositions of extant assemblages are based on a census of counts of living individuals, then (abundance-based) diversity values cannot be compared directly to fossil values, given the attritional accumulation of the latter.

5.3.1.2. Taphonomic bias

Unfortunately, a detailed taphonomical study of the Spanish succession could not be performed until now. Nevertheless, there are some arguments which support the assumption of more or less isotaphonomic conditions within the succession:

1) Localities are selected in the field on the basis of a specific lithology, typically being a several dm thick grey/black marl/clay containing bone and/or gastropod fragments. In addition, several of the sections show rhythmic alternations between the fine-grained fossiliferous beds and limestone beds, suggesting a repetition of

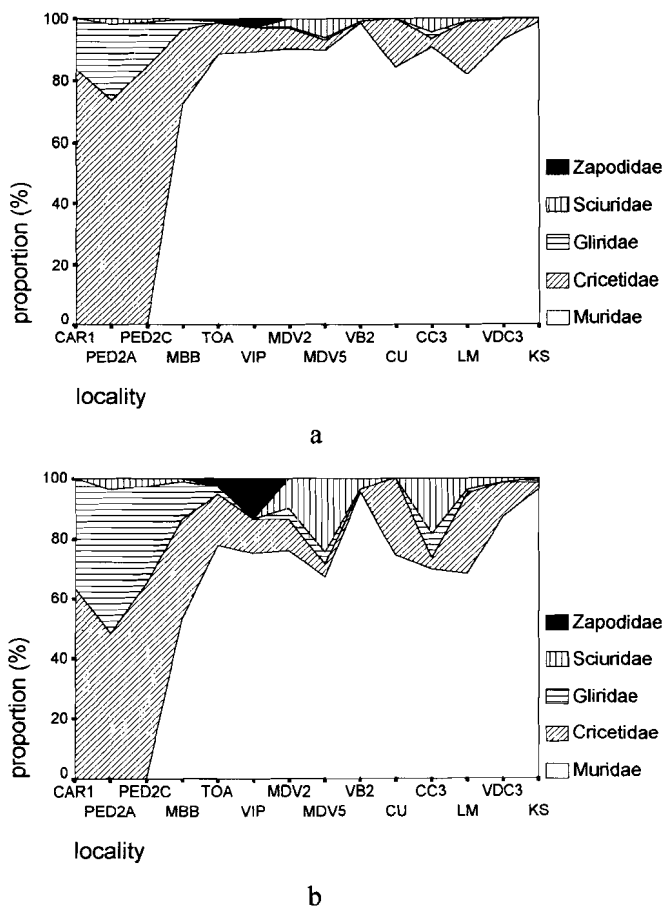


Figure 5.6. The effect of demographic bias on the proportions of upper Miocene rodent families of the Calatayud-Daroca and Teruel basins. Only localities with more than 300 first and second molars are included. Castoridae and Hystricidae are not included. a) uncorrected death assemblages; b) corrected death assemblages; proportions are multiplied by correction factors and re-scaled to 100%. The correction factors correspond to the mid-points of ranges of life-expectancy at birth values for the three demographic groups distinguished by French et al. (1975): 1.80 month for Muridae, 3.35 month for Cricetidae, and 9.95 months for Zapodidae, Sciuridae, and Gliridae. Note that the adjusted faunas (b) are more heterogeneous than the unadjusted ones (a).

sedimentary environments. The variations in organic content of the sampled layers may reflect variations between swamp, pond or small lake environments. According to Alvarez-Sierra et al. (1990) these differences in environments may be associated with slight differences in preservation of teeth of some groups, but this was not tested statistically.

2) Isotaphonomy with regard to predation is more difficult to assess. The critical point is whether the pellets and scats of selective predators differ in preservation potential. The presence of selective predators as such does not exclude the possibility of isotaphonomic conditions, as long as the predation regime remains constant. Owls are generally recognized as a main source of micromammals in sediments. Like mammal carnivores, most owl species are more or less opportunistic in their search for food, although some extant owl species are known to have specialized on specific micromammal groups like voles (Andrews, 1990a, 1990b; Kowalski, 1990). However, if the ecological rule that specialists are less abundant than generalists (e.g. Cockburn, 1991) also holds in this case, the effects of selective predation may remain small. It is possible to identify predators from breakage, digestion effects, and relative proportions of the skeletal elements of preys (Andrews, 1990a) or from chemical properties (Dauphin et al., 1997). However, to perform such analyses on complete successions is extremely time-consuming.

Reworking does not seem to be an important factor disturbing small mammal sample compositions from lacustrine sediments. Rare "anachronisms" can normally be explained by contamination between samples during processing. One of the reasons for the rarity of reworking could be the fragility of micromammal remains (Alvarez-Sierra et al., 1990). Another reason may be that mixing occurs only at a very local scale in low-energy environments. Especially young, uncompacted clays and marls may erode relatively easy, but stratigraphic displacement may be small, at least smaller than the stratigraphic distance between successive localities in the sequence.

The extensive work on the sections in the Calatayud-Daroca and Teruel basins has shown that compositions are surprisingly predictable. Composition of levels could be successfully predicted from the compositions from levels below and above it. In addition, local "noise" not related to the general patterns of co-occurrences of groups can effectively be filtered out *a posteriori* by statistical methods (chapter 6).

5.3.2. Humidity reconstructions

41 localities of the late Miocene small mammal succession in the Calatayud-Daroca and Teruel basins were selected for humidity reconstructions. Chiroptera were not included in the calculations. Four humidity-related measures were compared:

1) % non-grazing individuals. Calculation of this percentage was based on an initial classification into four dietary groups, to which the following taxa were assigned: a) insectivorous/carnivorous: all Insectivora and the glirid *Eliomys*; b) omnivorous with about equal amounts of vegetarian and non-vegetarian food: Zapodidae (*Eozapus*). (The remaining omnivores were assigned to one of the other categories if either animal or vegetarian food predominates.); c) grazing or partly grazing vegetarian: the hypsodont cricetids *Hispanomys*, *Ruscinomys*, and *Blancomys*, the stephanodont,

"broad-molared" murids *Occitanomys* and *Stephanomys* (see appendix C) and the Lagomorpha *Prolagus* and *Alilepus*; d) non-grazing vegetarian: all other micromammals. The proportion of non-grazing individuals (a+b+d) is regarded as a measure for relative humidity. Similarly, the relative abundance of c is regarded as a measure for relative aridity. The assignment of the taxa to the groups was based on both neontological literature (Niethammer and Krapp, 1978; Chapman and Flux, 1990; Nowak, 1991; Lange et al., 1994) and paleontological literature (van de Weerd and Daams, 1978; van der Meulen and de Bruijn, 1982; Daams and van der Meulen, 1984; Farjanel and Mein, 1984; Daams et al., 1988; van der Meulen and Daams, 1992; appendix C).

2) % arboreal/scansorial + semi-aquatic individuals. To the arboreal/scansorial group were assigned: Eomyidae (*Leptodontomys*), Petauristidae, and Gliridae except for *Myomimus* and *Tempestia*. The talpid *Archaeodesmana* and Castoridae were considered to be semi-aquatic. The rest of the micromammals were assigned to the terrestrial/fossorial category, and their relative abundance is regarded as a measure for relative aridity. (*Talpa* was considered to be the only true fossorial genus in the data set.) Attributions were based on the literature mentioned under 1.

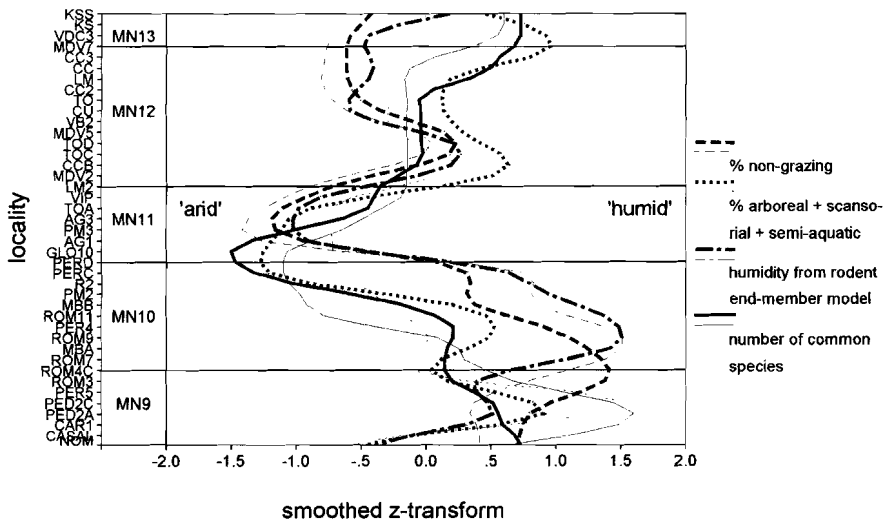


Figure 5.7. Smoothed standardized humidity-related curves for the upper Miocene of the Calatayud-Daroca and Teruel basins. Thick curves are adjusted for demographic bias, whereas the corresponding thin curves are not. The absolute number of common micromammal species varies between 5 and 11. See text for more information on the specific measures.

3) Humidity as modelled in chapter 6. In this chapter a multivariate technique (end-member modelling) is applied to a data set of 67 rodent compositions from Spain and some other parts of Europe, including the 41 localities used here. Prior to modelling, rodents were classified into nine ecologically defined groups on the basis of life

history/taxonomy, diet, locomotion, and to a lesser degree paleobiogeographic distribution. Muridae, Cricetidae, Gliridae, and Sciuridae were subsequently split into a "wet" and a "dry" group. "Wet" Sciuridae were included in one group together with Petauristidae and Eomyidae. Castoridae were kept as a separate "wet" group. The contributions of the 41 compositions to four theoretical end-member compositions were used to construct a humidity signal.

4) Species richness of common species. This measure indicates the heterogeneity, or non-dominance aspect of diversity. It is calculated as the number of species counted after 95% of all the specimens, with the taxa ranked from the most to the least abundant taxon (Johnson, 1964). By using the 95% criterium the effect of differential sample size is removed ($n \geq 20$). This measure is considered as a humidity-related measure, because it is generally believed that a) diversity is higher in more "favourable" environments and b) humid environments are more favourable.

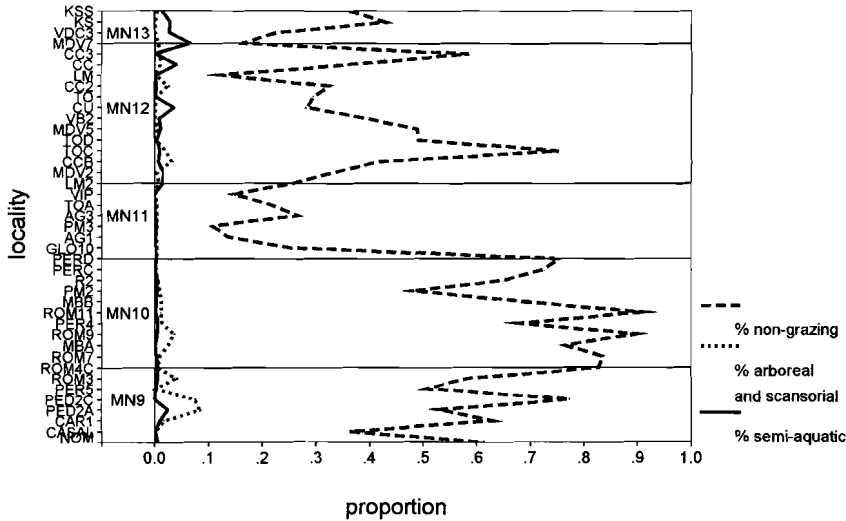


Figure 5.8. Humidity-related curves for the upper Miocene of the Calatayud-Daroca and Teruel basins, based on proportions of individuals having certain types of dietary and locomotory adaptations. See text for more information on the specific measures.

5.3.2.2. Comparison and discussion

Figure 5.7 shows the various curves. Thick lines indicate adjustment for demographic bias whereas thin lines are not adjusted. (The rodent end-member curve is robust against this bias, see chapter 6). The curves are standardized to facilitate mutual comparison, and a smoothing procedure is applied. The influence of life-expectancy correction appears to be relatively small. It appears from figure 5.7 that

there are two broad "humid" intervals, one corresponding to Neogene Mammal Zones MN9 and 10 (~11-9 Ma), and another corresponding to MN12-13 (~ 8-6 Ma). These humid intervals are separated by an arid interval corresponding to MN11 and the MN10-11 transition (9-8 Ma). The values of the grazing curve and rodent end-member curve are higher (more humid) for the MN9-10 interval than for the MN12-13 interval, whereas the levels of the other two curves are about equal. Another, smaller aridity maximum within MN12 at ~7 Ma is indicated by some of the curves. Figure 5.8 shows the raw proportions of the non-grazing, arboreal/scansorial and semi-aquatic groups. Despite the low frequencies of the latter two locomotory groups (the rest belongs to the terrestrial group), it can be observed that the humidity signal in the lower part of the record is more vegetation-related (higher frequencies of arboreal/scansorial), whereas in the higher part it is more related to open water (higher frequencies of semi-aquatic).

The differences in shape between the four curves in figure 5.7 might be caused by wrong assumptions on preferences or adaptations of genera. In addition, some taxa were forced into one dietary or locomotor category, although they show characteristics of two categories. The differences in the curves may also be related to the different ecological aspects expressed by the four measures. The relation between frequencies of animal adaptations to certain plant types and the frequencies of these plant types themselves is complex and certainly not linear, and will differ for locomotion and diet. Equally complex is the relation between the relative abundances of plant groups and levels of humidity. Animal diversity still measures another aspect, and although it is known to increase with humidity, it is also dependent on other environmental features such as predictability.

A clear difference between the curves relates to the position of the first humidity maximum. The diversity and locomotor curves show a maximum in MN9 whereas the dietary and rodent end-member curves have their highest values in MN10. The diversity maximum during MN9 could be related to the higher environmental predictability during this interval (see next application). The high correlation of diversity with non-terrestrial locomotion ($r = .54, p < .001$) points to another, possibly related explanation for higher species diversities in structurally more heterogeneous vegetation types (see Giller, 1984, and Putman, 1994). (It should be realized, however, that the absolute number of common micromammal species in the studied basins is low: it varies between 5 and 11, which is much lower than in contemporaneous Central European assemblages.). If a choice has to be made between the curves, the rodent end-member curve is preferred. On the one hand it is based on more data, both ecologically and geographically, and on the other hand "noise" in the compositions and the humidity signal is filtered out by the underlying end-member model (chapter 6).

The rodent-based climatic reconstructions by van der Meulen and Daams (1992) point to a gradually rising humidity in the Calatayud-Daroca basin from the middle-late Aragonian transition to the lower Vallesian. This humidification occurs after a middle Aragonian aridity maximum at ~17-14 Ma (ages after Krijgsman et al., 1996). Figure 5.7 shows that renewed aridification takes place during the late Vallesian to

earliest Turolian (i.e. between 9.5-8.5 Ma). It is interesting to note that an important turnover in Spanish large mammals marking the Vallesian-Turolian transition also leads to an increase in forms adapted to more open environments (Moyà-Solà and Agustí, 1990; Köhler, 1993) and to a decrease in diversity (Pickford and Morales, 1994; Cerdeño and Nieto, 1995). A pollen record from the Rhone basin (France) with an age close to the Vallesian-Turolian transition also indicates aridification (Farjanel and Mein, 1984), although micromammals from the same area indicate that aridification is not so strong as in Spain (chapter 6; data from Mein, 1984).

The possibility should not be ruled out that this aridification in SW Europe is an expression of Northern Hemisphere-wide climatic change. The estimations of the age of the North American land mammal age boundary between the Clarendonian and Hemphillian vary between 9.0 Ma (Woodburne and Swisher, 1996) and 8.4 Ma (Alroy, personal communication 1997). Both the Vallesian-Turolian and Clarendonian-Hemphillian boundaries are characterized by a diversity drop and a supposed extension of more open vegetation; Shotwell (1964) evidenced that grassland communities made their first appearance in the Northern Great Basin at the base of the Hemphillian.

During the late early Turolian (late MN11) or early middle Turolian (early MN12) humidity starts to increase again (figs. 5.7-5.8). A humidity maximum during MN12 for the Teruel basin during this interval was also inferred by Alcalá (1994) on the basis of the body size distributions of a set of selected late Vallesian-Turolian assemblages containing both macro- and micromammals. Unfortunately, there are not many data from Europe to compare with for this specific interval. The rodent-based analyses of chapter 6 include three MN11 and two MN12 localities from Alicante, southern Spain (data after de Bruijn et al., 1975). Although average modelled humidity is slightly higher for the MN12 localities compared to the ones from MN11, the differences are small. Renewed sampling (Freudenthal et al., 1991) has refined the record for this area and will allow more detailed reconstructions in the future.

A second small aridity maximum seems to occur within MN12, at ~ 7 Ma (fig. 5.7). The main interval for evaporite deposition in the Mediterranean (Messinian salinity crisis) occurs after 6 Ma (Gautier et al., 1994), and is not covered by our succession. Some localities described by Mein et al. (1990) and Adrover et al. (1993) from the Teruel area probably belong to this interval, but their ecological composition is not very different from that of older localities. This observation is consistent with the conclusion of de Bruijn (1989), who noted that Eastern Mediterranean Messinian-equivalent small mammal faunas are ecologically similar to both older and younger faunas.

5.3.3. The cricetid-murine replacement during the early late Miocene

In chapter 6 the classification of demographic types of rodents and a multivariate analysis of their relative abundances is used to reconstruct seasonality and predictability signals for the late Miocene of Spain and other parts of Europe (fig. 5.9). According to the results, an important shift towards a more unpredictable, wet-

dry seasonal climate occurred in Spain during MN10-11 between 9.4 and 8.2 Ma. This is about the interval that Murinae show their strongest diversification in SW Europe (chapter 3). Also in other areas of the Old World (eastern Mediterranean, Anatolia, and the supposed source area South Asia) murines expand and diversify during the early late Miocene (Jacobs and Downs, 1994; de Bruijn et al., 1996).

Why did murines become so successful from the early late Miocene onwards, and how were they able to replace the low-crowned cricetids which dominated the rodent faunas in these areas during the middle Miocene? On the basis of the discussion in 2.3, it is suggested here that such a replacement could be the consequence of a competitive advantage gained by the extremely reproduction-oriented murines as the result of environmental change. Selection for the murine life-history strategy would

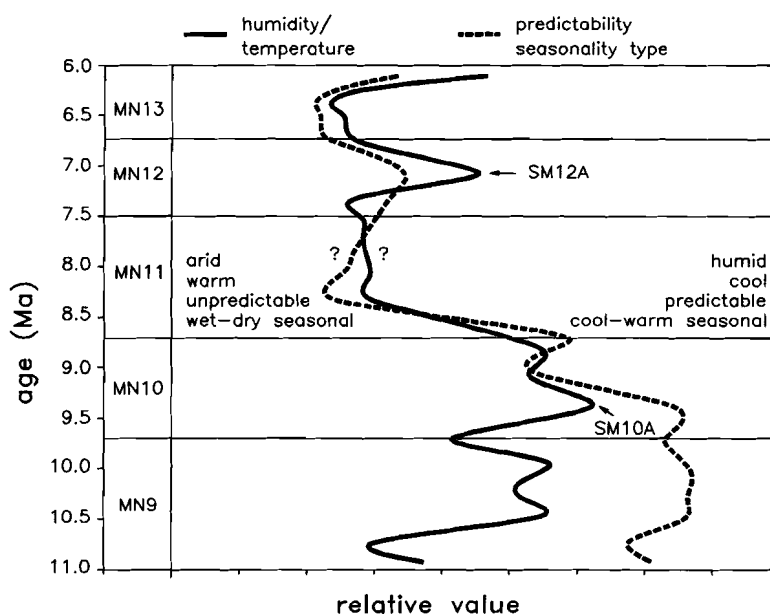


Figure 5.9. Climate curves for the Calatayud-Daroca and Teruel basins relative to numerical time (ages were converted to the time scale of Cande and Kent, 1995), based on end-member modelling of rodent compositions (chapter 6). Ages are based on magnetobiostratigraphic data (Krijgsman et al., 1996; Garcés et al., 1996, in press; appendix B). Parameter values were averaged per 0.2 m.y. (missing values were replaced by linear interpolation), and smoothed. Question marks indicate uncertainty because of missing data at 7.5, 7.7 and 7.9 Ma.

have occurred after an environmental change towards a stronger wet-dry seasonal and unpredictable climate. Obviously, the cricetid-murine replacement did not take place everywhere: cricetids remained superior in certain areas of the Old World where they persisted with large numbers until the present day (e.g. Central Asia). Nonetheless, their distributional area has undergone important shrinkage since the early late

Miocene. Today, the northern boundaries of the monsoonal region (fig. 5.2) seem to be the areas where Murinae and Cricetidae (particularly Cricetinae and Gerbillinae) are more or less in a competitive equilibrium.

An increasing number of studies stress the importance of Cenozoic climatic forcing by uplift of areas like the Tibetan plateau, Himalayas and Rocky Mountains (e.g. Ruddiman and Kutzbach, 1989; Raymo and Ruddiman, 1992; Kutzbach et al., 1993; see Hay, 1996 for a review). Recently, it has been proposed on the basis of geological evidence that an important phase of Tibetan-Himalayan uplift occurred between ~12-9 Ma (Amano and Taira, 1992; Prell et al., 1992; Harrison et al., 1993; Hodell and Woodruff, 1994; Raymo, 1994). The temporal correlation between uplift and rodent community change suggests a relation, and therefore it is proposed that:

- 1) An intensification of Tibetan-Himalayan uplift between ~12-9 Ma, leading to the onset or intensification of the monsoonal system in South Asia, guided the evolution towards modern, reproduction-oriented murines in this region around this time.
- 2) Northern Hemisphere-wide atmospheric circulation effects resulting from this uplift, leading to more arid, wet-dry seasonal, and unpredictable climates in the Mediterranean area, created ecological space for murines, and allowed them to expand into, and diversify in this region at the cost of other groups such as cricetids.

The idea that monsoonal circulation in Asia develops as a consequence of high topography is generally accepted (Flohn, 1950; Hay, 1996). Indications for monsoon intensification between 11-7 Ma come from Indian-Ocean diatom records (Schrader, 1974; Burckle, 1989), radiolarian and planktonic foraminifer records (Prell et al., 1992; Prell and Kutzbach, 1992), and Pakistan paleosol records (Quade et al., 1989, 1995; Retallack, 1991). A relation between a developing monsoon system and evolutionary change leading to reproduction-oriented murines is to be expected. Such life-history strategies are advantageous in monsoonal areas, because of a) the large food availabilities during wet seasons, b) a significant interannual variability in the onset and duration of these wet seasons (Fairbridge, 1986), and c) the frequent occurrence of fires. It is striking that the northern limit of the typical monsoonal conditions (running through northern Africa, northern India and southern China, see fig. 5.2) corresponds to the isoline of murine species number 5, which is considered to be an important boundary (Misonne, 1969; Montuire, 1994). North of this line there are only a few murid species, whereas just south of the line the number of species rapidly rises to more than ten to reach numbers more than 50 in SE Asia and more than 30 in Central Africa. Although not defined as a monsoonal region in terms of reversing winds, southeastern Australia falls within a region of highly seasonal and erratic precipitation (Leeper, 1970), favouring a murine reproductional strategy.

The early evolutionary history of murines in South Asia consists of various steps. The first murines (*Antemus*) (Jacobs, 1978; de Bruijn and Hussain, 1984; de Bruijn et al., 1996) appear in Pakistan at ~ 14 Ma (Jacobs and Downs, 1994). The evolution

towards a modern murine dental morphology occurs at ~12 Ma when *Antemus* develops into *Progonomys*. By that time murines become the dominant small mammals in this area. Next (10-9 Ma) follows an episode of cladogenesis which results in three lineages (*Progonomys*, a small and a large *Karnimata* with the latter developing into *Parapelomys*) (Jacobs and Downs, 1994). Thus, estimations of 12-9 Ma for uplift intensification in South Asia and 11-9 Ma for onset or intensification of the monsoon correlate very well with important evolutionary events in South Asian murines, such as the rise of modern (i.e. post-*Antemus*) murines and their subsequent diversification into several genera.

The Spanish murine record starts at about 10 Ma (late early Vallesian or late MN9) (chapter 3). An important event within the Vallesian of Spain (and other areas) is the numerical explosion of murines (*Progonomys*) at the early-late Vallesian (MN9-10) boundary (9.7 Ma in Spain). This event is part of the so-called "Vallesian crisis", which affected both small and large mammal faunas in Europe (Moyà-Solà and Agustí, 1987; Agustí and Moyà-Solà, 1990). The main diversification phase of murines in Spain occurs somewhat later, at the end of the Vallesian (~9.0-8.7 Ma) when *Progonomys* is replaced by *Huerzelerimys*, *Occitanomys* and *Parapodemus* (van de Weerd, 1976; Mein et al., 1993; de Bruijn et al., 1996; chapter 3)

A relation between uplift in South Asia and the change towards more arid, wet-dry seasonal and unpredictable climates in Spain (fig. 5.9) is plausible according to recent simulations of the effects of Tibetan-Himalayan uplift on Northern Hemisphere atmospheric circulation. Effects on the Mediterranean climate include decreasing summer precipitation due to a shift in mean wind direction from westerly to northerly and northeasterly directions (Ruddiman and Kutzbach, 1989), which is due to the relation between topography (particularly high mountains and plateaus) and the occurrence of mid-latitude stationary atmospheric waves (Manabe and Terpstra, 1974). Climatic predictability has not been simulated by these models, but a relation between uplift and increased Northern Hemisphere climatic unpredictability is to be expected, because strength and shape of these waves is known to be highly variable from year to year (van Loon and Williams, 1980). The reasons of this variability are not quite clear, but they could be related to variations in the latitudinal position of westerly winds including the jet stream, and the specific spots where winds "hit" the western sides of the elevated areas (Agee, 1980).

The purpose of models is not to fit the data but to sharpen the questions.

Samuel Karlin
(11th R. A. Fisher Memorial Lecture, 1983)

Chapter 6

Reconstruction of the late Miocene climate of Spain using rodent paleocommunity successions: an application of end-member modelling

Abstract

End-member modelling is applied to a data set of relative abundances of 67 upper Miocene rodent associations (11-6 Ma) from Spain, France, Austria and Greece. The analysis results in the robust estimation of relative levels of four climatic parameters: humidity, temperature, seasonality type and predictability.

In the preparatory stage, species are aggregated into nine groups on the basis of ecological criteria. Humidity preferences and adaptations are based on actualistic and functional morphological interpretations of dentition and locomotion. Temperature preferences are inferred from paleobiogeographic distributions. Levels of adaptation to seasonality type (wet-dry or cool-warm seasonality) are assigned on the basis of diversities in present-day climate/vegetation zones, and the ability of extant relatives to hibernate. Demographic data are used to formulate adaptations to climatic (un)predictability.

In the modelling stage, the compositions are unmixed into the contributions of four end members. These four extreme, theoretical rodent compositions are interpreted in climatic terms, and their contributions to the samples are used for the estimation of climatic parameters. The subset of 44 well-dated rodent compositions from the Calatayud-Daroca and Teruel basins (NE Spain) is used to construct detailed climatic curves for the late Miocene, while the geographical dimension in the data set is used to calculate inter-basinal differences.

The model results for Spain indicate more humid and cooler conditions between 10.5 and 8.5 Ma, around 7, and around 6 Ma, and more arid and warmer conditions before 10.5, between 8.6 and 7.5 Ma and around 6.5 Ma. Superimposed on this pattern is a shift from a more predictable, cool-warm seasonal climate towards a more unpredictable, wet-dry seasonal climate between 9.4 and 8.2 Ma. Inter-basinal

comparisons per time slice show that the climate in Southern Europe was dryer, warmer, more wet-dry seasonal and more unpredictable than in Central Europe, and that the climatic and vegetational boundaries between the two regions were sharp. The occurrences of more humid and cooler episodes in Spain during the late Miocene might be explained by southward migrations of the boundary between a temperate and subtropical-dry climatic belt and their associated vegetation types.

Partial correlations are observed between the rodent-based climatic curves for Spain, and some other paleoclimatic records from the Mediterranean and NE Atlantic region (clay minerals, marine fauna, stable isotopes), although most comparisons show that there are sub-intervals without positive correlations. Nevertheless, the two cooling maxima at 9.4 and 7 Ma closely correspond to clusters of marine events which can be interpreted as maxima of global ice volume.

6.1. Introduction

The late Miocene is generally considered to represent an important episode in the trend known as "Cenozoic climatic deterioration". Although the evidence for global cooling during this period is less evident than that for the middle Miocene and Plio-Pleistocene (Barron, 1985; Frakes et al., 1992), the late Miocene is characterized by very marked changes in terrestrial ecosystems. Well known among these changes is the strong expansion of low-biomass vegetation: woodlands start to replace forests, and savannas and grasslands establish themselves on a global scale (Wolfe, 1985; Potts and Behrensmeyer, 1992; Quade et al., 1995). As a reaction to these changes faunal diversifications occur, for instance in open-vegetation herbivores and large mammalian carnivores (Van Couvering, 1980; Potts and Behrensmeyer, 1992; Janis, 1993). Although the general picture is clear, little is known about how and when this late Miocene paleoenvironmental transition occurred in the different continents and regions. In order to study this, more long, continuous, well-documented, and dated paleoclimatic records are needed (Badgley and Behrensmeyer, 1995).

Fossil mammal successions have been used more extensively in paleoecology during the last few decades. The classic successions of the Paleogene of North America and the Neogene of the Siwaliks have shown the large potential of mammal successions for terrestrial paleoecology (Barry et al., 1990; Gunnell et al., 1995; Morgan et al., 1995). Here we focus on NE Spain, where a high-resolution frame has been established, based on micromammal successions. This holds in particular for the Neogene sections of the Calatayud-Daroca and Teruel basins (van de Weerd, 1976; Daams et al., 1988; Mein et al., 1990; van der Meulen and Daams, 1992; chapter 2). Detailed quantitative climatic reconstructions for the early-middle Miocene were made by van der Meulen and Daams (1992) on the basis of rodents. Magnetostratigraphic studies (Krijgsman et al., 1994b, 1996) have allowed correlations to the Geomagnetic Polarity Time Scale (GPTS). As a result, major climatic changes, e.g. the global mid-Miocene cooling event, have been accurately dated in Spain (Krijgsman et al., 1994b).

Here we will concentrate on the upper Miocene rodent succession of the Calatayud-Daroca and Teruel basins (hereafter referred to as CT basins). We will subject relative abundance data to the multivariate approach called end-member modelling or mixing modelling (Full et al., 1981; Renner, 1993; Weltje, 1994, 1997). Algorithms of Weltje (1994, 1997) will be used to "unmix" the ecological composition of each sample into the contributions of a limited set of end members. These end members are extreme theoretical compositions, each of which can be interpreted rather easily in terms of climate, given the preferences of the rodents. The contributions of each sample to the end members are used to estimate values for climatic parameters. Because we will also include 23 compositions from other parts of Europe (France, Austria and Greece) in the analysis, end-member compositions are expected to show a geographical dimension.

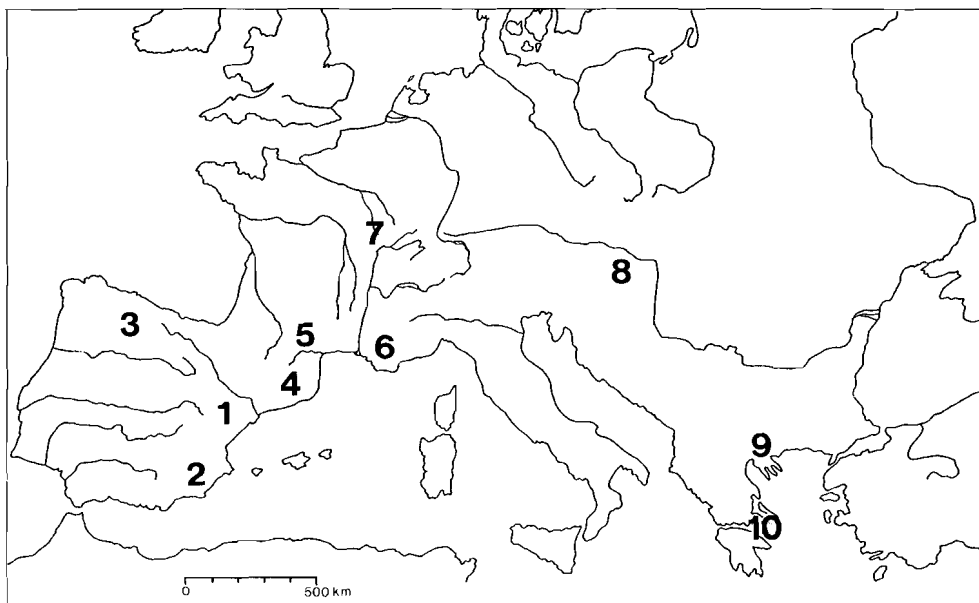


Figure 6.1. Positions of the basins/areas referred to in this study. 1) Calatayud-Daroca and Teruel; 2) Alicante; 3) Duero; 4) Vallès-Penedès; 5) Languedoc Central; 6) Cucuron-Basse Durance); 7) Rhone; 8) Vienna; 9) Strimon; 10) Rafina.

The method is applied to an ecology-based grouping of rodents. Functional morphological interpretations of the dentition and locomotion are used to formulate humidity preferences. (Paleo)biogeographic distributions are used to infer temperature preferences. Information on the demography and life-history strategies of extant rodent groups is used to model seasonality type (temperature- versus humidity-related seasonality), and predictability or interannual variation (see also chapter 5).

6.2. Material

Our data set consists of rodent compositions from 67 South and Central European late Miocene localities (table 6.1). 44 of these are located in the two adjacent basins of Calatayud and Teruel (CT basins), situated in the provinces of Teruel and Zaragoza, NE Spain (fig. 6.1). Taxon identifications are after van de Weerd (1976), Besems and van de Weerd (1983), van der Meulen and Daams (1992), van der Meulen (data base), and chapters 2, 3 and appendix A of this thesis). The studied time slice (~ 11 to 6 Ma) includes the Vallesian and a large part of the Turolian, which correspond to Neogene Mammal zones MN9-10 and MN11-13, respectively (Mein, 1990; de Bruijn et al., 1992). Numerical ages have been assigned to these localities within a framework of magneto-, litho, and biostratigraphy (Krijgsman et al., 1996; Garcés et al., submitted; appendix B). The material is stored in the Institute of Earth Sciences of Utrecht University, the Geology Faculty of the University Complutense of Madrid, the National Natural History Museum of Leiden, and the National Museum of Natural Sciences of Madrid.

A group of 25 localities from other basins in Spain, France, Greece and Austria is included into the data set to provide a regional dimension to the analysis (table 6.1; figure 6.1). Faunal information comes from Aguilar and Michaux (1990), Agustí (1981, 1990), Agustí and Gibert (1982a, 1982b), Alvarez Sierra (1983), Daxner-Höck (1980), de Bruijn (1976, 1989), de Bruijn et al. (1975), Huguency and Mein (1965), Mein (1984), Mein (personal communication 1995) and van der Meulen (data base). Lissieu (Lyon area, MN13) is the only karst locality in the data set. It is included because there are no other stratified northern localities of MN12-13 age for which quantitative data are available.

Relative abundances for the CT basins were based on the number of first and second molars. In case these were absent but other teeth or skeletal material was present, frequencies were counted as one. Frequencies were also counted as one, in case skeletal material (e.g. teeth of Castoridae) originated from a macromammal sample. Damaged molars were counted as one unless their surface amounted to less than half of the original surface. Relative frequencies from similarly aged samples were used to estimate these missing values. Differences with counts of van de Weerd (1976) are mainly due to a different treatment of damaged specimens, and the addition of some unpublished material collected by van de Weerd.

The counts for most of the other basins were also based on first and second molars. Relative abundances for Eichkogel (Austria) and most French localities were based on the available totals of first, second and third molars. The abundances for Montredon (Languedoc Central, France) for which the abundances were based on first and second molars for Gliridae and on first molars for the rest of the rodents.

End-member modelling

Table 6.1. Localities used in this study. Ages for the Calatayud-Daroca and Teruel (CT) basins (calibrated to the time scale of Cande and Kent, 1995) are based on magneto-, bio- and lithostratigraphic data and correlations in the CT basins (Krijgsman et al., 1996; Garcés et al., in press; chapter 2 and appendix B), on age estimates for the MN7-8/9, "MN9A/9B" (subdivision of MN9 according to Agustí and Moyà-Solà, 1991) and MN9/10 boundaries in the Vallès-Penedès basin (Garcés et al., 1996), and on the age estimate of the MN11/12 boundary in the Cabriel basin (Opdyke et al., 1990; reinterpretation by Krijgsman et al., 1996).

MN zone	locality	code	age (Ma)	MN zone	locality	code	age (Ma)
<i>Teruel-Alfambra region, Teruel basin, Spain</i>				<i>Teruel-Ademuz region, Teruel basin, Spain</i>			
13	Las Casiones superior	KSS	6.1	12	Cubla	CU	7.1
13	Las Casiones	KS	6.1	9	Casas Altas	CASAL	10.7
13	Valdecebro 3	VDC3	6.3	<i>Daroca region, Calatayud-Daroca basin, Spain</i>			
13	Masada del Valle 7	MDV7	6.7	9	Pedregueras 2C	PED2C	10.0
12	Concud	CC	6.8	9	Pedregueras 2A	PED2A	10.2
12	Concud 3	CC3	6.9	9	Carrilanga 1	CAR1	10.5
12	Los Mansuetos	LM	6.9	9	Nombrevilla	NOM	10.9
12	Concud 2	CC2	6.9	<i>Alicante, Spain</i>			
12	Tortajada	TO	6.9	12	Crevillente 5	CR5	
12	Villalba Baja 2	VB2	7.0	12	Crevillente 4	CR4	
12	Masada del Valle 5	MDV5	7.0	11	Crevillente 3	CR3	
12	Masada del Valle 4	MDV4	7.1	11	Crevillente 2	CR2	
12	Tortajada D	TOD	7.1	11	Crevillente 1	CR1	
12	Tortajada C	TOC	7.1	<i>Vallès-Penedès basin, Spain</i>			
12	Masada del Valle 3	MDV3	7.1	10	Trinxera Nort Autopista	TNA	
12	Concud B	CCB	7.1	10	Trinxera Sur Autopista 2	TSA2	
12	Masada del Valle 2	MDV2	7.3	9	Can Llobateres	CL	
12	Los Mansuetos 2	LM2	7.3	9	Can Ponsich	CP	
11	Vivero de Pinos	VIP	8.1	9	Hostalets superior	HSS	
11	Tortajada A	TOA	8.1	<i>Duero basin, Spain</i>			
11	Los Aguanaces 3	AG3	8.1	10	Torremormojón 1	TOR1	
11	Alfambra	ALF	8.2	<i>Languedoc central, France</i>			
11	Puente Minero 3	PM3	8.2	10	Montredon	MONTR	
11	La Gloria 10	GLO10	8.2	<i>Cucuron-Basse Durance basin, France</i>			
11	Los Aguanaces 1	AG1	8.3	12	Cucuron Stade	CUCS	
11	Puente Minero	PM	8.3	<i>Rhone basin / Lyon area, France</i>			
11	Peralejos D	PERD	8.7	13	Lissieu	LS	
10	Peralejos C	PERC	8.8	11	Ambérieu 3	AMB3	
10	La Roma 2	R2	8.9	11	Dionnay	DION	
10	Puente Minero 2	PM2	9.1	11	Ambérieu 2	AMB2	
10	Masía de la Roma 11	ROM11	9.2	11	Ambérieu 1	AMB1	
10	Masía del Barbo 2B	MBB	9.2	10	Soblay	SOBL	
10	Peralejos 4	PER4	9.3	10	Douvre	DOUVR	
10	Masía de la Roma 9	ROM9	9.4	<i>Vienna basin, Austria</i>			
10	Masía del Barbo 2A	MBA	9.4	11	Eichkogel	EICHK	
10	Masía de la Roma 7	ROM7	9.4	<i>Rafina basin, Greece</i>			
10	Masía de la Roma 4C	ROM4	9.5	12	Pikermi 4	PK4	
9	Masía de la Roma 3	ROM3	9.7	<i>Strimon basin, Greece</i>			
9	Peralejos 5	PER5	9.7	10	Lefkon	LEF	

6.3. End-member modelling

6.3.1. The linear mixing model

Various types of methods and techniques can be used to model compositional variation in paleoecological assemblages (Birks, 1985). Here principles of linear mixing modelling are used (Klovan and Miesch, 1976; Miesch, 1976; Full et al., 1981, 1982; Renner, 1993; Weltje, 1994, 1997). Linear mixing models of compositional data summarize variation among a series of observations in terms of proportional contributions of actual or theoretical end members. The end members represent a series of fixed compositions, which can be regarded as distinct subpopulations within the data set. For instance, variation among a series of chemical bulk compositions of samples from a single intrusive rock body may reflect varying proportional contributions of a fixed number of mineralogical constituents with fixed chemical compositions.

Compositional data are generally cast into the form of a matrix X , with n rows representing observations (samples), and p columns representing variables. The compositional variables are non-negative, and each row of the data matrix sums to a constant c , usually 1, 100, or 10^6 (for measurements recorded as proportions, percentages, or parts per million, respectively).

$$\sum_{j=1}^p x_{ij} = c \quad x_{ij} \geq 0 \quad (1)$$

If compositional variation among a series of samples results from a mixing process, each row of the matrix of compositional data X is a non-negative linear combination of the q rows of B , a matrix of end-member compositions. The matrix M represents the proportional contributions of the end members to each observation. In matrix notation, this perfect mixing can be expressed as

$$X = MB \quad (2)$$

subject to the following non-negativity and constant-sum constraints:

$$\begin{aligned} \sum_{k=1}^q m_{ik} &= 1 & m_{ik} &\geq 0 \\ \sum_{j=1}^p b_{kj} &= c & b_{kj} &\geq 0 \end{aligned} \quad (3)$$

Although this representation is acceptable from an algebraic point of view, it fails to account for the fact that perfect mixing cannot be demonstrated in practice, due to sampling and measurement errors in X . Therefore, it is assumed that the data matrix X is made up of a systematic part X' , attributable to perfect mixing, and a matrix of error terms E , representing non-systematic contributions to X . It is assumed that the errors are relatively small and X' closely resembles X . By definition, the rows of X' , the estimated matrix of perfect mixtures, consist of non-negative linear combinations M of q end-member compositions B :

$$\begin{aligned} X' &= X - E \\ X' &= MB \end{aligned} \tag{4}$$

The range of each variable in X' cannot exceed that of the corresponding variable in the end members B , due to the non-negativity constraint on M . In other words, the end-member matrix contains the extreme values of each variable. By definition, the rows of X' are also subject to the constant-sum constraint, and therefore

$$\begin{aligned} \sum_{j=1}^p x'_{ij} &= c & x'_{ij} &\geq 0 \\ \sum_{j=1}^p e_{ij} &= 0 \end{aligned} \tag{5}$$

The above considerations lead to the following mathematical formulation of the general mixing model (subject to the constraints listed above):

$$X = MB + E \tag{6}$$

6.3.2. Inverse modelling strategy

In terms of mathematical modelling, equation (6) is the forward model. Once a set of end members is specified, the composition of any mixture can be produced. In case no a priori information about the number of such end members and/or their compositions is available, the problem is much more complex, and all of the parameters of the mixing process have to be estimated from the data by means of inverse modelling techniques.

The inverse modelling procedure used here consists of two stages. In the first modelling stage, the mixing space is defined by partitioning the data into X' and E ("signal" and "noise") for each number of end members, following equation (4). A matrix of perfect mixtures is generated for every value of q ($2 \leq q \leq p$) using fundamental concepts of linear algebra (singular value decomposition and constrained weighted least squares approximation). Each approximated matrix conforms to the non-negativity constraint of equation (5). As will be illustrated in the faunal

application below, the "best" of these solutions is chosen in order to fix X' and q . A fundamental assumption is that the set of end members from which the observed variability has been generated is linearly independent in compositional space, because the dimensionality (shape) of the data in p -space is closely related to the number of linearly independent end-member vectors needed to span the mixing polytope. The requirement of linear independence thus limits the maximum number of end members in inverse models of a mixing process to p . In our application the columns of the data matrix were scaled to equal weights prior to the partitioning into signal and noise, so that each variable (i.e. a rodent group) is equally important in determining the approximate dimensionality of the data.

The problem to be solved in the second modelling stage consists of expressing X' , the matrix of perfect mixtures, as the product of two matrices M and B , subject to the constraints of equation (3). This is a constrained bilinear minimisation problem, which cannot be solved uniquely without additional information. The intrinsic non-uniqueness of the bilinear unmixing solution can be circumvented by specifying additional constraints, based on the trade-off between two apparently contradictory but equally desirable requirements: mathematical and physical (including ecological) feasibility. Of primary concern is that the modeled end members enclose the smallest possible mixing space, so that each end member contributes significantly to the observed compositional variation, and its composition can be easily interpreted in paleoecological and/or paleoclimatological terms. However, negative values of end-member contributions are not allowed in the model, and a good fit of the model to the approximated data requires that the number and magnitude of negative contributions are as small as possible. In a geometrical sense, the set of end members must enclose as many of the observations as possible, because any observation not enclosed by the end members is distorted in the modeled representation of the data. The apparent contradiction of these two requirements enables the optimal solution for a given (minimal) value of q to be defined as the smallest possible mixing space which encloses a sufficiently large proportion of the data points.

A new iterative algorithm has been developed for estimating the "optimal" M and B (Weltje, 1994, 1997). It is more robust, has better convergence properties, and is computationally more efficient than previously developed numerical schemes. Figure 6.2 shows the basic concept of the iterative construction of "optimal" end-member compositions as it was used in this study. The data in the ternary diagram of figure 6.2A consist of three source compositions and six mixtures. The number of end members is thus known *a priori*. Figure 6.2A also shows the locations of three centres of mass in the data set, that have been calculated using a Q-mode cluster algorithm (Full et al., 1982; Bezdek et al., 1984). These centres of gravity are the robust initial end-member estimates employed by the iterative procedure. Because a set of end members has been specified, the matrix of mixing proportions corresponding to these end members can be calculated from the exact bilinear relationship of equation (4). This matrix of mixing proportions is evaluated in order to define improvements to the end members, which aim at reducing the number and magnitude of negative mixing proportions. In the next iteration cycle, the updated matrix of end-member

compositions is used to generate a new mixing proportions matrix. In a geometrical sense, the mixing space grows in each iteration cycle, until the constraints on an optimal mixing model have been satisfied (fig. 6.2B). Eventually, all of the data points are enclosed by the final mixing space, indicating that the original source compositions are accurately identified (fig. 6.2C).

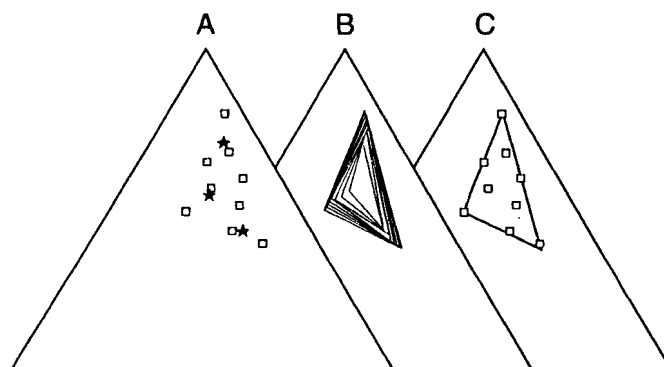


Figure 6.2. a) Synthetic data set consisting of nine three-part compositions. This data set was generated by mixing the three extreme observations in arbitrary proportions in order to generate six additional data points. An initial guess of the end-member compositions (shown as stars) is made by a "fuzzy clustering" algorithm (Full et al., 1982; Bezdek et al., 1984). b) A series of iteration cycles. The ternary mixing space (represented by a triangle in compositional space) grows in each iteration cycle until the mathematical constraints on a feasible solution have been satisfied. c) At convergence, the calculated end members are nearly identical to the three extreme observations. The true end members from which the mixtures have been generated are closely approximated. Parameter estimation is independent of sample locations or other considerations, because the mixing model is constructed in compositional space.

6.3.3. Paleoenvironmental extensions to modelling

6.3.3.1. The nature of the mixing space

It is important to realize that mixing of faunal compositions should not be interpreted as actual physical mixing of teeth. In this respect our application differs from most of the traditional geological and geochemical applications where physical mixing of sediment grains or chemical constituents is described. This application is different because the fossil assemblages are distributed over millions of years and across a broad range of sedimentary systems and basins. The "system" described here is the ecological/climatic system connecting all localities and basins by its control on the geographical and temporal distribution of the rodent groups. Employed in such a way, "mixing" is more conceptual than physical, and can best be viewed as the result of interaction between climatic factors on the one hand, and adaptations of and interspecific competition between species on the other hand. For rodents, the reality of interspecific competition has repeatedly been demonstrated (e.g. Grant, 1972).

6.3.3.2. Estimation of climatic parameters

The estimation of climatic parameters from rodent end-member compositions is done in three steps: 1) characterizing the end members as "cooler", "warmer", "more humid", etc. on the basis of their compositions; 2) calculating the ratios of the contributions of those pairs of end members which indicate opposite conditions (e.g. "cooler" versus "warmer"); and 3) taking the logarithms of these ratios (logratios). A logratio is the most appropriate form to describe variation within compositions and it is insensitive to closed-sum effects (Aitchison, 1986). A logratio of the contributions m_{ik} and m_{il} of the end members k and l (elements of M) to the sample i can be described as:

$$r_{ikl} = \ln(m_{ik}/m_{il}) \quad (7)$$

The logratio is undefined when m_{ik} or m_{il} is zero, and in such cases the following decisions are made: if m_{ik} is zero the ratio is set to 0.01; if m_{il} is zero the ratio is set to 100; and in case both m_{ik} and m_{il} are zero the ratio is set to 1. 4) The final parameter (e.g. "relative humidity") is calculated as the first principal component of all selected logratios that are used to describe that climatic parameter in step (2).

6.3.3.3. Model assumptions

A number of model assumptions have to be made, before the end-member method can be applied to our rodent paleocommunity successions.

Assumption 1): An important part of the signal in the data set is climate-related. This first assumption implies that the mixing space is mainly a climatic space (see 5.1). It reflects the fact that many abiotic, but also biotic features of the environment (such as vegetation type) are climate-related. However, it is for instance known that some rodent species prefer habitats not only because of climate or vegetation, but also because of specific soil or rock types. Such preferences are not dealt with here because they are assumed to be of minor importance.

Assumption 2): Communities are in equilibrium with the environment. This assumption implies that groups react "instantaneously" to environmental changes. Only then we may expect a one-to-one relation between a specific set of parameters and a certain composition resulting from it. Obviously, the concept of equilibrium is time-scale dependent (Giller and Gee, 1986). However, it is known that even in (geologically instantaneous) ecological time, rodent communities (like most other communities) respond very quickly to environmental changes. This means that in geological time the problem will be even much smaller, because of time-averaging effects within samples.

On the other hand, other problems may arise because of the length of geologic time. For instance, tectonic processes may induce the creation or removal of barriers such as mountains and water surfaces. If these barriers prevent groups from reaching certain

areas during a part of the studied interval structural zeros will enter the data set. This means in turn that estimates of environmental parameters will be distorted if the absence of these groups would be explained in ecological terms. This problem can be solved by the aggregation of groups, preferably in an ecological way. The result will be that faunal changes caused by the opening of new migration routes will not automatically be expressed in changes in the ecological composition, because the taxa competing or replacing each other may belong to the same ecological category. Structural zeros, representing the not-yet existence or extinction of a group, form another complication. Again, aggregation may solve the problem. Obviously, there is a limit to aggregation, because information is lost every time groups are combined.

Assumption 3): The equilibrium between compositions and climatic change is of the type described by equation (7). Obviously, equation (7) is a simplification of reality. However, our focus is on general climatic trends, and the exact shape of the function is less important than its monotonous increase. The assumption of monotony means for instance that if humidity is known to increase along some geographical gradient, the ratios of "humid" versus "arid" end members have to increase along this gradient also, i.e. without any reversals. Or to put it differently: if the environment becomes more favorable to group A than to group B, then the ratio of abundances of A and B is expected to increase. Formulated like this, the assumption of monotony comes close to the assumption that interspecific selection and competition are important in shaping community structure. Support for assumptions 1, 2 and 3 can be found by examining gradients in present-day climate and in rodent compositions and by checking for correlations. Until now we have not performed such a study.

Assumption 4): Intra-group variation is small compared to inter-group variation. This assumption means that the groups are not allowed to vary too much internally in their preferences and adaptations. Intra-group variation occurs because of evolution, and because groups may consist of several taxa which contribute in different ways.

Assumption 5): Assemblages are isotaphonomic. The composition of a vertebrate death assemblage is only partly determined by the structure of the original life assemblages, since taphonomical processes may cause serious biases. In this application of end-member modelling the main assumption is that biasing factors operate in a constant way, i.e. that the assemblages are isotaphonomic (Wing et al., 1992). For such a setting, it may be assumed that estimates of relative climate on the basis of the compositions are not disturbed by structural (i.e. constant) under- or overrepresentation of groups. This also holds for the end-member model, because the use of constant correction factors will distort the mixing space in an approximately linear way (see section 6.3). As discussed in chapter 5 the assumption of isotaphonomic conditions is reasonable for our data set, the major reasons being that almost all localities are formed in low-energy shallow lacustrine systems, and that the majority of localities comes from one basin (on which the final climatic curves are based). In addition, a type of bias which occurs in one or a few localities only will be filtered out during modelling.

A summary of the methodology is given in figure 6.3. The basic data are relative abundances of first and second molars of rodent species from time-ordered samples

from several geological basins (the species relative abundance matrix Y). Species abundances are converted into ecological abundances by grouping species on the basis of diet, locomotion, life history and energy expenditure, and (paleo)biogeographic distributions (see below). This conversion results in the ecological relative abundance matrix X (notation as in section 6.3.1). After an evaluation of sources of compositional bias, an end-member model is fitted to X . The matrix M of end-member contributions to the samples is used to calculate climatic parameters (the matrix R).

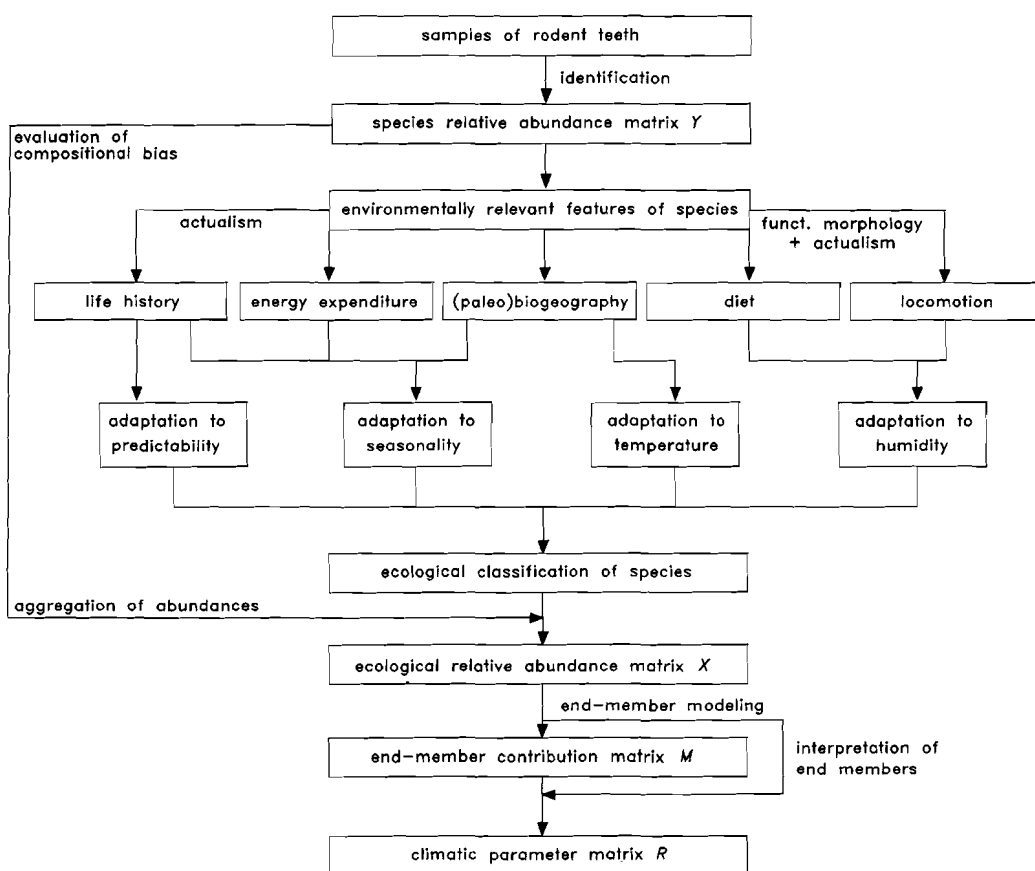


Figure 6.3. Methodological flow chart of this study.

6.4. The climatic parameters and their estimation from rodents

Four climatic parameters are estimated on the basis of a fitted end-member model: humidity, temperature, seasonality type and predictability. A general discussion on the

use of small mammals as proxies for these parameters was presented in chapter 5. Here we restrict ourselves to a short summary, in which we focus on rodents (see also fig. 6.3). The inferences of the preferences and adaptations for the particular groups used in the analysis will be discussed in the next section.

Humidity preferences are based on the functional morphology of the dentition, and on the extrapolation of habitats from those of extant relatives (the principle of actualism). Various dental features (hypsodonty, brachiodonty, stephanodonty, various types of lophodonty) are interpreted as adaptations to specific diets, which in turn are assumed to indicate certain habitats. Knowledge of extant habitats and phylogenetic relations is used to infer the habitats of fossil relatives.

Temperature preferences are primarily inferred from (a) Miocene paleobiogeographical distributions, and (b) abundance shifts in Spanish rodents (van der Meulen and Daams, 1992; Krijgsman et al., 1994b) related to the generally accepted global middle Miocene cooling episode. This cooling followed a late early to middle Miocene thermal optimum between 17 and 14.5 Ma (Flower and Kennett, 1993; Hodell and Woodruff, 1994), when Holarctic land temperatures were about 7° C higher than at present (Schwarzbach, 1968; Axelrod and Bailey, 1969; Burchardt, 1978; Wolfe, 1994).

Adaptations to inter-annual climatic variability (predictability) are mainly inferred from demographic patterns and associated life-history strategies. (Un)predictability is an important determinant of community structure (Pimm, 1978), and predictable variations in resource availability can be accommodated by groups with appropriate life histories (Giller and Gee, 1986). We use a demographic tripartition of rodents (French et al., 1975; extensions by van der Meulen and Daams, 1992, and chapter 5) to classify rodents into three groups in terms of adaptations to (un)predictability. The extremely production-oriented species of demographic group 1 (which includes Murinae) are optimally adapted to unpredictable environments. By contrast, strong "internal clocks" are (or are assumed to be) common in the efficiency-oriented taxa of group 3 (among which are Gliridae, Sciuridae, Petauristidae, Zapodidae and Eomyidae). Such clocks can only function in a predictable environment, because they regulate the tuning of many physiological and behavioural changes to the annual cycle (e.g. hibernation). Representatives of group 2, to which Cricetidae belong, are intermediately adapted with regard to predictability.

Adaptations to seasonality type are based on two considerations. In the first place, the ability to hibernate (Cade, 1964; Precht et al., 1973) is regarded as an adaptation to cool-warm seasonality. The second consideration relates to the climate types and biomes where extant relatives reach their highest diversities. E.g. murines (group 1) are assumed to have a competitive advantage over many other groups in monsoon-dominated zones, such as savannas, which are areas dominated by wet-dry seasonality. Where monsoon-dominated vegetation zones grade into drier, less productive biomes, murines give way to more survival-oriented groups of group 2, such as gerbils (type 2) in the North African (semi) desert, and cricetines in the Central Asian steppes. Superiority of members of group 3 is typically related to a higher fasting endurance, made possible by large fat stores and hibernation, during which body temperature and

Table 6.2. Ecological grouping of the late Miocene rodents studied and their assigned scores on climatic parameters. Positive, neutral and negative scores correspond to high, intermediate/mixed, and low values, respectively (see text for details). Humidity scores are based on diet and locomotion, and temperature scores on Miocene paleobiogeography. Scores on seasonality type (warm-cool vs. humid-arid) are based on present-day diversities in climatic/vegetational belts and on hibernation abilities. Predictability scores are based on demographic characteristics, reflecting survival- or reproduction oriented life history strategies.

rodent group			scores assigned to climatic parameters			
name	ecologically relevant features	taxonomy	humidity (humid: +) (arid: -)	temperature (warm: +) (cool: -)	seasonality (in temp.: +) (in hum.: -)	predictability (high: +) (low: -)
Castoridae	beavers, semi-aquatic	Castoridae	+	-	+	+
Cricetidae I	hamsters with relatively high-crowned molars	Cricetodontini, <i>Blancomys</i>	-	0	0	0
Cricetidae II	hamsters with relatively low-crowned molars	Cricetinae, <i>Megacricetodon</i> ¹	0	0	0	0
Gliridae I	terrestrial dormice with few lophs on molar crowns	Myomiminae except <i>Ramys</i> and <i>Vasseuromys</i>	-	0	+	+
Gliridae II	arboreal/scansorial dormice with many lophs on molar crowns	Bransatoglirinae, Dryomyinae, Glirinae, <i>Ramys</i> , <i>Vasseuromys</i>	+	-	+	+
Muridae I	mice with relatively broad molars with well-developed longitudinal ridges	<i>Occitanomys</i> , <i>Stephanomys</i>	-	0	-	-
Muridae II	mice with relatively slender molars with less well-developed longitudinal ridges	Muridae except <i>Occitanomys</i> and <i>Stephanomys</i> ²	0	0	-	-
Sciuridae I	ground squirrels preferring relatively open habitats	Xerini	-	+	-	+
Sciuridae II + Eomyidae + Petauristidae	squirrels and eomyids preferring relatively closed habitats	Tamiini, Petauristidae, Eomyidae ³	+	-	0	+

¹ rest groups *Anomalomys*, *Eumyarion*, *Epimeriones* are included in Cricetidae II

² rest groups Zapodidae and Hystricidae are included in Muridae II

³ rest group Marmotini is included in Sciuridae II

End-member modelling

Table 6.3. Ecological abundance matrix X. Totals are numbers of first and second molars, unless indicated otherwise. Prior to modelling, zeros are replaced by small values corresponding to half a tooth (which is the measurement error).

locality	Castoridae	Crice-tidae I	Crice-tidae II	Gliri-dae I	Gliri-dae II	Muri-dae I	Muri-dae II	Sciuri-dae I	Sc. II+ Pet. + Eomy.	total number
KSS	0	5.23	10.47	0	1.16	42.44	40.70	0	0	172
KS	0.65	0	1.06	0	0.24	58.06	39.98	0	0	1228
VDC3	1.02	1.79	4.59	0	0	72.96	19.39	0	0.26	392
MDV7	1.59	0	1.59	0	1.59	92.06	3.17	0	0	63
CC	5.41	8.11	0	0	0	54.05	29.73	0	2.70	37
CC3	0	2.72	0	0	1.97	39.27	51.73	3.09	1.22	1067
LM	0.11	16.91	0.16	0	0.32	72.57	9.18	0.75	0	1863
CC2	0	4.49	0	0	4.49	50.56	38.20	1.12	1.12	89
TO	0	11.36	0	0	0	64.77	17.05	6.82	0	88
VB2	0	0.62	0	0	0	64.71	34.06	0.62	0	323
MDV5	0	2.56	0.51	0	1.03	46.41	43.59	1.54	4.36	390
MDV4	0	5.13	0	0	0	51.28	41.03	0	2.56	39
TOD	0	7.08	0	0	0	49.56	40.71	0	2.65	113
TOC	0	4.17	0	0	4.17	12.50	79.17	0	0	24
MDV3	0	3.33	0	0	0	26.67	70.00	0	0	30
CCB	0	2.08	0	0	4.17	54.17	39.58	0	0	48
MDV2	0.43	5.25	1.29	0	0.75	44.59	45.55	0.64	1.50	933
LM2	0	31.58	2.63	0	0	55.26	10.53	0	0	38
VIP	0	7.40	0.24	0	0	80.43	11.93	0	0	419
TOA	0	9.31	1.06	0	0.53	76.06	13.03	0	0	376
AG3	0	6.01	1.09	0	0.55	68.85	23.50	0	0	183
ALF	0	0	1.85	0	0	72.22	25.93	0	0	54
PM3	0	19.12	1.47	0	0	58.82	20.59	0	0	68
GLO10	0	6.62	1.32	0	0.66	70.20	21.19	0	0	151
AG1	0	4.07	0	0	0	89.43	6.50	0	0	123
PERD	0	17.04	0	1.48	0	0	81.48	0	0	135
PERC	0	15.45	0	0	0.28	0	84.27	0	0	356
R2	0	7.14	2.38	2.38	0	0	88.10	0	0	42
PM2	0	29.27	2.44	2.44	2.44	0	60.98	2.44	0	41
ROM11	0	4.93	1.41	0.70	1.41	0	91.55	0	0	142
MBB	0.47	23.94	0.23	1.41	1.64	0	72.07	0.23	0	426
PER4	0	6.38	0	12.77	2.13	0	78.72	0	0	47
ROM9	0	5.08	0	6.78	5.08	0	83.05	0	0	59
MBA	0	19.57	0.72	3.62	4.35	0	71.74	0	0	138
ROM7	0	18.75	2.50	16.25	1.25	0	61.25	0	0	80
ROM4C	0	7.14	0	22.86	0	0	70.00	0	0	70
ROM3	0	28.07	19.30	47.36	0	0	0	0	5.26	57
PER5	0	51.81	10.84	37.53	0	0	0	0	0	83
CU	0	15.55	0	0	0	57.42	27.03	0	0	418
CASAL	0.71	42.76	35.69	18.37	0.35	0	0	1.77	0.35	283
PED2C	0	22.17	62.43	4.84	9.36	0	0.11	0.65	0.43	929
PED2A	3.09	46.34	25.04	13.33	10.41	0	0	1.79	0	615
CAR1	1.86	18.58	63.62	12.53	3.41	0	0	0	0	646
NOM	0.81	37.25	44.94	13.77	0.40	0	0	2.83	0	247
CR5	0	9.00	13.00	0	2.00	30.00	32.00	0	14.00	100
CR4	0	1.16	31.40	0	0	17.44	50.00	0	0	86
CR3	0	2.00	19.00	0	2.00	44.00	31.00	2.00	0	100
CR2	0	1.46	28.64	0	0.97	24.76	40.78	3.40	0	206

locality	Casto- ridae	Crice- tidae I	Crice- tidae II	Gliri- dae I	Gliri- dae II	Muri- dae I	Muri- dae II	Sciuri- dae I	Sc. II+ Pet. + Eomy.	total number
CR1	0	0	23.38	0	2.60	37.66	35.06	1.30	0	77
TNA	0	1.54	75.38	0	1.54	0	1.54	0	20	65
TSA2	0	13.64	56.82	0	0	0	15.91	0	13.64	44
CL	0.76	6.44	85.98	0	1.33	0	0.38	1.89	3.22	528
CP	1.67	64.02	15.06	0.84	2.09	0	0	13.81	2.51	239
HSS	0	52.15	21.47	2.45	0	0	0	23.93	0	163
TOR1	7.27	5.45	0	0	20.00	0	67.27	0	0	55
MONTR	0	3.04	63.69	0	9.22	0	22.03	1.47	0.55	1052 ²
CUCS	0	4.20	4.90	0	1.40	72.03	16.08	0	1.40	143 ¹
LS	0	0	1	0	29	1	68	0	1	3099 ¹
DION	2	11	5	0	4	0	71.5	0.25	6	1249 ¹
AMB3	0	0	34	0	10	2	29	0	25	126 ¹
AMB2	0	2	41	0	7	0	38	0	12	567 ¹
AMB1	0.25	9	22	0	8	0	53.75	0	7	341 ¹
SOBL	2	0.16	32.84	0	6	0	39	0.25	19.75	612 ¹
DOUVR	2	0	40	0	5	0	32	0	21	95 ¹
EICHK	0.08	0	34.5	3.17	8.87	0	45.57	0	7.81	1230 ¹
PK4	0	9.28	3.09	14.44	1.03	15.46	56.7	0	0	97
LEF	0	13.64	4.55	3.03	4.55	0	71.21	0	3.03	66

¹ totals are numbers of first, second and third molars; proportions are based on these numbers

² proportions are based on first and second molars for Gliridae and on first molars for other groups

Table 6.3. (continued)

activity are lowered. Glirids, which occur in all-year-wet temperate zones dominated by cool-warm seasonality (particularly cold winters) are a good example.

6.5. Ecological grouping of the rodents

6.5.1. Ecology and taxonomy

The studied rodent species are classified into nine ecological groups (table 6.2). Their relative abundances (the matrix X in fig. 6.3) are shown in table 6.3 and figure 6.4. Families are considered to represent certain "ways of life", which are related to their demography and energy expenditure strategies as discussed above. Most families are split into two groups according to preferences for open or closed habitats, based on inferred diet (Cricetidae, Gliridae, Muridae) or locomotion (Gliridae, Sciuridae). As a result, ecological and taxonomic boundaries coincide in the Sciuridae, whereas in Gliridae the ecological boundary runs through a subfamily (see the description of the nine groups below). Because of the uncertain taxonomic status of *Blancomys* in the Cricetidae it is difficult to ascertain whether the ecological boundary in this family corresponds to a taxonomic boundary. No tribes or subfamilies are defined for the Muridae studied here.

Overall, phylogenetic relations within each of the nine groups are tight. This has the additional advantage, that most of them also function as geographical units, facilitating

the attribution of temperature preferences. The close relation between taxonomy and ecology in our data set is in agreement with the general notion that ecological designations tend to include closely related species (Simberloff and Dayan, 1991). Our final grouping may be regarded as the result of a consensus between ecological, taxonomical, and statistical considerations (with the latter resulting in aggregation of genera, as discussed in the previous section). An important asset of this subdivision is that each group is characterized by a unique set of preferences in table 6.2, implying that each group occupies a unique position in "ecological space".

6.5.2. Scores on preferences and adaptations

Adaptations or preferences are assigned in the form of positive (+), neutral (0) or negative (-) scores (table 6.2), and follow the principles mentioned in section 4. For clarity, a remark has to be made on the temperature scores. A neutral score in table 6.2 indicates a late Miocene geographical distribution which was restricted to, or had its centre at the latitude of Spain, i.e. the northwestern part of the Mediterranean area. A positive score is assigned to groups which late Miocene distribution had a major extension into lower latitudes (Africa), and/or showed a decline in Spain during the middle Miocene cooling. Similarly, a negative score is assigned to groups that had their centres of distribution at higher (Central European) latitudes, and/or increased their numbers and/or diversity during the middle Miocene cooling. Unfortunately there is no Miocene rodent record for high-latitude areas, but indirect evidence for at least temporary presence of a group at high latitudes is indicated by occurrences in both Eurasia and North America, implying intercontinental migration across the Bering Street.

We admit that some +, 0 and - assignments may be wrong. However, we will show that the method is robust against a limited number of errors in the assignments (see 7.3).

6.5.3. The nine groups (tables 6.2-6.3 and fig. 6.4)

The nine rodents groups and their preferences and adaptations will now be described.

1) **Castoridae**. In spite of their rareness in the associations studied here, beavers are kept as a separate group because of their specific ecological requirement for permanent open water. Beavers are given a negative score on temperature, because their late Miocene paleobiogeographic distribution includes the mid-latitudes, and because their fossil record indicates repeated migration across the Bering Street (Korth, 1994). Their score on seasonality type is positive because the present-day distribution of beavers can be associated with the middle- to high-latitude zones of cool-warm seasonality. Their score on predictability is positive because of their high life expectancies.

2) Relatively high-crowned Cricetidae (**Cricetidae I**) (use of Cricetidae according to Chaline et al., 1977). Late Miocene Cricetodontini (including *Cricetodon*, *Hispanomys*, *Ruscinomys*, *Byzantinia*) and *Blancomys* are included because of their hypsodonty and similar geographic distribution. Their hypsodonty is interpreted as an adaptation to diets containing a significant proportion of fibrous plant parts, including grasses. Because of this, a preference for open, more arid environments is assumed (de Bruijn et al., 1993). A neutral score on temperature is assigned because the records from Spain (MN9-13), Greece and Anatolia (MN9-12) show that the southern part of western Eurasia was the main area where Cricetodontini lived by then (de Bruijn et al., 1993). Seasonality and predictability preferences are assumed to be identical to those of the Cricetidae II group (see below).

3) Relatively low-crowned Cricetidae (**Cricetidae II**). This heterogeneous group includes all Cricetidae in the data set which do not belong to Cricetidae I. The most abundant genera are *Megacricetodon*, *Cricetulodon*, *Rotundomys* and *Kowalskia*. The group is not split up in order to prevent a high frequency of structural and statistical zeros in the data matrix. A neutral score is assigned to humidity, because some genera are assumed to prefer more open, others to prefer more closed habitats while still others do not seem to have any preference (Daams et al., 1988). An intermediate temperature preference is assigned. Some genera were more restricted to southern Europe (*Cricetulodon-Rotundomys*), whereas others had distribution areas across both South and Central Europe (*Megacricetodon*, *Kowalskia*, *Cricetus*).

A neutral score on seasonality type is assigned to this group on the basis of the diversity patterns of the two extant groups of Cricetinae and Peromyscini. Cricetinae are particularly successful in the Asiatic steppes. Generally, these areas have a wet-dry seasonality which is less extreme than in savannas. Cool-warm seasonality is rather strong also, and weak hibernation occurs in a number of genera (*Cricetus*, *Mesocricetus*). Cool-warm seasonality is not so strong in the Mexican steppes, where peak diversities of extant Peromyscini occur (Nowak, 1991). Neither is hibernation known for this tribe. Nevertheless, we will test also for a positive score on seasonality type, i.e. for an adaptation to cool-warm seasonality. Because of their membership to the intermediate demographic group 2, a neutral score on predictability is assigned.

4) Ground-dwelling Gliridae (**Gliridae I**) (use of Gliridae after Daams and de Bruijn, 1995). This group consists of dormice with molars that have occlusal surfaces with a relatively low number of transverse crests. This dental feature is observed in the extant ground-dwelling dormouse *Myomimus* and many extinct representatives of the subfamily Myomiminae, and is thought to be indicative of a life on the ground and of an open, relatively dry habitat (van der Meulen and de Bruijn, 1982; Daams and van der Meulen, 1984). The Gliridae I group consists of the three Myomiminae genera *Myomimus*, *Miodromys* and *Tempestia*. Two other Myomiminae have many ridges (*Vasseuromys* and *Ramys*). We follow the interpretation of Daams and van der Meulen (1984) and include these into Gliridae II.

An intermediate score is assigned to temperature. Although the Myomiminae were flourishing across Europe during the early and middle Miocene, late Miocene genera had a more restricted distribution. *Myomimus* is documented from Spain to Pakistan,

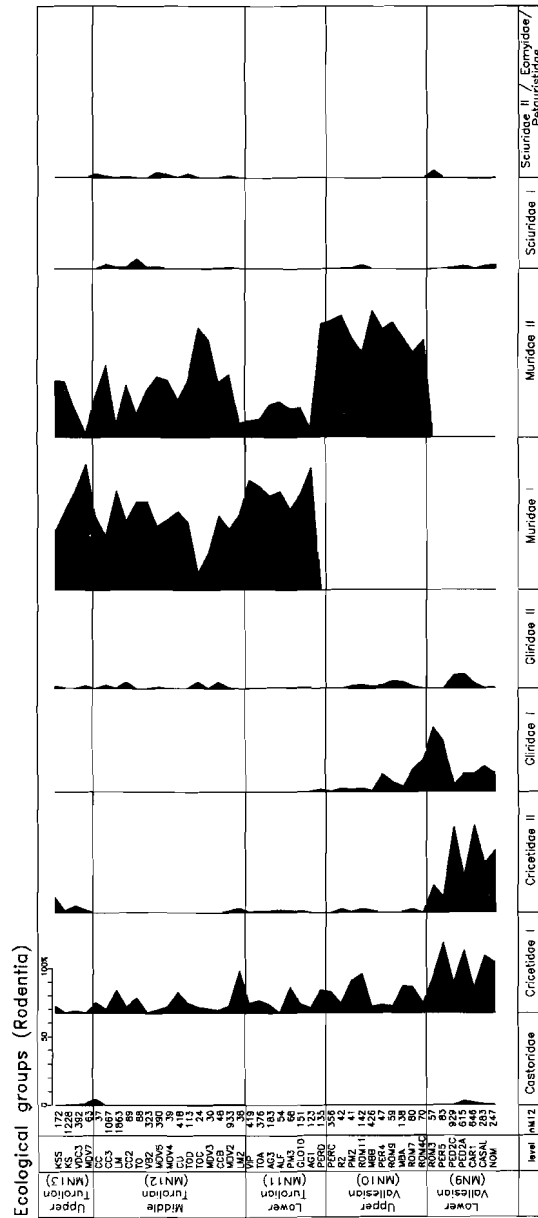


Figure 6.4. Relative frequencies of ecological groups in the Calatayud-Daroca and Teruel basins (together representing a large part of the ecological relative abundance matrix X).

but its absence in the late Miocene localities of France of our data set shows that it had a limited north-south range in Europe during this period. Similarly, *Miodromys* was wide-spread across Europe during the early-middle Miocene in Europe, but its later Miocene occurrence was restricted to southern areas (Vallès-Penedès, Spain, early MN9). *Tempestia* was endemic to Spain. On the basis of the occurrence of hibernation in *Myomimus* a preference for cool-warm seasonality is assigned. Because of their membership to demographic group 3, a positive score on predictability is assigned.

5) Arboreal/scansorial Gliridae (**Gliridae II**). This group includes representatives of the subfamilies Glirinae (*Glis*, *Muscardinus*, *Myoglis*, *Glirudinus*), Dryomyinae (*Eliomys*, *Glirulus*, *Microdyromys*, *Paraglrulus*) and *Bransatoglrinae* (*Bransatoglis*), as well as the two Myomiminae genera mentioned above (*Vasseuromys*, *Ramys*). A positive score on humidity is attributed to Gliridae II because of their assumed arboreal-scansorial way of life, which is attributed to the group on the basis of the habitats of extant relatives, and a molar morphology characterized by many transverse crests (Storch, 1978; van der Meulen and de Bruijn, 1982; Daams and van der Meulen, 1984). The rare dryomyine *Graphiurops* is not separated from the other genera of its subfamily, although its molar pattern with relatively few ridges suggests that inclusion in Gliridae I would perhaps have been better. A negative score on temperature is assigned because relative abundances and diversity of forms with many-lophed molars are small in the late Miocene in Spain compared with contemporary associations from more northern areas (Mayr, 1979; Mein, 1984). A preference for cool-warm seasonality is ascribed to this group because maximum diversities occur in the temperate zones of Eurasia and because they show the habit of deep hibernation. The predictability score is positive as in the previous group.

6) Muridae of the *Occitanomys-Stephanomys* group (**Muridae I**). (Use of Muridae according to Chaline et al., 1977). Stephanodonty (Schaub, 1938) is well developed in this group. The stephanodont pattern is characterized by a garland-type pattern of ridges between the posterior cusps of the upper molars. The well-developed longitudinal valleys indicating a strong power stroke (van Dam, 1996 or chapter 4) and the relatively large width-length ratios of the molars (appendix C) indicate a diet which at least partly consists of fibrous components. It is therefore suggested that the group is adapted to relatively open and dry environments. An intermediate temperature preference is assigned to both genera because their late Miocene distribution was almost exclusively restricted to southwestern Europe (*Stephanomys*) and southern Europe and Anatolia (*Occitanomys*) (de Bruijn et al., 1996). Seasonality and predictability scores are identical to those of Muridae II (see below).

The Muridae I group is the only group with structural zeros in the data matrix, because it was non-existent during the Vallesian (MN9-10). However, its unique combination of adaptations and preferences (table 6.2) is not shared with any of the other groups living in the Vallesian, so it may be argued that the group was adapted to a type of environment that was not yet existing by then.

7) Muridae: *Progonomys*, *Huerzelerimys*, *Parapodemus* and *Apodemus* and some very rare *Castromys* and cf. *Rhagapodemus*. (**Muridae II**). A neutral humidity score is given to this group. The only still living genus, *Apodemus*, is tolerant to different kinds

of habitats. Most of its species have broad frugivorous to omnivorous diets, but do not graze (Niethammer and Krapp, 1978; Nowak, 1991). A biometric analysis on cheek teeth of extant and fossil murids (appendix C) suggests that *Progonomys*, *Huerzelerimys*, and *Parapodemus* were grazing rodents neither.

An intermediate temperature preference is assigned to Muridae II because of their relatively high abundances and diversity in southern Europe during the late Miocene. This means that we do not regard the recent high diversity of murids in tropical areas as an indication for a high-temperature preference of Miocene Murinae. A negative score on seasonality type is assigned to Muridae because they reach their highest present-day diversities in vegetation zones characterized by a wet-dry monsoon-seasonality, such as savannas. Unfortunately for our purposes, Montuire (1994) did not include annual differences in precipitation as a parameter in her study on the relation between extant murid diversity and climate. However, the authors did find a negative correlation between murid diversity and the annual difference in temperature. This is consistent with our negative score on cool-warm seasonality. A relative preference of murids for seasonal dry climates is also corroborated by studies on compositional changes on extant rodent communities in Italy, which confirm that *Rattus rattus* and *Mus musculus* are more favoured by the Mediterranean climate than other groups (Amori et al., 1984). A negative score is given to predictability, because of the classification of Muridae into demographic group 1.

We consider the rare Zapodidae of age MN11 as a rest group and combine them with the Muridae, which is most abundant family in Spain at this time. Assignment to Muridae II group is preferred, because the presence of Zapodidae is more correlated to the presence of *Parapodemus* (Muridae II) than to *Occitanomys* (Muridae I) in the data set. Hystricidae occur only in one locality (Las Casiones, Teruel basin) and are also included into this group.

8) Sciuridae: ground squirrels of the tribe Xerini (**Sciuridae I**). The ground squirrels *Heteroxerus* and *Atlantoxerus* are assumed to be indicators for relatively open habitats and hence low humidity. The two extant *Xerus* species are living in the drier savannas, and the NW African relict species *Atlantoxerus getulus* lives in an arid mountainous environment (Kingdon, 1974; Nowak, 1991). A positive score on temperature is assumed for Xerini, because they flourished during the late early to middle Miocene thermal optimum in Spain and declined during the subsequent middle Miocene cooling episode (Daams et al., 1988). A positive score on temperature is supported by the regular occurrence of *Atlantoxerus* in the upper Miocene of the Maghreb (Jaeger, 1977; Coiffait, 1991).

Adaptation to wet-dry seasonality is assumed because of the adaptation of extant *Xerus* to savanna environments (Kingdon, 1974). Xerini are not known to hibernate, and it is uncertain whether they possess any type of torpidity (Cade, 1964). Being Sciuridae, their energy expenditure strategy may be expected to be relatively survival-oriented. The positive score of Xerini on predictability is assigned because of their assumed membership to demographic group 3.

9) Sciuridae: ground squirrels of the tribe Tamiini (**Sciuridae II**), flying squirrels of the family **Petauristidae**, and **Eomyidae**. All three taxa are put in one group because their supposed common preference for forested environments, and the low abundances of each individual subgroup. It is assumed that the extinct genus *Spermophilinus*, like the majority of extant Tamiini (Nowak, 1991), preferred closed, relatively humid biotopes. This assumption is consistent with the high abundances of *Spermophilinus* in very "wet" faunas such as Dorn-Dürkheim (fig. 6.1) in the German Rhine basin (Franzen and Storch, 1975). Undoubtedly, flying squirrels were adapted to a life in forests like their extant relatives. Eomyids are extinct, but there are sufficient indications that they preferred closed vegetation (Daams et al., 1988; van der Meulen and Daams, 1992 and unpublished data). The recent discovery of a flying membrane on a late Oligocene eomyid (Storch et al., 1996) from Germany is in agreement with this hypothesis. The shared biotope preference of *Spermophilinus*, Petauristinae and Eomyidae is confirmed by their simultaneous occurrences in (the more northern localities in) our data set.

This ninth group is given a negative score on temperature. *Spermophilinus* is a very common element in late Miocene northern localities such as Dorn-Dürkheim in the Rhine basin and Eichkogel in the Vienna basin. During the late early to middle Miocene thermal optimum the genus is temporarily absent in Spain (van der Meulen and Daams, 1992; unpublished data), whereas it is present at higher latitudes (e.g. Puttenham). Today, Tamiini are particularly successful in North America. An adaptation to cool environments is indicated by their apparent migration across the Bering Street. The Eomyidae are a similar case. This family was especially abundant in Spain during the late Oligocene-early Miocene (Alvarez Sierra, 1987). The detailed record from the CT basins shows that they disappeared during the thermal optimum, but reappeared afterwards in MN6 (Manchones, Las Planas 5K, see Daams et al., 1988) and MN 9 (Masía de la Roma 3, see table 2.1). In more northern areas however, Eomyidae bridge the interval in which they were absent in Spain (Engesser, 1990; Bolliger, 1992; Fahlbusch and Bolliger, 1996). The group remains well-represented at relatively high latitudes during younger intervals. For example, three different genera occur in Podlesice in Poland (Fahlbusch, 1978). A northern transcontinental migration route is assumed for the Eomyidae, because of their supposed North American origin (Fahlbusch, 1979; Korth, 1994). Petauristidae are today particularly diverse in tropical South East Asia, but during the Neogene they flourished in forested areas all across central Europe (de Bruijn, 1995), and showed a high diversity in latitudes at least as high as Poland (Kowalski, 1990).

A tentative neutral score is given to seasonality type. Whereas present-day diversity of Tamiini is high in (cool-warm seasonal) temperate zone forests (e.g. western United States), hibernation is weak and accompanied by food hoarding. Petauristinae are particularly diverse in tropical SE Asia and do not hibernate. Information is absent for extinct Eomyidae. The predictability score of the complete group is positive because all subgroups belong to demographic group 3.

6.6. Model results

6.6.1. End-member interpretation

Figure 6.5 shows goodness of fit statistics (R^2 values) for each rodent group as a function of the number of end members. A mixing model with four end members seems to be a reasonable choice considering the level of noise on the one hand, and the desire for a simple description on the other hand. This model implies a very low goodness of fit for the Castoridae, which means that variation in this group is mainly regarded as noise. The remaining groups are adequately reproduced, although Sciuridae I and Gliridae II show a lower goodness of fit than other groups.

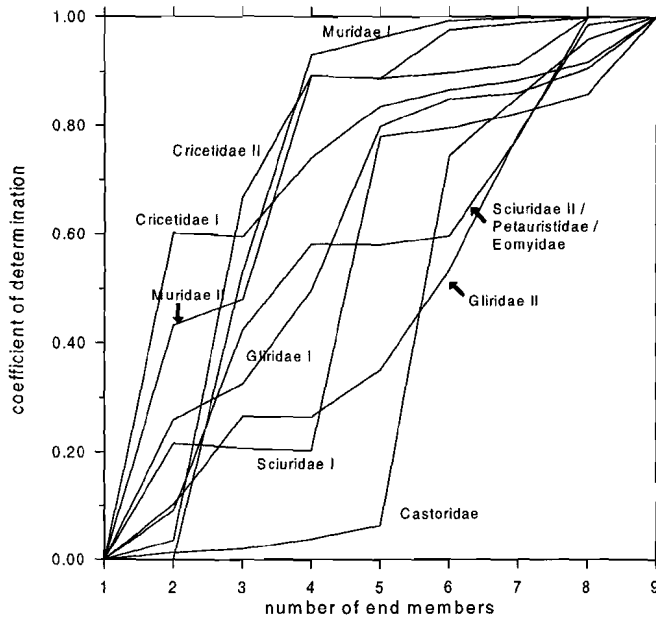


Figure 6.5. Goodness of fit for ecological groups as a function of the number of end members. Estimating the number of end members is the first step in the modelling procedure. The number of end members is equal to the smallest number of dimensions required for a reasonable approximation of the data set. This approach does not require any knowledge of the end-member compositions. The curves show that some of the variables can be reproduced fairly well with only two end members. A four end-member model is a reasonable minimum scenario.

The four end-member compositions are shown in figure 6.6 and table 6.4. In addition, table 6.4 shows how the end members are interpreted in terms of climate. If a group has a positive score on a specific parameter in table 6.2, it scores positively (+) on end members containing a large proportion of this group compared to other end members (row-wise comparison in table 6.4). Similarly, a positive score in table 6.2 results in a negative (-) or neutral (0) score in table 6.4 in case of low or intermediate proportions

respectively. The same reasoning applies to negative scores in table 6.2. Neutral scores in table 6.2 always translate into neutral scores in table 6.4.

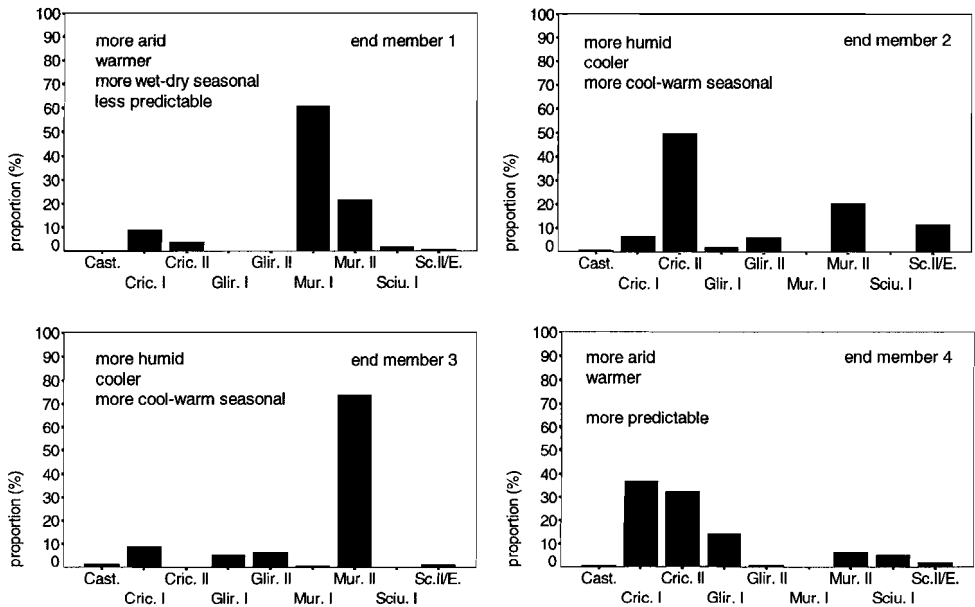


Figure 6.6. The four end-member compositions and their climatic interpretations. For further explanation see text. Note that the group indicated as Sc.II/E. (Sciuridae II-Eomyidae) also includes the Petauristidae.

The net scores for the end members enable a straightforward interpretation, because in most cases the scores of the nine ecological groups appear to point in the same direction, allowing the identification of "humid", "warm", etc. end members. Here we regard net scores higher than 1 or lower than -1 as indicative, which implies that we attribute four climatic characteristics to end members 1 and 4, and three to 2 and 3. It appears that end members 1 and 4 can be described as relatively dry and warm, whereas 2 and 3 can be described as relatively humid and cool. End members 2 and 3 are at the same time characterized by cool-warm seasonality, whereas 1 is characterized by wet-dry seasonality. End member 1 can also be described as unpredictable, and 4 as predictable.

Table 6.5 shows the end-member contributions for all localities, while figure 6.7 shows the contributions for the subset of localities from the CT basins. **End member 1** is an (extreme) Spanish "Turolian" composition, containing more than 80% murids and no glirids. Its composition resembles mostly that of the lower Turolian localities of the CT basins, to which it contributes more than 90%. **End member 2** is identical to the (filtered) compositions of AMB3 (Rhône basin, lower Turolian) and TNA (Vallès-Penedès basin, upper Vallesian). It is a relatively northern, humid end member containing significant numbers of both cricetids and murids (fig. 6.6). With a proportion of 50%, cricetids are

End-member modelling

the dominant family. The low humidity-adapted Cricetidae I and Muridae I groups are scarce. Humid groups such as the Gliridae I and Sciuridae II-Petauristidae-Eomyidae group score high. **End member 3** closely resembles the late Vallesian compositions from the CT basins (ROM9, ROM11), Duero basin (TOR1) and Greece (LEF), but some of the younger middle Turolian localities such as TOC (CT basins) and PK4 (Greece) show a high contribution of end member 3 as well. Approximately 75% of the composition of this end member consists of the Muridae II group, whereas the Cricetidae II group is totally absent (fig. 6.6). Both glirid groups are well-represented, whereas Xerini (Sciuridae I) are absent. Finally, **end member 4** has a composition which is typical for early MN9 localities (NOM and CASAL from the CT basins, and HSS and CP from the Vallès-Penedès basin), and several latest MN9 localities (PER5 and ROM3 from the CT basins). Cricetidae are dominant in this fourth end member (~70%), with about equal representations of high- and low-crowned groups. Very characteristic are the peak abundances for the ground-dwelling groups Gliridae I and Sciuridae I, and the very low numbers of Muridae.

Table 6.4. End-member compositions and climatic interpretations. Interpretations are based on the total net score of +, - and 0 scores calculated across columns. The individual scores are determined as follows: A positive score of a group in table 6.2 may translate into a positive, negative or neutral score on an end member in this table, if the group has a high, low or intermediately high proportion, respectively, in the end member, relative to other end members (comparison along rows of this table). Similarly a negative score in table 6.2 may translate into a negative, positive or neutral score. A neutral score in table 6.2 will always translate into a neutral score in this table. H = humidity, T = temperature, S = seasonality type, P = predictability.

group	end member																			
	1					2					3					4				
	%	H	T	S	P	%	H	T	S	P	%	H	T	S	P	%	H	T	S	P
Castoridae	0.67	-	+	-	-	1.07	0	0	0	0	1.51	+	-	+	+	0.77	-	+	-	-
Cricetidae I	9.44	+	0	0	0	6.77	+	0	0	0	9.10	+	0	0	0	36.92	-	0	0	0
Cricetidae II	3.76	0	0	0	0	49.99	0	0	0	0	0.00	0	0	0	0	32.62	0	0	0	0
Gliridae I	0.00	+	0	-	-	2.43	+	0	-	-	5.91	0	0	0	0	14.41	-	0	+	+
Gliridae II	0.00	-	+	-	-	6.37	+	-	+	+	6.93	+	-	+	+	1.21	-	+	-	-
Muridae I	61.22	-	0	-	-	0.44	+	0	+	+	0.75	+	0	+	+	0.00	+	0	+	+
Muridae II	21.77	0	0	+	+	20.54	0	0	+	+	74.18	0	0	-	-	6.54	0	0	+	+
Sciuridae I	2.20	0	0	0	0	0.69	+	-	+	-	0.00	+	-	+	-	5.38	-	+	-	+
Sciuridae II+	0.94	-	+	0	0	11.70	+	-	0	0	1.61	-	+	0	-	2.15	-	+	0	0
Petauristidae+ Eomyidae																				
net score		-	+	-	-		+	-	+	+		+	-	+			-	+		+
		2	3	3	3		6	3	3	1		4	2	3	0		5	4	0	2
relative climate		arid warm					humid cool					humid cool					arid warm			
		wet-dry seasonal predictable					cool-warm seasonal					cool-warm seasonal					predictable			

Table 6.5. Estimated end-member contributions and climatic parameters. See table 6.6 for estimation of climatic parameters.

locality	contribution of end member (total = 1)				climatic parameter (relative values)	
	1	2	3	4	humidity = - temperature	predictability = cool/warm seasonality = - wet/dry seasonality
<i>Teruel-Alfambra region, Teruel basin, Spain</i>						
KSS	0.696	0.056	0.248	0	0.12	-.65
KS	0.806	0	0.194	0	-0.46	-.95
VDC3	0.990	0	0.010	0	-1.27	-1.42
MDV7	0.983	0.013	0.004	0	-1.20	-1.39
CC	0.643	0.003	0.353	0	-0.24	-.79
CC3	0.665	0	0.335	0	-0.26	-.81
LM	0.949	0.040	0	0.011	-0.90	-1.22
CC2	0.694	0	0.306	0	-0.30	-.84
TO	0.929	0.009	0	0.062	-1.72	-1.19
VB2	0.919	0	0.081	0	-0.72	-1.12
MDV5	0.732	0.044	0.224	0	0.02	-.72
MDV4	0.725	0.003	0.272	0	-0.34	-.87
TOD	0.770	0	0.230	0	-0.40	-.91
TOC	0.223	0	0.777	0	0.27	-.28
MDV3	0.404	0	0.596	0	0.03	-.54
CCB	0.690	0	0.310	0	-0.29	-.83
MDV2	0.705	0	0.295	0	-0.31	-.85
LM2	0.755	0	0	0.245	-1.96	-.92
VIP	0.975	0.020	0	0.005	-0.91	-1.42
TOA	0.978	0.018	0	0.004	-0.94	-1.43
AG3	0.984	0	0.016	0	-1.15	-1.36
ALF	0.941	0	0.059	0	-0.81	-1.17
PM3	0.885	0	0.037	0.078	-1.40	-.95
GLO10	0.989	0	0.011	0	-1.25	-1.41
AG1	0.960	0.031	0	0.009	-0.90	-1.30
PERD	0.073	0	0.811	0.116	0.02	.45
PERC	0.080	0	0.845	0.075	0.10	.37
R2	0.127	0	0.873	0	0.46	-.06
PM2	0.090	0	0.601	0.309	-0.36	.45
ROM11	0.076	0	0.924	0	0.63	.15
MBB	0.032	0	0.787	0.181	0.14	.81
PER4	0.005	0	0.863	0.132	0.78	1.48
ROM9	0.025	0	0.964	0.011	0.94	.58
MBA	0	0	0.843	0.157	0.53	1.24
ROM7	0	0	0.656	0.344	0.28	1.30
ROM4C	0	0	0.743	0.257	0.38	1.28
ROM3	0	0	0.110	0.890	-0.41	1.19
PER5	0	0	0.060	0.940	-0.57	1.11
<i>Teruel-Ademuz region, Teruel basin, Spain</i>						
CU	0.942	0	0.052	0.006	-0.75	-1.23
CASAL	0	0	0	1.000	-1.04	.88

End-member modelling

locality	contribution of end member (total = 1)				climatic parameter (relative values)	
	1	2	3	4	humidity = - temperature	predictability = cool/warm seasonality = - wet/dry seasonality
<i>Daroca region, Calatayud-Daroca basin, Spain</i>						
PED2C	0	0.573	0	0.427	0.28	1.28
PED2A	0	0.017	0.321	0.662	0.08	1.36
CAR1	0	0.465	0	0.535	0.16	1.28
NOM	0	0.042	0	0.958	-0.64	1.05
<i>Alicante, Spain</i>						
CR5	0.435	0.528	0.038	0	0.40	-0.45
CR4	0.346	0.342	0.312	0	0.88	-0.14
CR3	0.720	0.186	0.094	0	0.20	-0.65
CR2	0.529	0.262	0.141	0.068	0.02	-0.20
CR1	0.588	0.250	0.162	0	0.48	-0.46
<i>Valles-Penedès basin, Spain</i>						
TNA	0	1.000	0	0	1.33	.88
TSA2	0	0.884	0	0.116	0.71	1.17
CL	0	0.824	0	0.774	0.59	1.21
CP	0.168	0	0	0.832	-1.82	-0.21
HSS	0.230	0	0	0.770	-1.89	-0.33
<i>Duero basin, Spain</i>						
TOR1	0.041	0.034	0.925	0	1.14	.53
<i>Languedoc Central, France</i>						
MONTR	0	0.884	0.009	0.107	0.70	1.14
<i>Cucuron-Basse Durance, France</i>						
CUCS	0.978	0.017	0	0.005	-0.96	-1.44
<i>Rhone basin / Lyon area, France</i>						
LS	0	0.126	0.874	0	1.89	1.21
DION	0.067	0.158	0.775	0	1.38	.51
AMB3	0	1.000	0	0	1.33	.88
AMB2	0	0.890	0.110	0	1.91	1.18
AMB1	0	0.497	0.503	0	2.13	1.31
SOBL	0.011	0.819	0.170	0	1.97	1.19
DOUVR	0.025	0.872	0.104	0	1.62	.83
<i>Vienna basin, Austria</i>						
EICHK	0	0.666	0.334	0	2.11	1.29
<i>Strimon basin, Greece</i>						
PK4	0.170	0	0.611	0.219	-0.45	.17

locality	contribution of end member (total = 1)				climatic parameter (relative values)	
	1	2	3	4	humidity = - temperature	predictability = cool/warm seasonality = - wet/dry seasonality
<i>Rafina basin, Greece</i>						
LEF	0.051	0.049	0.821	0.080	.65	.73

Table 6.5. (continued)

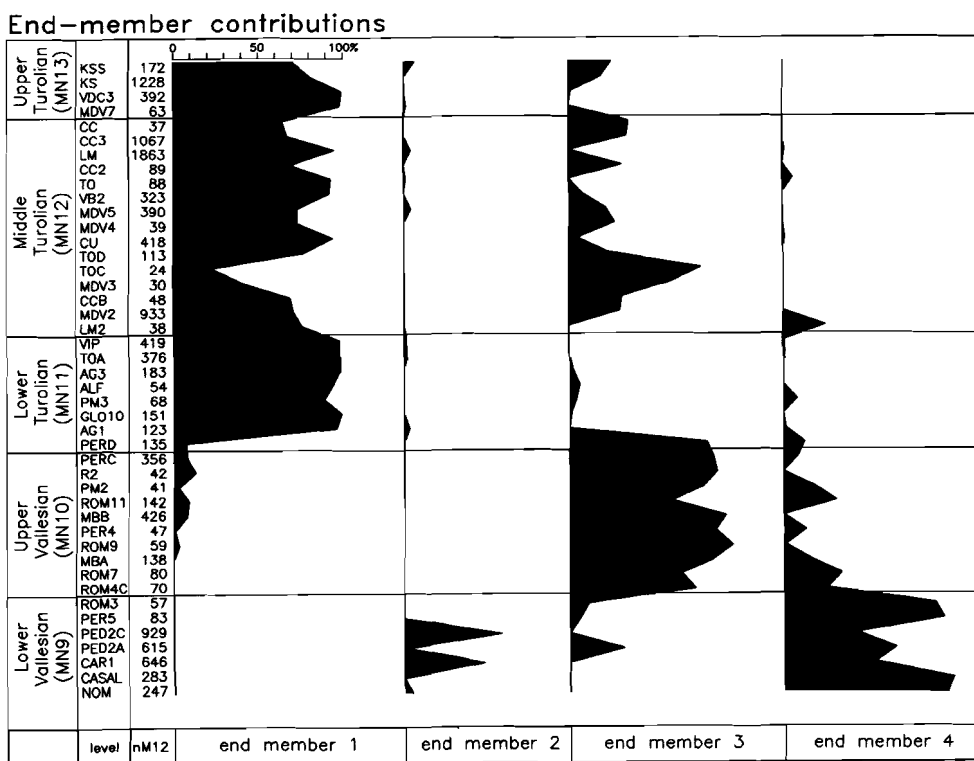


Figure 6.7. End-member contributions to the compositions of the localities from the Calatayud-Daroca and Teruel basins (together representing a large part of the end-member contribution matrix *M*).

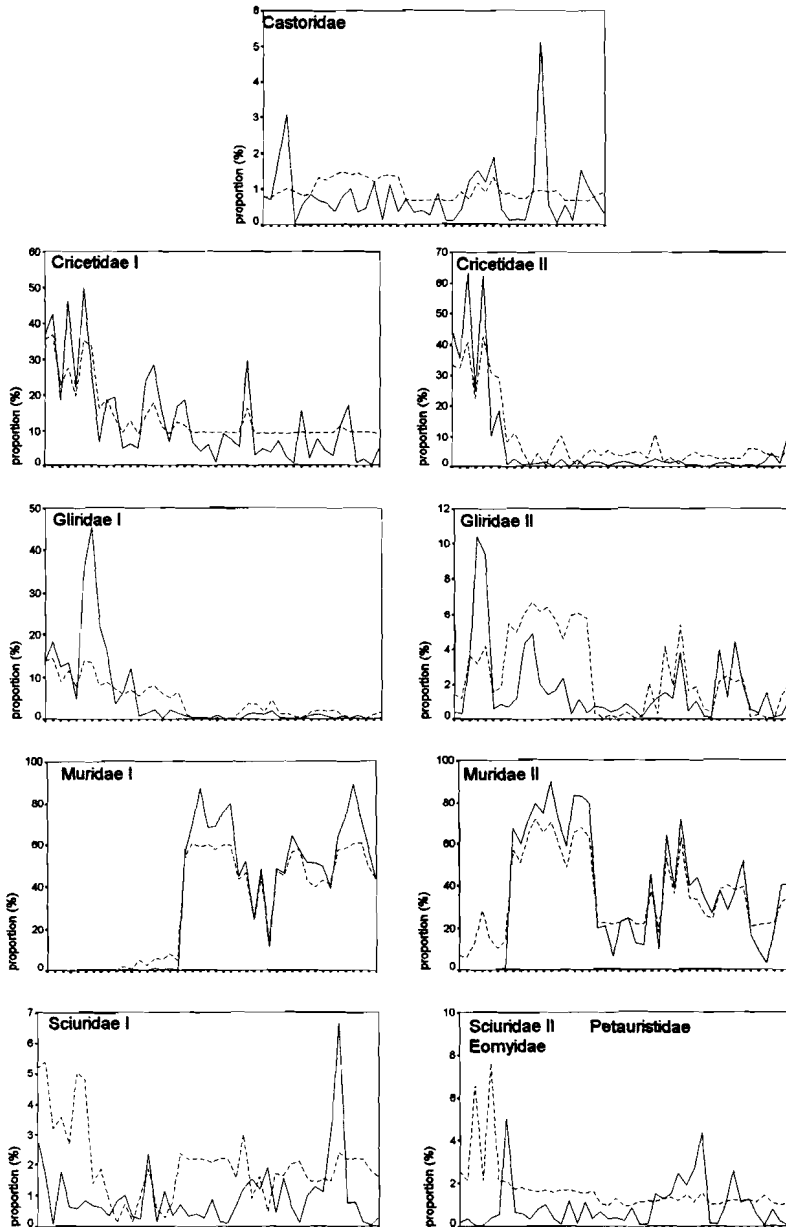


Figure 6.8. Comparison between model input (continuous line) and output (dashed line) for the nine environmental groups for the Calatayud-Daroca and Teruel basins. x axes represent localities from old (left) to young (right). Note the different scales on the y axes.

Figure 6.8 compares input and estimated model output for the CT basins. This figure shows that a significant amount of noise has been removed from the data. The general smoothing effect is shown by the reduction of extreme values. In some individual cases, filtering leads to pronounced modifications in proportions: for instance, a 45% maximum in terrestrial Gliridae (Gliridae 1) is not recognized as relevant in the model, and completely eliminated. An interesting result is the consistent generation of proportions up to 7% of Muridae I (*Occitanomys/Stephanomys*) just before their actual entry in the early Turolian. Supposedly, on the basis of the covariations between all groups, the model "expects" already some Muridae I in the late Vallesian (note that time is not included in the model, but only added afterwards.). This virtual presence is acceptable, given the gradual morphological change from *Progonomys hispanicus* (Muridae II) leading to *Occitanomys* (Muridae I) during this interval (van de Weerd, 1976; chapter 3). A similar effect occurs in Muridae II, which show substantial estimated proportions (in one case even 28%) during MN9, although it is still an extremely rare group by then. The interpretation could be that the environment was suitable for this group in principle, but that some other factor may have prevented the group from becoming abundant (which implies the violation of model assumptions 1 and 2, see 4.3.2). Figure 6.8 also shows that proportional variation in the rare Castoridae and the Sciuridae II / Eomyidae group are largely interpreted as noise for the CT basins. Particularly the latter group is more abundant in other basins, where its abundances are not interpreted as noise.

Table 6.6. Selection procedure for sets of end-member pairs for each climatic parameter. The choice of an initial set is made as follows: first, those end-member pairs are selected which correspond to complementary states in table 6.4 (e.g. cooler vs. warmer). Next, those pairs are selected which correspond to a net score difference larger than 2 (numbers between brackets), with a maximum of four pairs (or more in the case of ex-aequo values). Finally, the logratios of end-member contributions are calculated according to equation (7), and used in a principal component analysis. The first component (PC1) is considered as the best estimator of the climatic parameter. Loadings of the logratios on the PC1's are shown. The procedure results in identical sets of pairs for humidity and temperature (first and third column). In the case of seasonality type, negative loadings on PC1 of pairs 2-4 and 3-4 appear (sixth column). Omission of these pairs yields the same set as selected for predictability (seventh column).

humidity		temperature		seasonality type (preparatory step 1)		seasonality type/ predictability	
selected pair (net score difference table 6.4)	loading on PC1 (43.5% explained)	selected pair (net score difference table 6.4)	loading on PC1 (43.5% explained)	selected pair (net score difference table 6.4)	loading on PC1 (46.7% explained)	selected pair (net score difference table 6.4)	loading on PC1 (74.9% explained)
2-1 (8)	.77	1-2 (6)	.77	2-1 (6)	.78	2-1 (6/4)	.75
2-4 (11)	.61	1-3 (5)	.74	2-4 (3)	-.27	3-1 (6/3)	.71
3-1 (6)	.74	4-2 (7)	.61	3-1 (6)	.71	4-1 (3/5)	.79
3-4 (9)	.48	4-3 (6)	.48	3-4 (3)	-.42		
				4-1 (3)	.98		

6.6.2. Climatic parameter estimation

As explained above, the final values of the climatic parameters (table 6.5) are based on logratios of end members with opposite interpretations. For each parameter, those end-member pairs are selected which correspond to high differences in net scores in table 6.4. Only differences

End-member modelling

larger than 2 are considered, and the maximum number of end member pairs is set to four. For instance, the final humidity index is calculated as the first principal component of the four logratios corresponding to the end-member pairs 2-1, 2-4, 3-1 and 3-4. These pairs correspond to differences of 8, 11, 6 and 9 respectively (table 6.6). It appears that the sets of pairs for humidity and temperature are identical, which implies that these two parameters are fully correlated. In other words they can be represented by a single signal, reflecting the variation between the two combinations cool-humid and warm-arid. Table 6.6 also shows that seasonality type and predictability can be represented by a single signal, because two pairs with low net score differences can be omitted because of a negative loading on the first principal component. The resulting combinations are predictability and cool-warm seasonality on the one hand, and unpredictability and wet-dry seasonality on the other hand.

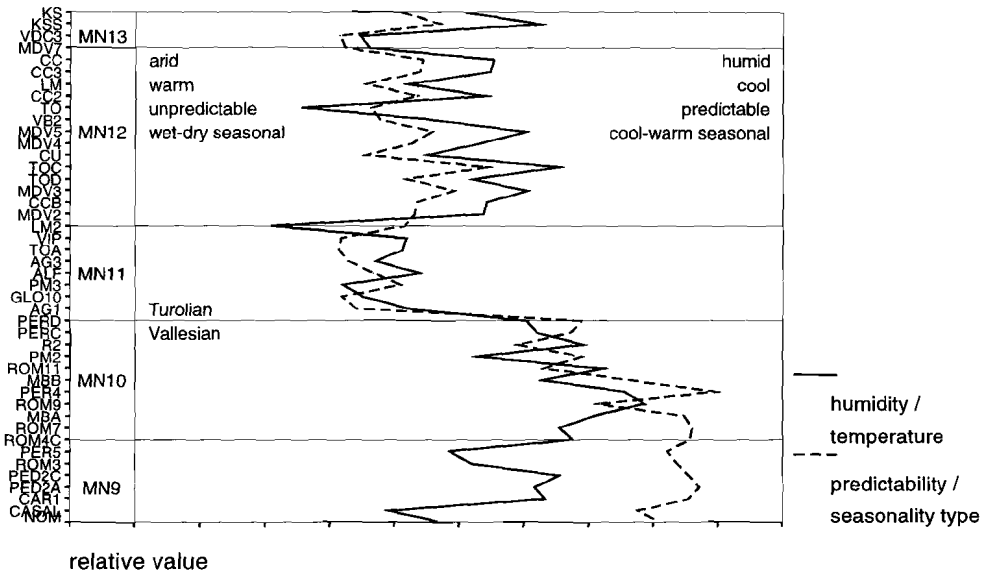


Figure 6.9. Relative humidity/temperature parameter and seasonality/predictability parameter for the localities of the Calatayud-Daroca and Teruel basins. For the full locality names see table 6.1.

The final values of the climatic parameters for all localities are shown in table 6.5. Figure 6.9 shows the raw values for the subset of localities from the CT basins. Figure 6.10 shows the smoothed curves against numerical time. The combined humidity-temperature curve shows a long humid and cool phase between ~10.5-8.5 Ma, and shorter ones around 7 and 6 Ma. Two peaks (called small mammal (SM) events SM10A and SM12A in chapter 7), occur at 9.4 and ~7 Ma. Arid and warm phases occur between 11.0 and 10.5, between 8.5 and 7.5 Ma and around 6.5 Ma. The seasonality-predictability signal shows a shift from a more predictable cool-warm seasonal climate to a more unpredictable wet-dry seasonal climate in two steps occurring at 9.4 to 9.0 and 8.7 to 8.2 Ma. The humidity-temperature and seasonality-predictability signals are strongly correlated ($r=.68, p<.001$ for all localities; $r=.64, p<.001$ for the CT basins). This means that the cooler and humid climates are also more cool-warm seasonal and more predictable. Figures 6.9 and 6.10 show that a main divergence between the two signals occurs in MN9 where relatively

warm and dry conditions are combined with a relatively high predictability and strong cool-warm seasonality.

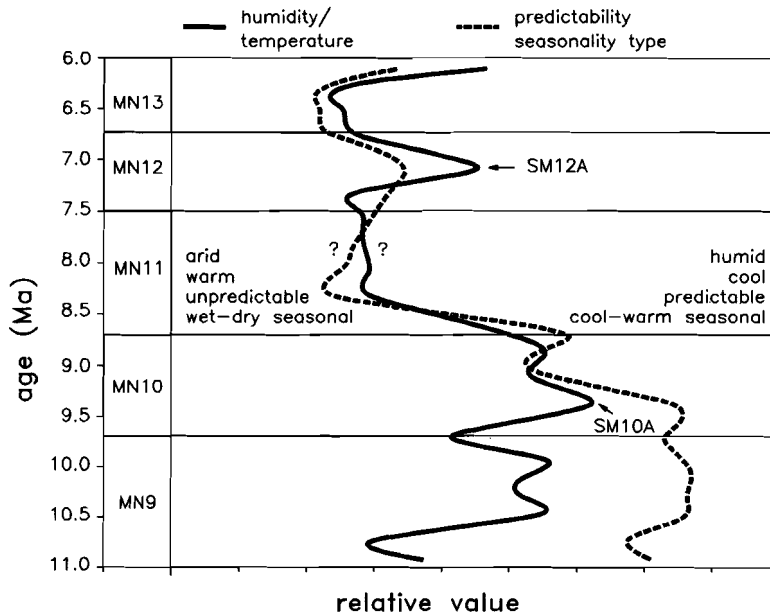


Figure 6.10. Proposed climate curves for the Calatayud-Daroca and Teruel basins relative to numerical time (ages converted to the scale of Cande and Kent, 1995). Parameter values were averaged per 0.2 m.y. interval, with linear interpolation used to replace missing values. Question marks indicate an interval for which estimations are uncertain, because of three subsequent missing values at 7.5, 7.7 and 7.9 Ma. Curves were smoothed by spline interpolation.

Figure 6.11 shows paleogeographic maps with mean parameter values per basin and MN zone. It should be stressed that some "mean" values are based on one locality only, whereas others are based on many. Nevertheless, the figure shows some interesting patterns, such as a similarity between Spanish bardiagrams for MN10 (fig. 6.11c) and the northern diagrams of both figures 6.11d and e (MN11-12). In some cases, strong similarities exist between areas from the same latitude and time slice, for instance Spain and Greece during MN10 and 12, and France and Austria during MN11. In addition, figure 6.11 shows climatic differences between coastal and continental areas. For example, the coastal Vallès-Penedès area scores higher on aridity and temperature, unpredictability and wet-dry seasonality than the CT area during early MN9 (fig. 6.11a). During late MN9 and MN10 the situation is reversed with regard to humidity and temperature. Another example is Alicante (South Spain), which shows somewhat higher humidities and lower average temperatures than the interiorly situated CT area during MN11-12.

The scatter diagram of figure 6.12 shows the inferred climatic features of all 67 localities. Three major and two minor clusters can be distinguished. The transition from cluster 2 via cluster 3 to 4 reflects the general transition in Spain from a cool-warm seasonal, predictable climate during MN9-10 (cluster 2) towards a wet-dry seasonal and unpredictable climate in MN11-13 (cluster 4). The early MN9 localities, particularly HSS and CP from the Vallès-Penedès basin (cluster 1), fall outside the main trend. They are warm and dry, but relatively cool-warm seasonal.

End-member modelling

The northern localities EICHK from the Vienna basin and DOUVR, SOBL, AMB1-3, and DION from the Rhone area fall in the most humid-cool part of the diagram (in cluster 3). The northern MN11 localities (e.g. EICHK, AMB3, DION) are much more temperate than the contemporaneous Spanish localities. The three localities from the Teruel basin of cluster 5 differ climatically from the time-equivalent localities of cluster 4. Their aridity/temperature level is equal to that of cluster 1.

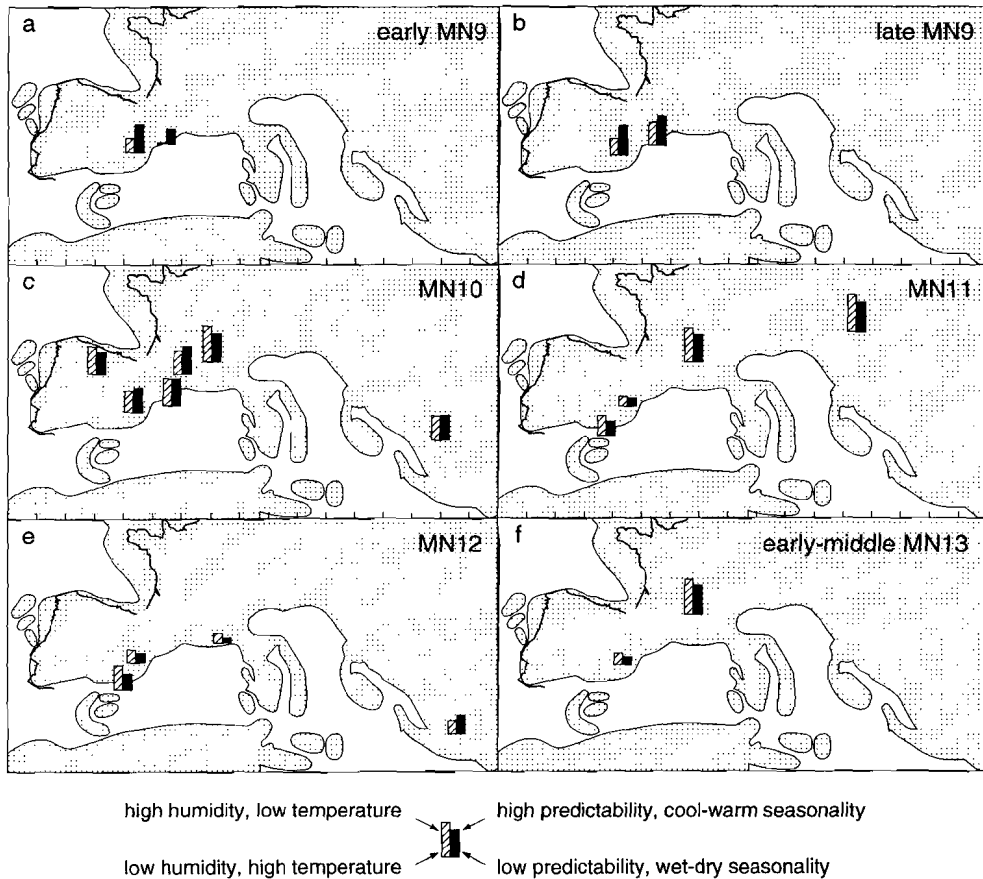


Figure 6.11. Mean values for the relative humidity/temperature, and seasonality/predictability parameter per basin and zone. Note that some values are based on one locality only, whereas others are based on more. "Early" MN9 localities are NOM, CASAL, CARI, HSS and CP. Paleogeographic basemap for the Tortonian after Dercourt et al. (1993).

6.6.3. Robustness

Both the selection procedure for end-member pairs and the filtering effect of the principal component analysis (table 6.6) contribute to the robustness of the method against errors in preferences and adaptations of groups in table 6.2. Firstly, a change of a preference score does not necessarily lead to a different set of logratio pairs in table 6.6, and secondly, if it does lead to

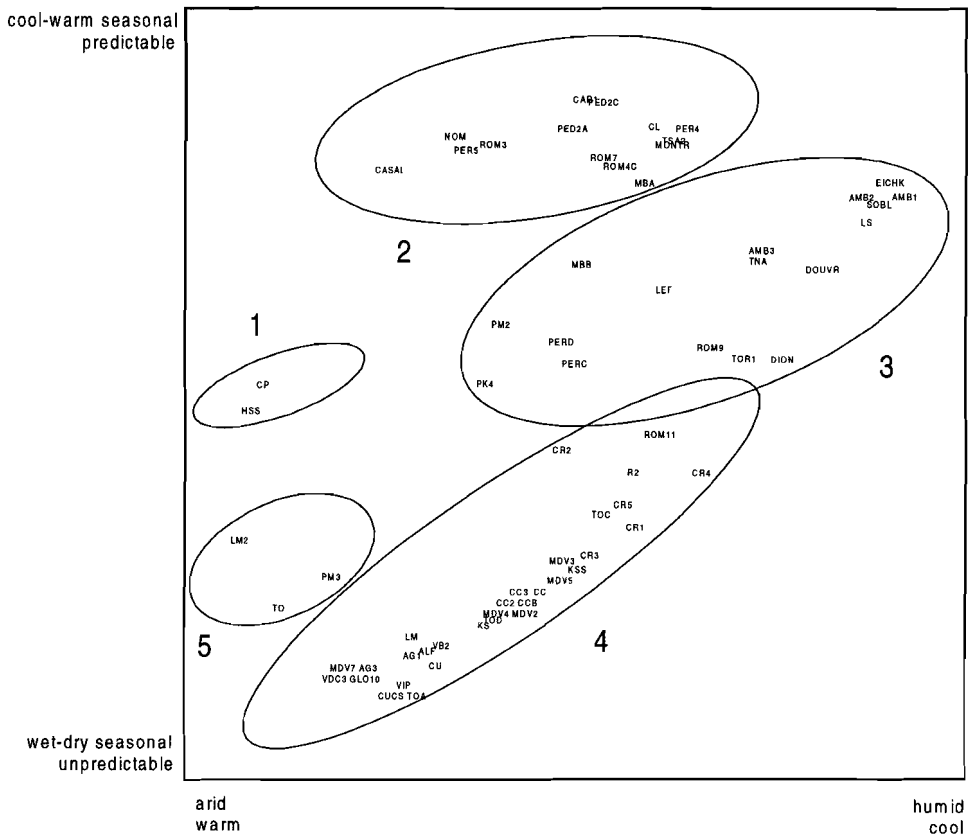


Figure 6.12. Scatter diagram with positions of all 67 localities. Three major and two minor clusters can be distinguished. The transition from cluster 2 via cluster 3 to 4 reflects the general transition in Spain from a cool-warm seasonal, predictable climate during MN9-10 (cluster 2) towards a wet-dry seasonal and unpredictable climate in MN11-13 (cluster 4). The early MN9 localities, particularly HSS and CP from the Vallès-Penedès basin (cluster 1), fall outside the main trend. They are warm and dry, but relatively cool-warm seasonal. The northern localities EICHK from the Vienna basin and DOUVR, SOBL, AMB1-3, and DION from the Rhone area fall in the most humid-cool part of the diagram (in cluster 3). The northern MN11 localities (e.g. EICHK, AMB3, DION) are much more temperate than the contemporaneous Spanish localities. The three localities from the Teruel basin of cluster 5 differ climatically from the time-equivalent localities of cluster 4. Their aridity/temperature level is equal to that of cluster 1.

another pair, PCA conservatively extracts the common signal contained by all logratios. Table 6.7 shows an example of this robustness: various alternatives for preferences and adaptations of Cricetidae result in identical sets of end-member pairs.

A second type of robustness relates to the sensitivity of climatic interpretations to structural under- or over-representation of groups. As an example, in table 6.8 we check robustness against systematic demographic bias in gradually accumulating assemblages caused by differences in life expectancies of groups (van Valen, 1964; Damuth, 1982). (The same

End-member modelling

Table 6.6. Selection procedure for sets of end-member pairs for each climatic parameter. The choice of an initial set is made as follows: first, those end-member pairs are selected which correspond to complementary states in table 6.4 (e.g. cooler vs. warmer). Next, those pairs are selected which correspond to a net score difference larger than 2 (numbers between brackets), with a maximum of four pairs (or more in the case of ex-aequo values). Finally, the logratios of end-member contributions are calculated according to equation (7), and used in a principal component analysis. The first component (PC1) is considered as the best estimator of the climatic parameter. Loadings of the logratios on the PC1's are shown. The procedure results in identical sets of pairs for humidity and temperature (first and third column). In the case of seasonality type, negative loadings on PC1 of pairs 2-4 and 3-4 appear (sixth column). Omission of these pairs yields the same set as selected for predictability (seventh column).

humidity		temperature		seasonality type (preparatory step 1)		seasonality type/ predictability	
selected pair (net score difference table 6.4)	loading on PC1 (43.5% explained)	selected pair (net score difference table 6.4)	loading on PC1 (43.5% explained)	selected pair (net score difference table 6.4)	loading on PC1 (46.7% explained)	selected pair (net score difference table 6.4)	loading on PC1 (74.9% explained)
2-1 (8)	.77	1-2 (6)	.77	2-1 (6)	.78	2-1 (6/4)	.75
2-4 (11)	.61	1-3 (5)	.74	2-4 (3)	-.27	3-1 (6/3)	.71
3-1 (6)	.74	4-2 (7)	.61	3-1 (6)	.71	4-1 (3/5)	.79
3-4 (9)	.48	4-3 (6)	.48	3-4 (3)	-.42		
				4-1 (3)	.98		

Table 6.7. Robustness of climatic parameter estimation against alternative choices for preferences and adaptations of Cricetidae. 0 scores are from table 6.2, + and - scores are alternatives. Net score calculation as in table 6.4. End-member pair selection and PC1 calculation as in table 6.6. Pairs between brackets can be omitted because of negative loadings on PC1. Alternatives result in identical sets of end-member pairs and hence in identical climatic parameter estimations.

parameter and group	score	net score of all groups on end members				resulting end-member pairs
		end m. 1	end m. 2	end m. 3	end m. 4	
humidity (Cricetidae I)	0	-2	+6	+4	-5	2-1, 2-4, 3-1, 3-4
	-	-1	+5	+5	-6	2-1, 2-4, 3-1, 3-4
temperature (Cricetidae I)	0	+3	-3	-2	+4	1-2, 1-3, 4-2, 4-3
	-	+4	-4	-1	+3	1-2, 1-3, 4-2, 4-3
	+	+2	-2	-3	+5	1-2, 1-3, 4-2, 4-3
seasonality type (Cricetidae I)	0	-3	+3	+3	0	2-1, 3-1, 4-1, (2-4, 3-4)
	+	-4	+4	+2	+1	2-1, 3-1, 4-1, (2-4)
seasonality type (Cricetidae I & II)	+	-5	+3	+1	+2	2-1, 3-1, 4-1

reasoning applies to robustness against systematic taphonomic bias.) Correction factors are only approximate and represent typical life expectancy values for demographic types after French et al. (1975). Corrected end-member compositions are calculated by multiplication of the percentages by the correction factors and scaling to 100%. It appears that end-member compositions are very different from those in table 6.4, but that row-

wise comparisons result in identical +, -, and 0 scores for eight of the nine groups except in one case (a shift from a negative to a neutral score for the contribution of Castoridae to end member 1). Therefore, it may be concluded that our method of climatic interpretation of end members is very robust against systematic under- or over-representation in general, even when correction factors differ by a factor five.

6.7. Discussion of the results

6.7.1. Other paleoclimatic records from the Mediterranean

Martin and Braga (1994) and Brachert et al. (1996) discuss the climatic significance of the vertical alternation of coral reefs and bryozoan/mollusc-dominated carbonate ramps in Neogene basins of the Betic Cordillera (southern Spain) (fig. 6.13f). Warm episodes characterized by reefs occurred during the latest Serravallian(?) to earliest Tortonian, the early late Tortonian, the early Messinian, and the latest Messinian. Cooler intervals characterized by the dominance of bryozoans and molluscs occurred during the rest of the early Tortonian (including an radiometrically dated interval of which the onset and end are dated at 9.6 and 8.6 Ma, respectively), the latest Tortonian to earliest Messinian, and the middle to late Messinian. These climatic inferences fit our climatic interpretations (figs. 6.10 and 6.13c) fairly well. It is not impossible that their latest Serravallian(?) - earliest Tortonian reef phase corresponds to our earliest Vallesian warming around 11 Ma, but because the reef-associated highstand is supposed to precede a marked lowstand at ~ 11 Ma (fig. 6.13g) this correlation remains questionable.

Clay-mineral records from Sicily show abundant smectite in the middle Tortonian and Messinian sediments (Chamley et al., 1986; de Visser, 1991). Unfortunately, age control for the Tortonian part is poor, due to the lack of a refined biozonation. Linear interpolation between two tie points (*Neogloboquadrina* coiling change at 9.24 Ma, and Tortonian-Messinian boundary at 7.12 Ma, Krijgsman et al., 1994a, 1995) results in an age of 9.0 Ma for the onset of a gradual smectite increase, culminating in a marked spike at 8.5-8.3 Ma. According to de Visser (1991), this smectite increase may be attributed to various processes, one of which is the development of a warm climate with strong seasonal contrasts in humidity. Other possibilities are rejuvenation of relief, regression, and marine authigenesis. If the climatic hypothesis is true, then timing and interpretation are strikingly similar to that based on our rodents, which indicate warming and increasing wet-dry seasonality between 9.4 and 8.2 Ma, with a maximum occurring at ~ 8.3 Ma. Unfortunately, data for the interval 8.0 -7.5 Ma can not be compared because of a gap in the Spanish rodent record.

A second smectite increase starts at about the Tortonian-Messinian transition and continues well into the Messinian. This rise correlates less well with our interpretation of the Spanish record. This record shows a maximum of warm and wet-dry seasonal conditions in a more restricted interval between 6.8 and 6.3 Ma (fig. 6.10). No comparison can be made for the interval after 6 Ma because we have no rodent data covering this time slice.

Oxygen isotope values of planktonic foraminifera from sections on Sicily (van der Zwaan and Gudjonsson, 1986) do not show important trends or excursions over the studied interval. The carbon isotope record, however, shows a marked shift towards lighter values between ~8.3 and 7.1 Ma. According to van der Zwaan and Gudjonsson (1986), this shift could correlate to the late Miocene carbon shift as recognized in all major oceans (Keigwin and Shackleton, 1980; Vincent et al., 1980) between ~7.5 and 6.5 Ma, although the earlier start and larger amplitude of the Mediterranean shift is not well understood. Interesting are recent suggestions (Cerling et al., 1993; Hodell et al., 1994) for a relation between the global marine $\delta^{13}\text{C}$ shift and an opposite shift in $\delta^{13}\text{C}$ as recorded in various terrestrial paleosol and mammal enamel records across the world. Some of these records show an abrupt shift towards heavier isotopes between 7.5 and 6.5 Ma, whereas others show a more gradual shift between ~9 and ~6.5 Ma (Quade et al., 1989; Harrison et al., 1993; Morgan et al., 1994; Quade and Cerling, 1995). This terrestrial shift, which is interpreted as a (global) replacement of C3 plants (trees, shrubs and cool-growing season grasses) by C4 plants (warm-growing season grasses), is not observed in a carbon isotope record from Greece. This record indicates a continuation of C3 vegetation, in the form of dry forest and woodland in a regime of winter or mixed-seasonal rain (Quade et al., 1994). Given these results, it is not unreasonable to suggest that the shift towards more arid and wet-dry seasonal conditions as we inferred from the Spanish record between 9.4 and 8.2 Ma, is more related to summer than to winter dryness.

6.7.2. North-south gradients

Our reconstruction of a wetter and climatically more predictable zone (Central Europe) north of a more arid and unpredictable zone (Spain and probably also Greece), is confirmed by an analysis of diversity. We counted the number of common rodent genera in our data set covering the late Miocene, which is the number of genera after counting 95% of the specimens, with the genera ranked from the most to the least abundant (Johnson, 1964). It appears that this number is about nine in the upper Vallesian-lower Turolian localities of the Rhone and Vienna basins, whereas in the CT basins in Spain it is only three on the average. Relations between climatic factors and diversity were studied by Slobodkin and Sanders (1969), who considered the diversity of a community as a function of the three environmental factors severity, variability and predictability. According to them the highest diversities occur in less severe, and/or more predictable environments. According to Putman (1994, p.125), a "temperate climax woodland with regular seasonal fluctuations" is an example of a favourable (= non-severe), variable and predictable terrestrial environment. Such type of environment probably corresponds to the Central European part of our data set, which is characterized by large contributions of the end members 2 and 3.

Our model results seem to agree with reconstructions of Miocene vegetation zones (Wolfe, 1985; Tallis, 1991; Janis, 1993). These reconstructions point to a broad zone of temperate, broad-leaved deciduous woodlands or temperate seasonal forests north of a zone of sclerophyllous woodlands or Mediterranean shrublands. The latter zone becomes

more distinct from the latest middle Miocene onwards, when xerophytisation of floras leads to "Troockenfloren" (dry floras) (Mai, 1995). Whether the distinction between the two vegetation belts also corresponds to a difference in climate types (*sensu* Köppen) is not sure. Macrofloral evidence from the late Miocene of Europe points to the general presence of a Cfa climate (temperate-warm without a dry season), although also Cs and Cw climates (temperate-warm summer-dry and winter-dry, respectively) have been postulated for Mediterranean sites (review in Mai, 1995).

6.7.3. Low-frequency shifting of climate belts?

The next question is whether the long-term climatic fluctuations as observed for instance in Spain, are related to changes in the size and position of climate belts. Or more explicitly: do intervals of more humid-cooler conditions in Spain correspond to southward migrations of a Cfa climate and/or the associated seasonal forest or woodland zone?

Latitudinal migration of climate belts seems to be a common phenomenon on all time scales, resulting from changes in meridional thermal gradients and associated changes in the position of polar ice fronts and ocean surface temperatures. For example, precipitation zones shift seasonally, leading to a more southern position of the mid-latitude westerly winds and associated depressions during Northern Hemisphere winters. This southern migration of precipitation belts is assumed to occur also at the levels of decades (Agee, 1980), millennia (Lamb, 1972), and glacial maxima (e.g. Nicholson and Flohn, 1980). Variations in solar radiation at the scale of Milankovitch cycles are also expected to lead to circulation changes in about the same way, with polar cooling leading to the migration of zones and contraction of the Hadley cell (Perlmutter and Matthews, *in press*). High-resolution records of marine flora and fauna indicate that astronomical forcing leads to migrational patterns with Milankovitch periodicities of ~ 20, 40, and 100 m.y. (Hays et al., 1976; Ruddiman and McIntyre, 1984; Beaufort and Aubry, 1990; Lourens et al. 1992) and their low-frequency modulations of 1.2 and 2.3 m.y. (Beaufort, 1994; Lourens and Hilgen, 1997).

Whether these types of low-frequency fluctuations also underlie or trigger the million-year scale variations in humidity and temperature as inferred for the late Miocene of Spain is difficult to test with our data alone, because of the small number of areas per time slice. At best the figures 6.11c and e seem to indicate similar climatic trends in Spain, southernmost France, and Greece between MN10 and MN12. Furthermore, persistence of cooler and more humid climatic conditions in the Rhone area between MN10 and 13 (fig. 6.11c-f) suggest that the boundary with the subtropical Mediterranean zone remained south of this area during that interval. Clearly, more data are needed to test the hypothesis of latitudinal shifting.

Insectivores were not included in our quantitative analyses. Nevertheless, some interesting examples of north-south migrations seem to confirm the results based on rodents. For instance, the intermittent presence of Anourosoricini (Soricidae, Insectivora) in the CT basins (fig. 6.13b) corresponds fairly well with peaks of more humid and cool conditions (fig 13c). The presence of Anourosoricini in Spain during more temperate intervals can be seen as the result of occasional southward expansions, given the

End-member modelling

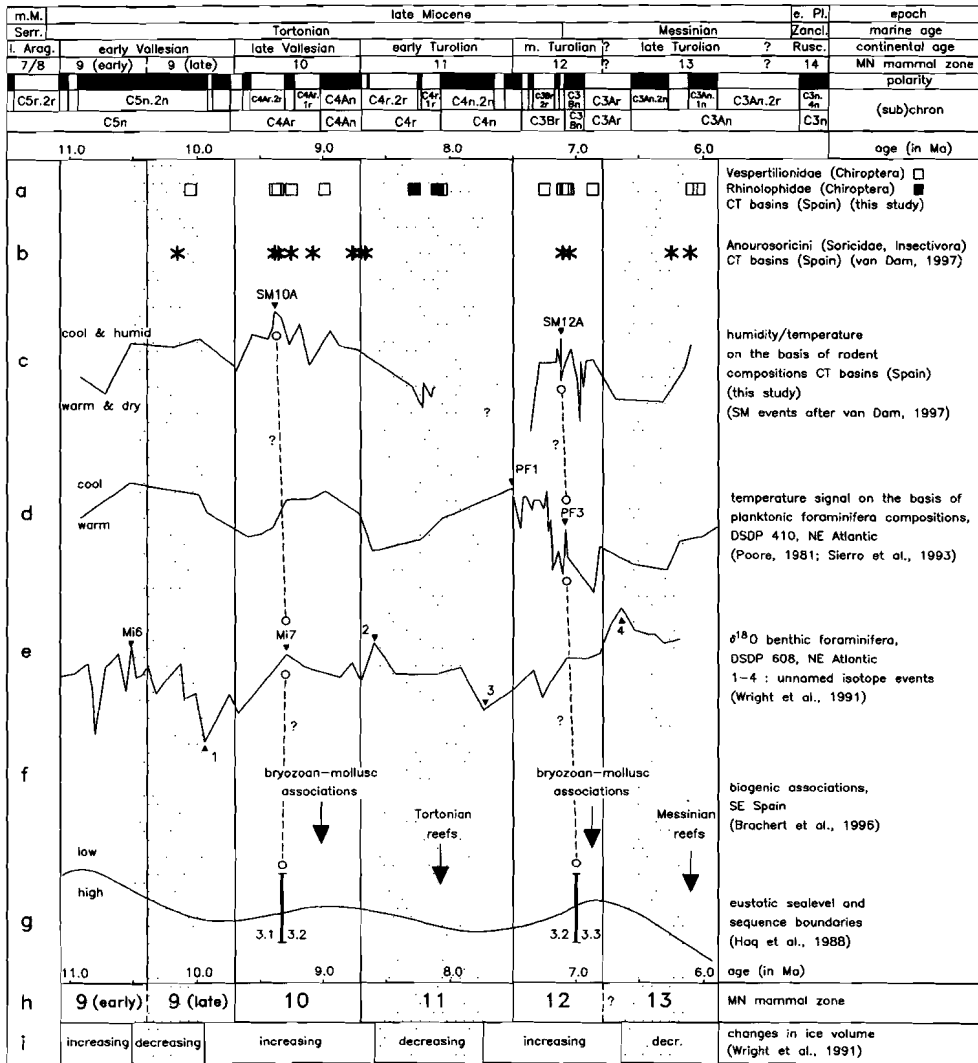


Figure 6.13. Various late Miocene climate-related records, with a special emphasis on the NE Atlantic / W Mediterranean region. Solid vertical lines: continental age and mammal zone (MN) boundaries; "early" and "late" MN9 correspond to MN9 "a" and "b" of Agustí and Moyà-Solà (1991). Dashed lines: proposed correlations. Stippled areas: intervals of decreased ice volume according to Wright et al. (1991). Ages calibrated to the time scale of Cande and Kent (1995). The data for curve d were recalibrated by linear interpolation between five calibration points: base of chron C5r.1r (10.949 Ma), FAD of *Discoaster berggreni* (8.6 Ma; Berggren et al., 1996), planktonic foraminifer events PF1 (7.09 Ma) and PF3 (7.51 Ma) (ages according to Hodell et al., 1994), and Miocene-Pliocene boundary (5.3 Ma according to Berggren et al., 1996) which is regarded by Poore (1981) as equivalent to the highest unequivocal Miocene in core 410. The data for curve e were recalibrated by linear interpolation between ten calibration points: isotope events Mi6 (10.53 Ma) and Mi7 (9.31 Ma) (ages after Oslick et al., 1994, recalibrated to the Cande and Kent, 1995 time scale), chron boundaries C5An.1n-C5r.3r, C5r.1r-C5n.2n, C5n.1n-C4Ar.3r, C4Ar.2r-C4Ar.1n, C4Ar-C4r.2r, C4r.1r-C4n.2n, C4n.1n-C3Br.3r, and recalibration of age of core top (Wright et al., 1991: figs. 2 and 3). Range of absolute values for curve e: 1.77-2.37 parts per thousand. For curve g we used Haq et al.'s (1988) calibration to the geomagnetic polarity pattern. Range of sealevel in curve g: ~ -50 - +50 m relative to the present-day level.

generally northern distribution of this tribe across Eurasia during the Neogene (Bachmayer and Wilson, 1970; Franzen and Storch, 1975; Storch and Zazhigin, 1996). A second example relates to the gradual southward migration of the Crocidoloricinae from central to southern Europe during the early to early late Miocene, followed by their final extinction. These events were attributed to general cooling by Reumer (1994). New data from the Teruel basin (chapter 2) show that the group disappeared from this area around the late Vallesian temperature minimum. Possibly, the sparse Chiroptera (bat) record from the CT basins (fig. 6.13a) is also a reflection of north-south migrations: Rhinolophidae are restricted to the early Turolian (MN11), which is a warm interval according to the rodent-based model (fig. 6.13c). Today this family of bats lives in tropical and temperate zones. Open squares represent Vespertilionidae, a group which presently lives in temperate and polar areas. Their clustering in MN10 and MN12/13 assemblages seems to confirm the lower temperatures during these intervals.

A scenario of latitudinal migration of climatic belts is advocated by Pickford and Morales (1994) who present a zoogeographic model based on ranges of Neogene macromammals from Spain and East Africa. These authors suggest that north-south shifts of the boundary zone between the "Paleo-Palaeartic" and "Paleo-Ethiopian" zoogeographic regions either opened or blocked critical passages through the Middle East and Afghanistan. During some intervals Spain would more belong to the "Paleo-Palaeartic" region (for the late Miocene this applies to MN9, MN10 and MN12), whereas during others it would belong to the "Paleo-Ethiopian" region (early MN9, MN11, MN13). These results fit our rodent-based results very well except for MN13, for which the authors suggest a very northern position of their boundary (i.e. warm conditions). At least part of the lack of correspondence for MN13 may be explained by the absence of early MN13 macromammal localities in the data set of Pickford and Morales, and the absence of late MN13 micromammal localities in our data set.

If such low-frequency migrations of belts occurred, then their effects are expected to show up in oceanic records from the same latitude and region. Figure 6.13c shows our humidity/temperature curve for Spain, which is compared to a principal component curve (fig. 6.13d) based on planktonic foraminiferal abundances from DSDP Site 410 from the NE Atlantic (Poore, 1981; Sierro et al., 1993), a benthic $\delta^{18}\text{O}$ curve (fig. 6.13e) from DSDP site 608, NE Atlantic (Wright et al., 1991), and the eustatic sealevel curve (fig. 6.13g) after Haq et al. (1988). The foraminiferal signal is supposed to indicate long-term cycles in sea surface temperature (Poore, 1981) while the oxygen isotope signal from site 608 has been interpreted in terms of low-frequency glacial-interglacial cycles (the stippled areas and fig. 13i). Assuming that the sealevel signal is of glacioeustatic origin, it may be expected to reflect glacial-interglacial cycles and, like curves d and e, to fit the scenario of shifting climate belts. The correspondence between the rodent and planktonic foraminiferal curve is fairly good. However, the correspondence between these two curves and the oxygen isotope curve is poor, especially after 8 Ma. The main differences between the sealevel curve and the rodent and foraminiferal curves concern the intervals before ~10.5 Ma and after ~6.5 Ma. The isotope and sealevel curves show a positive correlation, although low sealevels after 6.5 Ma correspond to an interval of relatively high $\delta^{18}\text{O}$ values. The alternation of coral reefs and bryozoan/mollusc-dominated

associations (see above and fig. 6.13f), of which the interpretation in terms of temperature fits well our results, is interpreted as the consequence of climate-controlled latitudinal shifting of the northern margins of the Miocene reef belt (Martin and Braga, 1994; Brachert et al., 1996). A general correlation of lower temperatures in Spain to sea-level lowstands (figs. 6.13c and g) is also inferred by the latter authors, who correlate the warmer reef episodes to sea-level highstands and the cooler bryozoan/mollusc-dominated episodes to lowstands on the basis of the geometries and approximate datings of the various biogenic units (figs. 6.13f and g).

Both the rodent-based cooling peaks SM10A and SM12A are close in time to clusters of (related?) marine events. SM10A (9.4 Ma) correlates well with global oxygen isotope event Mi7 (9.31 Ma) (Wright and Miller, 1992; age after Oslick et al., 1994) and to sequence boundary 3.1/3.2 (Haq et al., 1988). Sequence boundaries are generally thought to correlate with times of most rapid glacio-eustatic lowerings, and therefore to be stratigraphically close to Mi events (Miller et al., 1991). The clustering of events around 9.4-9.3 Ma could represent a climatic minimum within an early late Miocene predominantly cool episode. Studies on Antarctic and Southern Ocean deep sea cores indicate that the West Antarctic ice sheet probably started to develop by this time (Cieselski and Weaver, 1983; Robin, 1988; Kennett and Barker, 1990). Scattered ice build-up at Northern Hemisphere high latitudes around this time is indicated by ice-rafted debris (IRD) and glacier-related deposits (Denton and Armstrong, 1969; Hamilton, 1986; Schaeffer and Spiegler, 1986; Jansen et al., 1995; Wolf-Welling et al., 1995). Palynological data from Iceland indicate a strong cooling between 10 and 9.5 Ma (Mudie and Helgason, 1983), i.e. slightly before our maximum at 9.3-9.4 Ma.

Although alternative paleomagnetic interpretations are possible for the middle to late Turolian sections in the CT basins (appendix B), the most probable solution points to an age around 7 Ma for cooling event SM12A, which is temporally close to sequence boundary 3.2/3.3 and close to the base of the Messinian (7.12 Ma, Krijgsman et al., 1994a, 1995) and planktonic foraminiferal cooling event PF3 (7.09 Ma, Sierro et al., 1993; Hodell et al., 1994). However, there is no oxygen isotope excursion analogous to Mi7 at Site 608 around 7.1 Ma, although Hodell et al. (1994) note a two-step increase in $\delta^{18}\text{O}$ around the Tortonian-Messinian transition in Morocco, the first of which occurs at 7.17 Ma. The general shift towards heavier isotopes, which is observed at various oceanic sites at this time, probably marks the onset of a latest Miocene (Messinian) phase of renewed glacial expansion on the Southern Hemisphere (Mercer, 1983; see also Cita and McKenzie, 1986). Supposedly, the West Antarctic ice sheet became a permanent, stable feature by then (Kennett, 1986; Kennett and Barker, 1990; Ehrmann et al., 1992). In addition, there is evidence for scattered Northern Hemisphere glaciation at these times (Jansen and Sjøholm, 1993; Larsen et al., 1994, Wolf-Welling et al., 1995). The lack of correspondence between the curves of figure 6.13 for the interval after ~ 8 Ma may be indicative of the complex relation between ice accumulation and temperature at Northern Hemisphere mid-latitudes. The apparent lack of correspondence between polar and Mediterranean cooling during the Messinian is perhaps not surprising, because of the high probability of a regional climatic overprint in the Mediterranean in connection with the salinity crisis.

Lourens and Hilgen (1997) correlate Plio-Pleistocene third-order sea level cycles to astronomical cycles, in particular to a low-frequency (1.2 m.y.) modulation of the 41 k.y. earth obliquity signal. However, they note that such correlations work less well for the middle to late Miocene, where a modulation of the ~100 k.y. eccentricity signal with a periodicity of 2.3 m.y. seems to be more pronounced. This 2.3 m.y. signal is recognized in sapropel patterns (Hilgen et al., 1995) and planktonic foraminiferal abundances (Lourens and Hilgen, 1997). The % left-coiling neogloboquadrinids (from 10 to 6.6 Ma), which species type is used by the latter authors as a low-temperature proxy, indicates warmings at 10-9.5 and 7.7-7.3 Ma, together bracketing one complete cycle of ~2.3 m.y. Cooler conditions occur between 9.4 and 8.4 Ma and 6.8 and 6.6 Ma. The temperature signal corresponds more or less to our temperature signal for Spain, except for the latter cooling (fig. 6.10). It is interesting that our interval of most marked faunal and climatic turnover (9.0 to 8.3 Ma) around the Vallesian-Turolian boundary (8.7 Ma) is close in time to an interval of strong oscillations in neogloboquadrinids between 8.7-8.3 Ma. These oscillations would indicate a cooling maximum at 8.7 Ma, followed by a warming maximum at 8.5 Ma, which is immediately followed by a strong cooling at 8.4 Ma and a more permanent return to warmer conditions at 8.3 Ma. Indirect links between long-term astronomical forcing and changes in terrestrial ecosystems, if existing, will undoubtedly be complex. More long, detailed, and dated time series from different areas are needed to be able to demonstrate the reality and nature of such relations.

6.8. Conclusions

The main conclusions are:

1) End-member modelling is a useful method to extract paleoclimatic information from series of fossil rodent assemblages. The specific bilinear unmixing solution used here yields well-interpretable sets of end members. The contributions of these members to the samples can easily be converted to relative values for climatic parameters, given the preferences and adaptations of the rodent groups.

2) Life-history characteristics deserve to be used more in small-mammal based paleoecological and -climatological reconstructions, because they carry valuable information on the seasonal aspects of climate.

3) The model results for Spain indicate more humid and cooler conditions between 10.5 and 8.5, around 7, and around 6 Ma, and more arid and warmer conditions prior to 10.5, between 8.6-7.5 Ma and around 6.5 Ma. Superimposed on this pattern is a shift from a more predictable, cool-warm seasonal climate towards a more unpredictable, wet-dry seasonal climate between 9.4-8.2 Ma. A fairly abrupt transition existed between a southern and northern climate zone in Europe during at least a part of the studied interval. The southern climate is dryer, warmer, more wet-dry seasonal and more unpredictable than the northern one.

Time is what prevents everything from happening at once.

John Archibald Wheeler
American Journal of Physics (1978, Vol. 46: 323)

Chapter 7

The small mammals from the upper Miocene of the Teruel-Alfambra region: faunal dynamics and events

Abstract

The small mammal succession of the Teruel-Alfambra region is analyzed in order to test for the occurrence of "coordinated stasis", a pattern characterized by the alternation of long intervals of stability and short episodes of abrupt faunal change. During stable intervals taxonomic membership, species richness, relative abundance patterns and guild structure are supposed to remain nearly constant, whereas during periods of faunal change, concurrent changes in all faunal aspects are supposed to occur. The results for the Spanish small mammals only partially support the coordinated stasis hypothesis. In contrast to the predictions, changes in different faunal aspects (relative abundance, immigration, extinction, size) do not occur simultaneously, and neither do changes in rodents and insectivores. Nevertheless, various important small mammal events (called SM events) did occur: the expansion of murids at ~9.6 Ma (SM10), extinction amongst rodents and insectivores at ~9.1 Ma (SM10B) leading to a rodent diversity drop at ~8.9 Ma (SM10C), rodent immigration at ~8.7 Ma (SM11), immigration of mainly insectivores at ~8.1 Ma (SM11A), and rodent extinction and migration between 7.0 and 6.6 Ma (SM13). The faunal analyses of this chapter confirm the results of chapter 6 in the sense that they give further support to the presence of coeval correlated climate-induced changes in the marine and continental records. Two "glacial"- "interglacial" reversals at 8.6 and 6.7 Ma, as indicated by stable oxygen isotope records from the NE Atlantic (Wright et al., 1991), more or less coincide with SM11 and SM13 respectively. These correlations between marine and continental events can best be explained in terms of major climatic warmings.

7.1. Introduction

Since the mid-eighties there is a growing interest among paleontologists in the subject of faunal dynamics, especially with regard to the concepts of stability and turnover. The

"turnover-pulse hypothesis" of Vrba (1985) has stimulated discussion because of its extreme view that changes in unrelated lineages (speciation, extinction, migration) occur in pulses, which are thought to be initiated by extrinsic, physical causes. More recently, Brett and Baird (1992, 1995) introduced the concept of "coordinated stasis", based on the observation of regional, concurrent stability of coexisting Palaeozoic marine benthic lineages over extended intervals of geologic time, and the separation of these intervals by episodes of abrupt faunal change. During stable intervals taxonomic membership, species richness, relative abundance patterns and guild structure are nearly constant. Causes remain poorly understood, and both abiotic (physical, environmental) and biotic (evolutionary or ecological) mechanisms could account for such patterns (Ivany, 1996).

In any case, bimodality of turnover rates (stasis versus turnover) appears to be more common in the marine record than in the continental record. Vrba's claim that turnover in African antelope communities and hominids around 2.5 Ma ago was related to global late Pliocene climatic deterioration has recently got under fire in the light of new faunal data (see Kerr, 1996). Patterns that emerged from a huge database of North American Cenozoic mammals disconfirm various predictions of the coordinated stasis model (Alroy, 1996). Perhaps the strongest attack on the idea of long-term community stability comes from detailed studies on spatial changes of late Quaternary mammals of the United States. These studies show that species responded individually to climate change, and that their geographical ranges shifted at different times, in different directions and at different rates (FAUNMAP Working Group, 1996).

In order to test bimodality of turnover rates it is necessary to obtain: 1) long sequences with high faunal resolution, 2) excellent time control, and 3) rich and relatively unbiased samples. Bias in mammalian faunas is very common, and often there is an under-representation of either large or small mammals. This is the reason that analyses of sequences of complete mammal faunas (including both macro- and micromammals) are very rare. This problem can be partly solved by time-averaging (e.g. Barry et al., 1995).

Resolution can be increased if analyses are restricted to micromammals only. Large quantities of small mammal teeth can relatively easily be obtained by bulk-sampling and efficient screen-sieving, allowing the construction of rich "high-resolution" sequences (e.g. van der Meulen and Daams, 1992; this thesis). Although the number of micromammal species constitutes only a part of the total mammal fauna (roughly half), many studies have shown that the paleoecology and faunal dynamics of these smaller animals (rodents, insectivores, hares and rabbits, bats) can be studied separately. (Note that mammals as a whole are also part of larger terrestrial communities together with reptiles, birds etc.).

Our study focuses on a Vallesian-Turolian (MN9-13, late Miocene) sequence of small mammal assemblages from NE Spain, which largely meets the above requirements. The Vallesian is generally considered to be an interval of marked change in western European mammalian faunas, which has led to the concept of the "Vallesian" or "late Vallesian crisis" (Agustí and Moyá-Solá, 1990). Faunistically, the Vallesian (11.1-8.7 Ma) represents an interlude between the Aragonian (18-11.1 Ma) and Turolian (8.7-5 Ma). During the latter interval an open country "savanna fauna" of large mammals fully established itself in the western Mediterranean (Bernor et al., 1996). Low-resolution

diversity analyses on the level of MN zones indicate that western Europe lost about half of its species within the Vallesian. Turnover in this area reaches a maximum in MN9 (=early Vallesian), when per-species entry and exit levels peak at 50 and 70% respectively. Among the victims are hominoids, and small-sized carnivores and omnivores (Fortelius et al., 1996).

Also western Mediterranean small mammal communities change markedly during the Vallesian. Murids replace cricetids as the dominant group, and various other groups such as glirids, eomyids, and soricids decline (chapters 3 and 5). On the other hand, Turolian small mammal faunas appear to be far from stable either, both taxonomically (e.g. chapter 2) and in terms of relative abundances (e.g. chapter 5).

In this final chapter, various faunal aspects of the small mammal succession of the Teruel-Alfambra region will be analyzed, and a number of major small mammal events (called SM events) will be defined. (Note that these events are already indicated in the figures 7.1 to 7.5 in section 7.3). Event-correlations with the marine record will be shortly discussed.

7.2. Material and basic assumptions

The studied material consisted of a sequence of 66 assemblages of small mammal teeth collected from shallow lacustrine sediments in the Teruel-Alfambra region in NE Spain (10-6 Ma). The teeth were identified at the species level (rodents) or genus level (insectivores and lagomorphs). Teeth of bats appeared to be extremely rare and were not considered here. A large part of the localities are in direct stratigraphic superposition, and were dated within a magnetobiostratigraphic framework (Krijgsman, 1994; Krijgsman et al., 1996; Garcés et al., in press; this thesis: chapter 2 and appendix B). In order to improve the documentation for the early Vallesian we extended the data set with the rich locality Pedregueras 2C (see Daams et al., 1988).

For the reconstruction of taxon ranges, we used the convention that a taxon has to be undocumented for more than 1 m.y. before it could be recorded as (temporarily) absent. Furthermore, 'singletons' (presence in one locality only) were ignored. In order to study faunal dynamics the studied time slice was subdivided into 200 k.y. intervals. This resulted in a distribution of teeth shown in table 7.1. An additional subdivision into 500 k.y. intervals was also used, mainly because of the uncertainties in age estimations for the interval 7.5-6 Ma (see chapter 2 and appendix B). The number of taxa for a specific 200 k.y. or 500 k.y. interval was calculated as the mean of the number of taxa present at the beginning and the number of taxa present at the end of each interval. In the diversity and turnover calculations equal probability partitioning (e.g. Barry et al., 1990) was used to spread out an entry or exit over intervals with few or missing data (8.5, 7.9, 7.7, 7.5, and 6.5 Ma, see table 7.1). The differences in sample size for the other intervals were not considered to be a major problem, because of the flatness of the curve relating the number of micromammal species to the number of specimens, when the latter exceeds 100-200 (van de Weerd and Daams, 1978). In addition, the sample-size effects are reduced by ignoring 'singletons', which usually only occur in very rich intervals. Without doubt, samples are affected by taphonomic bias. However, given the characteristic lithology of

the sampled layers, and the opportunistic strategies of most predators (see chapter 3), isotaphonomy, or similarly operating taphonomic bias throughout a sequence, is a reasonable assumption.

Table 7.1. Number of teeth per 200 k.y.

age (Ma)	number of rodent cheek teeth	number of rodent M12+m12	number of insectivore M12+m12
6.1	1565	1407	726
6.3	450	396	79
6.5	0	0	0
6.7	108	70	23
6.9	4006	3492	602
7.1	779	644	144
7.3	1111	970	149
7.5	21	14	6
7.7	0	0	0
7.9	3	3	0
8.1	1383	1099	101
8.3	2178	1884	594
8.5	0	0	0
8.7	202	170	16
8.9	480	430	60
9.1	225	182	25
9.3	904	705	94
9.5	243	191	29
9.7	285	197	82
9.9*	1272	929	111
total	15215	12783	2755

* This age estimation is not accurate. The age of the locality Pedregueras 2C, which represents the 200 k.y. interval around 9.9 Ma, probably lies somewhere between 10.2 and 9.7 Ma, given mean sedimentation rates in the Daroca area, and magnetostratigraphic correlation of the *Cricetulodon* zone to the GPTS (Garcés et al., 1996).

7.3. Results

7.3.1. Relative abundances of (sub)families

Relative abundances were calculated on the basis of the number of first and second molars. The results for rodent families are shown in figure 7.1. This figure shows a major event at 9.6 Ma, corresponding to the sudden restructuring from a cricetid- to a murid-dominated rodent community. Between 9.6 and 8.9 Ma murid dominance is due to the presence of one murid genus only (*Progonomys*), and between 9.6 and 9.3 Ma it is even due to a single species (*P. hispanicus*).

Relative abundance changes in Insectivora (fig. 7.2) are best illustrated at the level of subfamilies or tribes. (Genus names are used in figure 7.2, because in almost all cases there is only one genus present per subfamily or tribe.) The figure shows that no restructuring occurs at 9.6 Ma, but that important changes in the insectivore community occur between 9.4 and 8.8 Ma and between 8.1 and 7.3 Ma. The first interval is

Faunal dynamics and events

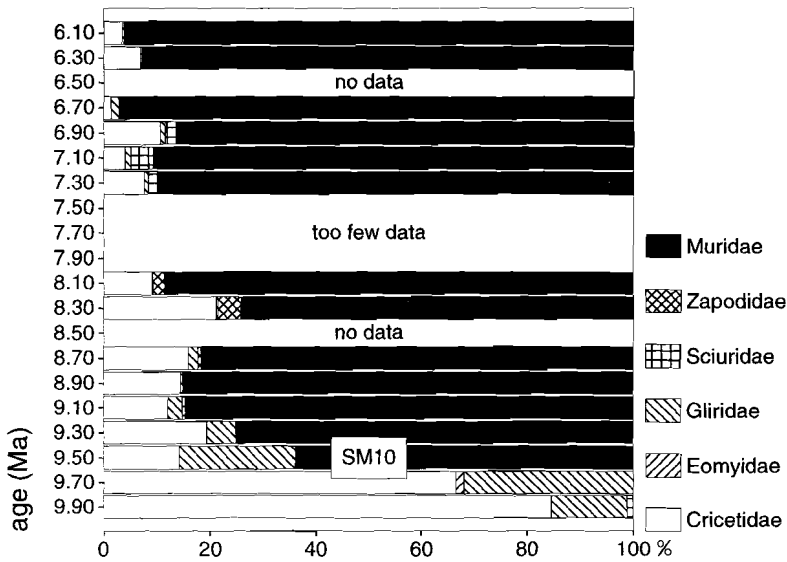


Figure 7.1. Relative abundances of rodent families per 200 k.y. interval based on the number of first and second molars. The very rare Eomyidae, Castoridae and Hystricidae have been omitted. For explanation of SM number/letter symbols see section 7.4.

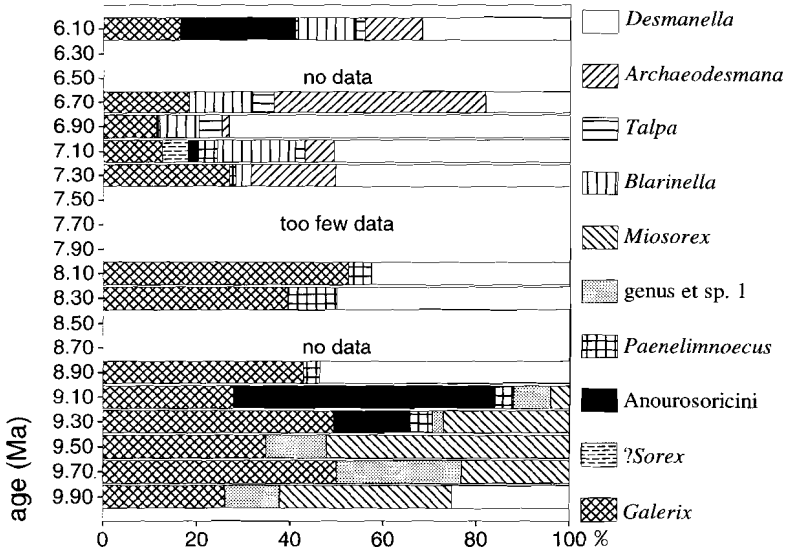


Figure 7.2. Relative abundances of insectivore groups (mainly genera) per 200 k.y. interval based on the number of first and second molars. The rare Erinaceinae are put in one group with *Galerix*.

characterized by the entry of *Paenelimnoecus*, by the entry, acme and rapid decrease of the tribe Anourosoricini (*Crusafontina*), by the decrease and disappearance of *Miosorex* and soricid genus et species 1, and by the re-expansion of the talpid *Desmanella*, which was absent between 9.9 and 9.3 Ma. The second interval of insectivore change is characterized by the expansion of *Archaeodesmana* and *Blarinella*. Due to a lack of data it is not possible to date the expansion of these groups more precisely. In addition to these two major changes, minor changes occurred. Notable are the re-occurrences of Anourosoricini around 7.1 and 6.1 Ma respectively (see also chapter 6).

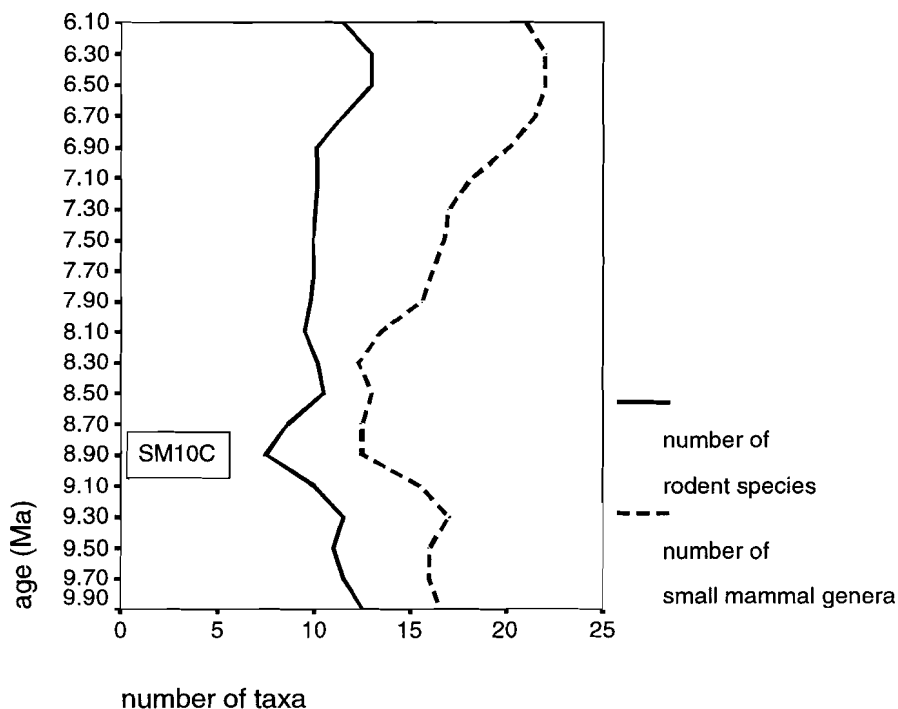


Figure 7.3. Number of rodent species and small mammal genera per 200 k.y. For explanation of SM number/letter symbols see section 7.4.

7.3.2. Diversity

Diversity and turnover were studied at two levels: the rodent species level and the small mammal genus level (excluding bats). Figure 7.3 shows that the number of rodent species is higher (12-13 species) in the earliest (9.9 Ma) and latest (6.5-6.1 Ma) part of the studied interval. Diversity is lower (~ 10 species) in the middle part with a minimum of 8 species at 8.9 Ma. The small mammal genus curve has its lowest values between 8.9 and 8.3 Ma. High values up to 23 genera are attained after 7 Ma, which is mainly due to an increase in insectivore genera.

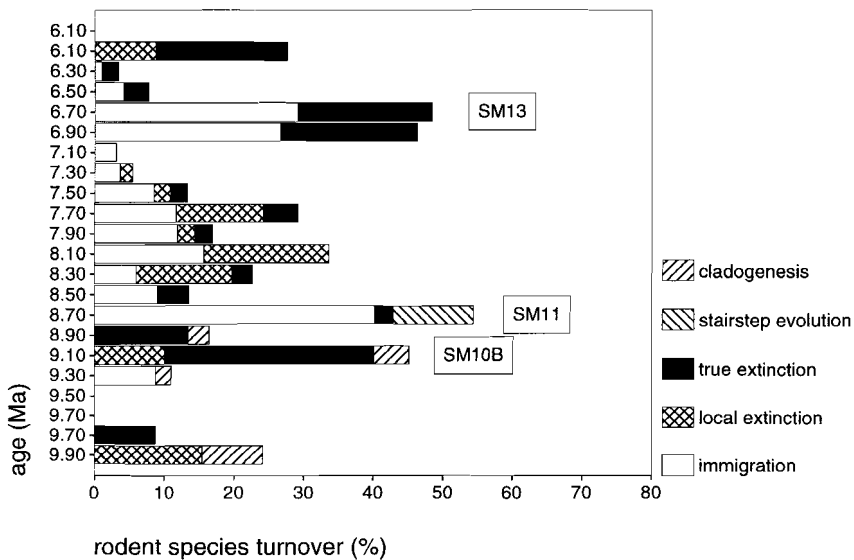
7.3.3. Turnover

Per-taxon turnover percentages were calculated as the number of events (appearances/disappearances) occurring in a 200 and 500 k.y. interval, divided by the number of taxa present. The following five types of event were recognized: 1) appearance in the area by immigration; 2) disappearance from the area by "local extinction"; 3) disappearance from the area by "true extinction"; 4) appearance by "stairstep" evolution (Stanley, 1985), i.e. by a sudden shift in the mean or median of a lineage as documented in the area; 5) appearance by cladogenetic evolution, presumably close to the study area. The number of First Occurrences (FO) was calculated as the sum of the number of events of types 1, 4 and 5, and the number of Last Occurrences (LO) was calculated as the sum of the events of types 2 and 3. Pseudo-extinctions and pseudo-originations presumably related to slow, anagenetic evolution (*Progonomys hispanicus*-*Occitanomys sondaari*-*O. adroveri*, *Progonomys cathalai*-*Huerzelerimys minor*, *Hispanomys aragonensis*-*H. peralensis*-*H. freudenthali*-*Ruscinomys schaubi*, see also fig. 7.6) were not counted as events. The age of an event was taken as the midpoint of the ages of the two bracketing localities, provided that these were relatively rich (we used the *ad hoc* criterium that they have to belong to one of the 44 rich localities used in chapter 6).

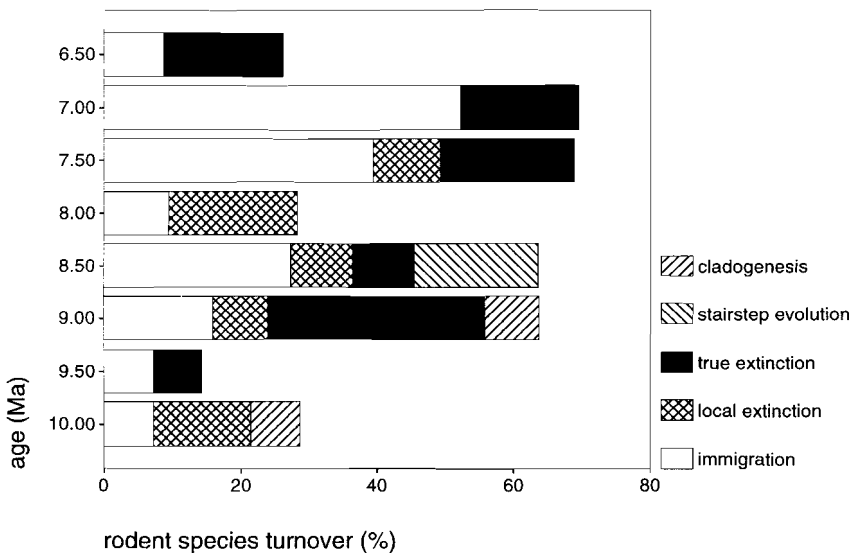
Table 7.2. Kolmogorov-Smirnov tests of uniform distribution of turnover. $p < .05$ indicate significance higher than the 95% level. FO=First Occurrence; LO=Last Occurrence.

taxonomic level	unit of analysis (k.y.)	type of event	<i>p</i>
rodent species	200	FO	.000
		LO	.003
		FO+LO	.201
rodent species	500	FO	.309
		LO	.173
		FO+LO	.172
small mammal genus	200	FO	.000
		LO	.000
		FO+LO	.015
small mammal genus	500	FO	.112
		LO	.160
		FO+LO	.465

Results are shown in figures 7.4 and 7.5. A Kolmogorov-Smirnov test was done for each combination of taxonomic levels (rodent species and small genera), standard interval (200 and 500 k.y.), and type of event (FO, LO and FO+LO) (table 7.2). Whereas the 500 k.y. patterns differ from the uniform distribution of events at low levels of significance (50-90%) only, the 200 k.y. patterns are significant at the 95% level, except for one case (the summed FO and LO for rodents). In our opinion the lower significance levels at the 500 k.y. level can be attributed to increased time-averaging. The 200 k.y. signal contains several sharp peaks, indicating the short duration of various turnover events. Although

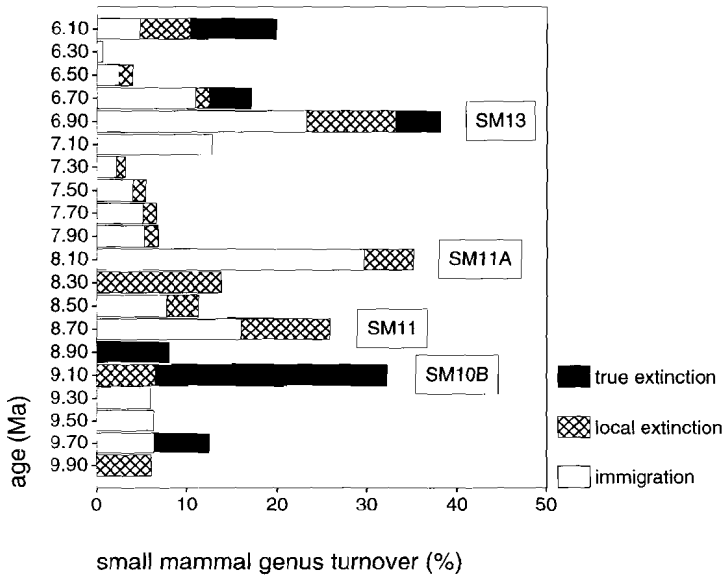


a

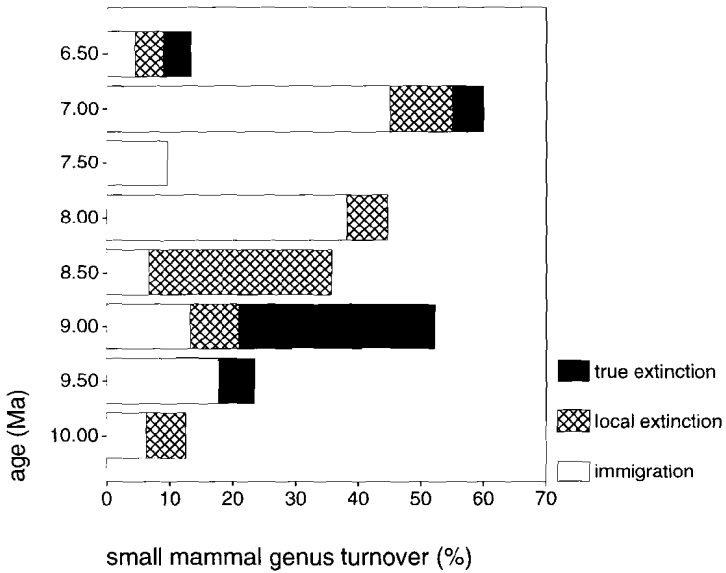


b

Figure 7.4. Per species turnover by event type for rodents for a) 200 k.y. intervals, and b) 500 k.y. intervals. For explanation of SM number/letter symbols see section 7.4.



a



b

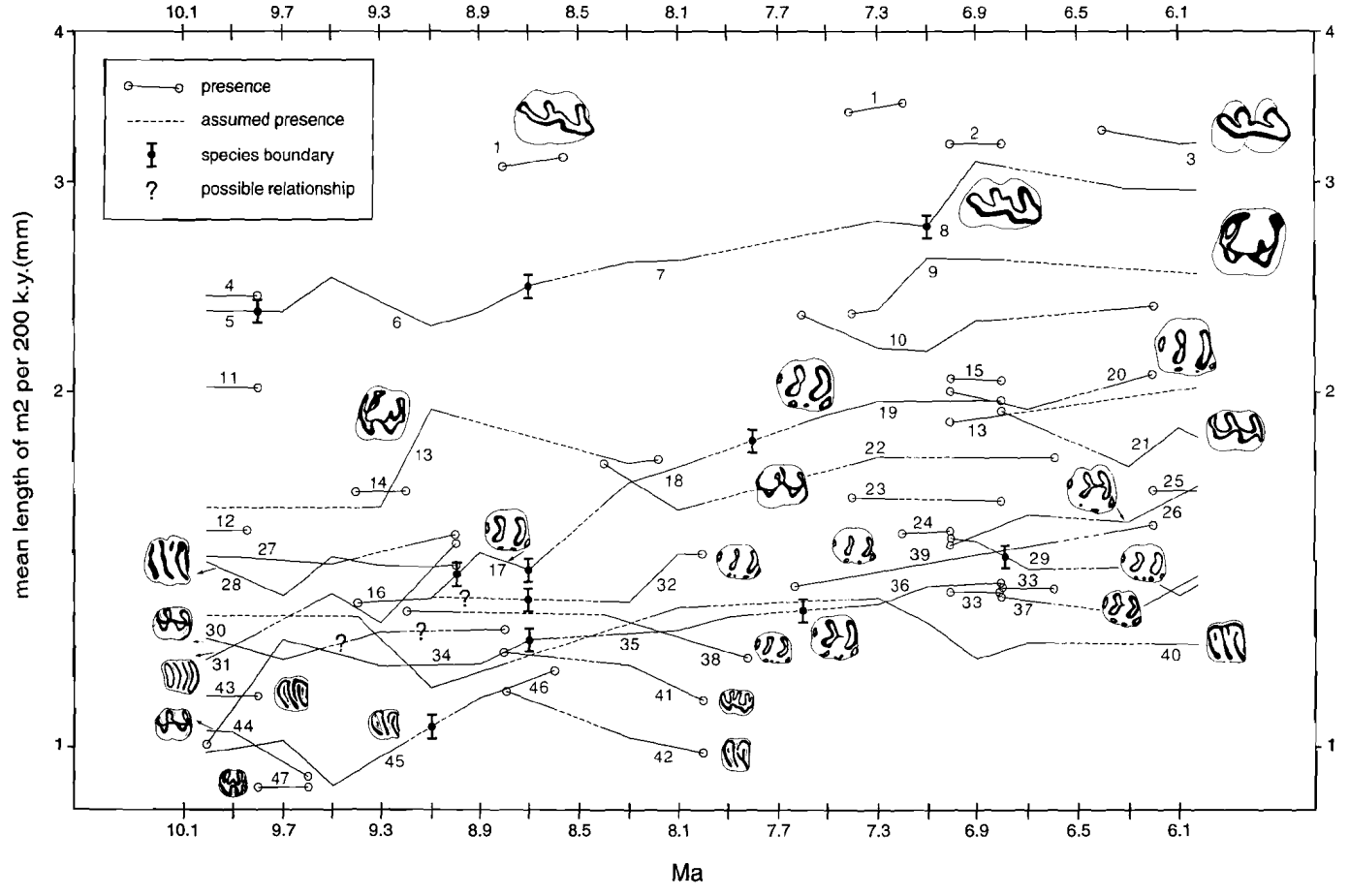
Figure 7.5. Per genus turnover by event type for small mammals (rodents, insectivores and lagomorphs) for a) 200 k.y. intervals, and b) 500 k.y. intervals. For explanation of SM number/letter symbols see section 7.4.

dating imprecision is thought to have no important effects on the 200 k.y. signal prior to 7.5 Ma, a standard interval of 200 k.y. could be too short for the interval between 7.5 and 6 Ma, which is less well dated. Nevertheless, the broad 400 k.y. interval of higher turnover in rodents (fig. 7.4a) between 7.0 and 6.6 Ma stands out clearly and is probably no artifact. Similarly, the 6.9 Ma peak in small mammal genus turnover (fig. 7.5a) is probably real. Higher turnover is still recognizable in the 500 k.y. pattern as a peak around 7 Ma (fig. 7.5b).

In the 200 k.y. diagrams, four intervals of relatively rapid change can be recognized. Around 9.1 Ma, i.e. within the late Vallesian, 40% of the rodent species and more than 30% of the small mammal genera disappear by (mainly true) extinction. Most victims are among the Gliridae, Cricetidae and Soricidae. This extinction event is followed by an immigration event around 8.7 Ma. It includes the entry of the murid *Parapodemus lugdunensis*, which defines the base of the Turolian (chapter 2). Other immigrants are *Eozapus* and *Eliomys* sp. A., two very small rodent species. A third event occurs around 8.1 Ma, i.e. within the early Turolian. It consists of the entry of three insectivore genera and one castorid (*Dipoides*), although all are still very rare by that time. The fourth interval of change occurs between 7.0 and 6.6 Ma and consists of various immigrations and extinctions, together constituting an almost complete turnover in murids and cricetids at both the species and genus level. One of the entries is that of *Stephanomys ramblensis*, which defines the base of the upper Turolian. It is remarkable that the insectivore community hardly changed at the time (see also chapter 2).

As shown by figure 7.4, local evolution by cladogenesis occurs very rarely in the studied interval. The only two cases which can be considered to represent this type of event are the branching off of a small-sized *Hispanomys* lineage from the main lineage around 10 Ma (see van de Weerd, 1976; appendix A), and the evolution from *M. dehmi* to *M. sp. A* between 9.3 and 8.9/8.7 Ma (appendix A). Accelerated "stairstep" change was observed in *Huerzelerimys*, which shows rapid size increase around 8.7 (chapter 3).

Figure 7.6. Mean length of lower second molar (m2) per rodent lineage per 200 k.y. In case m2 were absent, other elements were used to estimate the length of m2. Data from faunas older than 10 Ma and younger than 6 Ma were used for the construction of curves. Size of the drawn molars is adapted to the logarithmic scale. Castoridae and Hystricidae have been omitted. Part of the size fluctuation within lineages is due to low numbers of teeth. 1. *Hispanomys* sp. A.; 2. *Ruscinomys bravoii*; 3. *Blancomys sanzi*; 4. Marmotini gen. et sp. indet.; 5. *Hispanomys aragonensis*; 6. *Hispanomys peralensis*; 7. *Hispanomys freudenthali*; 8. *Ruscinomys schaubi*; 9. *Atlantoxerus adroveri*; 10. *Spermophilinus turoliensis* (*S. bredai-turoliensis* at 7.3 Ma); 11. ?*Atlantoxerus* sp.; 12. *Heteroxerus* cf. *rubricati*; 13. *Heteroxerus* cf. *grivensis* (*H. sp.* at 6.9 Ma); 14. cf. *Eumyarion* sp.; 15. Cricetinae gen. et sp. indet.; 16. *Progonomys cathalai*; 17. *Huerzelerimys minor*; 18. *Huerzelerimys vireti*; 19. *Huerzelerimys turoliensis*; 20. *Castromys inflatus*; 21. *Cricetus* cf. *kormosi*; 22. *Kowalskia occidentalis*; 23. Muridae gen. et sp. indet.; 24. *Occitanomys* sp. A.; 25. cf. *Rhagapodemus* sp.; 26. *Stephanomys ramblensis*; 27. *Cricetulodon hartenbergeri*; 28. *Tempestia hartenbergeri*; 29. *Apodemus gudrunae*; 30. *Democricetodon sulcatus* (*D. sp.* at 9.7 Ma, *D. sp. A* at 9.3 Ma, cf. *D. sp.* at 8.9 Ma); 31. *Muscardinus hispanicus*; 32. *Parapodemus gaudryi*; 33. *Muscardinus* aff. *hispanicus* at 6.9 Ma; *M. pliocaenicus* at 6.7 Ma; 34. *Progonomys hispanicus* (cf. *P. hispanicus* at 9.9 Ma); 35. *Occitanomys sondaari*; 36. *Occitanomys adroveri*; 37. *Occitanomys alcalai*; 38. *Parapodemus lugdunensis*; 39. *Parapodemus barbara*; 40. *Eliomys truci*; 41. *Eozapus intermedius*; 42. *Eliomys* sp. A.; 43. *Ramys multicrestatus*; 44. *Megacricetodon debruijnii*; 45. *Myomimus dehmi*; 46. *Myomimus* sp. A (Gliridae gen. et sp. indet at 8.9 Ma); 47. *Leptodontomys catalaunicus*.



Although this change may be due to true evolution in the local population, it is also possible that larger-sized populations immigrated from elsewhere. In that case, the event should be classified as an immigration event.

7.3.4. Size

In order to analyze trends in size the mean length of the second lower molar per rodent lineage per 200 k.y. interval was plotted (fig. 7.6). The m2 is preferred to the m1, because part of the size variation in rodent m1 is related to the presence or absence of a p4. A plot with body size instead of tooth size would have been more informative from an ecological point of view, but unfortunately tooth size to body size equations are not known for all rodent groups in the data set. The cricetid equation of Martin (1996) may be considered more or less valid for murids and zapodids. Data on the extant glirids *Eliomys* and *Muscardinus* (Storch, 1978) show that this cricetid equation underestimates the body size of these glirids by ~30 %. A sciurid equation has been calculated by Martin (1996), and it appears that sciurid body size is under-estimated by about 70%, when the cricetid equation is applied to the sciurids of our data set.

Prior to 8.0 Ma, the distribution is rather disharmonious with the majority of species having an m2 length between 0.9 and 1.5 mm, which is equivalent to body sizes of about 5-30 g. Almost all of these small species (cricetids, murids, zapodids and glirids) are considered to be non-grazing. They are either frugivorous (which includes granivorous), omnivorous or insectivorous. Of these small species, probably only *Occitanomys sondaari* was partially grazing (appendix C). A size gap exists between the small-sized species and the partially grazing cricetid *Hispanomys peralensis* (no. 6 in fig. 7.6, ~2.5 mm or ~80 g). (With a length of the m2 which is about equal to that of *H. peralensis*, the also partially grazing lagomorph *Prolagus* may have accompanied *H. peralensis* in this size class.)

The figure shows that the size distribution prior to 8 Ma is different from the distribution after about 7.5 Ma. A more precise dating of the transition can not be established, because the interval between 8 and 7.5 Ma is an interval for which there are almost no data. Mean rodent size increases during this time interval because of the disappearance of two very small-sized lineages (*Eozapus* and *Eliomys* sp. A, no. 41-42), the appearance of two relatively large-sized lineages (the ground squirrels *Atlantoxerus* and *Spermophilinus*, no. 9-10), and the evolution towards larger size within murids (18 to 19, 34 to 36, and 38 to 39). The mean size of the m2 per individual reaches a maximum of 2.1 mm (equivalent to ~45-50 g body size) at 6.9 Ma. This would imply more than a doubling of mean body size since 9.7 Ma.

Size distribution remains more or less constant after 7.5 Ma, in spite of the taxonomic turnover at ~ 7 Ma. Guild distribution changes gradually after 7 Ma when two partially grazing lineages, the large-sized *Blancomys* (no. 3) and the middle-sized *Stephanomys* (no. 26) enter.

7.4. Faunal dynamics: synthesis

Table 7.3 summarizes the major small mammal faunal changes in the Teruel basin between 10 and 6 Ma. We name the most important events by using the abbreviation SM ("Small Mammal"), by using the numbers 10-13 to indicate the MN zones, and the letters A, B or C to indicate the chronological order of events within MN zones. We also included in table 7.3 the various relative abundance-based changes and events corresponding to climatic minima and maxima as inferred in chapter 6. All faunal changes will be discussed in chronological order below.

The first important small mammal faunal change in the Calatayud-Daroca and Teruel basins after 10 Ma is the numerical expansion of murids at ~ 9.6 Ma (SM10, see fig. 7.1). This is a wide-spread event in the Mediterranean and southern Asia, although the degree of diachronism associated with both the FO and FRO (First Regular Occurrence) of murids is still under discussion (chapter 3). In Spain, age estimations for the FRO of *Progonomys hispanicus* in the Teruel, Vallès-Penedès and Duero basins are consistent, and pointing to an age of 9.7-9.6 Ma. An important role for competition is indicated by the fact that the extinction of various small brachiodont cricetids (notably *Megacricetodon*) in Europe, occurs more or less simultaneously with the expansion of the murid *Progonomys*. Cricetid-murid competition was already discussed in chapter 5, where it was hypothesized that murids, like today, were better adapted to an unpredictable, wet-dry seasonal - type of climate than cricetids. A shift towards the latter type of climate could have opened up forested areas which previously functioned as ecological barriers, and could have allowed murids to expand westward during the Vallesian.

A second abundance-based event occurs at 9.4-9.3 Ma (SM10A). The rodent composition indicates a relative maximum of humidity and a relative minimum of temperature at this time (see chapter 6). It was already noted in chapter 6 that this maximum is temporally close to an acme of the insectivore tribus Anourosoricini, the presence of which can be regarded as an indication of a more temperate climate (chapter 6).

Slightly later, around 9.1 Ma, various rodent and insectivore taxa disappear forever (extinction event SM10B). The relative abundances of most of these taxa had already decreased during the murid explosion (SM10) around 9.6 Ma (e.g. the cricetids *Cricetulodon* and *Democricetodon*, see fig. 5.5), or around the cooling maximum SM10A at 9.4-9.3 Ma (e.g. the glirid *Myomimus* and the soricid *Miosorex*, the latter being the last known representative of the Crocidosoricinae, see figs. 7.2 and 5.5). The final extinction of various groups at 9.1 Ma may have been related to another, minor cooling event at 9.0-8.9 Ma (fig. 6.10). Extinction by cooling is a plausible scenario for the Crocidosoricinae, given the general pattern of their southward migration during the mid-Miocene cooling (Reumer, 1994). Other disappearances could be related to the transition towards a new subtropical-dry climatic mode (chapter 6), which is estimated to have taken place between 9.4 and 8.2 Ma. The regional character of SM10B is difficult to assess at the moment, because there are no comparable mammal records for this interval which are both rich and well-dated.

Table 7.3. Small mammal faunal changes and relative abundance-based paleoclimatic interpretations for the Teruel basin between 10 and 6 Ma. The most important events are named. The numbering of these SM (= Small Mammal) events corresponds to the system of Neogene Mammal (MN) zones (Mein, 1990). Events without letters (SM10, SM11 and SM13) correlate to MN zone "transitions", with the number of the event corresponding to the youngest MN zone. SM events with letters (A, B or C) occur within MN zones.

SM event	age (Ma)	faunal aspect	description / interpretation
SM10	~9.6	rel. abund.	murid-dominated assemblages replace cricetid-dominated assemblages; FRO (First Regular Occurrence) of <i>Progonomys</i> (Muridae)
SM10A	9.4-9.3	rel. abund.	humidity maximum & temperature minimum as inferred from rodents (chapter 6)
-	~9.3-9.1	rel. abund.	first acme Anourosoricini (Soricidae)
-	9.4-8.2	rel. abund.	shift towards more wet-dry seasonal and unpredictable climate as inferred from rodents (chapter 6)
SM10B	~9.1	extinction	true: <i>Tempestia</i> (Gliridae); <i>Cricetulodon</i> , <i>Hispanomys</i> aff. <i>peralensis</i> (Cricetidae); <i>Miosorex</i> , genus and sp. 1 (Soricidae) local: <i>Myomimus dehmi</i> , <i>Muscardinus</i> (Gliridae)
-	~9.1	rel. abund.	<i>Desmanella</i> (Talpidae) expands; <i>Miosorex</i> , <i>Crusafontina</i> , and genus and sp. 1 (Soricidae) decay
SM10C	~8.9	diversity	number of rodent species reaches minimum
-	8.9-8.3	diversity	number of small mammal genera reaches minimum
SM11	~8.7	immigration	<i>Eliomys</i> sp. A (Gliridae); <i>Eozapus</i> (Zapodidae); <i>Parapodemus</i> (Muridae)
-	8.4-?	rel. abund.	humidity minimum & temperature maximum as inferred from rodents (chapter 6)
SM11A	~8.1	immigration	<i>Dipoides</i> (Castoridae); <i>Archaeodesmana</i> and <i>Talpa</i> (Talpidae); <i>Blarinella</i> (Soricidae)
-	8.1-7.3	rel. abund.	<i>Archaeodesmana</i> (Talpidae) and <i>Blarinella</i> (Soricidae) expand
-	8.0-7.5	size	change towards a larger mean size per lineage and individual in rodents
SM12A	7.2-6.9	rel. abund.	humidity maximum & temperature minimum as inferred from rodents (chapter 6)
-	~7.1	rel. abund.	second acme Anourosoricini (Soricidae)
SM13	7.0-6.6	immigration	<i>Muscardinus</i> (Gliridae); <i>Cricetus</i> (Cricetidae); <i>Occitanomys alcalai</i> , <i>Stephanomys</i> , <i>Castromys</i> , and perhaps <i>Apodemus</i> (Muridae); <i>Alilepus</i> (Leporidae)
-	7.0-6.6	extinction	<i>Occitanomys adroveri</i> , <i>Huerzelerimys</i> , and genus et sp. indet. (Muridae). Temporary LO: Erinaceinae and ? <i>Sorex</i> (Soricidae)
-	6.9-6.2	rel. abund.	humidity minimum & temperature maximum as inferred from rodents (chapter 6)
-	6.2-?	rel. abund.	humidity maximum & temperature minimum as inferred from rodents (chapter 6)
-	6.2-?	rel. abund.	third acme Anourosoricini (Soricidae)

The disappearance of glirids and cricetids at SM10B results in a marked rodent diversity minimum around 8.9 Ma (SM10C, fig. 7.3). Diversity is restored again around 8.7 Ma (SM11) when various central European immigrants (*Parapodemus lugdunensis*, *Eozapus* and possibly *Kowalskia*) enter. The more prolonged diversity low in small mammal genera between 8.9 and 8.3 Ma (fig. 7.3) more or less corresponds to a diversity minimum during MN11 in western European mammalian faunas in general (Fortelius et al., 1996). In the Teruel basin, diversity increases again around 8.1 Ma (fig. 7.3), when two semi-aquatic genera *Dipoides* and *Archaeodesmana* and two other insectivore genera enter (event SM11A), indicating a return to more humid conditions. From this moment

onwards small mammal genus diversity steadily increases until 6.5 Ma. Humidity does not increase in concert with diversity, but remains low until 7.2-6.9 Ma, when rodent data point to another maximum of (relatively) high humidity and low temperature. The Anourosoricini show an acme during this event, which is a repetition of the situation during cooling/humidity event SM10A.

It is interesting that the diversity trend described above coincides with an increase in faunal similarity between the eastern and western parts of Western Eurasia, which occurs between MN11 and MN12 (Fortelius et al., 1996). During MN12 large-mammal open-country "Pikermian" or "savanna" faunas have their maximum expansion and reach western Europe (Bernor et al., 1996). Although small mammal faunas of SW Europe are more endemic, marked similarities between small mammal faunas within the SW European region during MN12, e.g. between Spain and southern France as evidenced by the fauna of Cucuron Stade (Mein and Michaux, 1979). The small mammal diversity increase in the Teruel basin might be a direct result of this "uniformization" of Mediterranean fauna, because of the availability of a new and larger species pool. Alternatively, it might be the result of increased habitat diversity as a consequence of increased humidity (chapter 5).

A marked change in the size structure of rodents occurs between 8.0 and 7.5 Ma. The increase in mean rodent size is difficult to interpret, because size is related to many ecological and evolutionary variables. On the one hand, changes in life-history strategy and/or predator structure may have played a role. On the other hand, size appears just to be a simple function of time, because most anagenetically evolving lineages obey "Cope's rule", with size increase being just the consequence of the fact that founder species are usually small (Stanley, 1975).

The last major faunal change in the studied interval is the rodent "crash" associated with the major turnover (SM13) between 7.0 and 6.6 Ma. One of the remarkable aspects of this change is that the insectivore community remains unaffected. Furthermore, the analyses in chapter 6 have made clear that SM13 is a "taxonomic event", i.e. no marked changes occur in the ecological or guild structure of the rodents (and the reconstructed climatic parameters based on it). Most murid and cricetid taxa which disappear during SM13, are replaced by taxa of comparable size and dental morphology: *Huerzelerimys* by *Castromys*, *Parapodemus* by *Apodemus*, *Occitanomys adroveri* by *O. alcalai*, *Kowalskia* by *Cricetus*, *Ruscinomys* partly by *Blancomys*). In contrast to what happened around 9 Ma, immigration may have preceded extinction: generally there are no time lags between the exit of one species and the entry of its ecological counterpart, and in one case (*Parapodemus barbarae* and *Apodemus gudrunae*) ranges are known to overlap (see fig. 7.6). It should be noted, however, that the observed pattern could be biased and the degree of turnover associated with SM13 could be overestimated, because of the possibility of a gap in the record. Recent excavations in southern Spain (e.g. Martín Suárez and Freudenthal, 1994) have produced various new rodent species, among which are ancestors of *Stephanomys ramblensis* and *Castromys inflatus*. The latter mark the base of the upper Turolian (~6.8 Ma) in the Teruel basin.

Finally, a third humidity increase/temperature decrease is indicated by rodent and Anourosoricini abundances at the top of the studied interval, from ~6.2 Ma onwards.

These changes are assumed to have occurred before the onset of the main interval of evaporite deposition in the Mediterranean (salinity crisis), which occurred after 6 Ma (Gautier et al., 1994).

In summary, the studied data set reveals a dynamic small mammal history. Changes do not occur in all faunal aspects (relative abundance, diversity, immigration, and extinction) simultaneously, as predicted for instance by the model of coordinated stasis. Extinction may occur well before immigration (e.g. SM10B before SM11), and immigration prior to expansion (e.g. murid presence pre-dates expansion at SM10, immigration at SM11A pre-dates later expansion), reduction may occur before extinction (SM10 and 10A before SM10B), etc. In only two cases a mix of two event types is observed: important relative abundance changes take place on the insectivore (sub)family level during the extinction event SM10B, and both immigration and extinction occur during SM13. Furthermore, size increase in rodents between 8.0 and 7.5 Ma occurs more or less simultaneously with a relative abundance change in insectivores, but due to an informational gap the durations and possible synchronicity of these two changes remains questionable.

In addition, "taxonomic decoupling" occurs: rodents and insectivores behave rather uncoordinated. For instance, SM10, SM11 and SM13 are typical rodent events, whereas SM11A is mainly an insectivore event. The extinction event SM10B is the only major event which shows coordinated behaviour of the two orders. In addition to SM10B, various minor relative abundance fluctuations in insectivores (the three Anourosoricini acmes) co-occur with relative abundance peaks in rodents (SM10A, SM12A, and an interval of high values starting around 6.2 Ma). The uncoordinated behaviour of the two orders at SM11, 11A and 13 will partly be a reflection of ecological differences (diet, life history, etc.).

7.5. Discussion and conclusions

On the basis of the faunal analysis of the upper Miocene small mammal record of the Calatayud-Daroca and Teruel basins it may be concluded that:

1) Changes in different faunal aspects (relative abundance, immigration, extinction, size) do not occur simultaneously as predicted by the coordinated stasis model. Furthermore, an important change in a particular faunal aspect in rodents is usually not accompanied by an important change in that aspect in insectivores. The opposite is true as well. Nevertheless, various important small mammal turnover events (SM events) were found: the expansion of murids at ~9.6 Ma (SM10), the extinction amongst rodents and insectivores at ~ 9.1 (SM10B) leading to a rodent diversity drop at ~ 8.9 Ma (SM10C), the rodent immigration at ~8.7 Ma (SM11), the immigration of mainly insectivores at ~ 8.1 Ma (SM11A), and the rodent extinction and migration between 7.0 and 6.6 Ma (SM13).

2) Brett and Baird (1995) found 3-7 m.y. periods of stability (coordinated stasis) at the species level for Palaeozoic benthic assemblages. Although for example characteristic small mammal "associations" persist for 6-7 m.y. for example in the Neogene of SW

Europe (glirid/eomyid-, cricetid-, and murid-dominated associations, respectively), such taxonomic stability exists only at the family level.

3) The small mammal communities from the Teruel basin are characterized by an increase of murid dominance in both numbers of individuals and numbers of species. In terms of number of individuals murid dominance is achieved rapidly. The number of murids relative to the total number of rodents increases from almost zero to more than 60% at ~9.6 Ma, and further to more than 80 % at ~9.2 Ma. Levels of 90-95% are reached after 7.5 Ma. The number of species increases much more gradually. It raises from one to two at 9.3 Ma, from two to three at 8.7 Ma, and from three to four at 8.3 Ma. Between 8.0 and 7.5 (gap in the record) Ma species richness returns to three, which is finally followed by an increase to five at 6.9 Ma (see also chapter 3).

4) In chapter 6 it was noted that the cooling maxima at 9.4-9.3 (SM10A) and 7.2-6.9 Ma (SM12A) correspond to clusters of marine events which can be related to maxima in global ice volume. The faunal analyses of this chapter give further support to the existence of coeval climate-induced changes in the marine and continental records. The ages of two positive benthic $\delta^{18}\text{O}$ excursions at 8.6 and 6.7 Ma in the NE Atlantic (fig. 6.13) are close to the ages of turnover events SM11 (8.7 Ma) and SM13 (7.0-6.6 Ma). These two $\delta^{18}\text{O}$ events are interpreted by Wright et al. (1991) as onsets of decreasing global ice volume, i.e. the beginning of periods of long-term interglacial conditions (fig. 6.13). According to these authors, the $\delta^{18}\text{O}$ event at 8.6 Ma would correspond to an important change in paleoceanographic conditions, being the renewed onset of Northern Component Water (NCW) production. Both mentioned coeval changes can be explained in terms of climatic warmings. The model results of chapter 6 indicate onsets of warmer conditions at 8.7-8.6 and 7.0-6.6 Ma, which is consistent with the ice volume decrease indicated by the $\delta^{18}\text{O}$ reversals. In order to induce turnovers, climate change had probably to be fairly rapid and/or strong.

5) It is tempting to correlate the extinction event SM10B (~9.1 Ma) to a $\delta^{13}\text{C}$ maximum around 9 Ma (event "MC3") as observed in several oceans (Loutit et al., 1983; Kennett, 1986; Wright et al., 1991). Various authors (Cerling et al., 1993; Hodell et al., 1994) explicitly link a commonly observed shift from positive to negative benthic $\delta^{13}\text{C}$ values during the late Miocene ("late Miocene carbon shift") to a reduction in the amount of terrestrial biomass. Although the studied rodent abundances from Spain do indicate a change towards low-biomass environments (chapters 5 and 6), this change is supposed to have started already at 9.4 Ma. Whether there is a relation between SM10B and any marine event remains unclear for the time being. No marine event was found to correlate to immigration event SM11A at 8.1 Ma. Perhaps this event had only local significance.

Appendix A

Taxonomic remarks

Most rodent populations from the studied Vallesian and Turolian localities (see table 2.1) were placed within the existing species described by van de Weerd (1976) and others. The upper Vallesian to lower Turolian Muridae are reviewed in chapter 3. Additional new observations are included here.

1. *Occitanomys* sp. A (Muridae) from Masada del Valle 5 (middle Turolian, MN12, zone L) (fig. A.1)

The *Occitanomys adroveri* assemblage of Masada del Valle 5 as described by van de Weerd (1976) contains one murine M2 (MDV5-150) which differs in size and morphology from the remaining M2. I consider this specimen to belong to another species, *Occitanomys* sp. A.

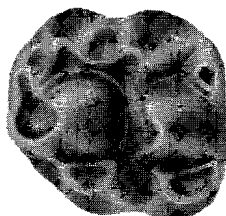


Figure A.1. M2 dex. of *Occitanomys* sp. A from Masada del Valle 5 (MDV5-150). Enlargement $\pm 20\times$.

Its size is large (length: 1.50, width: 1.57) and falls outside the range of the M2 of *O. adroveri* from the same locality (length range: 1.37-1.48, width range: 1.29-1.47, $n=32/33$). t12 is better developed than in most specimens of *O. adroveri* from the same locality. t6 is relatively large and extends towards the buccal side of t3, whereas in *O. adroveri* the t6 does not generally reach the level of t3. MDV5-150 shows a strong t6-t9 connection. This feature also occurs in a part of the *O. adroveri* assemblage from the same locality.

The size of MDV5-150 is intermediate between that of *Occitanomys adroveri* and the primitive *Stephanomys* species *S. stadii* (Mein and Michaux, 1979) and *S. ramblensis* (van de Weerd, 1976). The distinct t12, the very weak t1-t5 connection, and the brachiodont aspect of the M2 of *Occitanomys* sp. A do not support an assignment to *Stephanomys*.

2. *Hispanomys peralensis* and *H. aff. peralensis* (Vallesian, MN9-10, zones I-J2/?J3)

Van de Weerd (1976, pp.108-109) noted a bimodality in the size distribution of the m3 of the cricetid *Hispanomys* in three upper Vallesian assemblages (MBA, MBB and PER4). Since he could not recognize a bimodality in the distribution of other elements, he used the designation *H. cf. peralensis* for the small m3, and attributed the rest of the material to *H. peralensis* (type locality Peralejos C). Normality (Kolmogorov-Smirnov) tests and "range tests" (cf. Freudenthal and Cuenca Bescos, 1984) were applied to both van de Weerd's and new material in order to analyze the variation. These analyses show the presence of bimodality and/or unusual broad ranges in other elements as well. Analyses on the m3 indicate the presence of two co-occurring species in the interval ranging from PER5 (zone I) up to MBB (zone J2). Tests on the M2 and M3 indicate the presence of two species in the intervals PER5 up to PER4 (I-J2) and PER5 up to MBA (I-J1) respectively. Bimodality could not be demonstrated for the M1, m1 and m2.

In short, there is further additional evidence for the presence of two co-occurring *Hispanomys* species in the upper Vallesian of the Teruel-Alfambra region. The small species will be designated as *H. aff. peralensis*. In table 2.1 the entry *H. peralensis/H. aff. peralensis* is used for localities, which have too poor material to test for the presence of two species.

3. Gliridae gen. et sp. indet. from La Roma 2 (upper Vallesian, MN10, zone J3) (fig. A.2a)

The rodent assemblage from La Roma 2 contains one glirid tooth (R2-106), which is a right P⁴. Length and width are .75 and .87, respectively. Its outline is rounded. The protocone is prominent. Paracone and metacone are similar in size. The anteroloph almost reaches the protocone. Proto- and metaloph fuse in the centre of the occlusal surface, producing a typical "Y-shape". Centrolophs are absent. The posteroloph is weakly developed, especially its buccal part. The posteroloph is separated from both paracone and protocone.

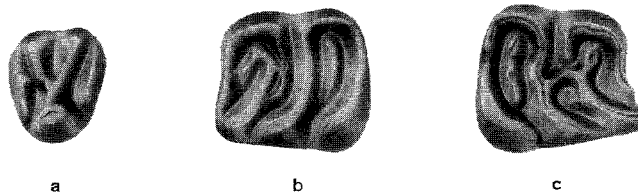


Figure A.2. a) Gliridae genus et species indet. P4 dex. from La Roma 2 (R2-106); b) m2 sin. of *Myomimus* sp. A from Peralejos D (PERD-151); c) m2 dex. of *Myomimus* sp. A from Peralejos D (PERD-152). Enlargement $\pm 20 \times$.

The general habitus of the tooth is similar that of early-middle Miocene *Pseudodryomys* species with simple dental patterns (Daams and de Bruijn, 1994).

Taxonomic remarks

Similarities include the rounded outline, the Y-shape of protoloph and metaloph, and the regular absence of centrolophs. However, an assignment to *Pseudodryomys* is very doubtful, because this genus is supposed to be extinct since MN6, i.e. long before the Late Vallesian. A comparison with the P⁴ of *Myomimus dehmi* from the type locality Pedregueras 2C (de Bruijn, 1976) and from Peralejos 5 and La Roma 3 (this thesis) also shows some similarities, especially with regard to size, to the fusion of proto- and metaloph situated buccally of the protocone, and to the relative length of anteroloph and posteroloph with the latter being longer. The absence of centrolophs fits the late Neogene trend towards simplification of the dental pattern in *Myomimus* (Daams, 1981). However, in the P⁴ of *Myomimus dehmi* proto- and metaloph fuse at a more lingual position (the "Y" tends to become a "V"), and the protocone is typically connected to the posteroloph. Although an assignment to *Myomimus dehmi* or *Myomimus* sp. A (see next paragraph) cannot be excluded, it is preferred to use Gliridae gen. et sp. indet. until new material becomes available.

4. *Myomimus* sp. A from Peralejos D (lower Turolian, MN11, zone K) (figs. A.2b and c)

The last occurrence of the genus *Myomimus* in western Europe is represented by two m1 from the earliest Turolian locality of Peralejos D. The length and width of PERD-151 are 1.18 and 1.11 mm, respectively. Length and width of PERD-152 are 1.11 and 1.15 mm, respectively (measuring method after Daams, 1981). The specimens are larger than m1 from older, Vallesian localities in the area (fig. A.3). The morphology of both specimens is peculiar because of their irregular running metalophids. In figure A.2b the metalophid does not run towards the base of the metaconid, but curves towards the anterolophid. In the other specimen (fig. A.2c) the metalophid branches off towards the mesolophid.

Van de Weerd (1976) had only few upper Vallesian *Myomimus* at his disposal (Peralejos 4 and D). He used the designation *M. cf. dehmi* for the material from Peralejos 4 and D, because size was generally larger than that of *Myomimus dehmi* from various early Vallesian localities, including its type locality Pedregueras 2C (de Bruijn, 1966; Daams, 1981). Later, Daams (1981) included the specimens from Peralejos 4 and D into *Myomimus dehmi*. With the new material from the Peralejos area, it has become clear that the m1 from Peralejos D differ in size and morphology from the m1 of the Vallesian assemblages, which all can unambiguously ascribed to *Myomimus dehmi*. The material from Peralejos D will be designated as *Myomimus* sp. A until more material is available. In addition to a morphological gap there is also a temporal gap with older assemblages, because *Myomimus* is absent in the middle part (zone J2) and probably also in the upper part of the upper Vallesian (zone J3), assuming that the P4 from La Roma 2 described above does not belong to the genus. *Myomimus* sp. A probably branched off from *M. dehmi* in Spain, and migrated into the Teruel area during the latest Vallesian (?) - earliest Turolian.

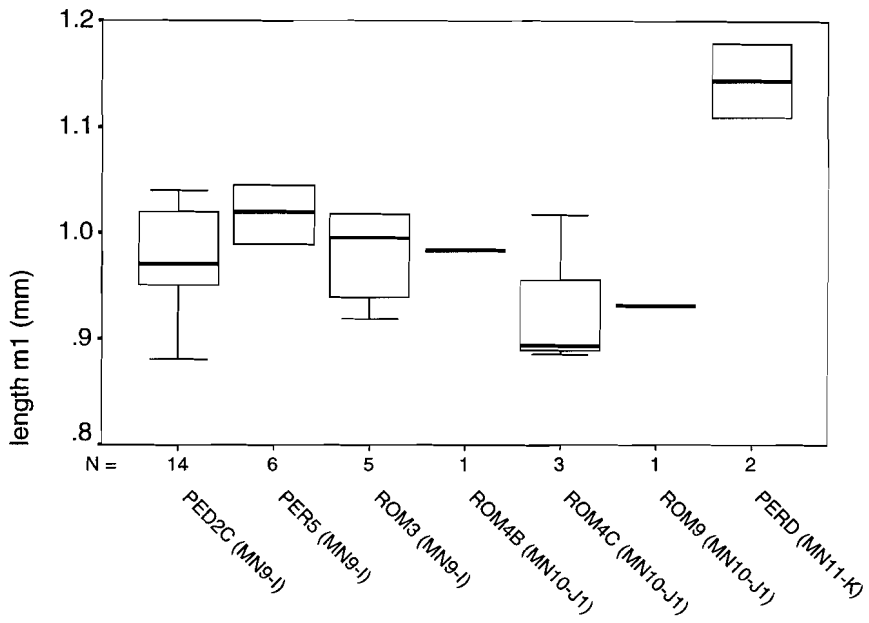


Figure A.3. Box plots of the length of the m1 in *Myomimus* populations from the Vallesian of the Calatayud-Daroca and Teruel basins. The line in the middle of the box represents the median, the box extends from the 25th percentile to the 75th percentile, and the lines emerging from the box extend to values three-halves the interquartile range rolled back to where is data. PED= Pedregueras, PER= Peralejos, ROM= Masía de la Roma.

Appendix B

Age estimates for mammal localities

Magneto-, litho- and biostratigraphic criteria are used to estimate the numerical ages for most of the fossil mammal localities of the Teruel-Alfambra region. The estimations are based on the stratigraphic and chronologic framework presented in chapter 2. Final estimates with a precision of 0.1 m.y. are given in table 2.1. The procedure followed is illustrated in the following 12 steps.

1. La Gloria and El Bunker parallel sections

The magnetic polarity patterns of the La Gloria section and the lower part of the overlapping El Bunker section have been correlated to interval C5n.2n-C4n.2n of the GPTS of Cande and Kent (1995) (figure 2.7). This correlation allows the estimation of the Vallesian-Turolian (MN10-11) boundary at 8.7 Ma between the localities AG5B and AG7 (Krijgsman et al., 1996). AG5B contains *Progonomys hispanicus* and consequently indicates the presence of zone J (upper Vallesian), while AG7 contains *Huerzelerimys vireti* indicating zone K (lower Turolian). Within the 5 m interval between these two localities, two other small localities with a mixed MN10/11 composition are present (table 2.1). The lower one (AG6) contains *Crusafontina*, which is characteristic for zone J, and *Hispanomys* cf. *freudenthali* which is only known from zones K and L. The second locality (GLO11) is not positioned in the section itself, but its bed can be correlated directly to the La Gloria section at a stratigraphic position about one meter higher than AG6 (see figs. 2.3 and 2.6). The composition of the association of this locality is typical for J, except for the presence of *Eliomys* sp. A, the distribution of which is further restricted to zone K.

Ages of the upper Vallesian (MN10) and lower Turolian (MN11) localities associated with these sections (AG4, AG5A, AG5B, AG6, GLO11, AG7, AG1, AG3, BUN6, BUN7) are made by linear interpolation within polarity zones (i.e. by assuming constant sedimentation rates).

2. Masía de la Roma section

The magnetobiostratigraphic data for the lower part of the Masía de la Roma section are consistent with the age of 9.7 Ma for the lower-upper Vallesian (MN9-10) boundary in the Vallès-Penedès basin as determined by Garcés et al. (1996). Although only two reversals are recorded, there are two biostratigraphic constraints which make the correlation to the interval C4Ar.2n-C4An (fig. 2.7) highly probable: 1) the lower-upper Vallesian (MN9-10) boundary as estimated in the Vallès-Penedès basin (9.7 Ma) is probably is close to the base of the section. Although the levels of the lower Vallesian

(zone I) localities ROM2-3 (~100 m south of the main section, see fig. 2.5) cannot be correlated directly to the main section due to the presence of a down-glided block (the block containing the locality R1, see fig. 2.5), the stratigraphic distance between ROM2-3 and ROM 4B will be small (maximally a few meters), given the observed continuity of the top of the facies unit M₃ (see section 2.2 and fig. 2.5). (Because of its early Vallesian age, it can be assumed that no down-gliding of the ROM2-3 block occurred). 2) The majority of localities belong to zone J1. The combination of both constraints implies that the age of the small mammal-containing part of the Masía de la Roma section will lie between 9.7 and ~ 9 Ma. On the basis of the length of the upper normal magnetozone in the Masía de La Roma section (fig. 2.7) this interval most likely corresponds to C4An, which means that C4Ar.1n is not recorded in the low-intensity middle part of the section.

Ages of all localities in and close to the section (ROM2, ROM3, ROM4B, ROM4C, ROM5, ROM6, ROM7, ROM8, ROM9, ROM11, PER4, PER5) are estimated by assuming constant sedimentation rates. The age for PER5, a locality sampled in the seventies, is considered to be the same as that of ROM3. The documentation of the exact position of PER5 has been lost, but it can be assumed that its stratigraphic position is identical to that of ROM3, because this is the only rich locality of early Vallesian age in the near vicinity.

3. Masada Rueva and Masía del Barbo parallel sections

The magnetic polarity pattern of the Masada Rueva section is correlated to chrons C5r and C4Ar (Garcés et al., press; see fig. 2.7). The ages of the localities MBA and MBB (Masía del Barbo section) are estimated by linear interpolation between two marker beds which connect the Masía del Barbo to the Masada Rueva section (fig. 2.3). Linear interpolation yields ages of 9.37 and 9.25 Ma for MBA and MBB, respectively. Upward linear extrapolation of sedimentation rates results in an age of 8.71 for MRU, which is consistent with a latest Vallesian age of this locality.

4. Peralejos and La Roma parallel sections

An age estimate of 8.7 Ma for PERD is based on three arguments: 1) Its rodent composition (table 2.1) indicates an age around the Vallesian-Turolian transition, which has been dated at 8.7 Ma in the La Gloria section. The presence of *Eozapus*, *Hispanomys freudenthali* and *Parapodemus* indicates a Turolian age, whereas *Progonomys hispanicus* and *Huerzelerimys minor* indicate a Vallesian age; 2) Assuming a) isochrony of the marker bed which forms the top of facies unit M₃ (see chapter 2), and b) equal sedimentation rates in both sections, the age of PERD can be estimated at 8.79 Ma; 3) PERD can be biochronologically correlated to the lower Turolian (MN11) localities AG1 (8.26 Ma) and AG3 (8.11 Ma) (La Gloria area) by means of a quantification of evolutionary stages in the *Progonomys hispanicus-Occitanomys sondaari* lineage. Frequency distributions of three morphological characters in this lineage (chapter 3) are calculated for all major lower Turolian localities, and summarized in one principal component score (table B.1). Assuming a linear relation between this score and numerical

Age estimates

time, the age of PERD can be estimated at 8.61 Ma. We use the average of the values calculated on the basis of arguments 2) and 3), resulting in an average value of 8.70 Ma, which corresponds to the age of the Vallesian-Turolian boundary as estimated under 1.

Table B.1. Estimation of numerical ages of MN11 localities using evolutionary stages in the early Turolian part of the *Progonomys hispanicus*-*Occitanomys sondaari* lineage. Three variables are standardized and used in a principal component analysis: the frequency distributions of the t6-t9 connection in M1, the t1-bis in M1, and the longitudinal spur in m1 (see chapter 3). The first principal component (PC1) is assumed to be linearly related to numerical time. Ages of AG1 and AG3 are used as calibration points. Note that the estimated ages for PERD and PM are not the final estimates as included in table 2.1 (see text).

MN11 locality	t6-t9 connection M1		t1 bis M1		longitudinal spur m1		PC1 (expl. 87.3%)	age equivalent (Ma)
	n	%	n	%	n	%		
	VIP	55	75	55	67	87	62	.90
TOA	50	79	53	64	44	59	.78	8.10
AG3	20	75	20	65	36	58	.69	8.11
ALF	4	75	6	67	13	46	.32	8.17
PM3	5	40	6	67	13	46	.23	8.18
GLO10	19	53	14	57	25	60	.08	8.21
AG1	19	58	18	50	24	54	-.24	8.26
PM	138	48	142	50	208	56	-.37	8.28
PERD	31	32	29	24	20	30	-2.40	8.61

The ages of the localities PERB, PERC, R1 and R2 were estimated by linear interpolation between the C4Ar.1r-C4An reversal (9.03 Ma) as recorded in the Masía de la Roma section, and the assumed age for PERD (8.70 Ma).

5. Other lower Turolian (MN11) localities

The quantified evolutionary stage of *Occitanomys sondaari* in PM (Puente Minero section) (table B.1) is used to estimate the age of this locality, using 8.70 (PERD) and 8.26 (AG1) as calibration points (This estimate is preferred to the one under 4.) The ages of AG1 and AG3 are used as calibration points for the estimation of the ages of PM3 (Puente Minero section), TOA (Tortajada section), ALF (Alfambra section), VIP (isolated locality) and GLO10 (lateral of La Gloria section). The thus inferred age for ALF is preferred to an age based on lithostratigraphic criteria, because of the presence of a gap corresponding to the upper part of the lower Turolian in the Alfambra-Masada del Valle section (fig. 2.7).

6. Additional check on ages of upper Vallesian (MN10) localities

Table B.2 shows the results of a statistical analysis of evolutionary stages of *Progonomys hispanicus*, the direct ancestor of *Occitanomys sondaari*. The first principal component successfully groups the localities according to the subzones J1-3. An

inconsistency (probably due to low sample sizes) appears within subzone J1, where ROM4C has a higher score than the lithostratigraphically higher positioned localities ROM7 and ROM9.

Linear interpolation of the first principal component between ROM9 (9.36 Ma) and ROM11 (9.16 Ma) results in an age of 9.32 Ma for MBA, whereas downward linear extrapolation on the basis of ROM11 (9.16 Ma) and PERC (8.84 Ma) yields 9.34 Ma. Both are very close to the age of 9.37 Ma for MBA as inferred in step 3. For MBA the two estimates are 9.23 and 9.25, which perfectly correspond to the magnetostratigraphically inferred age of 9.25 Ma.

Table B.2. Quantification of upper Vallesian evolutionary stages in *Progonomys hispanicus*. Three variables are standardized and used in a principal component analysis: the frequency distributions of the t6-t9 connection in M1, the t1bis in M1, and the longitudinal spur in m1. The first principal component (PC1) is used to check the ages for MBA and MBB (see text). Only those localities with an average sample size >7 are shown.

locality	t6-t9 connection M1		t1 bis M1		longitudinal spur m1		PC1 (explanation: 54.7%)
	n	%	n	%	n	%	
PERC	68	40	54	24	56	45	1.25
ROM11	11	9	7	14	11	27	.12
MBB	43	9	46	9	42	21	-.19
MBA	19	5	20	0	26	15	-.54
ROM4C	10	0	13	0	12	17	-.61
ROM9	12	0	12	8	10	0	-.73
ROM7	10	0	13	0	12	8	-.77

The number of *Progonomys hispanicus* specimens in PM2 (Puente Minero section) is too small for a reliable age estimation. If isochrony of the correlation lines between the Puente Minero section and Masía del Barbo sections, as well as constant sedimentation rates in the former are assumed, then ages of 9.59, 8.48 and 8.41 Ma result for PM2, PM, and PM3, respectively. These ages are, however, not consistent with other data. Firstly, PM2 belongs to subzone J2 (presence of both *P. hispanicus* and *cathalai*), the base of which is estimated at 9.3 Ma. Secondly, the age of 8.48 Ma for PM is older than the age of 8.28 Ma as calculated on the basis of evolutionary rates (step 5) is younger than inferred by lithostratigraphic correlation to the Masía del Barbo section. The age of PM2 is estimated by downward extrapolation from PM, assuming an age of 8.48 for PM and equal sedimentation rates in the Puente Minero and Masía del Barbo sections. The resulting age of 9.08 Ma for PM2 implies that it is positioned in the top part of zone J2.

7. The lower-middle Turolian (MN11-12) boundary

For the age of the MN11-12 boundary we use 7.5 Ma on the basis of a reinterpretation by Krijgsman et al. (1996) of Opdyke et al. 's (1990) results for the Cabriel Basin (eastern Spain).

8. The middle-upper Turolian (MN12-13) boundary

A tentative age of 6.8 Ma is assigned to the MN12-13 boundary on the basis of a) the polarity pattern and the presence of lower upper Turolian (zone M1) micromammals in the upper part of the El Bunker section (table 2.1 and fig. 2.7), and b) a constraint for a minimum age of about 6 Ma (5.9 or 6.3 Ma according to two different recalibrated interpretations of Opdyke et al., 1990) for the locality Venta del Moro in the Cabriel basin, which can be correlated to our zone M3. Assuming a constant sedimentation rate in the top part of the El Bunker section, the only magnetostratigraphic correlation for the small normal interval at the top (fig. 2.7), which results in a realistic estimation of the age of the locality BUN (6.7 Ma), is the correlation to C3An.1n. Alternative correlations to C3An.2n or C3An.1n-C3An.2n (combined) yield ages of 7.8 and 8.4 Ma for BUN, respectively, both of which are very unlikely given the age of 7.5 Ma for the MN12/13 boundary. We consider 6.8 Ma to be about the lower limit for the age of the MN12/13 boundary: on the one hand BUN (6.7 Ma) is not the lowest locality in zone M1 (table 2.1), and on the other hand a much higher age is not to be expected because it would imply a very short duration for MN12.

9. Tortajada section

Using 8.10 Ma as the age of TOA (step 5), a maximum age of 7.08 Ma results for TOC, given the constraints of a middle Turolian age of TOB and constant average sedimentation rates. The age of 7.08 Ma for TOC, leaves only ~0.3 m.y. for a large series of localities characterized by the common occurrence of *Parapodemus barbarae* and *Ruscinomys schaubi* (table 2.1). We assume that this co-occurrence did not last shorter than ~0.3 m.y., thereby constraining the age of TOB to 7.5 Ma.

10. Masada del Valle section

The evolutionary (size) stages of *Occitanomys adroveri* are used as the primary criterium for the chronological ranking of middle Turolian (MN12) localities. The first principal component of the mean lengths of lower and upper first and second molars is used for interpolation (table B.3). The resulting order of localities is consistent with the lithostratigraphic order of the MDV2, 4 and 5 localities, and with the grouping of localities in two clusters, one containing *Hispanomys* (LM2, MDV3), and one containing its descendant *Ruscinomys* (MDV5, LM, CC3).

TOC and TOD (two localities from approximately the same level) are correlated to the midpoint of the interval between MDV3 and MDV4 on the basis of the length of the lower first molar in the lineage *Hispanomys-Ruscinomys* (table B.3). (The *Occitanomys* size scores for TOC and TOD show some difference). Ages for MDV2, 3, 4 and 5, and 7 are estimated by linear inter- and extrapolation on the basis of the inferred ages for TOC-D (7.08 Ma; step 8) and MDV6 (6.8 Ma, lowermost upper Turolian locality in the area and older than BUN, which has an estimated age of 6.7 Ma (see step 8)).

Table B.3. Quantification of evolutionary stages in *Occitanomys adroveri*, and comparison with data from *Hispanomys freudenthali-Ruscinomys schaubi*. Four variables are standardized and used in a principal component Analysis: the mean lengths of the M1, M2, m1 and m2 of *O. adroveri*. Both the first principal component (PC1) and the mean length of m1 in *Hispanomys-Ruscinimys* are used for age estimations of MN12 localities (see text). Only those localities are shown with the total number of *O. adroveri* molars ≥ 20 . Only those lengths of *Hispanomys-Ruscinimys* molars are shown which are based on $n \geq 3$.

locality (MN12)	PC1 of mean lengths M1, M2, m1, m2 <i>Occitanomys adroveri</i> (55,9 % explanation)	total number of M1, M2, m1, m2 <i>Occitanomys adroveri</i>	mean length m1 <i>Hispanomys freudenthali- Ruscinomys schaubi</i> lineage	total number of m1 <i>Hispanomys freudenthali- Ruscinomys schaubi</i> lineage
CC3	1.33	194	3.21	3
LM	1.26	273	3.25	40
CC2	1.20	21		
TO	1.17	48		
VB2	0.37	112		
MDV5	-0.03	121	3.20	3
TOD	-1.04	36	3.11	3
MDV4	-1.05	20		
MDV2	-1.07	321	2.94	7
TOC	-1.28	21		
LM2	-1.34	21	3.08	4

11. Other middle Turolian (MN12) localities

Downward linear extrapolation of the *Occitanomys*-based size score in table B.3 results in an age estimate of 7.32 Ma for LM2 (Los Mansuetos section). On the basis of the scores, the ages of TO (isolated locality), LM (Los Mansuetos locality), CC2 and CC3 (Concud area) can be assumed to be younger than MDV5 (7.00 Ma, step 10), and older than MN13 locality MDV6 (6.8 Ma, step 8), i.e. ~ 6.9 Ma. The age of the (isolated) locality VB2 is estimated at 6.95 Ma. Because of the low number of teeth in CCB and CC (Concud section), their ages (7.12 and 6.83 Ma respectively) are based on their mean PC1 score (0.15), the 5 m stratigraphic distance between them (van de Weerd, 1976), and the assumption that the sedimentation rate is uniform and equal to that of the Tortajada section.

12. Other upper Turolian (MN13) localities

Age estimations for VDC3 (Rio Seco area), KS and KSS (Las Casiones section) are bound to be imprecise, because of the uncertainties concerning the age of the middle-upper Turolian (MN12-13) boundary (step 8), and the lack of reliable litho- and biostratigraphic correlations. An age of 6.3 Ma for VDC3 is based on the presence of *Castromys* (diagnostic for subzone M1) and *Amblycoptus* (table 2.1), a combination which is also observed in BUN4-5 (assigned age 6.3 Ma, see chapter 2). We tentatively assign ages of 6.1 Ma to the localities KS and KSS (subzone M2), because

Age estimates

biostratigraphically they are positioned between BUN4-5 (subzone M1, 6.3 Ma), and Venta del Moro in the Cabriel basin (M3, assumed age 5.9 Ma, see chapter 2).

Appendix C

A biometric analysis on fossil and extant murine molars

Unfortunately, only few functional morphological studies on murine dentitions have been performed. In Australian as well as in South East Asian murines a number of characters were observed that correlate with grazing diet (Crabb, 1976; Braidwaithe, 1979; van der Meulen and Musser, 1987). These characters are also recognized in herbivorous mammals in general and include hypsodonty, relative width of molars and

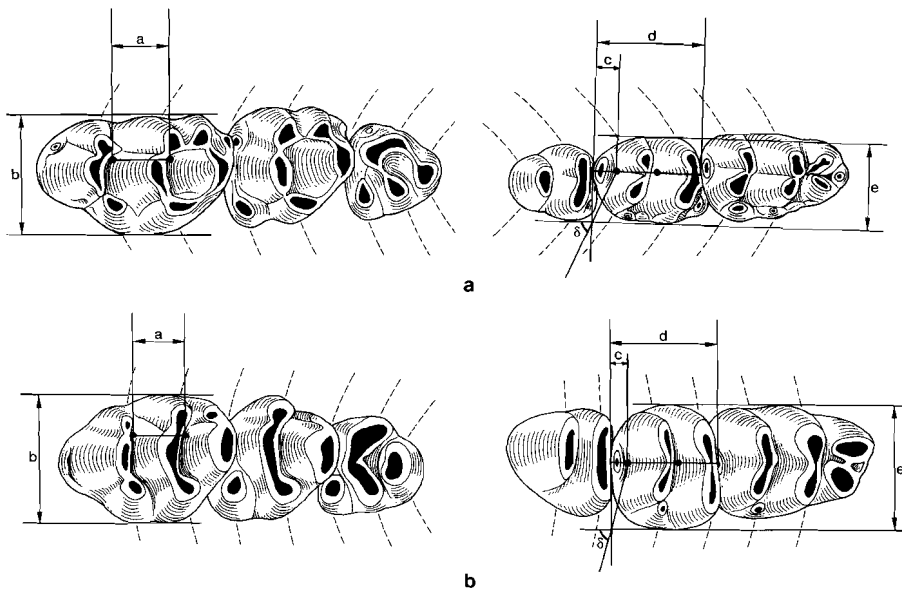


Figure C.1. Representative upper and lower tooth rows of a) *Parapodemus* (late Miocene of Eurasia, reconstructed), and b) *Aethomys* (extant, Africa). Transverse lamina may be either more curved (a) or more straight (b). a/b , d/e and 2δ were used as measures.

orientation of the transverse ridges. The specific aim of the analysis on murine molars presented here is the search for parameters which indicate a grazing component in the diet of fossil taxa. The identification of a grazing component is important for paleoenvironmental reconstructions, because (by definition) grazing indicates the presence of grass, which replaces forest vegetation with decreasing humidity.

In their typical habitus, upper and lower molar rows of murines consist of seven regularly spaced transverse structures (with the posterior one usually reduced) (fig. C.1).

These transverse structures (chevrons) consist of cusps, which may be fused into ridges. The chevrons are oriented more or less perpendicularly to the direction of (propalinal) chewing. As shown in the upper molar row in figure C.1, some of the "ridges" cross boundaries between molars.

Table C.1. Mean values (n=5) for d/e , 2δ , b/a (see fig. C.1) and their first principal component (PC1) for extant and fossil murine populations.

species	locality	e/d	2δ	b/a	PC1
extant:					
<i>Aethomys kaiseri</i>	Wangeregeze Forest, Uganda	0.94	144	2.40	0.20
<i>Apodemus mystacinus</i>	Scalita, Turkey	0.96	130	2.00	-0.60
<i>Apodemus sylvaticus</i>	Ethe, Belgium	0.94	131	2.00	-0.65
<i>Arvicanthis niloticus</i>	Nakuru, Kenia	1.09	157	2.70	1.73
<i>Dasymys incomtus</i>	Chaya, Nr. Ruchuru,	1.20	179	2.80	3.03
<i>Grammomys dolichurus</i>	Namaganga Forest, Uganda	0.95	130	2.00	-0.66
<i>Hybomys univittatus</i>	Wangeregeze Forest, Uganda	0.97	129	2.50	0.07
<i>Lemniscomys striatus</i>	Queen Elizabeth Park, Uganda	1.11	146	2.70	1.46
<i>Lenothrix canus</i>	Kepong, Malaysia	0.88	120	2.20	-1.01
<i>Oenomys hypoxanthus</i>	Namaganga Forest, Uganda	0.94	135	2.40	-0.05
<i>Thallomys paedulus</i>	Stampriet, Namibia	0.96	129	2.10	-0.57
<i>Thammomys rutilans</i>	Ghana	0.94	131	2.10	-0.57
fossil:					
<i>Apodemus gudrunae</i>	Valdecebro 3, Spain	0.89	129	2.10	-0.94
<i>Huerzelerimys turolensis</i>	Concud 3, Spain	0.89	134	2.20	-0.59
<i>Huerzelerimys vireti</i>	Puente Minero, Spain	0.96	137	2.00	-0.37
<i>Occitanomys adroveri</i>	Los Mansuetos, Spain	0.99	152	2.50	0.75
<i>Occitanomys alcalai</i>	Valdecebro 3, Spain	0.97	139	2.30	0.02
<i>Occitanomys sondaari</i>	Tortajada A, Spain	0.96	142	2.30	0.09
<i>Parapodemus barbarae</i>	Los Mansuetos, Spain	0.94	129	2.00	-0.68
<i>Parapodemus lugdunensis</i>	Lefkon, Greece (M1)	0.89	132	1.90	-1.07
	Crevillente 2, Spain (m2)				
<i>Progonomys cathalai</i>	Masía del Barbo 2B, Spain	0.88	127	2.20	-0.85
<i>Progonomys hispanicus</i>	Masía del Barbo 2B, Spain	0.93	137	2.20	-0.35
<i>Stephanomys donnezani</i>	Layna, Spain	1.04	144	2.60	0.98
<i>Stephanomys ramblensis</i>	Valdecebro 3, Spain	1.01	143	2.50	0.64

The regular spacing of chevrons defines a kind of wavelength, which is used to define longitudinal distances. For instance, in figure C.1, distance a is about one, and d is about two wavelengths. Three indices are defined (see fig. C.1): (1) b/a , an index of relative width of the first upper molar (M1). a is a distance corresponding to one wavelength, and is measured between two landmarks: one in the anterior transverse valley between the buccal and central cusp, and the other at the same position in the next more posterior valley. (Both landmarks have been used earlier in a geometric morphometric context, see van Dam, 1996, or chapter 4). b is the maximum width perpendicular to a . (2) e/d , an index of relative width of the second lower molar (m2). d corresponds to two wavelengths and runs through the central longitudinal valley, and is defined by the two valley landmarks indicated in figure C.1. e is the maximum width perpendicular to d . (3) δ , an angle indicating the curvature of the chevrons. It is estimated as $\arctan(c/0.5e)$, where c

Biometric analysis

is the length of the posterior cusp along *d*. Here we follow earlier suggestions that the relative length of the posterior cingulum (cp) is a good measure of "grazing" in murines because this cingulum tends to disappear with increasing hypsodonty and straightening of the chevrons (Crabb, 1976; Braidwithe, 1979).

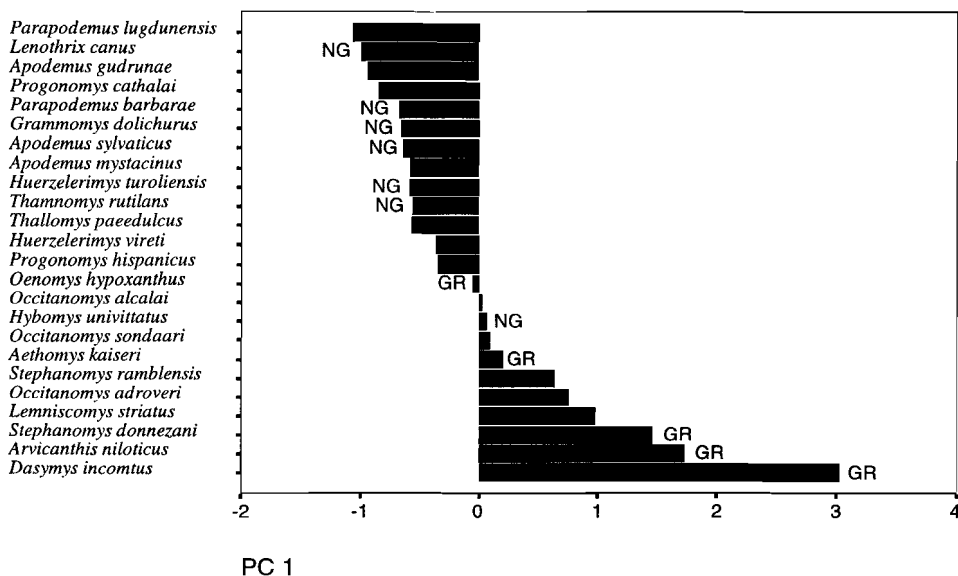


Figure C.2. Ranked values of the first principal component of an analysis on standardized *a/b*, *d/e* and 2δ , for fossil and extant murid populations. GR: grass in diet, NG: no grass in diet. Information on diets from Kingdon (1974), Nowak (1991), and Corbett and Hill (1992). The diet of *Dasymys incomtus* is badly known. This animal is known to consume grass in captivity (Hanney, 1965).

The data consist of 24 sets of molars, each containing five M1 and five m2. 12 sets are from extant, mainly African populations from collections of the Natural History Museum of London. The other 12 sets consist of isolated teeth from fossil populations, mostly from the upper Miocene of the Teruel-Alfambra region (table C.1). A Wild drawing microscope was used to draw the specimen, and measurements were taken from the drawings. The indices were calculated and standardized, and the first principal component of the three standardized values (PC1) for the indices was calculated as a summary index. The separation of murines into genera with and without a grazing component is based on the scores of the first principal component summarizing the three variables *b/a*, *e/d* and δ (table C.1 and fig. C.2). The first component explains 88% of the variation and the loadings of the three variables on this component are .92, .95 and .94 respectively. Broad molars with more straight lamellae in the lower tooth row cluster in the lower part of figure C.2, whereas slender molars with curved lamellae cluster in the upper part. When information on extant diets is added to the figure (GR and NG for the presence or absence of a grazing component, data from Kingdon, 1974, Nowak, 1991, and Corbett and Hill),

the correlation between grazing and broad molars with straight lophs is obvious. The score for *Hybomys univittatus* is higher than expected on the basis of its non-grazing diet. In this respect it is interesting to note that on the basis of its dental morphology this species is included in the "*Arvicanthis* division" (Misonne, 1969), which is a line of true herbivorous African murines. Kingdon (1974) suggests that *Hybomys* could be a modified relict of a formerly dominant type which has been eliminated outside the forest.

We use the break between *Progonomys hispanicus* and *Oenomys hypoxanthus* to separate the dental morphologies. This implies that we assume that the two extinct taxa *Stephanomys* and *Occitanomys* consumed tough food (grass) to some extent, and that *Progonomys*, *Huerzelerimys*, and *Parapodemus* probably did not. *Stephanomys* and *Occitanomys* are closely related genera (van de Weerd, 1976; Cordy, 1976). Besides large width/length ratios and tendency for straight lophs in the lower molars, they both show well-developed longitudinal ridges in upper and lower molars. This feature was noted by Schaub (1938) when he defined stephanodonty as a crown feature consisting of a garland-type pattern of ridges between the posterior cusps of the upper molars of murids. The concept was broadened by Cordy (1976) who included also other longitudinal crests into the definition. Stephanodonty was a common dental feature in late Miocene and Pliocene southwestern European murids, but disappeared afterwards. In its most typical habitus (*Stephanomys*) stephanodonty is a special combination of hypsodonty and selenodonty. Hypsodonty is special, because the cusps are not elongated in a vertical but in a oblique direction. Selenodonty differs from the common (ungulate) pattern, because chevrons are positioned not parallel to the tooth row, but at right angles to it. This pattern enables the longitudinal power stroke to function optimally (van Dam, 1996, or chapter 4).

References

- Adrover, R. 1986. Nuevas faunas de roedores en el Mio-Plioceno continental de la region de Teruel (España). Interes bioestratigráfico y paleoecológico. Instituto de Estudios Turoleses, Teruel.
- Adrover, R., L. Alcalá, P. Mein, E. Moissenet and J. Orrios. 1986. Mamíferos del Turoliense medio en la Rambla de Valdecebro (Teruel). Estudios geológicos 42: 495-509.
- Adrover, R., L. Alcalá, P. Mein, E. Moissenet, and J. Paricio. 1982a. Micromamíferos vallesienses del yacimiento La Salle en las Arcillas Rojas de Teruel. Acta Geológica Hispanica 17: 89-93.
- Adrover, R., L. Alcalá, P. Mein, E. Moissenet, and J. Paricio. 1984. Presencia en el barranco del Regajo (Tortajada, Teruel) de una serie continua con micromamíferos cubriendo los tres niveles del Turoliense. Estudios geológicos 40: 473-479.
- Adrover, R., L. Alcalá, J. Paricio, P. Mein, and E. Moissenet. 1982b. Dos nuevos yacimientos de vertebrados terciarios continentales: La Roma II (Alfambra, Teruel) y Búnker de Valdecebro (Teruel). Teruel 67: 7-21.
- Adrover, R., and P. Mein. 1996. Nuevo *Ruscinomys* (Rodentia, Mammalia) en el Mioceno Superior de la region de Teruel (España). Estudios geológicos 52: 261-365.
- Adrover, R., P. Mein, and E. Moissenet. 1993. Roedores de la transición Mio-Plioceno de la región de Teruel. Paleontología i Evolució 26-27: 47-84.
- Agee, E. M. 1980. Present climatic cooling and a proposed causative mechanism. Bulletin American Meteorological Society 61: 1356-1367.
- Aguilar, J.-P. 1982. Contribution a l'étude des micromammifères du gisement Miocène supérieur de Montredon (Herauld). 2. Les rongeurs. Palaeovertebrata 12: 81-117.
- Aguilar J.-P., M. Calvet, and J. Michaux. 1991. Présence de *Progonomys* (Muridae, Mammalia, Rodentia) dans une association de rongeurs de la fin du Miocène moyen (Castelnou 1B, Pyrénées-Orientales, France). Géobios 24: 503-508.
- Aguilar, J.-P., and J. Michaux. 1990. A paleoenvironmental and paleoclimatic interpretation of a Miocene rodent faunal succession in southern France. Critical evaluation of the use of rodents in paleoecology. Paléobiologie continentale 16: 311-327.
- Aguilar J.-P., and J. Michaux. 1996. The beginning of the age of Murinae (Mammalia: Rodentia) in southern France. Acta Zoologica Cracoviensia 39: 35-45.
- Aguirre, E., M. T. Alberdi, and A. Pérez-González. Turolian. 1975. Pp. 149-152 in F. F. Steininger and L. A. Nevevskaya, eds. Stratotypes of Mediterranean Neogene stages. Veda, Publishing House of the Slovak Academy of Sciences 2: 149-152.
- Agustí, J. 1981. Roedores miomorfos del Neógeno de Catalunya. Ph.D Thesis, Barcelona.
- Agustí, J., L. Cabrera, M. Garcés, and J. M. Parés. The Vallesian mammal succession in the Vallès-Penedès basin (northeast Spain): Paleomagnetic calibration and correlation with global events. Palaeogeography, Palaeoclimatology, Palaeoecology 133: 148-180.
- Agustí, J., and J. Gibert. 1982a. Roedores e insectívoros del Mioceno Superior dels Hostalets de Pierola (Vallès-Penedès, Catalunya). Butlletí Informatiu - Institut de Paleontologia de Sabadell 14: 19-37.
- Agustí, J., and J. Gibert. 1982b. Roedores e insectívoros (Mammalia) del Mioceno Superior de Can Jofresa y Can Perellada (Vallès-Penedès, Catalunya). Paleontología i Evolució 17: 29-41.
- Agustí, J., and S. Moyà-Solà, J. Gibert, J. Guillén, and M. Labrador. Nuevos datos sobre la bioestratigrafía del Neógeno continental de Murcia. Paleontología i Evolució 18: 83-93.
- Agustí, J., and S. Moyà-Solà. 1990. Mammal extinction in the Vallesian. Lecture Notes in Earth Sciences 30: 425-432.
- Agustí, J., and S. Moyà-Solà. 1991. Spanish Neogene mammal succession and its bearing on continental biochronology. Newsletters on Stratigraphy 25: 91-114.
- Aitchison, J. 1986. The statistical analysis of compositional data. Chapman and Hall, London.
- Alberdi, M.T., and L. Alcalá. 1990. El género *Hipparion* en la fosa de Alfambra-Teruel. Paleontología i Evolució 23: 105-109.
- Albesa, J., J. P. Calvo, L. Alcalá, and A. M. Alonso-Zarza. 1997. Interpretación paleoambiental del yacimiento de La Gloria 4 (Plioceno, Fosa de Teruel) a partir del análisis de facies y de asociaciones de gasterópodos y de mamíferos. Cuadernos Geología Ibérica 22: 239-264.
- Alcalá, L. 1987. Los Aljezares de Teruel. Historia y estado actual. Geogaceta 3: 61-63.
- Alcalá, L. 1994. Macromamíferos neógenos de la fosa de Alfambra-Teruel. INO Reproducciones, Zaragoza.
- Alcalá, L., and P. Montoya. 1990. Las faunas de macromamíferos del Turoliense inferior español. Paleontología i

- Evolució 23: 111-119.
- Alcalá, L., P. Montoya, and J. Morales. 1994. New large mustelids from the Late Miocene of the Teruel Basin (Spain). *Comptes Rendus de l'Académie des Sciences Paris* 319: 1093-1100.
- Alcalá, L., and J. Morales. 1997. A primitive caprine from the Upper Vallesian of La Roma 2 (Alfambra, Teruel, Aragón, Spain). *Comptes Rendus de l'Académie des Sciences Paris* 324: 947-953.
- Alcalá, L., C. Sesé, E. Herráez, and R. Adrover. 1991. Mamíferos del Turoliense inferior de Puente Minero (Teruel, España). *Boletín de la Real Sociedad Española de Historia Natural* 86: 205-251.
- Alcalá, L., C. Sesé, and J. Morales. 1986. Hallazgo de hircos en el área de Teruel. Nuevos datos sobre el tránsito Vallesiense-Turoliense. *Paleontología i Evolució* 20: 69-78.
- Alonso Zarza, A. M., J. P. Calvo, and M. A. García del Cura. 1992. Palustrine sedimentation and associated features - grainification and pseudo-microkarst - in the Middle Miocene (Intermediate Unit) of the Madrid Basin, Spain. *Sedimentary Geology* 76: 43-61.
- Alroy, J. 1992. Conjunction among taxonomic distributions and the Miocene mammalian biochronology of the Great Plains. *Paleobiology* 18: 326-343.
- Alroy, J. 1996. Constant extinction, constrained diversification, and uncoordinated stasis in North American mammals. *Palaeogeography, Palaeoclimatology, Palaeoecology* 127: 285-312.
- Alvarez Sierra, M. A. 1983. Paleontología y biostratigrafía del Mioceno superior del sector central de la Cuenca del Duero. Estudio de los micromamíferos de la Serie de Torremormojón (Palencia). Tesis de Licenciatura. Universidad Complutense de Madrid.
- Alvarez Sierra, M. A. 1987. Estudio sistemático y biostratigráfico de los Eomyidae (Rodentia, Mammalia) del Oligoceno superior y Mioceno inferior español. *Scripta Geologica* 86: 1-207.
- Alvarez Sierra, M. A., M. Díaz Molina, J. I. Lacombe, and N. López Martínez. 1990. Taphonomic and sedimentary factors in the fossil record of mammals. Pp. 461-474 in E. H. Lindsay, V. Fahlbusch, and P. Mein, eds. *European Neogene Mammal Chronology*. Plenum, New York.
- Amano K., and A. Taira. 1992. Two-phase uplift of Higher Himalayas since 17 Ma. *Geology* 20: 391-394.
- Ambid, L., I. Castan, C. Atgié, and M. Nibbelink. 1990. Food intake and peripheral adrenergic activity in a hibernating rodent, the garden dormouse. *Comparative Biochemistry and Physiology* 97: 361-366.
- Amori, G., M. Cristaldi, and L. Contoli. 1984. Distribution of rodents (Gliridae, Arvicolidae, Muridae) in peninsular and insular Italy with respect to the Mediterranean bioclimate. *Animalia* 11: 217-269.
- Anadón, P., and E. Moissenet. 1996. Neogene basins in the Eastern Iberian Range. Pp. 68-76 in P.F. Friend and C. Dabrio, eds. *Tertiary Basins of Spain. The stratigraphic record of crustal kinematics*. World and Regional Geology Series 6. Cambridge University Press, Cambridge.
- Andrewartha, H. G. 1961. Introduction to the study of animal population. University of Chicago Press, Chicago.
- Andrews, P. 1990a. Owls, caves and fossils. Natural History Publication, London.
- Andrews, P. 1990b. Small mammal taphonomy. Pp. 487-494 in E. H. Lindsay, V. Fahlbusch, and P. Mein, eds. *European Neogene Mammal Chronology*. Plenum, New York.
- Andrews, P. 1995. Mammals as palaeoecological indicators. *Acta Zoologica Cracoviensia* 38: 59-72.
- Andrews, P., J.M. Lord, and E.M. Nesbit. 1979. Patterns of ecological diversity in fossil and modern mammalian faunas. *Biological Journal of the Linnean Society* 11: 177-205.
- Artemiou, C. 1984. Mammalian community palaeoecology: a review of recent methods with special reference to Miocene mammalian faunas of Europe. *Paléobiologie Continentale* 14: 91-109.
- Axelrod, D. I., and H. P. Bailey. 1969. Paleotemperature analysis of tertiary floras. *Palaeogeography, Palaeoclimatology, Palaeoecology* 6: 163-195.
- Azanza, B., M. Nieto, D. Soria, and J. Morales. 1997. El registro neógeno de los Cervoidea (Artiodactyla, Mammalia) de España. Pp. 41-44 in J.P. Calvo and J. Morales, eds. *Avances en el conocimiento del Terciario Ibérico*. UCM-CSIC, Madrid.
- Bachmayer, F., and R. W. Wilson. 1970. Die Fauna der altploziänen Höhlen- und Spaltenfüllungen bei Kohfidisch, Burgenland (Österreich). *Annalen der Naturhistorischen Museums in Wien* 74: 533-587.
- Badgley, C. E., and K. A. Behrensmeier. 1995. Preservational, paleoecological, and evolutionary patterns in the Wyoming-Montana Paleogene and Siwalik Neogene fossil records. *Palaeogeography, Palaeoclimatology, Palaeoecology* 115: 1-11.
- Banet, M. 1988. Long-term cold adaptation in the rat. *Comparative Biochemistry and Physiology* 89A:137-140.
- Barron, E. J. 1985. Explanations of the Tertiary global cooling trend. *Palaeogeography, Palaeoclimatology, Palaeoecology* 50: 45-61.
- Barry, J. C., L. J. Flynn, and D. R. Pilbeam. 1990. Faunal diversity and turnover in a Miocene terrestrial sequence. Pp. 381-421 in R. Ross, and W. Allmon, eds. *Causes of evolution: a paleontological perspective*. University of Chicago Press, Chicago.

References

- Barry, J. C., E. H. Lindsay, and L. L. Jacobs. 1982. A biostratigraphic zonation of the middle and upper Siwaliks of the Potwar Plateau of northern Pakistan. *Palaeogeography, Palaeoclimatology, Palaeoecology* 37: 95-130.
- Barry, J. C., M. E. Morgan, L. J. Flynn, D. Pilbeam, L. L. Jacobs, E. H. Lindsay, S. Mahmood Raza, and N. Solounias. 1995. Patterns of faunal turnover and diversity in the Neogene Siwaliks of northern Pakistan. *Palaeogeography, Palaeoclimatology, Palaeoecology* 115: 209-226.
- Beaufort, L. 1994. Climate importance of the modulation of the 100 kyr cycle inferred from 16 m.y. long Miocene records. *Paleoceanography* 9: 821-834.
- Beaufort, L., and M.-P. Aubry. 1992. Fluctuations in the composition of late Miocene calcareous nannofossil assemblages as a response to orbital forcing. *Paleoceanography* 5: 845-865.
- Behrensmeyer, J. Damuth, W. DiMichele, R. Potts, H. D. Sues, and S. Wing, eds. *Terrestrial ecosystems through time*. University of Chicago Press, Chicago.
- Behrensmeyer, A. K., and R. W. Hook. 1992. Paleoenvironmental contexts and taphonomic modes. Pp. 183-203 in A.K. Behrensmeyer, A. K., D. Western, and D. Dechant Boaz. 1979. *New perspectives in vertebrate paleoecology from a Recent bone assemblage*. *Paleobiology* 5: 12-21.
- Behrensmeyer, A. K., and S. M. Kidwell. 1985. Taphonomy's contributions to paleobiology. *Paleobiology* 11: 105-119.
- Benton, M. J. 1991. Extinction, biotic replacements, and clade interactions. Pp. 89-102 in E. C. Dudley, ed. *The unity of evolutionary biology*. Dioscorides Press, Portland.
- Benton, M. J. 1996. On the nonprevalence of competitive replacement in the evolution of tetrapods. Pp. 185-210 in D. Jablonski, D.E. Erwin, and J. H. Lipps, eds. *Evolutionary paleobiology*. University of Chicago Press, Chicago.
- Berggren, W. A., D. V. Kent, C. C. Swisher III, and M. Aubry. 1996. A revised Cenozoic geochronology and chronostratigraphy. *Society of Economic Paleontologists and Mineralogists Special Volume* 54: 129-212.
- Bernor, R., N. Solounias, C. C. Swisher III, and J. A. Van Couvering. 1996. The correlation of three classical "Pikermian" mammal faunas - Maragheh, Samos, and Pikermi - with the European MN Unit System. Pp. 137-154 in R. L. Bernor, V. Fahlbusch, and H.-W. Mittmann, eds. *The evolution of western Eurasian Neogene mammal faunas*. Columbia University Press, New York.
- Bernstein, A. D., and C. A. Klevezal. 1965. Age determination of *Ochotona rutila* and *Ochotona macrotis*. *Zoologiceskij Zhurnal* 44: 787-789.
- Besems, R. E., and A. van de Weerd. 1983. The Neogene rodent biostratigraphy of the Teruel-Ademuz Basin (Spain). *Proceedings of the Koninklijke Nederlandse Academie van Wetenschappen*, B 86: 17-24.
- Bezdek, J. C., R. Ehrlich, and W. E. Full. 1984. FCM: the fuzzy c-means clustering algorithm. *Computers and Geosciences* 19: 191-204.
- Birks, H. J. B. 1985. Recent and possible future mathematical developments in quantitative palaeoecology. *Palaeogeography, Palaeoclimatology, Palaeoecology* 50: 107-147.
- Bolliger, T. 1992. Kleinsäugerstratigraphie in der miozänen Hörnlichüttung (Ostschweiz). *Documenta naturae* 75: 1-296.
- Bookstein, F.L., 1991. *Morphometric tools for landmark data*. Cambridge University Press, Cambridge.
- Bookstein, F. L. 1996. Standard formula for the uniform shape component in landmark data. Pp. 153-168 in Marcus, L. F., M. Corti, A. Loy, G. J. P. Naylor, and D. E. Slice, eds. *Advances in Morphometrics*. NATO volume 284. Plenum, New York.
- Boyce, M. S. 1979. Seasonality and patterns of natural selection for life histories. *American Naturalist* 114: 569-583.
- Boyce, M. S. 1984. Restitution of r- and K selection as a model of density-dependent natural selection. *Annual Review of Ecology and Systematics* 15: 427-447.
- Boyce, M. S. 1988. Evolution of life histories: theory and patterns from mammals. Pp. 3-32 in M. S. Boyce ed. *Evolution of life histories of mammals*. Yale University Press, New Haven.
- Brachert, T.C., C. Betzler, J.C. Braga, and J.M. Martin. 1996. Record of climatic change in neritic carbonates: turnover in biogenic associations and depositional modes (Late Miocene, southern Spain). *Geologische Rundschau* 85: 327-337.
- Braithwaite, R. W. 1979. Natural selection in *Rattus* molars. *Notes from the Mammal Society* 39: 545-548.
- Brett, C. E., and G. C. Baird. 1992. Coordinated stasis and evolutionary ecology of Silurian-Devonian marine biotas in the Appalachian basin. *Geological Society of America. Abstracts with Programs* 24: 39.
- Brett, C. E., and G. C. Baird. 1995. Coordinated stasis and evolutionary ecology of Silurian-Devonian marine biotas in the Appalachian basin. Pp. 285-315 in D. H. Erwin, and R. L. Anstey, eds. *New approaches to speciation in the fossil record*. Columbia University Press, New York.
- Bronson, F. H. 1989. *Mammalian reproductive biology*. University of Chicago Press, Chicago.
- Brujin, H. de. 1966. On the mammalian fauna of the *Hipparion*-beds in the Calatayud-Teruel Basin (Prov. Zaragoza, Spain). Part II. The Gliiridae. *Proceedings of the Koninklijke Nederlandse Academie van Wetenschappen*, B 78:367-387.
- Brujin, H. de. 1976. Vallesian and Turolian rodents from Biota, Attica and Rhodes (Greece). *Proceedings of the Koninklijke Nederlandse Academie van Wetenschappen*, B 79: 361-384.
- Brujin, H. de. 1989. Smaller mammals from the Upper Miocene and Lower Pliocene of the Strimon Basin, Greece. Part 1. Rodentia and Lagomorpha. *Bollettino della Società Paleontologica Italiana* 28: 189-195.

- Brujin, H. de. 1995. The vertebrate locality Maramena (Macedonia, Greece) at the Turolian-Ruscianian boundary. 8. Sciuridae, Petauristinae and Eomyidae (Rodentia, Mammalia). *Münchner Geowissenschaftliche Abhandlungen, Reihe A* 28: 87-102.
- Brujin, H. de, J. A. van Dam, G. Daxner-Höck, V. Fahlbusch, and G. Storch. 1996. The genera of Murinae, endemic insular forms excepted, of Europe and Anatolia during the Late Miocene and Early Pliocene. Pp. 253-260 in R. L. Bernor, V. Fahlbusch, and H.-W. Mittmann, eds. *The evolution of western Eurasian Neogene mammal faunas*. Columbia University Press, New York.
- Brujin, H. de, V. Fahlbusch, G. Saraç, and E. Ünay. 1993. Early Miocene rodent faunas from the eastern Mediterranean area. Part III. The genera *Deperetomys* and *Cricetodon* with a discussion of the evolutionary history of the Cricetodontini. *Proceedings of the Koninklijke Nederlandse Academie van Wetenschappen*, B 96:151-216.
- Brujin, H. de, and S. T. Hussain. 1984. The succession of rodent faunas from the lower Manchar formation in southern Pakistan, and its relevance for the biostratigraphy of the Mediterranean Miocene. *Paléobiologie continentale* 14: 191-204.
- Brujin, H. de, P. Mein, C. Montenat, and A. van de Weerd. 1975. Correlations entre les gisements de rongeurs et les formations marines du Miocène terminal d'Espagne meridionale (provinces d' Alicante et de Murcia). *Proceedings of the Koninklijke Nederlandse Academie van Wetenschappen*, B 78:1-32.
- Brujin, H. de, P. Y. Sondaar, and W. J. Zachariasse. 1971. Mammalia and Foraminifera from the Neogene of Kastellios Hill (Crete), a correlation of continental and marine biozones. *Proceedings of the Koninklijke Nederlandse Academie van Wetenschappen*, B 74: 1-22.
- Brujin, H. de, and W. J. Zachariasse. 1979. The correlation of marine and continental biozones of Kastellios Hill reconsidered. *Annales Géologiques des Pays Helléniques*, Tome hors serie: 219-226.
- Burchard B. 1978. Oxygen isotope paleotemperatures from the Tertiary period in the North Sea area. *Nature* 275: 121-123.
- Burckle, L. H. 1989. Distribution of diatoms in sediments of the northern Indian Ocean: Relationship to physical oceanography. *Marine Micropaleontology* 15: 53-65.
- Cade, T. J. 1964. The evolution of torpidity in rodents. *Annales Academiae Scientiarum Fennicae Series A, IV Biologica* 71: 77-112.
- Cande, S. C., and D. K. Kent. 1995. Revised calibration of the geomagnetic polarity time scale for the Late Cretaceous and Cenozoic. *Journal of Geophysical Research* 100: 6,093-6,095.
- Cerdeño, E., and M. Nieto. 1995. Changes in Western European Rhinocerotidae related to climatic variations. *Palaeogeography, Palaeoclimatology, Palaeoecology* 114: 325-338.
- Cerling, T. E., Y. Wang, and J. Quade. 1993. Expansion of C4 ecosystems as an indicator of global ecological change in the Late Miocene. *Nature* 361: 344-345.
- Chaline, J., and P. Mein. 1979. *Les rongeurs et l'évolution*. Doin Éditeurs, Paris.
- Chaline, J., P. Mein, and F. Petter. 1977. Les grandes lignes d'une classification évolutive des Muroidea. *Mammalia* 41: 245-251.
- Chamley, H., J. E. Meulenkamp, W. J. Zachariasse, and G. J. van der Zwaan. 1986. Middle to Late Miocene marine ecostratigraphy: clay minerals, planktonic foraminifera and stable isotopes from Sicily. *Oceanologica Acta* 9: 227-238.
- Chapman, J. A., and J. E. C. Flux. 1990. *Rabbits, Hares and Picas*. IUCN, Gland.
- Cheeseman, C. L., and M. J. Delany. 1979. The population dynamics of small rodents in a tropical African grassland. *Journal of the Zoological Society of London* 188: 451-475.
- Cieselski, P. F., and F. M. Weaver. 1983. Neogene and Quaternary paleoenvironmental history of Deep Sea Drilling Project Leg 171 sediments, southwest Atlantic Ocean. *Initial Reports of the Deep Sea Drilling Project* 71: 461-477.
- Cita, M. B., and J. A. McKenzie. 1986. The terminal Miocene event. *Geodynamics Series* 15: 123-140.
- Cockburn, A. 1991. *An introduction to evolutionary ecology*. Blackwell, Oxford.
- Collinson, M. E., and J. J. Hooker. 1991. Fossil evidence of interactions between plants and plant-eating mammals. *Philosophical transactions of the Royal Society of London*, B 333: 197-208.
- Coiffait, B. 1991. *Contribution des rongeurs du Neogène d'Algérie à la biochronologie mammalienne d'Afrique nord-occidentale*. Ph.D Thesis, Nancy.
- Corbet, G. B., and J.E. Hill. 1992. *The mammals of the Indomalayan region*. Oxford University Press, New York.
- Cordy, J.M. 1976. *Essai sur la microévolution du genre Stephanomys (Rodentia, Muridae)*. Ph.D Thesis, Liège.
- Cordy, J.M., 1978. Caractéristiques générales de la microévolution du genre *Stephanomys* (Rodentia, Muridae). *Bulletin de la Société Géologique de France* 20: 815-819.
- Crabb, P. L., 1976. Fossil mammals of the lower Pleistocene Moorna Sand, southwest New South Wales, Australia, with an analysis of the Australian pseudomyine murid molars. Ph.D Thesis, Melbourne.
- Crusafont, M. 1965. Observations à un travail de M. Freudenthal and P.Y. Sondaar sur des nouveaux gisements à *Hipparion* d'Espagne. *Proceedings of the Koninklijke Nederlandse Academie van Wetenschappen*, B 68: 121-126.
- Daams, R. 1981. The dental pattern of the dormice *Dryomys*, *Myomimus*, *Microdryomys*, and *Peridyromys*. Utrecht

References

- Micropaleontological Bulletins Special Publication 3: 1-115.
- Daams, R., and H. de Bruijn. 1981. A classification of the Gliridae (Rodentia) on the basis of dental morphology. *Hystrix* 6: 3-35.
- Daams, R., and M. Freudenthal. 1981. Aragonian: the Stage concept versus Neogene Mammal Zones. *Scripta Geologica* 62: 1-17.
- Daams, R., M. Freudenthal, and A. J. van der Meulen. 1988. Ecostratigraphy of micromammal faunas from the Neogene of the Calatayud-Teruel Basin. *Scripta Geologica Special Issue 1*: 287-302.
- Daams, R., and A. J. van der Meulen. 1984. Paleoenvironmental and paleoclimatic interpretation of micromammal faunal successions in the Upper Oligocene and Miocene of north central Spain. *Paléobiologie Continentale* 14: 241-257.
- Dam, J.A. van. 1996. Stephanodonta in fossil murids: a landmark-based morphometric approach. Pp. 449-461 in Marcus, L. F., M. Corti, A. Loy, G. J. P. Naylor, and D. E. Slice, eds. *Advances in Morphometrics*. NATO volume 284. Plenum, New York.
- Damuth, J. 1982. Analysis of the preservation of community structure in assemblages of fossil mammals. *Paleobiology* 8: 434-446.
- Damuth, J. 1992. Taxon-free characterization of animal communities. Pp. 183-203 in A.K. Behrensmeier, J. Damuth, W. DiMichele, R. Potts, H. D. Sues, and S. Wing, eds. *Terrestrial ecosystems through time*. University of Chicago Press, Chicago.
- Dauphin, Y., C. Denys, and K. Kowalski. 1997. Analysis of accumulations of rodent remains: Role of the chemical composition of skeletal elements. *Neues Jahrbuch für Geologie und Paläontologie. Abhandlungen* 203: 295-315.
- Daxner-Höck, G. 1980. Rodentia (Mammalia) des Eichkogels bei Mödling (Niederösterreich). *Annalen der Naturhistorischen Museums in Wien* 83: 135-152.
- Delany, M. J. 1982. *Mammal ecology*. Blackie, Glasgow.
- Delany, M. J., and R. H. Monro. 1986. Population dynamics of *Arvicanthis niloticus* (Rodentia: Muridae) in Kenya. *Journal of the Zoological Society of London (A)* 209: 85-103.
- Demarcq, G., P. Mein, R. Balleisio, and J.-P. Romaggi. 1989. Le gisement d'Andance (Coiron, Ardèche, France) dans le Miocène supérieur de la vallée du Rhône: un essai de corrélations marin-continental. *Bulletin de la Société Géologique de France* 5: 797-806.
- Denton, G. H., and R. L. Armstrong. 1969. Miocene-Pliocene glaciations in Southern Alaska. *American Journal of Science* 267: 1121-1142.
- Dercourt, J., L. E. Ricou, and B. Vrielynck. 1993. *Atlas Tethys paleoenvironmental maps*. Gauthier-Villars, Paris.
- Ehrmann W. U., M. J. Hambrey, J. G. Baldauf, J. Barron, B. Larsen, A. Mackensen, S. W. Wise Jr., and J. C. Zachos. 1992. History of Antarctic glaciation: An Indian Ocean perspective. *Geophysical Monograph* 70: 423-446.
- Engesser, B. 1990. Die Eomyidae (Rodentia, Mammalia) der Molasse der Schweiz und Savoyens. *Schweizerische Paläontologische Abhandlungen* 112: 1-144.
- Fahlbusch, V. 1978. Pliozäne und Pleistozäne Eomyidae (Rodentia, Mammalia) aus Polen. *Acta Zoologica Cracoviensia* 23: 13-26.
- Fahlbusch, V. 1979. Eomyidae - Geschichte einer Säugetierfamilie. *Paläontologische Zeitschrift* 53: 99-97.
- Fahlbusch, V., and T. Bolliger. 1996. Eomyids and Zapodids (Rodentia and Mammalia) in the Middle and Upper Miocene of Central and Southeastern Europe and the Eastern Mediterranean. Pp. 208-212 in R. L. Bernor, V. Fahlbusch, and H.-W. Mittmann, eds. *The evolution of western Eurasian Neogene mammal faunas*. Columbia University Press, New York.
- Fairbridge, R. W. 1986. Monsoons and paleomonsoons. *Episodes* 9:143-149.
- Farjanel, G., and P. Mein. 1984. Une association de mammifères et de pollens dans la formation continentale des "Marnes de Bresse" d'âge Miocène supérieur, à Ambérieu. *Géologie de la France* 1-2: 131-148.
- FAUNMAP Working Group, 1996. Spatial response of mammals to late Quaternary environmental change. *Science* 272: 1601-1606.
- Fejoo, B. J. 1736. Teatro Crítico Universal, o discursos varios en todo género de materias, para desengaño de errores comunes. Pp. 28-68 in Imp. Herederos Francisco del Hierro. Tomo VII. Discurso Segundo: Peregrinaciones de la Naturaleza: 28-68.
- Firquet, E., H. Leirs, R. Verhagen, and W. Verheyen. 1995. Germinating grasses and reproductive seasonality in *Mastomys*-rats. Abstracts of lecture presentation. Second Benelux-congres on zoology. Leiden.
- Flohn, H. 1950. Studien zur allgemeinen Zirkulation der Atmosphäre. *Berichte des Deutschen Wetterdienstes* 18: 34-50.
- Flower, B. P., and J. P. Kennett. 1993. Middle Miocene ocean-climate transition: High-resolution oxygen and carbon isotopic records from Deep Sea Drilling Project Site 588A, southwest Pacific. *Paleoceanography* 8: 811-843.
- Flynn, L. J., and L. L. Jacobs. 1982. Effects of changing environments on Siwalik rodent faunas of northern Pakistan. *Palaeogeography, Palaeoclimatology, Palaeoecology* 38: 129-138.
- Flynn, L. J., J. C. Barry, M. E. Morgan, D. Pilbeam, L. J. Jacobs, and E. H. Lindsay. 1995. Neogene Siwalik mammalian lineages: species longevities, rates of change, and modes of speciation. *Palaeogeography, Palaeoclimatology,*

- Palaeoecology 115: 249-264.
- Fortelius, M. 1985. Ungulate cheek teeth: developmental, functional, and evolutionary interrelations. *Acta Zoologica Fennica* 180: 1-76.
- Fortelius, M., L. Werdelin, P. Andrews, R. L. Bernor, A. Gentry, L. Humphrey, H.-W. Mittmann, and S. Viranta. 1996. Provinciality, diversity, turnover and paleoecology in land mammal faunas of the later Miocene of western Eurasia. Pp. 414-448 in R. L. Bernor, V. Fahlbusch, and H.-W. Mittmann, eds. *The evolution of western Eurasian Neogene mammal faunas*. Columbia University Press, New York.
- Fowler, C. W. 1981. Density dependence as related to life history strategy. *Ecology* 62: 602-610.
- Fraile, S., B. Pérez, I. de Miguel, and J. Morales. 1997. Revisión de los carnívoros presentes en los yacimientos del Neógeno español. Pp. 77-80 in J.P. Calvo and J. Morales, eds. *Avances en el conocimiento del Terciario Ibérico*. UCM-CSIC, Madrid.
- Frakes, L. A., J. E. Francis, and J. I. Syktus. 1992. *Climate modes of the Phanerozoic*. Cambridge University Press, Cambridge.
- Franzen, J. L., and G. Storch. 1975. Die unterpliozäne (turoalische) Wirbeltierfauna von Dorn-Dürkheim, Rheinhessen (SW-Deutschland). *Senckenbergiana lethaea* 56: 233-303.
- French, N. R., D. M. Stoddart, and B. Bobek. 1975. Patterns of demography in small mammal populations. Pp. 73-102 in F. B. Golley, K. Petruszewicz, and L. Ryszkowski, eds. *Small mammals: their productivity and population dynamics*. Cambridge University Press, Cambridge.
- Freudenthal, M. 1968. On the mammalian fauna of the *Hipparion*-beds in the Calatayud-Teruel Basin (Prov. Zaragoza, Spain). Part IV: The genus *Megacricetodon* (Rodentia). *Proceedings of the Koninklijke Nederlandse Academie van Wetenschappen*, B 71: 57-72.
- Freudenthal, M., and G. Cuenca Bescós. Size variation in fossil rodent populations. *Scripta Geologica* 76: 1-28.
- Freudenthal, M., J.I. Lacomba, E. Martín Suárez, and J. A. Peña. 1991. The marine and continental Upper Miocene of Crevillente (Alicante, Spain). *Scripta geologica* 96: 1-8.
- Full, W. E., R. Ehrlich, and J. E. Klovan. 1981. Objective definition of external endmembers in the analysis of mixtures. *Mathematical geology* 13: 331-344.
- Full, W. E., R. Ehrlich, and J. C. Bezdek. 1982. FUZZY QMODEL-A new approach for linear unmixing. *Mathematical geology* 14: 259-270.
- Garcés, M., J. Agustí, L. Cabrera, and J. M. Parés. 1996. Magnetostratigraphy of the Vallesian (late Miocene) in the Vallès-Penedès Basin (northeast Spain). *Earth and Planetary Science Letters* 142: 381-396.
- Garcés, M., W. Krijgsman, J. van Dam, J. P. Calvo, L. Alcalá, and A. M. Alonso-Zarza. 1998. Late Miocene alluvial sediments from the Teruel area: Magnetostratigraphy, magnetic susceptibility, and facies organisation. *Acta Geológica Hispanica* (in press).
- Gautier, F., G. Clauzon, J.-P. Suc, and D. Violanti. 1994. Age et durée de la crise de la salinité méditerranéenne: Académie des Sciences *Comptes Rendus Série 2*: 527-533.
- Giller, P. S. 1984. *Community structure and the niche*. Chapman and Hall, London.
- Giller, P. S., and J. H. R. Gee. 1986. The analysis of community organization: the influence of equilibrium, scale and terminology. Pp. 519-542 in J. H. R. Gee, and P. S. Giller, eds. *Organization of communities*. Blackwell, Oxford.
- Gordon, C. J. 1993. *Temperature regulation in laboratory rodents*, Cambridge University Press, Cambridge.
- Grant, P. R. 1972. Interspecific competition among rodents. *Annual Review of Ecology and Systematics* 3: 79-106.
- Gunnell, G. F., M. E. Morgan, M. Maas, and P. D. Gingerich. 1995. Comparative paleoecology of Paleogene and Neogene mammalian faunas: Trophic structure and composition. *Palaeogeography, Palaeoclimatology, Palaeoecology* 115: 265-286.
- Hallam, A. 1972. Models involving population dynamics. Pp. 62-80 in T. J. M. Schopf, ed. *Models in paleobiology*. Freeman, Cooper, San Francisco.
- Hamilton, T. D. 1986. Correlation of Quaternary glacial deposits in Alaska. *Quaternary Science Review* 5: 171-180.
- Hanney, P. 1965. The Muridae of Malawi. *Journal of Zoology* 146: 577-633.
- Haq, B.U., J. Hardebol, and P. Vail, 1988. Mesozoic and Cenozoic chronostratigraphy and cycles of sea-level change. *SEPM Special Publication* 42: 71-108.
- Harris, J. 1993. Ecosystem structure and growth of the African savannah. *Global and Planetary Change* 8: 231-248.
- Harrison, T. M., P. Copeland, S. A. Hall, J. Quade, S. Burner, T. P. Oyha, and W. S. F. Kidd. 1993. Isotopic preservation of Himalayan/Tibetan uplift, denudation, and climatic histories in two molasse deposits. *Journal of Geology* 101: 157-175.
- Hay, W. W. 1996. Tectonics and climate. *Geologische Rundschau* 85: 409-437.
- Hays, J. D., J. Imbrie, and N. J. Shackleton. 1976. Variations in the earth's orbit: pacemaker of the ice ages. *Science* 194: 1121-1132.
- Heideman, P.D., and F. H. Bronson. 1993. Sensitivity of Syrian hamsters (*Mesocricetus auratus*) to amplitudes and rates of photoperiodic change typical of the tropics. *Journal of Biological Rhythms* 8: 325-337.
- Heisler, C. 1985. Zum interspezifischen Verhalten von *Phodopus sungorus* (Cricetinae) und *Mus Musculus* (Murinae).

References

- Biologische Rundschau 23: 381-383.
- Henderson-Sellers, A., and P. J. Robinson. 1994. Contemporary climatology. Longman, Harlow.
- Hernández, A., M. Alvaro, J. I. Ramírez, M. C. Leal, M. Aguilar, P. Anadón, A. Meléndez, J. J. Gómez, J. M. Martín, J. C. García, and F. Ortí. 1983. Memoria de la Hoja no 47 (Teruel) del Mapa Geológico de España E. 1:200.000. IGME, Madrid.
- Hilgen, F.J., W. Krijgsman, C.G. Langereis, L.J. Lourens, A. Santarelli, and W.J. Zachariasse. 1995. Extending the astronomical (polarity) time scale into the Miocene. *Earth and Planetary Science Letters* 136: 495-510.
- Hodell, D. A., R. H. Benson, D. V. Kent, A. Boersma, and K. Rakić-El Bied. 1994. Magnetostratigraphic, biostratigraphic, and stable isotope stratigraphy of an Upper Miocene drill core from the Salé Briqueterie (northwestern Morocco): A high-resolution chronology for the Messinian stage. *Paleoceanography* 9: 835-855.
- Hodell, D. A., and F. Woodruff. 1994. Variations in the strontium isotopic ratio of seawater during the Miocene: stratigraphic and geochemical implications. *Paleoceanography* 9: 405-426.
- Huguéney, M., and P. Mein. 1965. Lagomorphes et rongeurs du Néogène de Lissieu (Rhône). *Travaux des Laboratoires de Géologie de la Faculté des Sciences de Lyon* 12: 109-123.
- Ivany, L. C. 1996. Coordinated stasis or coordinated turnover? Exploring intrinsic vs. extrinsic controls on pattern. *Palaeogeography, Palaeoclimatology, Palaeoecology* 127: 238-256.
- Jacobs, L. J. 1978. Fossil rodents (Rhizomyidae & Muridae) from Neogene Siwalik deposits, Pakistan. *Museum of Northern Arizona Press Bulletin Series* 52: 1-103.
- Jacobs, L. L., and W. R. Downs. 1994. Evolution of murine rodents in Africa. Pp. 149-156 in Y. Tomida, C. K. Li, and T. Setoguchi, eds. *Rodent and lagomorph families of Asian origins and diversification*. National Science Museum Monographs 8. Tokyo.
- Jacobs, L., L. Flynn, and W. Downs. 1989. Neogene rodents of southern Asia. Pp. 157-177 in C. C. Black, and M. R. Dawson, eds. *Papers on fossil rodents honoring Albert Elmer Wood*. Natural History Museum of Los Angeles County, Special Publication.
- Jaeger, J. J. 1977. Les rongeurs du Miocène moyen et supérieur du Maghreb. *Palaeovertebrata* 8: 1-166.
- Janis, C. M. 1988. An estimation of tooth volume and hypsodonty indices in ungulate mammals, and the correlation of these factors with dietary preferences. *Mémoires du Musée national d'Histoire naturelle (C)* 53: 367-387.
- Janis, C. M. 1993. Tertiary mammal evolution in the context of changing climates, vegetation, and tectonic events. *Annual Review of Ecology and Systematics* 24: 467-500.
- Janis, C. M., and M. Fortelius. 1988. On the means whereby mammals achieve increased functional durability of their dentitions, with special reference to limiting factors. *Biological Review* 63: 197-230.
- Jansen, E., T. Fronval, and N. Koç. 1995. Miocene to Recent paleoclimatic evolution at high Northern latitudes: interhemisphere linkages. Abstracts and Program. 5th International Conference on Paleoclimatology, Halifax : 20.
- Jansen, E., and J. Sjøholm. 1991. Reconstruction of glaciation over the past 6 Myr from ice-born deposits in the Norwegian Sea. *Nature* 349: 600-603.
- Johnson, R. G. 1964. The community approach to paleoecology. Pp.107-134 in J. Imbrie, and N. Newell, eds. *Approaches to paleoecology*. Wiley and Sons, New York.
- Keigwin, L. D. Jr., and N. J. Shackleton 1980. Uppermost Miocene carbon isotope stratigraphy of a piston core in the equatorial Pacific. *Nature* 284: 613-614.
- Kennett, J. P. 1986. Miocene to early Pliocene oxygen and carbon isotope stratigraphy in the southwest Pacific, Deep Sea Drilling Project Leg 90. *Initial Reports of the Deep Sea Drilling Project* 90: 1383-1411.
- Kennett, J. P., and P. F. Barker. 1990. Latest Cretaceous to Cenozoic climate and oceanographic developments in the Weddell Sea, Antarctica: an ocean-drilling perspective. *Proceedings of the Ocean Drilling Project, Scientific Results* 113: 937-960.
- Kerr, R. A. New mammal data challenge evolutionary pulse theory. *Science* 273: 431-432.
- Kingdon, J. 1974. East African mammals. Volume II, Part B (Hares and rodents). University of Chicago Press, Chicago.
- Klovan, J. E., and A. T. Miesch. 1976. Extended CABFAC and QMODEL computer programs for Q-mode factor analysis of compositional data. *Computers & Geosciences* 22: 631-637.
- Köhler, M. 1993. Skeleton and habitat of recent and fossil ruminants. *Münchner Geowissenschaftliche Abhandlungen, Reihe A* 25: 1-87.
- Korth, W. W. 1994. The Tertiary record of rodents in North America. *Topics in Geobiology* 12. Plenum Press, New York.
- Kowalski, K. 1990. Stratigraphy of Neogene Mammals of Poland. Pp. 193-210 in E. H. Lindsay, V. Fahlbusch, and P. Mein, eds. *European Neogene Mammal Chronology*. Plenum, New York.
- Kretzoi, M. 1957. Wirbeltierfaunistischen Angaben zur Quartärchronologie der Jankovich-Höhle. *Folia Archaeologica* 9: 14-21.
- Krijgsman, W. 1996. Miocene magnetostratigraphy and cyclostratigraphy in the Mediterranean: extension of the astronomical polarity time scale. *Geologica Ultraiectina* 141: 1-207.

- Krijgsman, W., M. Garcés, C. G. Langereis, R. Daams, J. van Dam, A. J. van der Meulen, J. Agustí, and L. Cabrera. 1996. A new chronology for the middle to late Miocene continental record in Spain. *Earth and Planetary Science Letters* 142: 367-380.
- Krijgsman, W., F. J. Hilgen, C. G. Langereis, A. Santarelli, and W. J. Zachariasse. 1995. Late Miocene magnetostratigraphy, biostratigraphy and cyclostratigraphy in the Mediterranean. *Earth and Planetary Science Letters* 136: 475-494.
- Krijgsman, W., F. J. Hilgen, C. G. Langereis, and W. J. Zachariasse. 1994a. The age of the Tortonian / Messinian boundary. *Earth and Planetary Science Letters* 121: 533-547.
- Krijgsman, W., C. G. Langereis, R. Daams, and A. J. van der Meulen. 1994b. Magnetostratigraphic dating of the Middle Miocene climatic change in the continental deposits of the Aragonian type area in the Calatayud-Teruel basin (Central Spain). *Earth and Planetary Science Letters* 128: 513-526.
- Kurtonur, C. and B. Özkan. 1991. New records of *Myomimus roachi* from Turkish Thrace. *Senckenbergiana biologica* 71: 239-244.
- Kutzbach, J. E., W. L. Prell, and W. F. Ruddiman. 1993. Sensitivity of Eurasian climate to surface uplift of the Tibetan Plateau. *The Journal of Geology* 101: 177-190.
- Lamb, H. H. 1972. *Climate, present, past and future*. Volume 1. Methuen, London.
- Landry, S. O. 1970. The Rodentia as omnivores. *The Quarterly Review of Biology* 45: 351-372.
- Lange, R., P. Twisk, A. van Winden, and A. van Diepenbeek. 1994. Zoogdieren van West-Europa. KNNV Uitgeverij, Utrecht.
- Larsen, H. C., A. D. Saunders, P. D. Clift, J. Beget, W. Wei, S. Spezzaferri, and ODP Leg 152 Scientific Party. 1994. Seven million years of glaciation in Greenland. *Science* 264: 952-955.
- Leeper, G. W. 1970. Climates. Pp 12-20 in G. W. Leeper, ed. *The Australian environment*. CSIRO, Melbourne.
- Leirs, H., R. Verhagen, and W. Verheyen. 1993. Productivity of different generations in a population of *Mastomys natalensis* rats in Tanzania. *Oikos* 68: 53-60.
- Leirs, H., R. Verhagen, and W. Verheyen. 1994. The basis of reproductive seasonality in *Mastomys* rats (Rodentia: Muridae) in Tanzania. *Journal of Tropical Ecology* 10: 55-66.
- Loon, H. van, and J. Williams. 1980. The association between latitudinal temperature gradient and eddy transport. Part II: relationships between sensible heat transport by stationary waves and wind, pressure and temperature in winter. *Monthly Weather Review* 108: 604-614.
- López Martínez, N. 1989. Revisión sistemática y biostratigráfica de los Lagomorpha (Mammalia) del Terciario y Cuaternario de España. *Memorias del Museo Paleontológico de la Universidad de Zaragoza* 3: 1-343.
- López Martínez, N., E. García Moreno, and M. A. Alvarez Sierra. 1986. Paleontología y bioestratigrafía (micromamíferos) del Mioceno medio y superior del sector central del la Cuenca del Duero. *Studia Geologica Salmanticensia* 22: 191-212.
- Lourens, L., and F. J. Hilgen. 1997. Long-periodic variations in the earth's obliquity and their relation to third-order eustatic cycles and late Neogene glaciations. *Quaternary International* 40: 43-52.
- Lourens, L., F. J. Hilgen, L. Gudjonsson, and W. J. Zachariasse. 1992. Late Pliocene to early Pleistocene astronomically forced sea surface productivity and temperature variations in the Mediterranean. *Marine Micropaleontology* 19: 49-78.
- Loutit, T. S., J. P. Kennett, and S. M. Savin. 1983. Miocene equatorial and southwest Pacific paleoceanography from stable isotope evidence. *Marine Micropaleontology* 8: 215-233.
- Lungu, A. N. 1981. Gipparionovaya fauna srednego sarmata Moldavii (nasekomoyadnyye, zaytseobraznyye i grysuny). [The Middle Sarmatian Hipparion Fauna of Moldavia (insectivores, lagomorphs and rodents).] *Shtiintsa, Kishinev, MSSR*: 1-140.
- MacArthur, R. M. 1972. *Geographical ecology*. Harper and Row, New York.
- MacArthur, R. M., and E. O. Wilson. 1967. *The theory of island biogeography*. Princeton University Press, Princeton.
- Machette, M. N. 1985. Calcic soils of the southwestern United States. *Geological Society of America, Special Paper* 203: 1-21.
- Made, J. van der. 1997. Los Suides de la Península Ibérica. Pp. 109-112 in J.P. Calvo and J. Morales, eds. *Avances en el conocimiento del Terciario Ibérico*. UCM-CSIC, Madrid.
- Mai, D.H. 1995. Tertiäre Vegetationsgeschichte Europas. Gustav Fischer, Jena.
- Maiorana, V.C. 1990. Evolutionary strategies and body size in a guild of mammals. Pp. 69-102 in J. Damuth, and B. J. MacFadden. *Body size in mammalian paleobiology: estimation and biological implications*. Cambridge University Press, Cambridge.
- Manabe, S., and T. B. Terpstra. 1974. The effects of mountains on the general circulation of the atmosphere as identified by numerical experiments. *Journal of Atmospheric Sciences* 31: 3-42.
- Marcus, L. F. 1993. Some aspects of multivariate statistics for morphometrics. Pp. 95-130 in L. F. Marcus, E. Bello, and A. García-Valdecasas, eds. *Contribution to morphometrics*. Monografías del Museo Nacional de Ciencias Naturales. Museo Nacional de Ciencias Naturales, Madrid.
- Marks, P. 1971. Turolian. *Giornale di Geologia* 37: 215-219.
- Martin, J. M., and J. C. Braga. 1994. Messinian events in the Sorbas basin in southeastern Spain and their implication in the

References

- recent history of the Mediterranean. *Sedimentary Geology* 90: 257-268.
- Martin, L. D. 1993. Evolution of hypsodonty and enamel structure in Plio-Pleistocene rodents. Pp. 205-225 in R.A. Martin, and D. Barnosky, eds. *Morphological change in Quaternary mammals of North America*. Cambridge University Press, Cambridge.
- Martin, R. D. 1996. Tracking mammal body size distributions in the fossil record: a preliminary test of the 'rule of similarity'. *Acta Zoologica Cracoviensia* 39: 321-328.
- Martin Suárez, E., and M. Freudenthal. 1994. *Castromys*, a new genus of Muridae (Rodentia) from the Late Miocene of Spain. *Scripta Geologica* 106: 11-34.
- Martin Suárez, E., and P. Mein. Revision of the genus *Castillomys* (Muridae, Rodentia). *Scripta Geol.* 96: 47-81.
- Mayr, H. M. 1979. Gebissmorphologische Untersuchungen an miozänen Gliriden (Mammalia, Rodentia) Süddeutschlands. Ph.D Thesis, München.
- Mein, P. 1984. Composition quantitative des faunes de mammifères du Miocène moyen et supérieure de la région lyonnaise. *Paléobiologie Continentale* 14: 339-347.
- Mein, P. 1990. Updating of MN zones. Pp. 73-90 in E. H. Lindsay, V. Fahlbusch, and P. Mein, eds. *European Neogene Mammal Chronology*. Plenum, New York.
- Mein, P., E. Martín Suárez, and J. Agustí. 1993. *Progonomys* Schaub, 1938 and *Huerzelerimys* gen. nov. (Rodentia); their evolution in Western Europe. *Scripta Geologica* 103: 41-64.
- Mein, P., and J. Michaux. 1979. Une fauna de petits mammifères d'âge Turolien moyen (Miocène supérieur) à Cucuron (Vaucluse); données nouvelles sur le genre *Stephanomys* (Rodentia) et conséquences stratigraphiques. *Géobios* 12: 481-485.
- Mein, P., E. Moissenet, and R. Adrover, 1990. Biostratigraphie du Néogène supérieur de Teruel. *Paleontología i Evolució* 23: 121-139.
- Mercer, J. H. 1983. Cenozoic glaciation in the Southern Hemisphere. *Annual Review of Earth and Planetary Sciences* 11: 99-132.
- Meulen, A. J. van der, and H. de Bruijn. 1982. The mammals from the Lower Miocene of Aliveri (Island of Evia, Greece). Part 2. The Gliridae. *Proceedings of the Koninklijke Nederlandse Academie van Wetenschappen*, B 85: 485-524.
- Meulen, A. J. van der, and R. Daams. 1992. Evolution of Early-Middle Miocene rodent faunas in relation to long-term palaeoenvironmental changes. *Palaeogeography, Palaeoclimatology, Palaeoecology* 93: 227-253.
- Meulen, A. J. van der, and G. G. Musser. 1987. Progress report on the rodents from the Pleistocene of Trinil, Sangiran, Kali Glagah and Ci Saat (Java, Indonesia). Unpublished report.
- Michaux, J. 1971. Muridae (Rodentia) néogène d'Europe sud-occidentale. Evolution et rapports avec les formes actuelles. *Paléobiologie Continentale* 2: 1-67.
- Michaux, J., 1982. Aspects de l'évolution des Muridés (Rodentia, Mammalia) en Europe sud-occidentale. Pp. 195-199 in J. Chaline, ed. *Modalités, rythmes, mécanismes de l'évolution biologique. Gradualisme phylétique ou équilibres ponctués?* Éditions du Centre National de la Recherche Scientifique, Paris, France.
- Miesch, A. T. 1976. Q-mode factor analysis of geochemical and petrologic data matrices with constant sum rows. U. S. Geological Survey Professional Paper 574-G: 1-47.
- Miller, K. G., J. D. Wright, and R. G. Fairbanks. 1991. Unlocking the Ice House: Oligocene-Miocene oxygen isotopes, eustasy, and margin erosion. *Journal of Geophysical Research* 96: 6,829-6,848.
- Misonne, X. 1969. African and Indo-Australian Muridae. Evolutionary trends. *Musée Royal de l'Afrique Centrale, Sciences zoologique* 172: 1-219.
- Moissenet, E. 1983. Aspectos de la neotectónica en la Fosa de Teruel. Pp. 427-446 in *Geología de España, Libro Jubilar J.M. Ríos*, vol. 2. Instituto Geológico y Minero de España, Madrid.
- Moissenet, E. 1989. Les fossés néogènes de la Chaîne Ibérique: leur évolution dans le temps. *Bulletin de la Société Géologique de France*, série 8, 5: 919-926.
- Montuire, S. 1994. Communautés de mammifères et environnements. Ph.D Thesis, Montpellier.
- Morgan, M. E., C. Badgley, G. F. Gunnell, P. D. Gingerich, J. W. Kappelman, and M. C. Maas. 1995. Comparative paleoecology of Paleogene and Neogene mammal faunas: body-size structure. *Palaeogeography, Palaeoclimatology, Palaeoecology* 115: 287-318.
- Morgan, M. E., J. D. Kingston, and B. D. Marino. 1994. Carbon isotopic evidence for the emergence of C4 plants in the Neogene from Pakistan and Kenya. *Nature* 367: 162-165.
- Moyà-Solà, S., and J. Agustí. 1987. The Vallesian in the type area (Vallès-Penedès, Barcelona, Spain). 1987. Proceedings of the VIIIth RCMNS Congress, Budapest. *Annales Instituti Geologici Publici Hungarici* 52: 93-99.
- Moyà-Solà, S., and J. Agustí. 1990. Bioevents and small mammal successions in the Spanish Miocene. Pp. 357-404 in E. H. Lindsay, V. Fahlbusch, and P. Mein, eds. *European Neogene Mammal Chronology*. Plenum, New York.
- Mrosovsky, N. 1966. Acceleration of annual hibernating cycle to 6 weeks in captive dormice. *Canadian Journal of Zoology* 44: 903-910.

- Mrosovsky, N. 1976. Lipid programmes and life strategies in hibernators. *American Zoologist* 16: 685-697.
- Mudie, P. J., and J. Helgason. 1983. Palynological evidence for Miocene climatic cooling in eastern Iceland about 9.8 Myr ago. *Nature* 303: 689-692.
- Nesbit Evans, E. M., J. A. H. Van Couvering, and P. Andrews. 1981. Palaeoecology of Miocene sites in Western Kenya. *Journal of Human Evolution* 10: 99-116.
- Nicholson, S., and H. Flohn. 1980. African environmental and climatic changes and the general circulation in late Pleistocene and Holocene. *Climatic Change* 2: 313-348.
- Niethammer, J., and F. Krapp. 1978. *Handbuch der Säugetiere Europas*. Akademische Verlagsgesellschaft, Wiesbaden.
- Nowak, R. M. 1991. *Walker's mammals of the world*. John Hopkins University Press, Baltimore.
- Opdyke, N., P. Mein, E. Moissenet, A. Pérez-González, E. Lindsay, and M. Petko. 1990. The magnetic stratigraphy of the Late Miocene sediments of the Cabriel Basin, Spain. Pp. 507-514 in E. H. Lindsay, V. Fahlbusch, and P. Mein, eds. *European Neogene Mammal Chronology*. Plenum, New York.
- Osborn, J.W. and A. G. S. Lumsden. 1978. An alternative to "theogosis" and a re-examination of the ways in which mammalian molars work. *Neues Jahrbuch für Geologie und Paläontologie. Abhandlungen* 156: 371-392.
- Oslick, J., K. Miller, M. D. Feigenson, and J. D. Wright. 1994. Oligocene-Miocene strontium isotopes: Stratigraphic revisions and correlations to an inferred glacioeustatic record. *Paleoceanography* 5: 427-443.
- Pedley, H.M. 1990. Classification and environmental models of cool freshwater tufas. *Sedimentary Geology* 68: 143-154.
- Platt, N.H. 1989. Lacustrine carbonates and pedogenesis: sedimentology and origin of palustrine deposits from the Early Cretaceous Rupelo Formation, W Cameros Basin, N Spain. *Sedimentology* 36: 665-684.
- Pengelley, E. T., 1967. The relation of external conditions to the onset and termination of hibernation and estivation. Pp. 1-29 in K. C. Fisher, A. R. Dawe, C. P. Lyman, E. Schönbaum, and F. E. South, eds. *Mammalian Hibernation III*. Oliver and Boyd, Edinburgh.
- Perlmutter, M. A., and M. D. Matthews. In press. Global cyclostratigraphy - a model. In T. Cross, ed. *Quantitative dynamic stratigraphy*. Prentice Hall, Englewood Cliffs.
- Perrin, M. R. 1980. Ecological strategies of two co-existing rodents. *South African Journal of Science* 76: 487-491.
- Peshev, T. K., T. S. Dinev, and V. I. Angelova. 1960. *Myomimus personatus* Ogn. (Mammalia, Myoxidae) a rodent new to the fauna of Bulgaria. *Zoologiceskij Zhurnal* 59: 784-785.
- Pevzner, M. A., and E. A. Vangenheim. 1993. Magnetostratigraphic age assignments of Middle and Late Sarmatian Mammalian localities of the Eastern Paratethys. *Newsletters on Stratigraphy* 29: 63-75.
- Pianka, E. R. 1970. On r- and K- selection. *The American Naturalist* 104: 592-597.
- Pianka, E. R. 1972. r- and K- selection or b and d selection. *The American Naturalist* 106: 581-588.
- Pickford, M., and J. Morales. 1994. Biostratigraphy and palaeobiogeography of East Africa and the Iberian peninsula. *Palaeogeography, Palaeoclimatology, Palaeoecology* 112: 297-322.
- Pimm, S.L. 1978. An experimental approach to the effects of predictability on community structure. *American Zoologist* 18: 797-808.
- Poore, R. 1981. Late Miocene biogeography and paleoclimatology of the central North Atlantic. *Marine Micropaleontology* 6: 599-616.
- Potts, R., and A. K. Behrensmeyer. 1992. Late Cenozoic terrestrial ecosystems. Pp. 419-519 in A. K. Behrensmeyer, J. Damuth, W. DiMichele, R. Potts, H. D. Sues, and S. Wing, eds. *Terrestrial ecosystems through time*. University of Chicago Press, Chicago.
- Precht, H., J. Christopherson, H. Hensel, and W. Larcher. 1973. *Temperature and life*. Springer, Berlin.
- Prell, W. L., and J. E. Kutzbach. 1992. Sensitivity of the Indian monsoon to forcing parameters and implications for its evolution. *Nature* 360: 647-652.
- Prell, W. L., D. W. Murray, S. Clemens, and D. M. Anderson. 1992. Evolution and variability of the Indian Ocean Summer Monsoon: evidence from the Western Arabian Sea Drilling Program. *Geophysical Monograph* 70: 447-469.
- Putman, R. J. 1994. *Community ecology*. Chapman and Hall, London.
- Quade, J. T., and T. E. Cerling. 1995. Expansion of C₄ grasses in the Late Miocene of Northern Pakistan: evidence from stable isotopes in paleosols. *Palaeogeography, Palaeoclimatology, Palaeoecology* 115: 91-116.
- Quade, J.T., T. E. Cerling, and J. R. Bowman. 1989. Development of the Asian monsoon revealed by marked ecological shift in the latest Miocene of northern Pakistan. *Nature* 342: 163-166.
- Quade, J. T., N. Solounias, and T. E. Cerling. 1994. Stable isotope evidence from paleosol carbonates and fossil teeth in Greece for forest or woodlands over the past 11 Ma. *Palaeogeography, Palaeoclimatology, Palaeoecology* 108: 41-53.
- Raymo, M. E. 1994. The Himalayas, organic carbon burial, and climate in the Miocene. *Paleoceanography* 9: 399-404.
- Raymo, M. E., and W. F. Ruddiman. 1992. Tectonic forcing of late Cenozoic climate. *Nature* 359: 117-122.
- Reiss, M.J. 1989. *The allometry of growth and reproduction*. Cambridge University Press, Cambridge.
- Renner, R. M. 1993. The resolution of a compositional dataset into mixtures of fixed source compositions. *Appl. Statist., Jour. Roy. Stat. Soc.* 42: 615-631.

References

- Rensberger, J. M. 1973. An occlusion model for mastication and dental wear in herbivorous mammals. *Journal of Paleontology* 47: 515-528.
- Rensberger, J. M. 1975. Function in the cheek tooth evolution of some hypsodont geomyoid rodents. *Journal of Paleontology* 49: 10:22.
- Rensberger, J. M. 1982. Patterns of dental change in two locally persistent successions of fossil aplodontid rodents. Pp. 324-348 in B. Kurtén, ed. *Teeth: form, function and evolution*. Columbia University Press, New York.
- Rensberger, J. M. 1986. Early chewing mechanisms in mammalian herbivores. *Paleobiology* 12: 474-494.
- Retallack, G. J. 1991. *Miocene paleosols and ape habitats of Pakistan and Kenya*. Oxford University Press, New York.
- Reumer, J. W. F. 1994. Phylogeny and distribution of the Crocidoloricinae (Mammalia; Soricidae). *Carnegie Museum of Natural History Special Publication* 18: 345-356.
- Robin, G. de Q. 1988. The Atlantic ice sheet, its history and response to sea level and climatic changes over the past 100 million years. *Palaeogeography, Palaeoclimatology, Palaeoecology* 67: 31-50.
- Robinson, P. F. 1968. General aspects of physiology. Pp. 111-118 in R. A. Hoffman, P. F. Robinson, and H. M. Magelhaes, eds. *The golden hamster, its use in medical research*. Iowa State University Press, Ames.
- Rodríguez-Aranda, J.P., and J. P. Calvo. 1997. Trace fossils and rhizoliths as a tool for sedimentological and palaeoenvironmental analysis of ancient continental evaporite successions. *Palaeogeography, Palaeoclimatology, Palaeoecology* (in press).
- Rohlf, F.J. 1993a. Relative warp analysis and an example of its application to mosquito wings. Pp. 131-160 in L. F. Marcus, E. Bello, and A. García-Valdecasas, eds. *Contribution to morphometrics*. Monografías del Museo Nacional de Ciencias Naturales. Museo Nacional de Ciencias Naturales, Madrid.
- Rohlf, F.J. 1993b. TPSRW - Thin plate spline relative warp. Department of Ecology and Evolution, State University of New York, Stony Brook.
- Rohlf, F.J. 1993c. TPSREGR: A program for regression of partial warp scores. Department of Ecology and Evolution, State University of New York, Stony Brook.
- Ruddiman, W. F., and A. McIntyre. 1984. Ice-thermal response and climate role of the surface Atlantic Ocean, 40°N to 63°N. *Geological Society of America Bulletin* 95: 381-396.
- Ruddiman, W. F., and Kutzbach, J. E. 1989. Forcing of late Cenozoic Northern Hemisphere climate by plateau uplift in Southern Asia and the American West. *Journal of Geophysical Research* 94: 18,409-18,427.
- Rümke, C. G. 1974. A new *Desmanella* species (Talpidae, Insectivora) from the Turolian of Concu and Los Mansuetos (Prov. of Teruel, Spain). *Proceedings of the Koninklijke Nederlandse Akademie van Wetenschappen*, B 88: 415-426.
- Rümke, C. G. 1985. A review of fossil and recent Desmaninae (Talpidae, Insectivora). *Utrecht Micropaleontological Bulletin, Special Publication* 4: 1-241.
- Sanz, M.E., A. M. Alonso-Zarza, and J. P. Calvo. 1995. Carbonate pond deposits related to semi-arid alluvial systems: examples from the Tertiary Madrid Basin, Spain. *Sedimentology* 42: 437-452.
- Schaeffer, R., and D. Spiegler. 1986. Neogene Kälteeinbrüche und Vereisungsphasen im Nordatlantik. *Zeitschrift der Deutschen Geologischen Gesellschaft* 137: 537-552.
- Schaub, S., 1938. Tertiäre und Quartäre Murinae. *Abhandlungen der Schweizerischen Paläontologischen Gesellschaft* 61: 1-39.
- Schrader, H.-J. 1974. Cenozoic marine planktonic diatom stratigraphy of the tropical Indian Ocean. *Initial Reports of the Deep Sea Drilling Project* 24: 887-968.
- Schwarzbach, M. 1968. Das Klima des rheinischen Tertiärs. *Zeitschrift der Deutschen Geologischen Gesellschaft* 118: 33-88.
- Sen, S. 1997. The oldest late Miocene murids from Anatolia and their implications on the biochronology of the Old World murids. Abstracts. *Biochrom* 97. Montpellier.
- Sepkoski, J. J., Jr. 1996. Competition in macroevolution: the double wedge revisited. Pp. 211-255 in D. Jablonski, D.E. Erwin, and J. H. Lipps, eds. *Evolutionary paleobiology*. University of Chicago Press, Chicago.
- Shotwell, J. A. 1964. Community successions in mammals of the Late Tertiary. Pp. 135-150 in J. Imbrie, and N. Newell, eds. *Approaches to Paleocology*. Wiley and Sons, New York.
- Sierro, F. J., J. A. Flores, J. Civis, J. A. González Delgado, and G. Francés. 1997. Late Miocene globorotaliid event-stratigraphy and biogeography in the NE-Atlantic and Mediterranean. *Marine Micropaleontology* 21: 143-168.
- Simberloff, D., and T. Dayan. 1991. The guild concept and the structure of ecological communities. *Annual Review of Ecology and Systematics* 22: 115-143.
- Slobodkin, L. B., and H. L. Sanders. 1969. On the contribution of environmental predictability to species diversity. *Brookhaven Symposia in Biology* 22: 82-95.
- Sondaar, P. Y. 1971. The Samos *Hipparion*. *Proceedings of the Koninklijke Nederlandse Akademie van Wetenschappen*, B 74: 417-441.
- Stanley, S.M. 1973. An explanation for Cope's rule. *Evolution* 27: 1-26.
- Steininger, F., R. L. Bernor, and V. Fahlbusch. 1990. European Neogene marine/continental chronologic correlations. Pp. 15-

- 46 in E. H. Lindsay, V. Fahlbusch, and P. Mein, eds. *European Neogene Mammal Chronology*. Plenum, New York.
- Storch, G. 1978. Familie Gliridae Thomas, 1897 - Schläfer. Pp. 201-279 in J. Niethammer, and F. Krapp. 1978, eds. *Handbuch der Säugetiere Europas*. Akademische Verlagsgesellschaft, Wiesbaden.
- Storch, G., B. Engesser, and M. Wutke. 1996. Oldest fossil record of gliding in rodents. *Nature* 379: 439-441.
- Storch, G., and V. S. Zazhigin. 1996. Taxonomy and phylogeny of the *Paranourosorex* lineage, Neogene of Eurasia (Mammalia: Soricidae: Anourosoricini). *Paläontologische Zeitschrift* 70: 257-268.
- Tallis, J. H. 1991. *Plant community history*. Chapman and Hall, London.
- Taylor, K. D., and M. G. Green. 1976. The influence of rainfall on diet and reproduction in four African rodent species. *Journal of the Zoological Society of London* 180: 367-389.
- Tchernov, E. 1979. Polymorphism, size trends and Pleistocene paleoclimatic response of the subgenus *Sylvaemus* (Mammalia: Rodentia) in Israel. *Israel Journal of Zoology* 28: 131-159.
- Thackeray, J. F. 1987. Late Quaternary environmental changes inferred from small mammalian fauna, Southern Africa. *Climate Change* 10: 285-305.
- Thaler, L. 1966. Les rongeurs fossiles du Bas-Languedoc dans leur rapports avec l'histoire des faunes et la stratigraphie du tertiaire d'Europe. *Mémoires du Musée national d'Histoire naturelle C* 53: 367-387.
- Ünay, E., and H. de Bruijn. 1984. On some Neogene rodent assemblages from both sides of the Dardanelles, Turkey. *Newsletters on Stratigraphy* 13: 119-132.
- Van Couvering, J. A. H. 1980. Community evolution in Africa during the Late Cenozoic. Pp. 272-298 in A. K. Behrensmeyer, and A. P. Hill, eds. *Fossils in the making*, University of Chicago Press, Chicago.
- Van Valen, L. 1964. Relative abundance of species in some fossil mammal faunas. *The American Naturalist* 93: 109-116.
- Vincent, E., S. Killingley, and W. H. Berger. 1980. The Magnetic Epoch 6 carbon shift: a change in the ocean's ¹³C/¹²C ratio 6.2 million years ago. *Marine Micropaleontology* 5: 185-203.
- Visser, J. P. de. 1991. Clay mineral stratigraphy of Miocene to recent marine sediments in the central Mediterranean. *Geologica Ultraiectina* 75: 1-244.
- Voorhies, M. R. 1969. Taphonomy and population dynamics of an early Pliocene vertebrate fauna, Knox County, Nebraska. *University of Wyoming contributions to Geology Special Paper* 1: 1-69.
- Vrba, E. S. 1985. Environment and evolution: alternative causes of the temporal distribution of evolutionary events. *South African Journal of Science* 81: 229-236.
- Walter, H. 1994. *Vegetation of the earth*. Springer, Berlin.
- Weerd, A. van de. 1976. Rodent faunas of the Mio-Pliocene continental sediments of the Teruel-Alfambra region, Spain. *Utrecht Micropaleontological Bulletin, Special Publication* 2: 1-217.
- Weerd, A. van de, and R. Daams. 1978. Quantitative composition of rodent faunas in the Spanish Neogene and paleoecological implications. *Proceedings of the Koninklijke Nederlandse Academie van Wetenschappen, B* 81: 448-473.
- Weijjs, W.A. 1994. Evolutionary approach of masticatory motor patterns in mammals. *Advances in Comparative and Environmental Physiology* 18: 270-318.
- Weijjs, W.A., and R. Dantuma. 1975. Electromyography and mechanics of mastication in the albino rat. *Journal of Morphology* 146:1-34.
- Weijjs, W.A., and R. Dantuma. 1981. Functional anatomy of the masticatory apparatus in the rabbit (*Oryctolagus cuniculus*). *Netherlands Journal of Zoology* 31: 99-147.
- Welcomme, J. L., J.-P. Aguilar, and L. Ginsburg. 1991. Découverte d'un nouveau Pliopitèque (Primates, Mammalia) associé à des rongeurs dans les sables du Miocène supérieur de Priay (Ain, France) et remarques sur la paléogéographie de la Bresse au Vallésien. *Comptes Rendus de l'Académie des Sciences, Paris* 313: 723-729.
- Weltje, G. J. 1994. Provenance and dispersal of sand-sized sediments. *Geologica Ultraiectina* 121: 1-208.
- Weltje, G. J. 1997. End-member modelling of compositional data: Numerical-statistical algorithms for solving the explicit mixing problem. *Journal of Mathematical Geology* 29: 503-547.
- Western, D. 1980. Linking the ecology of past and present mammal communities. Pp. 41-54 in A. K. Behrensmeyer, and A. P. Hill, eds. *Fossils in the making*, University of Chicago Press, Chicago.
- Wing, S. L., H. D. Sues, R. Potts, W. DiMichele, and A.K. Behrensmeyer. 1992. *Evolutionary Paleocology*. Pp. 1-13 in A.K. Behrensmeyer, J. Damuth, W. DiMichele, R. Potts, H. D. Sues, and S. Wing, eds. *Terrestrial ecosystems through time*. University of Chicago Press, Chicago.
- Wolfe, J. A. 1994. An analysis of Neogene climates in Beringia. *Palaeogeography, Palaeoclimatology, Palaeoecology* 108: 207-216.
- Wolfe, J. A. 1985. Distribution of major vegetational types during the Tertiary. *Geophysical monographs* 32: 357-75.
- Wolf-Welling, T.C.W., A. Winkler, S. O'Connell, M. Cremer, F. Rack, K. Stattegger, and J. Thiede. 1995. Northern Hemisphere cooling starting at 10.5 Ma: Coarse fraction analysis of Fram Strait Sites 908 and 909 (Leg 151 NAAG). Abstract for congress: *Prediction in Geology*, Amsterdam.

References

- Woodburne, M. O., and C. C. Swisher III. 1996. Land-mammal high-resolution geochronology, intercontinental overland dispersals, sea level, climate and vicariance. *SEPM Special Publication 54*: 335-364.
- Wright, J. D., and K. G. Miller. 1992. Miocene stable isotope stratigraphy, Site 747, Kerguelen Plateau, Proceedings of the Ocean Drilling Project, Scientific Results 120: 855-866.
- Wright, J. D., K. G. Miller, and R. G. Fairbanks. 1991. Evolution of modern deepwater circulation: evidence from the late Miocene Southern Ocean. *Paleoceanography* 6: 275-290.
- Zwaan, G. J. van der, and L. Gudjonsson. 1986. Middle Miocene-Pliocene stable isotope stratigraphy and paleoceanography of the Mediterranean. *Marine Micropaleontology* 10: 71-90.

Acknowledgements

I would like to thank all my colleagues, friends and family; without their help and support this thesis could not have been accomplished.

Special thanks to my co-promotor Albert van der Meulen who always reserved time, when I needed him. His deep interest into all sorts of paleontological issues has always stimulated me in my work ever since I was a student. I appreciate the interesting discussions we had on such different subjects as evolution, sports, and complex rhythms in Balkan and jazz/rock music.

I thank my promotor Johan Meulenkamp for giving me the opportunity to do the research, for his supervision and his critical reading of the various manuscripts.

I am very grateful to Hans de Bruijn, who was my room mate for the last two years. This was a great luck because of Hans's awe-inspiring knowledge of fossil small mammals. He was always willing to try to identify an unsightly tooth fragment with which I came up, or to immediately phone a foreign colleague to solve any kind of problem.

I thank Remmert Daams for his great help in the field, collecting the small mammals, and for incorporating me into Spanish research projects. His numerous anecdotes and jokes contributed significantly to the pleasant atmosphere during the field campaigns. Remmert's advice during my Groningen study to contact Albert van der Meulen in Utrecht has eventually led to this thesis.

I am grateful to Luis Alcalá, who was always willing to guide me in Spain, and show me the fossil localities in the Teruel area. We made a good start for an integrated micro-macromammal approach for the area ("*and remember, one day we will reach this state of eternal fame*"). I thank him for his contribution to chapter 2.

Many thanks to Jose Pedro Calvo and Ana Alonso Zarza for their work constructing the lithostratigraphic framework, and for their contribution to chapter 2. Jose Pedro showed an admirable patience answering all the faxes and E-mails I sent.

From 1992 onwards almost three months were spent in the Daroca and Teruel areas in Spain for fieldwork. I am very grateful to Remmert Daams, Albert, Joke and Michiel van der Meulen, Pablo Pelaez Campomanes, Marian Alvarez Sierra, and Martine Bestebreurtje for their structural help with the collection of micromammals and pleasant company during all the campaigns. I hope that they can forgive me my selection not too close to the road of some localities. Many people joined the campaigns for shorter and longer time and digged, carried, and washed sediments from the Teruel-Alfambra region or helped otherwise in the field: I thank Berta Alcalá, Poppe de Boer, Hans and Jes de Bruijn, Michel Brunet, Rob Dikken, Pilar Garcia Somoza, Miguel Garcés, Cindy Gordon, Cor Langereis, Lars van den Hoek Ostende, Ton van Hoof, Wout Krijgsman, François Lévêque, Filip Levering, Bob Martin, Carmen Martin, Pierre and Marie-Therèse Mein, Johan Meulenkamp, Francisco Mieres, André Nieuwenhuizen, Fred Rögl, Ed van Slobbe, Karel Steensma, Constantin Theocharopoulos, Agnes and Paul Tijman op Smeijers, and Marleen Vriends.

Tengo un grato recuerdo de la hospitalidad y la amabilidad de la gente española. El Hostal Legido en Daroca fue el lugar apropiado sino perfecto durante el desarrollo de nuestras campañas. La comida (me encantó la ensalada mixta y el gazpacho) y las bebidas (los excelentes cafés con leche en vaso largo, las cañas refrescantes, los cuba-libres y los pacharanes) nos fueron eficazmente servidas por el amable Pepe ("*Ian ban Dan!*") y sus camareros, que a pesar de estar muy atareados, siempre nos atendieron a la perfección.

Muchas gracias a mis amigos Alberto y Delia del restaurante Los Caprichos en Teruel. Su hospitalidad en el restaurante y en su casa hizo muy agradable mi estancia en la zona. Pasamos noches muy agradables junto con sus vecinos del piso de arriba, Jordi y Corine (su traducción al holandés del menú que colgaba en el exterior fue la causa inmediata de entablar contacto) y Manolo, quien me cedió amablemente su apartamento.

The jury consisted of Dr H. (Hans) de Bruijn, Prof. Dr R. (Remmert) Daams, Mr. P. Mein, Prof. Dr H. Visscher, and Prof. Dr B. J. (Bert) van der Zwaan. In addition to my promotor, co-promotor, and members of the jury, I am grateful to the following persons for their suggestions on, and critical reading of various chapters: Wout Krijgsman on chapter 2, who is also thanked for his contribution to this chapter, Fred Bookstein, Marco Corti, Anna Loy, Gavin Naylor, Pablo Pelaez Campomanes, and Jim Rohlf on chapter 4, Mark Boyce on chapter 5, John Damuth, Frits Hilgen and Jelle Reumer on chapters 5 and 6, and Jan Willem Zachariasse on chapter 6. I thank Prof. Dr. C. J. E. Schuurmans for discussing the subject of topographic effects on atmospheric circulation, and Prof. W. A. Weijs for discussing the subject of mastication in small mammals.

I enjoyed the discussions and informal chatting on both scientific and non-scientific affairs with the above mentioned colleagues and with Hayfa Abdul Aziz, Poppe de Boer, Jelmer Cleveringa, Ivo Duijnste, Maryke den Dulk, Tanja Kouwenhoven, Natasja Jannink, Gerard Klein Hofmeijer, Cor Langereis, Lucas Lourens, Michiel van der Meulen, Niek Molenaar, Albert Oost, Pablo Pelaez Campomanes, Dolores Pipujol, George Postma, Maarten Prins, Andrea Santarelli, Paul Sondaar, Wim Sissingh, Andries Spaan, Rob Speijer, Joris Steenbrink, Henko de Stigter, Jan Berend Stuu, Johan ten Veen, Gert Jan Weltje, Wilma Wessels, and the students, all from the Faculty of Earth Sciences. Multidimensional discussions with Gert Jan Weltje have led to the application of his end-member algorithms to my data, which has resulted in a joint paper included as chapter 6. I enjoyed the pleasant company of Wilma as a roommate on her scientific (Mon- and Thurs)days. Jildou Nijboer so kind to check the English text of these acknowledgements, of which Dolores Pipujol translated the two paragraphs above into Spanish. Lucas, Michiel and Theo van Zessen helped me out with various network and computer problems. I really enjoyed Pablo Pelaez-Campomanes's stay in Utrecht, and thank him for drawing my attention to some valuable ecological literature.

I thank Jaap ("*you would not say so, but here lives an artist!*") Luteijn for his superb drawings (including the cover illustration) and retouch work. I am happy to have included in my thesis his first drawings made with the new successful airbrush technique. Thanks to Tom ("Mr. AUTOCAD") van Hinte for his computer assistance and patience with my requests for yet another version of some drawing. I thank Wil den Hartog for all his high-quality photographic work. (We still have to play a high-quality game of tennis!). Jaco van Berghenengouwen, Paul van Oudenallen, Izaak Santoe and Fred Trappenburg

Acknowledgements

prepared various figures. Thanks to Hans Brinkerink, Gerrit van 't Veld and Geert Ittmann for washing various samples in the laboratory, and not getting discouraged after the fifth or sixth treatment with acetic acid. Hans Brinkerink, together with Frank Geerts, Willem Renema and Juliette Richter were helpful in sorting residues. I thank Ank Pouw and Marnella van der Tol for all their small but indispensable favours. I am grateful to Willem van Hattem, Lidy Jansen, Jan Jansen, Agathe van Rhee, Marcel Stelling, en Frans Verdaasdonk for their excellent service in the library, one of my favourite places in the Institute. Our canteen ladies Margret and Berna looked well after my physical well being during the day. They let me be in their debt when I was out of money, and served my favourite Wednesday pea and Thursday bean soups sometimes even during summer.

Many other colleagues outside the Institute of Earth Sciences were helpful during the establishment of my thesis. Lars van den Hoek Ostende and Jelle Reumer helped me with the identification of insectivores. I still admire Jelle's craftsmanship as a driver in his brand new red mini-bus on the all-too-dangerous Polish highways on our trip to the 1994 Krakow congress. Lodewijk IJlst is thanked for letting me use his impressive overflow centrifuge machinery in order to reduce some samples. I thank Leslie Marcus and the other organizers and staff of the NATO ASI "Advances in Morphometrics", Il Ciocco, Italy (1993), for allowing me to participate and publish my results, and for helping me during the workshop with my trials (and errors) applying morphometric tools to my data. I thank the people from the Mammal Department of the Natural History Museum of London for their help during my working visits, when I studied extant murid dentitions. I thank Antonio Rosas, Jan van der Made and Ceniz for their hospitality during my stays in London and Madrid. Dr J.-P. Aguilar, Dr J. Michaux and Mr P. Mein are thanked for their hospitality during my working visits in Montpellier and Lyon. I thank the latter colleagues and Dr G. Storch for supplying me with a number of faunal data.

I thank my "precursor" Anne van de Weerd (whose thesis was my bible) for granting me a large collection of reprints and copies, which formed a fantastic starting point for this study.

I thank here also Em. Prof. L. M. J. U. van Straaten (Groningen) whose exciting lectures made me enthusiastic for geology and paleontology in the first place.

Chris was a wonderful source of distraction. Maria Panhuyzen, and the families Key and Roelen were very helpful taking care of him during crisis times.

I am very grateful to my parents Gijs and Ina van Dam, who kept on supporting me during my study, and who had to go through many sleepless nights, wondering what illustrious career steps their son would take this time. My father helped me fantastically with sorting the residues, and I am pleased to see that he has become an enthusiastic amateur geologist.

Above all, I thank Agnes for all her love, support, endurance, and household-organizational qualities during the years. I solemnly promise that I never will write a thesis again.

Curriculum vitae

Jan Arie van Dam was born on 20 March 1959 in Krimpen a/d IJssel, the Netherlands. He attended secondary school in Assen from 1971 to 1977. He obtained B.Sc. degrees in social geography in 1982 and geology in 1985, and a M.Sc. degree in social geography (demography) in 1986 at the University of Groningen. From 1986 to 1988 he was employed as a geographer/demographer at Utrecht University and TNO Delft. He obtained a M.Sc. degree in geology at Utrecht University in 1991 with mammal paleontology as his principal subject. From 1992 to 1996 he was employed as a Ph.D. candidate (AIO) at the Department of Geology, Faculty of Earth Sciences, Utrecht University.

ERRATA

p. 31

Zone J: "*Muscardinus hispanicus*" instead of "*Muscardinus hartenbergeri*"

p. 32

Zone J3: "*Myomimus* sp. A" instead of "*Myomimus* sp."

p. 54

Figure 3.9 is figured upside down

p. 55

Last line: 3.4.6 instead of 4.6

p. 80

Caption figure 4.4: "thick lines" instead of "thin lines", and vice versa

p. 81

Table 4.5: " $\alpha=0$, uniform component included" instead of " $\alpha=0$, uniform component not included", and vice versa

p. 146

Add:

Table 6.8. Robustness of climatic parameter estimation against structural under or over-representation of groups. The effect of demographic bias is tested by a posterior correction of end-member compositions from table 6.4. Correction factors are based on French et al. (1975) and represent mid-points of ranges of life-expectancy values for demographic groups. Only in one case (the proportion Castoridae in end member 1) row-wise comparison of proportions leads to scores different from those in table 6.4.

group	correction factor	corrected end members (%)			
		1	2	3	4
Castoridae	9.95	2.89	3.61	4.63	1.59
Cricetidae I	3.35	13.64	7.72	9.41	25.62
Cricetidae II	3.35	5.44	56.99	0.00	22.64
Gliridae I	9.95	0.00	8.23	18.41	29.70
Gliridae II	9.95	0.00	22.93	21.26	2.49
Muridae I	1.80	47.50	0.27	0.43	0.00
Muridae II	1.80	16.93	7.18	41.19	2.44
Sciuridae I	9.95	9.46	2.35	0.00	11.08
Sciuridae II & Petauristidae & Eomyidae	9.95	4.06	39.47	4.94	4.43
total		100.00	100.00	100.00	100.00

p. 166

SM13 includes both immigration and extinction between 7.0 and 6.6 Ma